The role of eIF2alpha kinases in the resistance to VSV infection and regulation of the stability of the tumor suppressor protein p53

by

Dionissios Baltzis

Experimental Medicine

McGill University, Montreal

February 2007

A thesis submitted to McGill University in partial fulfillment of the requirements of the degree of Doctor of Philosophy.

Your file Votre référence
ISBN: 978-0-494-32292-5
Our file Notre référence
ISBN: 978-0-494-32292-5

To the late Athanasios Baltzis,

Who never got the chance to see me graduate.

ABSTRACT

PKR has been shown to play an essential role against VSV infection by phosphorylating eIF2α leading to the inhibition of protein synthesis. Through this capacity PKR is thought to be a mediator of the anti-viral and anti-proliferative actions of IFNs. In addition to translational control, PKR has been shown to modulate the transcriptional activities of NF-κB, Stats and p53. However, experiments with two different $PKR^{-/-}$ mouse models have failed to verify many of the biological functions attributed to PKR. Here, we show that the two $PKR^{-/-}$ MEFs express different PKR truncated proteins suggesting that both $PKR^{-/-}$ models are incomplete knockouts. The expression of the PKR variants may account for the significant signaling differences between cells from the two $PKR^{-/-}$ mice.

We also demonstrate that another eIF2α kinase, PERK contributes to cellular resistance towards VSV infection. We demonstrate that $PERK^{-/-}$ MEFs are more susceptible to VSV-mediated apoptosis than $PERK^{+/+}$ MEFs. The higher replication capacity of VSV in $PERK^{-/-}$ MEFs results from their inability to attenuate viral protein synthesis due to an impaired eIF2α phosphorylation. We also show that VSV-infected $PERK^{-/-}$ MEFs are unable to fully activate PKR suggesting a cross-talk between the two eIF2α kinases in virus infected cells. These findings further implicate PERK in virus infection, and provide evidence that the anti-viral and anti-apoptotic roles of PERK are mediated, at least in part, via the activation of PKR.

Despite the translational control function of eIF2α kinases, we demonstrate their implications in p53 inactivation. Specifically, we show that PERK activation is

responsible for the proteasomal degradation of p53 in a manner that is independent of translational control. This role is not specific for PERK, since the PKR also promotes p53 degradation in response to dsRNA transfection. We established that activation of eIF2α kinases leads to the activation of GSK3β thus promoting the Mdm2-dependent degradation of p53. That is, induction of eIF2α kinases leads to the nuclear localization of GSK3β, and the nuclear export and proteasomal degradation of p53. Our findings establish a novel cross-talk between the eIF2α kinases and p53 with significant implications in stress responses that control cell proliferation and tumorigenesis.

RÉSUMÉ

La protéine kinase PKR joue un rôle essentiel contre l'infection virale par le VSV, elle phosphoryle eIF2α, provoquant l'inhibition de la synthèse des protéines. De cette action, PKR est perçue comme un médiateur des actions anti-virale et anti-prolifération des IFNs. En plus du contrôle traductionnel, PKR intervient dans la régulation des activités transcriptionnelles des facteurs NF-κB, Stats et p53. Cependant, des expériences avec deux modèles différents de souris $PKR^{-/-}$ n'ont pas permis de mettre en évidence certaines fonctions biologiques attribuées à PKR. Ici, nous montrons que les deux types de cellules $PKR^{-/-}$ expriment différentes protéines PKR tronquées, suggérant que les deux modèles de $PKR^{-/-}$ sont des knock-out incomplets. L'expression de ces variants de PKR peut justifier les différences significatives de signalisation observées dans les deux types de souris.

Nous démontrons aussi qu'une autre kinase phosphorylant eIF2α, PERK, contribue à la résistance cellulaire consécutive à l'infection par le VSV. Nous démontrons que les MEFs $PERK^{-/-}$ sont plus susceptibles à l'apoptose induite par VSV par rapport aux MEFs $PERK^{+/+}$. La plus forte capacité réplicative du VSV dans les MEFs $PERK^{-/-}$ résulte de leur incapacité d'atténuer la synthèse de protéine virale due au manque de phosphorylation de eIF2α. Nous montrons également que les MEFs $PERK^{-/-}$ infectés par VSV sont incapables d'activer totalement PKR, suggérant un lien étroit entre les deux kinases dans les cellules infectées par le virus. Ces travaux impliquent PERK dans l'infection virale, et fournissent la preuve que les rôles anti-virals et anti-apoptotiques de

PERK en réponse à l'infection virale sont régulés, au moins en partie, via l'activation de PKR.

En plus des fonctions dans le contrôle traductionnel des kinases phosphorylant eIF2α, nous démontrons leurs implications dans l'inactivation de p53. Nous montrons que l'activation de PERK est responsable de la dégradation de p53 via le protéasome, et ce, indépendamment du contrôle traductionnel. Ce rôle n'est pas spécifique de PERK, puisque PKR induit aussi la dégradation de p53 en réponse au traitement dsRNA. Nous avons également établi que l'activation des kinases phosphorylant eIF2α active GSK3β, permettant ainsi la dégradation de p53 d'une manière dépendante de Mdm2. En effet, l'induction des kinases eIF2α mène à la localisation nucléaire de GSK3β, à l'exportation nucléaire et à la dégradation de p53. Nos travaux établissent un nouveau lien étroit entre les kinases phosphorylant eIF2α et p53, avec des implications significatives dans les réponses aux stress qui contrôlent la prolifération cellulaire et la tumorigenèse.

ACKNOWLEDGEMENTS

Behind every able person, there are always other able people. Therefore I would like to thank and acknowledge all those people who helped achieve my goals. I owe them my never ending gratitude and appreciation because if not for these people, I wouldn't be where I am today.

First, I would like to thank my supervisor, Dr. Koromilas, who not only gave me my first laboratory experience, but for initially training me during a stressful transition period in his lab. I appreciate his trust in me, and for allowing me to contribute to the success we experienced along the way. Thank you for making me realize that ability can take you to the top, but it takes character to keep you there.

I would also like to thank all my committee members who gave me proper guidance and advice during my Ph.D. training. Also, my deepest respect goes to all those who donated to the Terry Fox Foundation, the National Cancer Institute of Canada (NCIC), and the Canadian Institutes for Health Research (CIHR) because all this work couldn't have been achieved without the financial support they've given me over the last five years.

Thanks to all my lab colleagues who helped me over the past five years, in particular Dr. Shirin Kazemi. Ever since I entered the lab, Dr. Kazemi has been a dear friend and a wonderful person to work with. She kept reminding me that a friend is one who knows who you are, understands where you have been, accepts what you become, and still gently invites you to grow. She made my lab experience a more pleasurable one,

and I couldn't have asked for a better partner to work with. Thank you for being my "Guardian Angel".

On a personal side, I deeply thank Mr. Marcel Paradis, Mr. & Mrs. Drblik, and especially Mr. Sam Erimos for giving me my first employment opportunity, and reference letter. I thank them for their support that got me threw my education prior to my Ph.D. training.

Next, I would like to thank my family whom I love more than life itself. I owe them for all my life's achievements and success, and I dedicate all this work to them. I would like to thank my little sister, Sophia, for being my number one supporter and best friend. She made my life enjoyable when times were tough and always made the proper sacrifices when I needed her the most. To my big brother, Tommy, who never stopped inspiring me, and played the positive role model when we were growing up. I'll always look up to him knowing that he'll always be there for me.

Finally, to my parents, Panagiotis and Roula, who taught me that failure, fear, and the lives we lead are inevitable; how we deal with them is the true test of our character. They gave me strength and courage that reminded me of how proud they were of me and my accomplishments. Their perseverance in supporting my education gave me a treasure that will follow me forever: knowledge.

PREFACE

In accordance with "Guidelines for Thesis Preparation", the candidate has chosen the option of presenting his results in the classical format. A general introduction is presented in Chapter I. Materials and methods for research presented in this document are detailed in Chapter II. The results described in Chapter III have been published, in part, in the stated journal article following subjection to the peer review process and in the manuscript which is in the process of preparation:

1. Baltzis D, Li S, Koromilas AE. **(2002)** Functional characterization of *pkr* gene products expressed in cells from mice with a targeted deletion of the N-terminus or C-terminus domain of PKR. J Biol Chem. 277 (41), Oct. 11, pp. 38364-38372.

2. Baltzis D, Qu L, Papadopoulou S, Blais JD, Bell JC, Sonenberg N, Koromilas AE. **(2004)** Resistance to vesicular stomatitis virus infection requires a functional cross-talk between the eIF2α kinases PERK and PKR. Journal of Virology. 78 (23), pp 12747-12761.

3. Baltzis D, Pluquet O, Papadakis AI, Kazemi S, Qu L, Koromilas AE. **(2007)** The eIF2α kinases PERK and PKR activate glycogen synthase kinase 3 to promote the proteasomal degradation of the tumor suppressor protein p53. (Manuscript in preparation).

All research presented in Chapter III was performed by the candidate, with the exception of these specific contributions:

1. Dr. Shirin Kazemi generated the HT1080/GyrB-PKR cells that were used in Chapter III section 3.
2. Dr. Olivier Pluquet performed the experiments in Fig. 39, 45, 47B, 48-51.
3. Dr. Ana Maria Rivas-Estillas provided guidance with the RT-PCR reactions in Fig. 23 and with the cloning of the *SF-mPKR* cDNAs.
4. Dr. Stavroula Papadopoulou helped with the 2D-PAGE analysis in Fig. 30D and 34C.
5. Dr. Suiyang Li initially cloned all *PKR* cDNAs in yeast vectors that were used in Fig. 20 and the PKRΔ6 in Fig. 35B.
6. Tetsu Ishii contributed to the cloning of ES-mPKR and performed the experiment in Fig. 26A.
7. Dr. Like Qu provided guidance with the VSV plaque assay in Fig. 29 and performed the experiments in Fig. 43.
8. Andreas Papadakis performed experiments in Fig. 38A.

The candidate was also involved in several collaborations with respect to research that is relevant to the data presented in this document. This research has been published in the following journal articles following subjection to the peer review process:

1. Pluquet O, Qu L, Baltzis D, Koromilas AE. **(2005)** Endoplasmic reticulum stress accelerates p53 degradation by the cooperative actions of Hdm2 and glycogen synthase kinase 3β. Mol Cell Biol. 25(21):9392-405.

2. Qu L, Huang S, Baltzis D, Rivas-Estilla A-M, Pluquet O, Hatzoglou M, Koumenis C, Taya Y, Yoshimura A, Koromilas A E. **(2004)** Endoplasmic reticulum stress induces p53 cytoplasmic localization and prevents p53-dependent apoptosis by a pathway involving glycogen synthase kinase-3β. Genes & Development. 18 (3), pp261-277.

The candidate was also involved in several collaborations with respect to research that is beyond the scope of this document. This research has been published in the following journal articles following subjection to the peer review process:

1. Kazemi S, Mounir Z, Baltzis D, Rivas-Estillas A-M, Qu L, Raven JF, Pluquet O, Wang S, Su Q, Pelletier J, Koromilas AE. **(2007)** A novel function of eIF2α kinases as inducers of the phosphoinositide-3 kinase signaling pathway. Molecular Biology of the Cell (Revised manuscript).

2. Su Q, Wang S, Baltzis D, Qu LK, Raven JF, Li S, Wong AH, Koromilas AE. **(2006)** Interferons induce the tyrosine phosphorylation of the eIF2α kinase PKR through activation of Jak1 and Tyk2. EMBO Reports. 8(3):265-70.

3. Wang S, Raven JF, Baltzis D, Kazemi S, Brunet DV, Hatzoglou M, Tremblay ML, Koromilas AE. **(2006)** The catalytic activity of the eukaryotic initiation factor-2alpha kinase PKR is required to negatively regulate Stat1 and Stat3 via activation of the T-cell protein-tyrosine phosphatase. J Biol Chem. 281(14):9439-49.

4. Su Q, Wang S, Baltzis D, Qu LK, Wong AH, Koromilas AE. **(2006)** Tyrosine phosphorylation acts as a molecular switch to full-scale activation of the eIF2alpha RNA-dependent protein kinase. PNAS 103(1):63-8.

CONTENTS

LIST OF TABLES AND FIGURES

CHAPTER I - INTRODUCTION

1. THE TUMOR SUPPRESSOR P53

1.1 HISTORY OF P53

The tumor suppressor protein p53 was first identified in 1979 by its ability to associate with the simian virus 40 (SV40) large T antigen (LT_{Ag}) and by its overexpression in chemically induced sarcomas or other transformed mouse cells (80,210,211). Other viral proteins were found to associate or bind to p53, such as the adenoviral E1B 55 kDa protein (285) and the HPV E6 protein (237). This suggested that DNA tumor viruses utilize common pathways in order to induce the transforming phenotype.

Although p53 was initially thought to be a tumor antigen further experiments suggested that p53 expression possesses oncogenic properties. Transfection of cloned p53 cDNA into primary mouse cells resulted in their immortalization (161) and co-transfection with the activated ras oncogene transformed primary rat fibroblasts (255). Also, p53 chromosomal translocations were detected in various tumors, such as acute promyelocytic leukemia (195). These studies favored the hypothesis that p53 behaved like an oncogene due to its overexpression in transformed cell lines. However, most of these experiments were misleading because this overexpressed p53 was in fact a mutated protein instead of the wild type protein (331).

The exact cellular role that p53 played still remained unclear until studies showed that p53 production was increased after nontransformed cells were exposed to ultraviolet (UV) radiation (223). This upregulation was explained by the fact that p53 undergoes post-translational modifications in order to bypass its degradation or to stabilize it (251).

Future experiments elucidated the cellular function of p53 when studies in colorectal carcinomas were done. Mutations commonly occurred in the p53 gene in combination with wild type p53 allelic deletions in colorectal carcinomas suggesting a tumor suppressor function of p53 (8,10). This hypothesis was tested and confirmed when wild type p53 was able to inhibit the growth of various cancer cells (9) and to suppress the transformation capacity of many oncogenes (102). These historical key experiments led to an explosion of research in determining the tumor suppressor function of p53 and it was shown to be the most commonly mutated gene in diverse human tumors (241). Subsequent work during the 1990's showed that p53 was a transcription factor that regulates many genes involved in cell cycle arrest, DNA repair, and apoptosis (130).

To date, great knowledge has been gathered regarding the mechanisms of activation and cellular functions of p53. Databases have been formed to categorize p53 alterations found in many human malignancies as well as the consequences of its inactivation (29,123,138,208). Applying this knowledge effectively into patient care such as early diagnosis, clinical outcome or prognosis as well as patient response to various treatments will be beneficial for designing novel anticancer therapies that are currently under investigation.

1.2 Molecular Biology of p53

The tumor suppressor protein p53, also known as tumor protein 53 (TP53), is a sequence-specific DNA-binding transcription factor that regulates a large number of target genes. These genes mediate cell cycle arrest, differentiation, senescence, DNA repair, inhibition of metastasis (angiogenesis), and apoptosis (130). Its primary function

is to suppress cancer via the activation of several cellular pathways targeted by its transcriptional activity (318,345). p53 has been described as "the guardian of the genome" due to its role in conserving genomic stability by preventing mutations. Its name is derived from its corresponding molecular weight of 53 kDa (193,201).

The importance of p53 in tumorigenesis was demonstrated by the fact that p53 is highly mutated in many different cancers and is rendered inactive in other types of cancers (194); and that mice homozygous for the *p53* null allele are prone to spontaneous neoplasms by 6 months of age (90). In about 50% of these tumours, p53 is directly inactivated as a result of mutations in the p53 gene (*TP53*) (145,146). Whereas in the remaining tumours, it is inactivated indirectly as a result of alterations in gene products that interact with or signal to p53 (146,337). Mutation or inactivation of p53 renders cancer cells resistant to current cancer therapies due to the lack of p53-mediated signaling pathways that are required to suppress the tumorigenesis process (318).

1.3 Structure of p53

1.3.1 The *TP53* Gene

The human *p53* gene (*TP53*) is located on the chromosome band 17p13.1, and stretches up to 20 kb containing 11 exons (Fig. 1A). The first exon is non-coding and is spaced some 10 kb from the other 10 exons. The fully processed and spliced mRNA is 2.5 kb in size and is expressed in all cells in the body (21,22,250). Although the *p53* mRNA levels have been shown to be relatively low in normal tissues (270), studies regarding *p53* mRNA transcription have shown that a number of transcription factors can maintain basal levels, enhance or repress *p53* mRNA expression (107,176,315,330). Most

transcription factors, particularly those from the AP-1 family (c-Jun, JDP-2), have been shown to repress p53 expression at the transcriptional level upon UV radiation (257,292,295). Although little is known about the promoter sequence regulating the transcription of p53, the highest level of *p53* mRNA was detected in the spleen and thymus (213,249,270).

1.3.2 The p53 Protein

The human *p53* gene (*TP53*) encodes for a 53 kDa protein consisting of 393 amino acids in which five evolutionary conserved regions have been described (Fig. 1B) (307). The first is located near the amino terminus and spans codons 13-19. The other four conserved regions are localized in the central area of the protein between codons 100-300. Functionally, the p53 protein is divided into three domains: the amino-terminus (N-terminus) domain; the central core domain; and the carboxy-terminus (C-terminus) domain (Fig. 1C) (131). The functional domains are further sub-divided into several other domains that possess specific functions that enable p53 to act as a transcription factor and/or tumor suppressor (131). Although p53 functions mainly as a transcription factor, p53 has been shown to form protein complexes by binding to heterologous proteins in order to modulate its activity (41). However, the biological functions of these complexes are still under investigation. Nevertheless, the regulation of the biochemical and biological outcomes of p53 are determined by combinatorial site specific modifications mediated by precise modulators (130).

1.3.2.1 Functional Domains of p53

The N-Terminus domain consists of the transactivation domain (TAD) and the proline-rich domain (PRD) (Fig. 1C). The transactivation domain (aa 1-44) is required for the transactivation activity of p53 in order to interact with various transcription factors and specific regulators, such as acetyltransferases and the Mdm2 ubiquitin ligase (131). Also a putative nuclear export signal (NES) has been identified within the transactivation domain (aa 11-24). The proline-rich domain (PRD) is a Src-homology 3-like (SH3) domain (aa 58-101) (Fig. 1C) and can mediate the interaction of p53 with Sin3a (238) in order to prevent its degradation (369) as well as to mediate the apoptotic function of p53 upon DNA damage.

The central core domain consists of the sequence-specific DNA-binding domain (DBD: aa 102-292) (Fig. 1C) (131). This is where most of the interactions between p53 and its target proteins occur. The DNA-binding domain contains a variety of structural motifs and is the target of 90% of p53 mutations found in human cancers. A single point mutation can cause serious conformational changes in p53 rendering it inactive in its ability to bind target DNA sequences.

The C-terminus domain consists of the oligomerization or tetramerization domain (TET), and the regulatory domain (REG) (Fig. 1C). The tetramerization domain (aa 325-356) is composed of a β-strand, which interacts with another p53 monomer to form a dimer, followed by a α-helix which mediates the dimerization of two p53 dimers to form a tetramer. Three nuclear localization signals (NLS) have been identified in the C-terminal domain. The first NLS (NLSI: aa 316-324) consists of three consecutive lysine

residues to a basic core, and is the most active and conserved domain. The regulatory domain (aa 363-393) comprises the other two NLS. NLSII is located between amino acids 370-376, whereas the NLSIII is between amino acids 380-386. A leucine-rich C-terminus NES has been identified within the tetramerization domain. The NES (aa 340-351) is highly conserved and it is believed that oligomerization can result in masking of the NES, resulting in p53 nuclear retention (131).

Figure 1. Structure of p53.

(A) The *TP53* gene spans some 20 kb, and comprises 11 exons (E1-E11) and 10 introns (I1-I10) of various length in which E1 is non-coding. The fully spliced *p53* mRNA is 2.5 kb. The numbers underneath the exons or above the introns indicate the length of that corresponding exon or intron in base pairs.

(B) The *p53* mRNA (exons shown in black) encode for a 53 kDa protein in which five conserved regions can be found (I-V).

(C) The p53 protein is a transcription factor containing 393 amino acids. The N-terminus contains the transactivation domain (TAD) and the proline-rich domain (PRD) both playing key roles in p53 activation. The central core domain consists of the DNA-binding domain (DBD) and is required for binding to promoters of genes with p53 responsive elements. The C-terminus contains the tetramerization domain (TET) in which the nuclear localization (NLS) and nuclear export (NES) signals have been described. Also, the regulatory domain (REG) is located at the very end of the protein, and is the region that undergoes many post-translational modifications that negatively regulate p53.

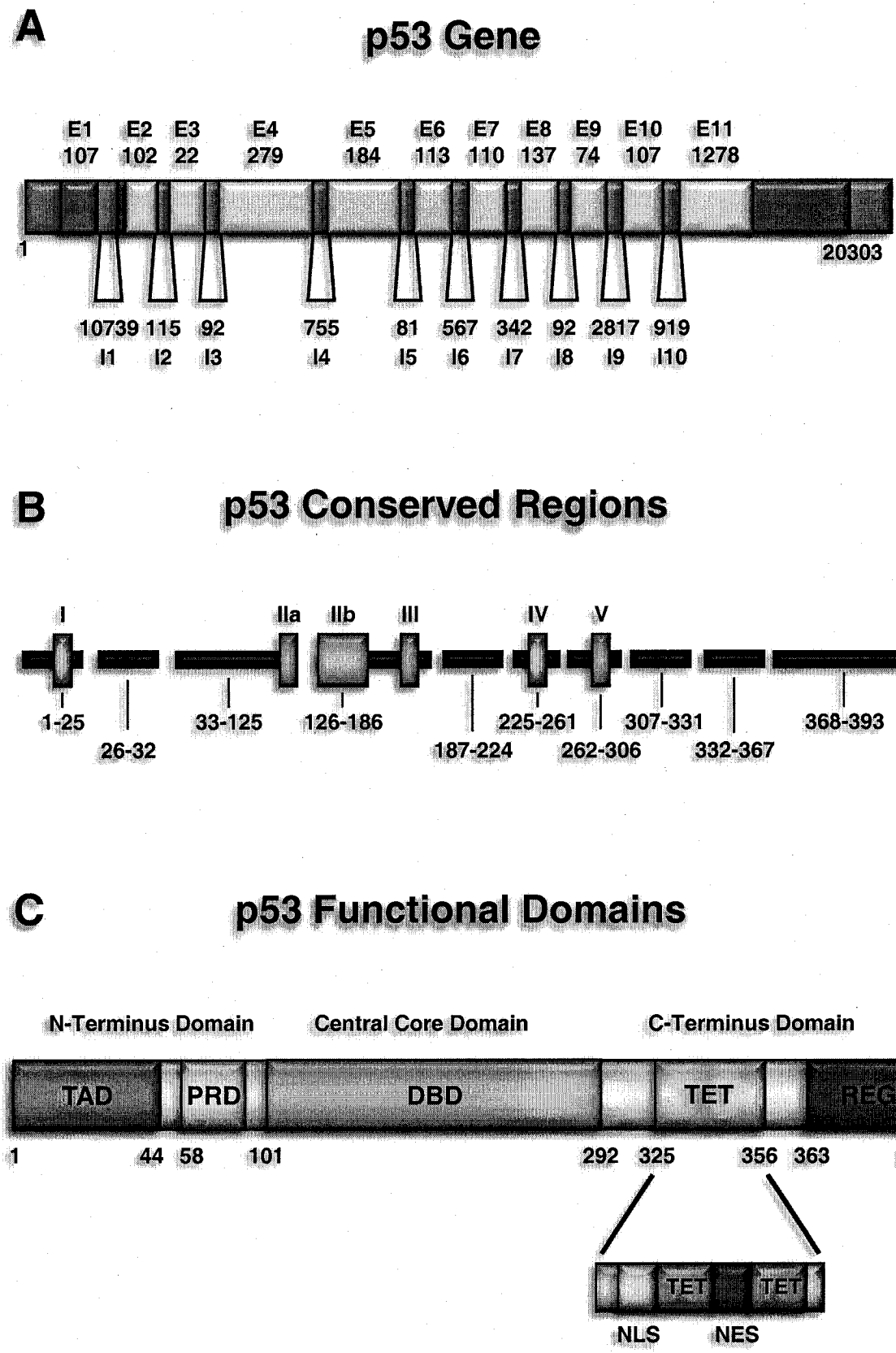
A
p53 Gene
E1 E2 E3 E4 E5 E6 E7 E8 E9 E10 E11
107 102 22 279 184 113 110 137 74 107 1278
1
20303
10739 115 92 755 81 567 342 92 2817 919
I1 I2 I3 I4 I5 I6 I7 I8 I9 I10
B
p53 Conserved Regions
I IIa IIb III IV V
1-25 26-32 33-125 126-186 187-224 225-261 262-306 307-331 332-367 368-393
C
p53 Functional Domains
N-Terminus Domain
Central Core Domain
C-Terminus Domain
TAD PRD DBD TET REG
1 44 58 101 292 325 356 363 393
TET TET
NLS NES

Figure 1

1.4 Activation of p53

Intrinsic and extrinsic stresses to the cell are capable of inducing the activation of p53. These stresses are categorized in three different groups: genotoxic, non-genotoxic and oncogenic stresses. The most studied stress capable of activating p53 is the cellular response upon DNA damage or any damage that affects the integrity of the genome (genotoxic stress). Damaging agents such as, gamma or UV irradiation, alkylation or depurination of DNA, reactive oxidative free radicals, and exposure to nitric oxide (NO) (104) can alter the DNA template in different ways that ultimately lead to the stability and activation of p53. The stabilization and activation of p53 is achieved by different modulators that are capable of sensing specific stresses in order to modify p53 at the post-translational level (35).

Different types of DNA damage activate different enzymes that modify p53 at specific amino acid residues capable of transmitting a specific cellular response according to the type of stress. The transmittance of the signal is dependent upon the post-translational modifications that p53 underwent once activated by specific modulators. These modifications can be phosphorylation on serine/threonine sites mainly in the N-terminus transactivation domain of p53, and acetylation, methylation, sumoylation or ubiquitination on different epsilon amino groups of lysine residues in the C-terminus domain (35). For instance different p53 modulators can modify p53 depending upon the type of DNA damage-inducing agent (Fig. 2). For example, gamma-radiation can induce the activation of ATM and CHK2 kinases, in which both can phosphorylate p53, whereas UV-radiation activates ATR and CHK1 kinases and modify p53 on different sites of phosphorylation. The combination of phosphorylation,

acetylation or other post-translational modifications of p53 will induce specific downstream signaling pathways upon the specific stress acting up on the cell (35).

The accumulation of genomic mutations is the key factor leading to carcinogenesis. The rapid induction of p53 activity in response to genotoxic stress thus serves to ensure that cells carrying such mutations are dealt with in order to avoid tumor progression. Furthermore, p53 also contributes, directly or indirectly, to repair the afflicted DNA (246), hence its nickname "guardian of the genome" (193).

Despite the activation of p53 upon DNA damage, a variety of other non-genotoxic conditions can lead to rapid induction of p53 stability (Fig. 2) (259). Although these conditions represent various types of stress (oxidizing or physical stress), they all have a common factor which is to favor the emergence of cancer-susceptible cells. Such conditions include ribonucleotide depletion (209), hypoxia (185), heat shock (247).

In addition, p53 activity is triggered by oncogenic stress. This response is mediated by a variety of oncogenic proteins, including myc (136), Ras (293), and β-catenin (74) for example, providing a direct link between oncogenic processes and the tumor suppressor action of p53.

Although most stress signals induce p53 protein accumulation, DNA synthesis inhibitors (116) and hypoxia (117,185) impair its transactivation function. Also our lab was the first to show that a particular type of stress inactivates p53 by downregulating its protein levels upon ER stress (263). These data show that despite stresses that induce p53 accumulation, its function is impaired under certain circumstances and that there may be other stresses that promote p53 degradation similar to the ER stress response (Fig.2).

Figure 2. Mediators of p53 core regulation.

Diverse stress signals (DNA damage, oncogene activation, etc.) that activate p53 contribute to the regulation of the central core by inducing the tumor suppressor activity of the p53 protein by activating a wide range of specific p53 mediators such as kinases, and acetyltransferases or other modifiers. However, some conditions promote p53 degradation such as ER stress. Other stress conditions, such as hypoxia, have remained controversial as to how it regulates p53 activation or degradation.

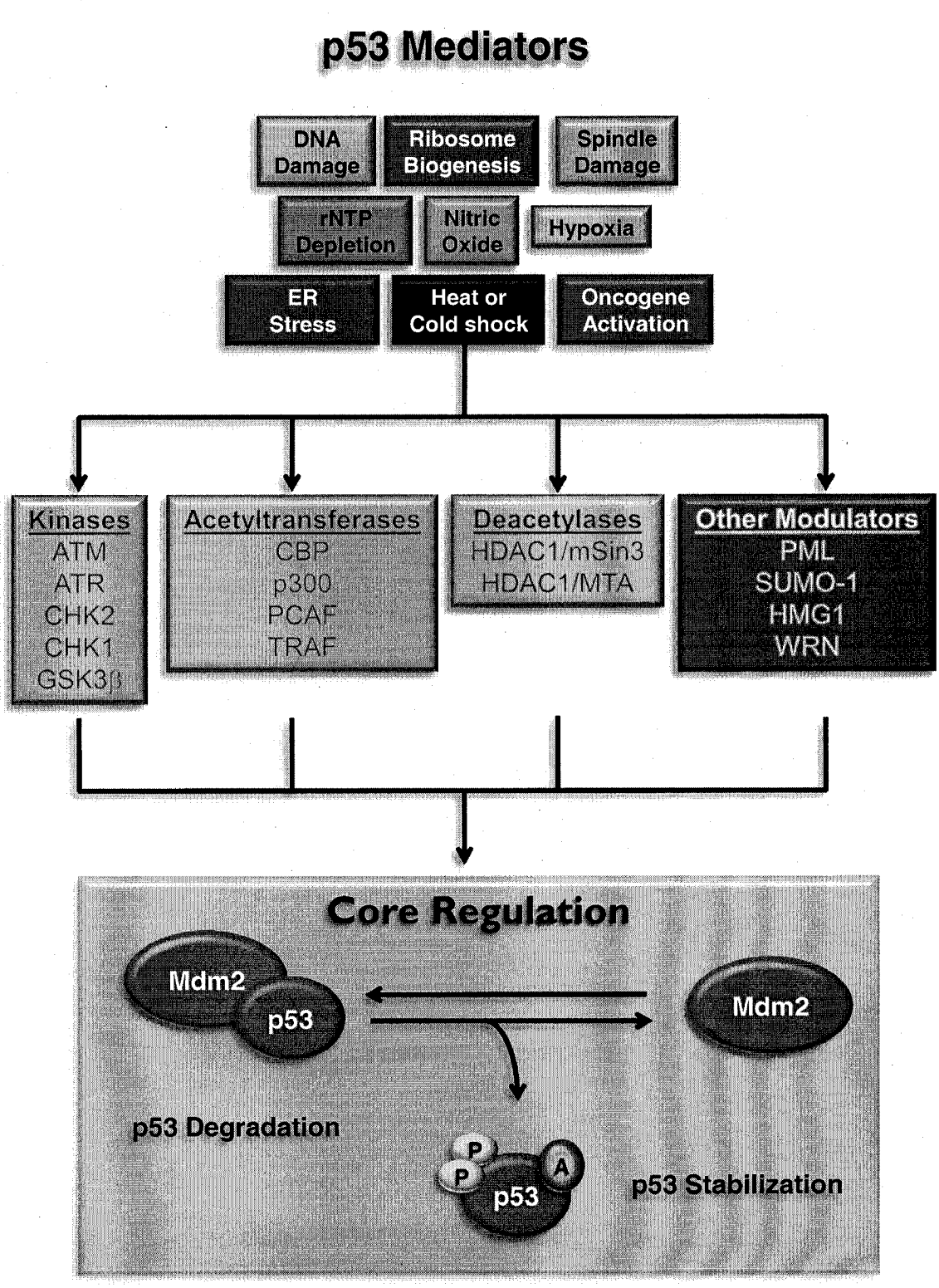
p53 Mediators
DNA Damage
Ribosome Biogenesis
Spindle Damage
rNTP Depletion
Nitric Oxide
Hypoxia
ER Stress
Heat or Cold shock
Oncogene Activation
Kinases
ATM
ATR
CHK2
CHK1
GSK3β
Acetyltransferases
CBP
p300
PCAF
TRAF
Deacetylases
HDAC1/mSin3
HDAC1/MTA
Other Modulators
PML
SUMO-1
HMG1
WRN
Core Regulation
Mdm2
p53
Mdm2
p53 Degradation
P
P
A
p53
p53 Stabilization

Figure 2

1.5 Regulation of p53 Transcriptional Activity

The transcriptional activity of p53 is controlled at the cellular level, its DNA-binding ability, and its subcellular localization. All these mechanisms are dependent on the different post-translational modifications imposed on the p53 protein itself.

1.5.1 Regulation of the Cellular p53 Level

1.5.1.1 p53 Ubiquitination & Degradation

For more than a decade, p53 protein turnover has been shown to be mediated by an ubiquitination-dependent mechanism mediated by the 26S proteasome pathway (55,222). A molecule of ubiquitin is first sequentially transferred through the ubiquitin-activating enzyme (E1), ubiquitin-conjugating enzyme (E2), and the ubiquitin-protein ligase (E3). The E3 ligase also transfers ubiquitin molecules to one or more lysine residues of the target substrate. When multiple ubiquitin molecules are attached to one another they form a polyubiquitin chain. This chain is sufficient to target the substrate protein for destruction by the proteasome (58).

One of the first E3 ubiquitin ligases identified to promote p53 degradation was Mdm2 (Fig. 3A) (147,221). It has been shown that Mdm2 can regulate the stability of p53 through the ubiquitin proteolysis pathway (36,133,187). More studies have demonstrated that Mdm2 has intrinsic E3 ligase activity suggesting that it can ubiquitinate p53 and Mdm2 itself (148).

The hydrophobic pocket domain in the N-terminus of Mdm2 binds to the N-terminus of p53. The Mdm2-binding site in p53 has been mapped within residues 19-26

(Fig. 3A) (232). Upon binding to p53, Mdm2 transfers monoubiquitin molecules onto lysine residues located mainly in the C-terminus of p53. Figure 4 shows the various C-terminus lysine residues of p53 modified by Mdm2. This monoubiquitination is sufficient to promote the nuclear export of p53, but not its degradation by the 26S proteasome pathway (204,355). It was recently shown that the histone acetyl transferase (HAT) p300 possesses intrinsic E3 ligase activity and is critical in the addition of polyubiquitin chains to p53 (Fig. 3A) (118,119). However, the mechanism that governs the switch between the HAT and ubiquitin ligase activity of p300 is not known.

Another study suggests that p53 ubiquitination can be reversible by the Herpes virus-associated ubiquitin-specific protease (HAUSP). Not only was HAUSP identified as a p53 binding protein, but it can also bind and stabilize Mdm2 by deubiquitinating it as well (150,203,205). Although HAUSP is not induced by DNA damage, its effect on p53 stability has not been determined yet. This suggests that perhaps other deubiquinating enzymes, such as the USP/UBP family of ubiquitin-specific processing proteases (7), may have a functional significance in regulating p53 activity.

As mentioned earlier, Mdm2 is one of the well known E3 ligases that control p53 stability (36). The identification of several other E3 ligases or proteins has been shown to mediate p53 ubiquitination and degradation. The list includes Pirh2 (200), COP1 (92), CHIP (99), ARF-BP1 (45), Topors (265), and the recently described ER-resident ubiquitin ligase Synoviolin (352). Since most of these E3 ligases have been recently discovered, the regulation and mechanism of activation that mediates p53 degradation still remains elusive. However, it is apparent that more E3 ligases remain to be discovered and that the cell utilizes different ubiquitin ligases to degrade p53 upon

specific types of stress. For example, while Mdm2 degrades p53 in unstressed conditions (Fig. 3A), Synoviolin induces the ubiquitination and degradation of p53 upon ER stress (352). Perhaps the cell has acquired more than one single ubiquitin ligase to compensate for the loss of another.

1.5.1.2 p53 Phosphorylation & Stabilization

Human p53 has 23 phosphorylation/dephosphorylation sites most of which are outside the DNA-binding domain (Fig. 4). These include serines 6, 9, 15, 20, 33, 37, 46, 149, 215, 313, 314, 315, 366, 376, 378, 392, and threonines 18, 55, 150, 155, 377, 378, 387. Most residues are phosphorylated by several different kinases in response to specific stresses that are associated with p53 activation. Several kinases can phosphorylate one specific residue (Ser15 is phosphorylated by 8 different kinases), and one specific kinase can phosphorylate several residues (CHK2 phosphorylates 7 different residues) (Fig. 4). This redundancy amongst different kinases and phosphorylation sites may provide a safety mechanism to allow various stresses to activate p53 (35). Although some residues appear to be phosphorylated by a unique kinase, the phosphorylation patterns imposed upon p53 determines its cellular and biological responses or functions (35).

In contrast, some residues that undergo dephosphorylation appear to activate p53 as well upon ionizing radiation (IR). Such is the case with the dephosphorylation of Ser376 and stabilization of p53 correlating with the binding to 14-3-3 proteins (312). Conversely, not all kinases that phosphorylate p53 can stabilize and activate its transcriptional activity. We previously showed that glycogen synthase kinase 3 beta (GSK3β) can phosphorylate p53 on Ser315/376 (Fig. 4) and induce its degradation upon

ER stress (263). However, other conditions that induce GSK3β kinase function can stabilize and activate p53 after Ser33 phosphorylation (332). This vast and complex pattern of phosphorylation/dephosphorylation is under intense study, and reflects our lack of knowledge that governs the regulation of the biological functions of p53.

1.5.1.3 p53-Mdm2 Interaction

The p53-Mdm2 interaction can be disrupted upon certain specific phosphorylated serine and threonine residues in the N-terminus of p53 (Fig. 3B) (35,341,349). The conformation of p53 is believed to be hindered once phosphorylated thereby preventing the binding of Mdm2 and thus promoting the buildup of p53 protein levels (Fig. 3B). In response to DNA damage (IR or UV irradiation), Ser15/20/37 and Thr18 are phosphorylated by either ATM (155), ATR (328) or CHK1/CHK2 (300) (Fig. 4). More so, the tetramerization of p53 is required for its N-terminus phosphorylation (301) and subsequent transactivation (Fig. 3D, 5).

The phosphorylation of Ser15 and Ser20 alone does not impede the binding of Mdm2 whereas the phosphorylation on Thr18 does. However, since p53 undergoes sequential phosphorylation, Ser15/20 phosphorylation is required first before inducing Thr18 phosphorylation in order to inhibit Mdm2 binding. Despite the well studied IR and UV pathways leading to p53 stabilization (Fig. 5), there is a plethora of phosphorylation cascades catalyzed by specific kinases which differentially regulate p53 (35) (Fig. 4).

Since p53 ubiquitination occurs within its C-terminus lysine residues (Fig. 4), any other modification on these residues would then hinder p53-Mdm2 interaction. The p300/CBP histone acetyltransferase acetylates Lys372/373/381/382 of p53 upon DNA

damage thereby promoting its accumulation by competing with Mdm2-mediated ubiquitination of these same residues (Fig. 3C and Fig. 4) (212,282). These studies suggest that the N-terminus phosphorylation of p53 is required to promote C-terminus acetylation in order to stabilize and activate the transcriptional activity of p53 (Fig. 5). However a recent study demonstrated that by mutating six C-terminus lysine residues of endogenous mouse p53, the stabilization of p53 appeared normal before or after DNA damage (101). This indicates that ubiquitination of these lysine residues is not required for efficient p53 degradation. However the transcriptional activity of this mutant form of p53 was affected suggesting that the C-terminus post-translational modifications may contribute to the outcome of the p53 response rather to its stability. This matter still remains debatable and would require much more insight before generalizing such a statement.

1.5.2 Regulation of p53 DNA-binding Activity

1.5.2.1 Acetylation/Deacetylation

The p300/CBP proteins mediate histone acetylation and function as co-activators for many transcription factors (43), including p53 (121). About a decade ago, p300/CBP was shown to also acetylate the C-terminus of p53, and promote its ability to bind DNA (Fig. 3C) (120,282). This increase in the DNA-binding function of p53 mediated by acetylation was later shown to enhance its transcriptional activity on selected target genes (216). However, when several acetylation sites were mutated in the C-terminus of p53, the mutant p53 was able to bind to the *p21* promoter to the same extent as the wild type p53 protein using a ChIP assay (16). This study demonstrated that p53 acetylation may

not favor its DNA-binding ability but rather to promote co-activator recruitment and histone acetylation in order to induce its transcriptional activity on selected target genes. Although the enhancement of DNA-binding of p53 by acetylation remains controversial, these data suggest that C-terminus acetylation modifies or induces conformational changes in the structure of p53 in order to activate its transcriptional activity.

Although p300/CBP acetylates lysines on p53 associated with Mdm2-mediated ubiquitination (Lys 372/373/381/382), the E4F1 ubiquitin ligase has recently been shown to ubiquitinate Lys320 (Fig. 4). This lysine residue is a distinct site than those targeted by Mdm2 and competes with the acetylation induced by PCAF on p53 (196). In contrast to Mdm2-dependent ubiquitination, E4F1 does not promote p53 degradation but instead it inhibits cell growth by arresting the cell cycle. However, this response does not induce pro-apoptotic target genes, as seen with the acetylation of Lys320 by PCAF (282,324). It appears that most acetylation that occurs on p53 has a positive effect on its transcriptional activity regardless the controversy surrounding the effect on its DNA-binding activity. Although p300/CBP stabilizes p53 by competing with the ubiquitination of Mdm2, E4F1-mediated ubiquitination has no effect on the lysine residues recognized by p300/CBP (196).

It was previously discovered that histone deacetylases (HDAC) downregulate the transcriptional activity of p53 (167). HDACs deacetylate lysine residues on p53 similar to those that are acetylated by p300/CBP. However, p53 and HDACs do not directly interact to promote deacetylation. This is mediated by another protein called metastasis-associated protein 2 (MTA2) which is a component of the NuRD ATP-dependent chromatin remodeling and histone deacetylase complex (357). MTA2 likely

recruits HDACs to p53 in order to reduce the acetylation levels of p53 (218). Other studies have shown that the Sin3a co-repressor recruits HDACs to p53 as well and inhibits its apoptotic function (238). Subsequent work has also identified that Sir2α, a NAD-dependent histone deacetylase, can physically bind and attenuate p53 function through deacetylation and repress its transcriptional activity upon DNA damage (217).

Other lysine covalent modifications on p53 have been described such as sumoylation (289,290) and methylation (57), both of which stabilize and induce p53 transcriptional activity (Fig. 4). In contrast, Mdm2-mediated neddylation (348) seems to inhibit its transactivation. The mechanisms by which these modifications affect p53 activity remains to be determined and the modified residues are briefly described in Figure 4.

Thus it appears that acetylation stabilizes p53 upon DNA damage and that the acetylated p53 is inactivated by deacetylation once the genomic damage has been repaired. These data suggest that a single post-translational modification does not determine the fate or function of p53, and that multiple covalent modifications encode for specific p53 biological outcomes. This "p53-code" would provide new insight as to how p53 chooses between the cell cycle or apoptotic transcriptional program.

1.5.2.2 Phosphorylation

Although the phosphorylation effect of p53 on its DNA-binding activity remains unclear (101), p53 phosphorylation can recruit the interaction of certain proteins such as Pin1, a peptidyl-prolyl isomerase which regulates the function of many proteins involved in cell cycle control and apoptosis (362). Upon DNA damage, p53 interacts with Pin1 and

is strictly dependent on p53 phosphorylation. Serine 33, Thr81 and Ser315 are required for this interaction (362). Proline 82 of the polyproline region of p53 was identified to be essential for its interaction with Chk2 and consequent phosphorylation of p53 on serine 20, following DNA damage. These physical and functional interactions are regulated by Pin1 through cis-trans isomerization of proline 82 (24).

It was previously shown that the p53 protein lacking the polyproline region has impaired apoptotic activity and altered specificity for certain apoptotic target genes (25). Also, p53 lacking the polyproline region was identified to be more susceptible to ubiquitination, nuclear export, and Mdm2-mediated degradation (25). These studies explain how Pin1 protects p53 from Mdm2-mediated proteasome degradation. Upon binding, Pin1 generates conformational changes in p53, enhancing its transactivation activity and impairing its association with Mdm2.

These are the first studies that provide a novel mechanism to the regulation of p53 DNA-binding activity in which p53 phosphorylation indirectly controls its cellular response upon DNA damage.

1.5.3 Regulation of p53 Localization

The activation and cellular functions of p53 are dependent on its localization. In unstressed cells, p53 is translated and localizes in the nucleus via its nuclear localization signal (NLS) (207,296). Nuclear p53 binds to and is ubiquitinated by Mdm2 thereby promoting its nuclear export and degradation (Fig. 5). The translation, nuclear translocation and degradation of p53 are dynamic processes that normal cells utilize to

maintain p53 levels relatively low. Any disturbance in this dynamic process would result in the stabilization and accumulation of p53 in the nucleus.

Recently the Parkin-like ubiquitin ligase, Parc has been shown to physically interact with p53 (242). Parc and p53 form a large cytoplasmic complex in unstressed cells and sequesters p53 in the cytoplasm and inhibits its apoptotic function (242). Our lab has shown that GSK3β binds and phosphorylates p53 on Ser315/376 in the nucleus, and enhances its cytoplasmic localization and degradation in cooperation with Mdm2 upon ER stress (Fig. 5) (260,263).

Another study demonstrated the role of HECT domain E3 ligase, WWP1, in regulating p53 localization and activity. WWP1 associates with p53 and induces p53 ubiquitination. Unlike other E3 ligases, WWP1 increased p53 stability in the cytoplasm with a concomitant decrease in its transcriptional activities. Although WWP1 limits p53 activity, p53 reduces the expression of WWP1, indicating a possible negative feedback loop mechanism. This finding identifies the first instance where an ubiquitin ligase stabilizes p53 while inactivating its transcriptional activities (192).

In conclusion, all the current p53 research suggests that a specific stress activates a different pool of p53 which in turn regulates a subset of target genes. All the different stresses employ various signaling pathways that differentially regulate the transcriptional activity of p53 in order to achieve a particular biological outcome. The enormous challenge that remains is to fully understand the dynamic processes that regulate or integrate these pathways together.

Figure 3. Regulation of p53 transcriptional activity.

(A) The transcriptional activity of p53 is regulated by the stability of the protein. In unstressed cells p53 is targeted for degradation by Mdm2-mediated ubiquitination. The p300 acetyltransferase has been shown to promote ubiquitin (U) chain additions to the Mdm2-directed mono-ubiquitinated p53 molecules.

(B, C, D) In stressed cells, p53 undergoes post-translational modifications such as phosphorylation (P), acetylation (A) thus promoting its stabilization, and its DNA-binding activity by tetramerization in order to induce its transcriptional activity.

Regulation of p53 Transcriptional Activity

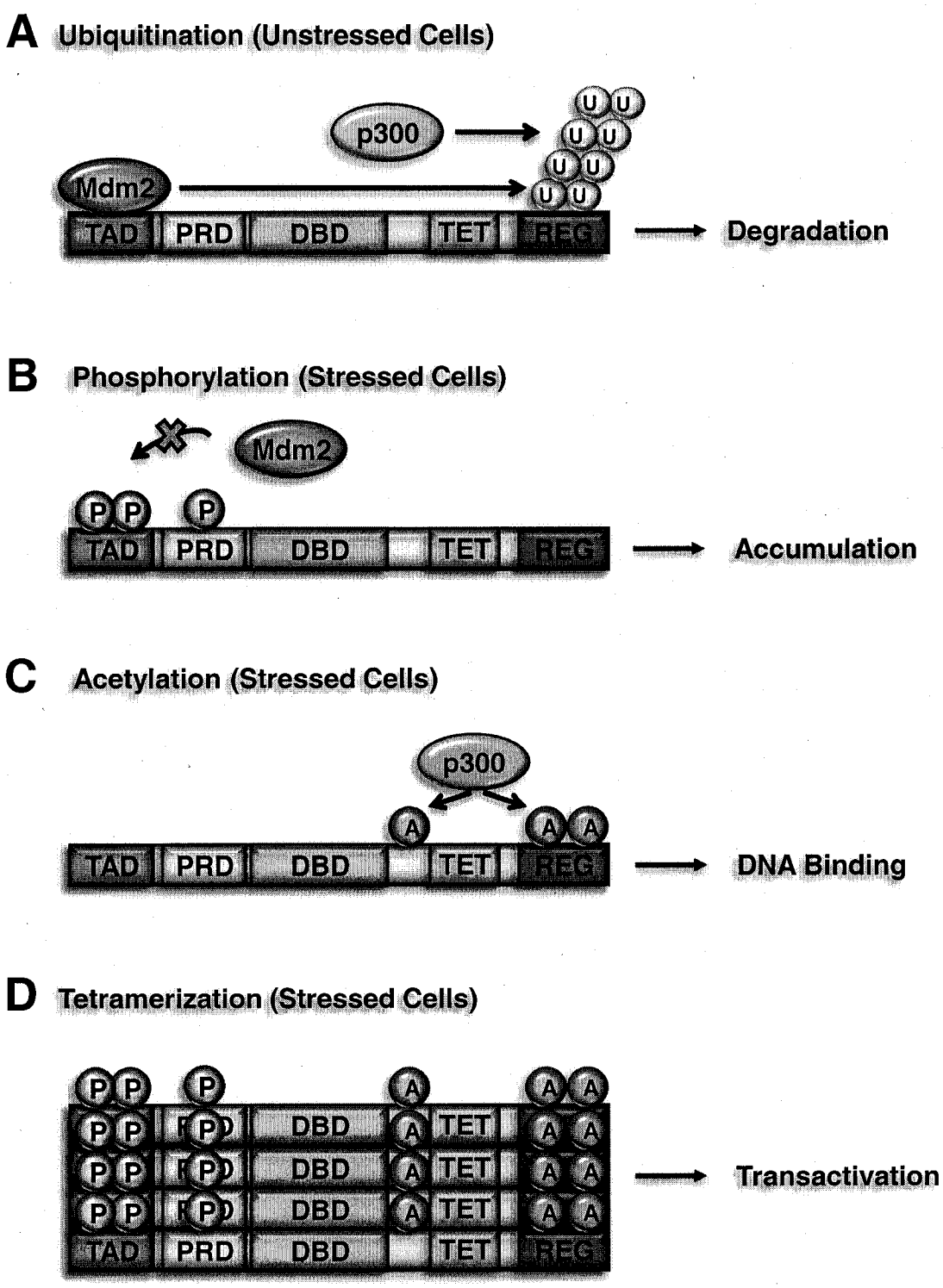

Figure 3

Figure 4. Post-translational modification of p53.

The p53 protein consists of several different domains (TAD: transactivation domain; PRD: proline-rich domain; DBD: DNA-binding domain; TET: tetramerization domain; REG: regulatory domain) that are post-translationally modified by phosphorylation (P), acetylation (A), ubiquitination (U), neddylation (N), methylation (M) and sumoylation (S). Residues for each of these modifications are indicated, including the kinases, acetyltransferases or E3 ligases responsible for specific modifications that have been previously described.

Figure 4

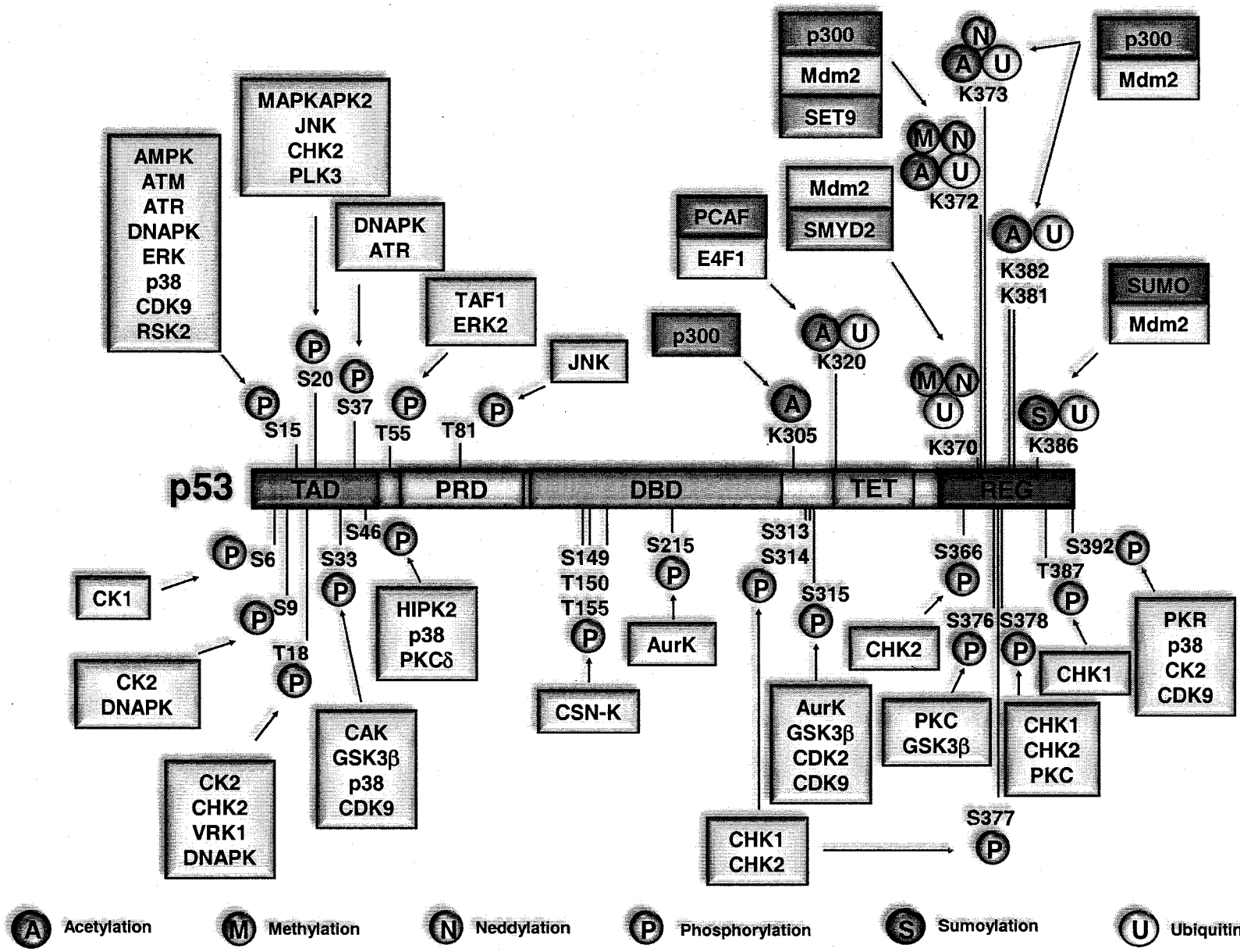
p53
TAD
PRD
DBD
TET
REG
AMPK
ATM
ATR
DNAPK
ERK
p38
CDK9
RSK2
MAPKAPK2
JNK
CHK2
PLK3
DNAPK
ATR
TAF1
ERK2
JNK
p300
PCAF
E4F1
p300
Mdm2
SET9
Mdm2
SMYD2
p300
Mdm2
SUMO
Mdm2
S15
S20
S37
T55
T81
K305
K320
K370
K372
K373
K381
K382
K386
S6
S9
T18
S33
S46
S149
T150
T155
S215
S313
S314
S315
S366
S376
S378
T387
S392
CK1
CK2
DNAPK
HIPK2
p38
PKCδ
CAK
GSK3β
p38
CDK9
CK2
CHK2
VRK1
DNAPK
CSN-K
AurK
AurK
GSK3β
CDK2
CDK9
CHK2
PKC
GSK3β
CHK1
CHK2
PKC
CHK1
PKR
p38
CK2
CDK9
CHK1
CHK2
S377
Acetylation
Methylation
Neddylation
Phosphorylation
Sumoylation
Ubiquitination

Figure 5. Regulation of p53-Mdm2 interaction.

In unstressed cells, p53 is kept inactive and at low levels by the action of Mdm2, which inhibits p53 by quenching its transcriptional activity, and through its ubiquitin-ligase activity to promote p53 degradation by the proteasome pathway. After various cellular stresses, stress-induced kinases phosphorylate p53 on several serine and threonine residues in the transactivation domain (TAD) thus reducing the binding of Mdm2. This leads to p53 accumulation, to form tetramers thus masking the nuclear export signal, so that stabilized p53 remains in the nucleus. The phosphorylation of the p53 TAD promotes the interaction with acetyltransferases such as p300. This leads to the acetylation of lysine residues in the p53 regulatory domain to promote p53 stabilization, and increase specific DNA binding at p53 target genes. Although accumulated p53 is located in the nucleus, some studies suggest that following stress, a pool of the p53 molecules remain in the cytoplasm to promote apoptosis by inhibiting the anti-apoptotic Bcl-2 or Bcl-xL proteins. The apoptotic response is also mediated by the pro-apoptotic proteins Bax, Bak, and PUMA. In contrast, since most stress conditions stabilize p53, we have previously shown that ER stress promotes the degradation of p53. These p53 molecules are targeted for degradation in the cytoplasm by phosphorylation of p53 on Ser315/376 mediated by the activation of GSK3β and the cooperative action of Mdm2.

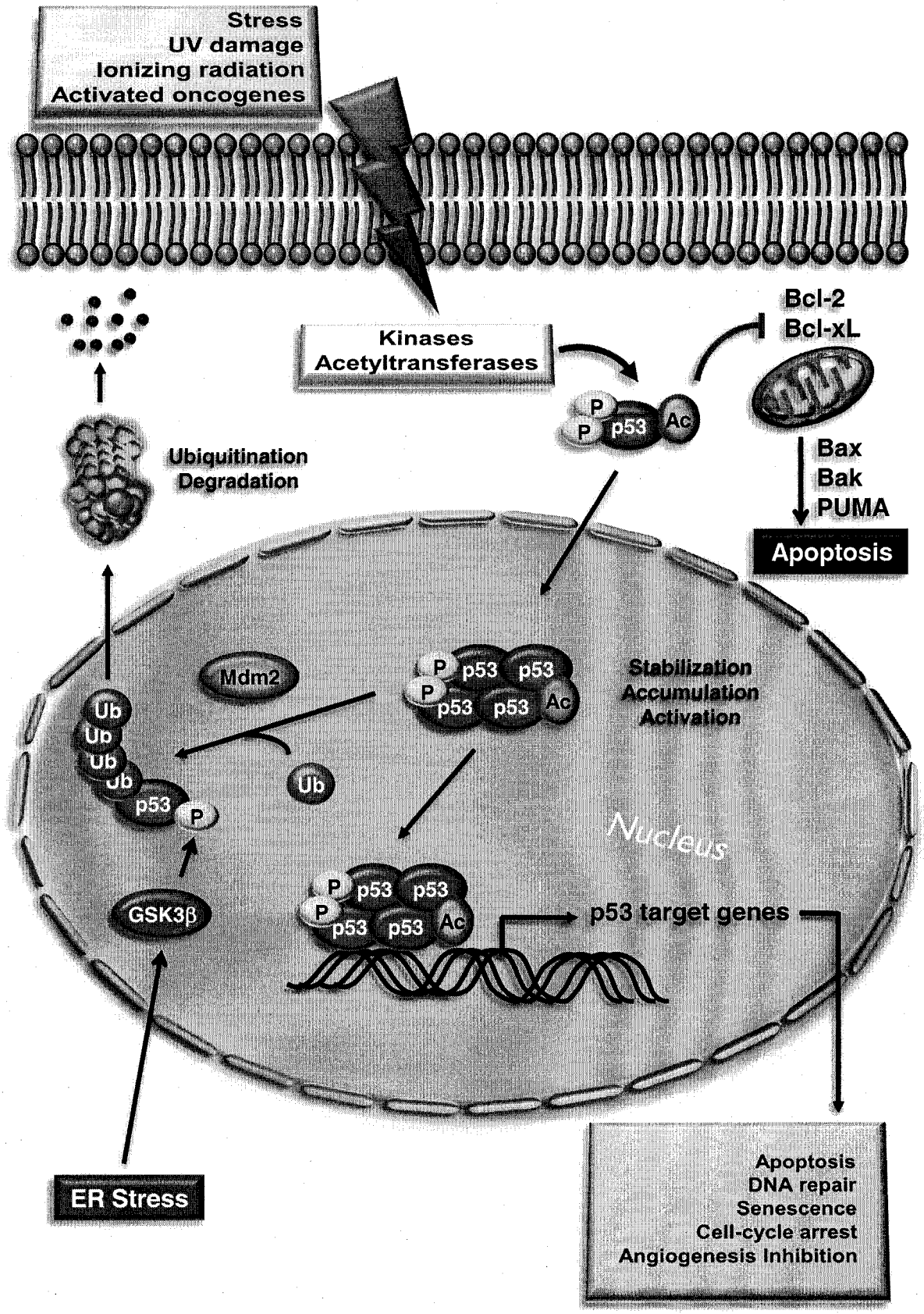
Stress
UV damage
Ionizing radiation
Activated oncogenes
Kinases
Acetyltransferases
Bcl-2
Bcl-xL
Bax
Bak
PUMA
Apoptosis
Ubiquitination
Degradation
Mdm2
Ub
p53
P
Ac
Stabilization
Accumulation
Activation
Nucleus
GSK3β
p53 target genes
ER Stress
Apoptosis
DNA repair
Senescence
Cell-cycle arrest
Angiogenesis Inhibition

Figure 5

1.6 Functions of p53

Since the demonstration of the DNA-binding activity of p53, intense p53-regulated gene expression patterns have been analyzed using the help of DNA microarray methods. The nature of the p53 response depends on the type of inducing agent, p53 protein levels, cell type, and the length of treatment (366). The p53-regulated genes fall into either induced or repressed gene clusters that have different cellular functions. These include cell cycle arrest, DNA repair, apoptosis, and feedback regulation just to name a few. Selected activated target genes will be discussed below and are summarized in Figure 6.

1.6.1 Downstream Targets of p53

Upon activation of p53 in response to stress signals, it binds to p53-responsive DNA sequence elements in the genome in order to transcribe target genes. The function of the p53-regulated genes falls into several categories (Fig. 6). The first are involved in G1/S or G2/M phase cell cycle arrest such as p21 (96), 14-3-3σ (137), Cdc25C (310), and GADD45 (303) in conjunction with DNA repair genes (p21, GADD45, p48 XPE) (304). The second set of genes is involved in apoptosis which in itself comprises the intrinsic and extrinsic apoptotic pathways (132). For the extrinsic pathway, genes such as Fas, KILLER/DR5 have been described, whereas Bax, PUMA, and Noxa comprise the intrinsic apoptotic pathway. Several p53-regulated genes such as Perp, Scotin, PIG3, and p53-AIP have been shown to enhance the apoptotic function of p53, but their mechanism of action remains unresolved (Fig. 6) (132).

Although the regulation and activation of apoptosis by p53 is still unclear, several groups have shown that p53 itself can localize to the mitochondria and promote apoptosis through the release of cytochrome c. This is partially mediated by the interaction of p53 with Bcl-2, Bcl-xL or Bax (53,233) and the involvement of PUMA (Fig. 5) (52).

Finally, the cell needs to assess whether its DNA has been repaired and re-enter the cell cycle or to reinforce the p53 response. For this, another set of p53-regulated genes initiate a positive or negative feedback loop that affect p53 and its core regulator of that specific pathway. These genes include the negative modulators such as Mdm2, Pirh2, COP1, WIP-1, SIAH-1, Cyclin G, and the positive modulator PTEN (Fig. 6) (132).

More and more p53-regulated genes are being discovered every year although their function or mechanisms of action are not fully elucidated. However, the discovery of new target genes emphasizes new p53 functions never before seen or thought. For instance, three new p53-regulated genes have recently been discovered and reveal new roles of p53 in glucose metabolism and autophagy (Fig. 6). The DRAM protein is regulated by p53 and may participate in the fusion of autophagosomes with lysozomes during autophagy (70). The pathways regulating glucose metabolism and mitochondrial respiration are regulated by p53-target gene products, TIGAR (23) and SCO2 (227). TIGAR blocks glycolysis, whereas SCO2 enhances oxygen consumption and mitochondrial respiration. Since all these pathways are regulated by metabolism, the data suggest that p53 may link all three metabolic pathways to ensure cell survival.

The identification of novel p53-target genes will help clarify some of the biological effects, cellular processes and phenotypes observed by the activation of p53.

However the regulation of the p53-gene expression profiles will have to be investigated further in order to understand these outcomes and find ways to control them regarding cancer therapy and drug treatment of patients.

1.7 p53 and Translational Control

Several reports have suggested that translational control may contribute to p53 regulation. The p53 protein was suggested to negatively regulate its own translation by direct binding to its 5'UTR stem-loop structure (235). A translation suppressor element was also reported in the 3'UTR of the *p53* mRNA (105). A recent study revealed that in response to DNA damage, the ribosomal protein L26 (RPL26) and nucleolin were found to bind to *p53* mRNA in cells and to compete with each other to regulate p53 synthesis through binding to the 5'UTR of *p53* mRNA (319). Also, two independent studies identified an Internal Ribosomal Entry Site (IRES) in the 5'UTR of the *p53* mRNA (268,354). They showed that p53 synthesis can be induced when cells are exposed to etoposide through a cap-independent translational mechanism mediated by IRES activity (354).

Recently, it was reported that dsRNA downregulates p53 in a PKR/translational-dependent manner (226), and that lack of p53 sensitizes cells to dsRNA-dependent apoptosis. Despite suggestions that translational control of p53 might be important, the extent and mechanism of p53 translational regulation has remained unclear.

Figure 6. Downstream targets of p53.

A variety of p53 target genes have been identified and play roles in the various cellular responses mediated by p53, such as DNA repair, cell cycle arrest, apoptosis, negative or positive feedback regulation, glucose metabolism, and autophagy. Each of these genes has been shown to contain p53 binding sites within its regulatory regions.

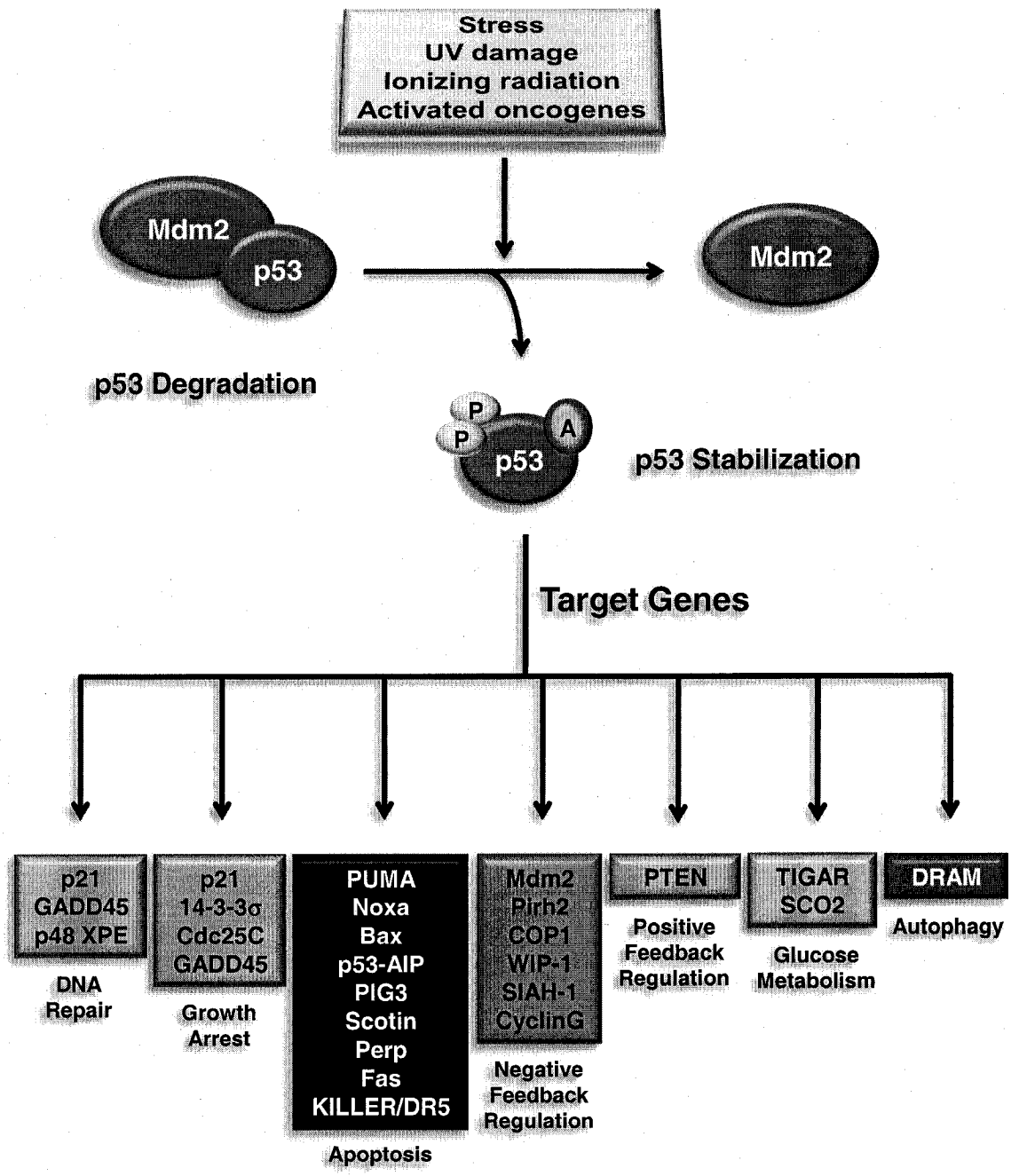
Stress
UV damage
Ionizing radiation
Activated oncogenes
Mdm2
p53
Mdm2
p53 Degradation
P
P
A
p53
p53 Stabilization
Target Genes
p21
GADD45
p48 XPE
DNA
Repair
p21
14-3-3σ
Cdc25C
GADD45
Growth
Arrest
PUMA
Noxa
Bax
p53-AIP
PIG3
Scotin
Perp
Fas
KILLER/DR5
Apoptosis
Mdm2
Pirh2
COP1
WIP-1
SIAH-1
CyclinG
Negative
Feedback
Regulation
PTEN
Positive
Feedback
Regulation
TIGAR
SCO2
Glucose
Metabolism
DRAM
Autophagy

Figure 6

2. TRANSLATIONAL CONTROL

2.1 REGULATION OF TRANSLATION

The regulation of gene expression at the translational level plays an important role in cell growth, proliferation, and development (343). Translation is controlled by many mechanisms notably at the level of initiation, elongation and termination (229). However, most of the regulation is modulated at the level of initiation. This step is crucial for the initiation codon to be recruited along with the ribosome onto an mRNA. Many initiation factors (eIFs) are involved in this recruitment process. The mammalian initiation steps consist first of the formation of the ternary complex (TC) composed of eIF2-GTP-$tRNA_{Met}$. Then, the TC binds to the 40S small ribosomal subunit facilitated by the initiation factors eIF1, eIF1A, and eIF3, forming the 43S pre-initiation complex. The eIF4F complex composed of eIF4A, eIF4G, and eIF4E binds to the 7-methylguanosine cap structure located on the 5'end of the mRNA and facilitates the loading of the 43S complex. The latter complex then scans along the mRNA, 5' to 3', in order to recognize the initiator AUG start codon. Once the start codon has been identified, the hydrolysis of GTP of eIF2 occurs promoted by eIF5, thus generating an eIF2-GDP complex in which it dissociates from the TC leaving behind the $tRNA_{Met}$ in the P-site of the 40S ribosomal subunit. The 60S ribosomal subunit then joins the 40S subunit via eIF5B, yielding an 80S initiation complex (IC) waiting for the next aminoacyl-tRNA to be delivered in the A-site of the IC in order to begin elongation (229).

In order to recycle to its active form and initiate another round of translation, eIF2-GDP must be converted to eIF2-GTP through the catalyzed reaction by eIF2B. The

hydrolysis of GTP to GDP as well as the recycling of eIF2 is tightly controlled by the phosphorylation of the alpha (α) subunit of eIF2, which prevents eIF2 recycling, thereby inhibiting translational initiation and protein synthesis (Fig. 7A) (229).

Although most mRNAs are inhibited by eIF2α phosphorylation, translation of several mRNAs is enhanced by this stress response. Such is the case for the yeast *GCN4* mRNA (87), and the *ATF3* (122), *ATF4* (215), and *CAT-1* (351) mRNAs in mammalian cells. In non-stressed cells, translation of these mRNAs is inhibited by upstream open reading frames (ORFs) in which ribosomes are stalled prematurely (110). This restricts the re-initiation and scanning of other ribosomes attempting to bind to the ORFs and thus preventing the translation of these mRNAs. When eIF2α is phosphorylated and limits the number of active 43S ribosomal complexes, only then can re-initiation occur and promote mRNA translation (110) (Fig. 7B).

Phosphorylation of the α subunit on serine 51 by certain specific eIF2α protein kinase family members (see section 2.2) results in the inhibition of the initiation of mRNA translation (173). The phosphorylated form of eIF2 functions as a dominant inhibitor of the guanine exchange factor eIF2B, and prevents the recycling of eIF2 between consecutive rounds of translation initiation (Fig. 7A) (317). Phosphorylation of eIF2α is induced by many physiological conditions including virus infection, heat shock, iron deficiency, amino acid or glucose deprivation, changes in intracellular calcium, and the accumulation of unfolded proteins in the endoplasmic reticulum (ER) (60).

Figure 7. Regulation of translation.

(A) eIF2 is a general translational initiation factor composed of three subunits (α, β, and γ) that forms two types of complexes: active eIF2-GTP and inactive eIF2-GDP. eIF2-GTP binds Met-tRNA$_i$ to form a ternary complex that is required for binding to the 40S ribosomal subunit and mRNA in order to initiate translation. Subsequently, upon joining of the 60S ribosomal subunit, GTP from eIF2-GTP is hydrolyzed to GDP. In order to recycle to its active form and initiate another round of translation, eIF2-GDP must be converted to eIF2-GTP through the catalyzed reaction by eIF2B. The recycling of eIF2 is inhibited by phosphorylation on Ser51 of its α subunit carried out by eIF2α kinases. Phosphorylated-eIF2-GDP has higher affinity for eIF2B than eIF2-GDP thereby preventing the GDP-GTP exchange activity of eIF2B thus inhibiting protein synthesis. **(B)** However, several specific mRNAs (*GCN4, ATF4, ATF3, CAT-1*) contain upstream open reading frames (uORF) that help bypass translational inhibition. The mechanism of GCN4 translation will only be discussed in this figure. Under unstressed conditions that result in high eIF2-GTP, translation re-initiation occurs more frequently after each uORF. As a result, re-initiation at the *GCN4* ORF (blue) becomes infrequent. Under stressed conditions that induce eIF2α phosphorylation and low levels of eIF2-GTP, re-initiation occurs less frequently at the uORFs. This increases the probability of the 40S ribosomal subunit to scan longer and read-through the uORFs, and subsequently initiate translation on the AUG initiation codon of the downstream ORF.

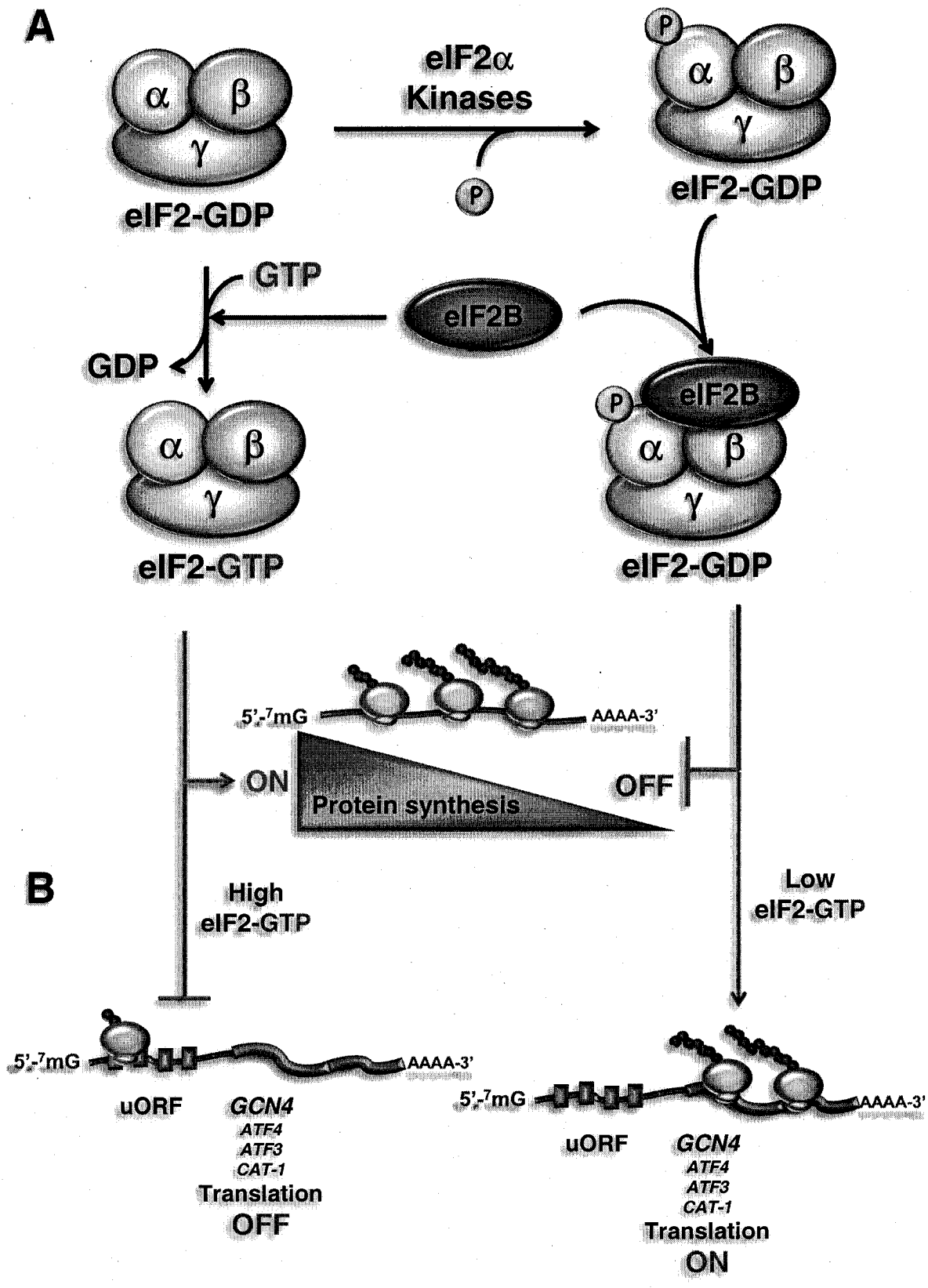
A
eIF2α
Kinases
P
eIF2-GDP
eIF2-GDP
GTP
GDP
eIF2B
eIF2B
P
eIF2-GTP
eIF2-GDP
5'-7mG
AAAA-3'
ON
Protein synthesis
OFF
B
High
eIF2-GTP
Low
eIF2-GTP
5'-7mG
AAAA-3'
uORF
GCN4
ATF4
ATF3
CAT-1
Translation
OFF
5'-7mG
AAAA-3'
uORF
GCN4
ATF4
ATF3
CAT-1
Translation
ON

Figure 7

2.2 The eIF2α Kinases

Phosphorylation of eIF2α is induced by several kinases including PKR (172), PERK (273), GCN2 (27) and HRI (47). Each kinase is activated upon a specific type of stress that generates different biological outcomes in order to cope with that specific stress response (Fig. 8). Each kinase is described below with emphasis on PERK and PKR.

2.2.1 HRI

HRI (heme-regulated eIF2α kinase) is expressed predominantly in erythroid cells and is regulated by heme, the prosthetic group of hemoglobin (46). HRI contains two heme-binding domains located in the N-terminus and the kinase insertion domains (264). The N-terminus domain is always stably bound to heme (44). In contrast, heme reversibly binds to the kinase insertion domain and inhibits HRI kinase activity (48). Consequently, HRI activity is dependent according to intracellular heme concentrations (Fig. 9A). It was previously documented that protein synthesis in reticulocyte lysates is dependent upon the availability of heme (48). Upon heme deficiency, inhibition of protein synthesis correlates with the activation of HRI and eIF2α phosphorylation (47). Small amounts of *HRI* mRNA are also found in non-erythroid tissues but no evidence of HRI protein expression has been reported (26). On the other hand, recent studies have implicated HRI in response to heat shock, osmotic and oxidative stresses (214).

2.2.2 GCN2

GCN2 was first cloned and identified in yeast (87). GCN2 functions in the coordinate regulation of genes involved in amino acid biosynthesis (139). Regulation of GCN2 kinase activity is mediated by homologous sequences to histidyl-tRNA synthetases (HisRS). During amino acid starvation, uncharged tRNAs accumulate and bind to the HisRS-related domain and stimulate GCN2-mediated phosphorylation of eIF2α. Phosphorylation of eIF2α leads to increased translational expression of GCN4, a transcriptional activator of genes involved in amino acid biosynthesis (Fig. 9B) (140).

Amino acid starvation has also been reported to control translation initiation in higher eukaryotes. Identification and characterization of GCN2 orthologs have been shown in many species from Drosophila, mice and humans (27). All GCN2 orthologs contain the HisRS-related sequences juxtaposed to the kinase domain. Expression of mammalian GCN2 proteins functionally complement GCN2 in the *gcn2*Δ yeast, and are able to phosphorylate eIF2α (86). This suggests that the mechanism of phosphorylation of eIF2α in response to nutrient deprivation is conserved from yeast to mammals.

Figure 8. The eIF2α kinase family.

Four eIF2α kinase family members have been identified to date (HRI, GCN2, PERK, and PKR). Although the signaling pathways converge in the phosphorylation of eIF2α and inhibition of protein synthesis, each kinase is activated upon specific conditions. HRI is activated upon heme deficiency, PKR is activated in response to virus infection and dsRNA, PERK activity is induced upon ER stress, whereas GCN2 kinases are activated during amino acid starvation.

The eIF2α Kinase Family

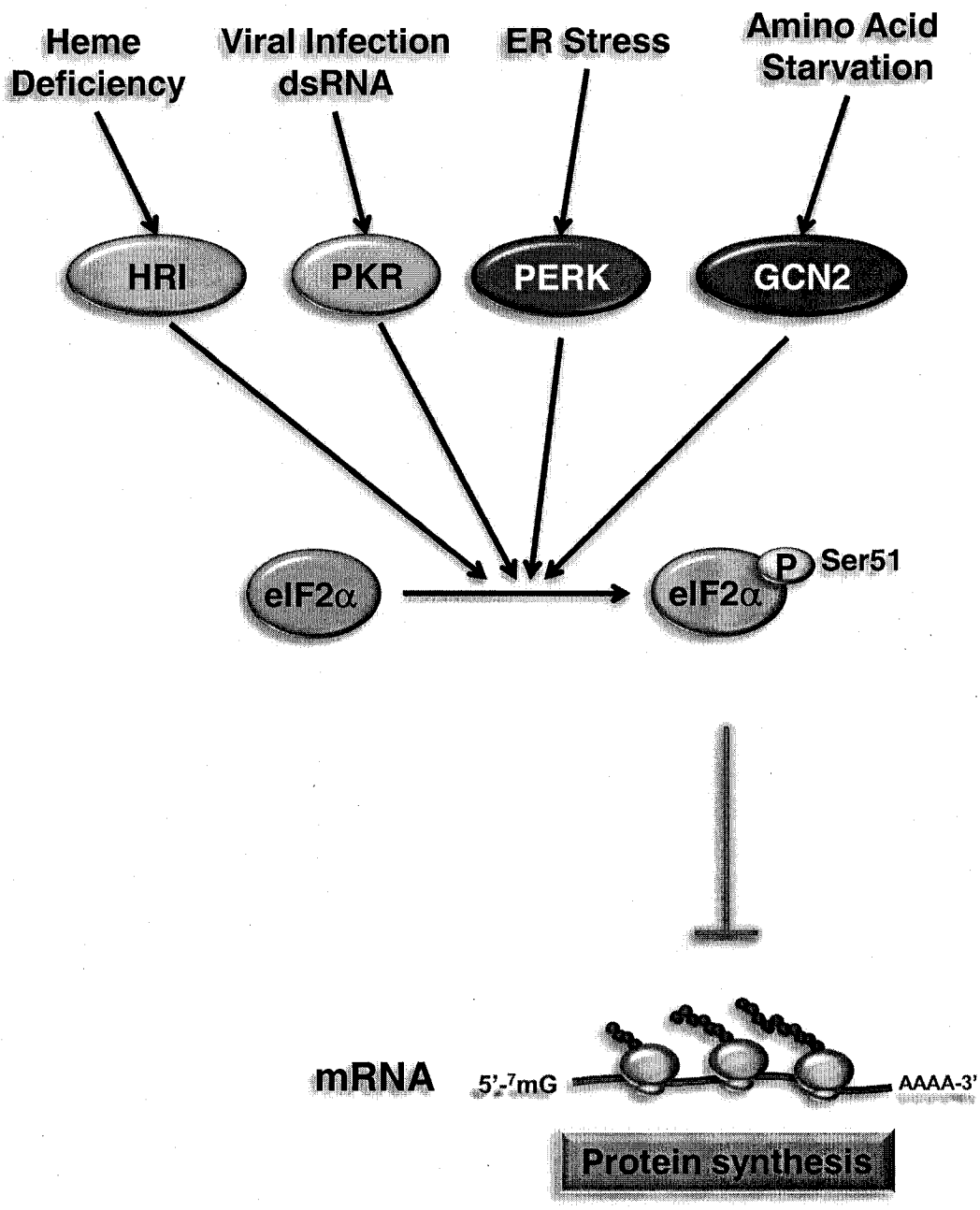

Figure 8

Figure 9. Translational control by HRI & GCN2.

(A) HRI is regulated by heme through the two heme-binding domains in the N-terminus and kinase domain (KD). Heme is constitutively bound to the N-terminus heme-binding domain (HBD), and HRI is kept inactive by heme bound to the HBD in the KD. Upon heme deficiency caused by a depletion of intracellular iron, HRI kinase activity is induced thereby inhibiting translation of *globin* mRNAs by phosphorylating eIF2α.

(B) Amino acid deprivation leads to the accumulation of uncharged tRNAs which in turn are recognized by the histidyl-tRNA synthetase-like domain (HisRS) of GCN2 thereby inducing its dimerization and activation. GCN2 subsequently inhibits protein synthesis by phosphorylating eIF2α except for the increased translation of GCN4, a transcriptional activator of amino acid biosynthesis. *GCN4* mRNA bypasses the negative regulation of eIF2α phosphorylation due to specific regulation in the 5'UTR containing upstream open reading frames (uORF).

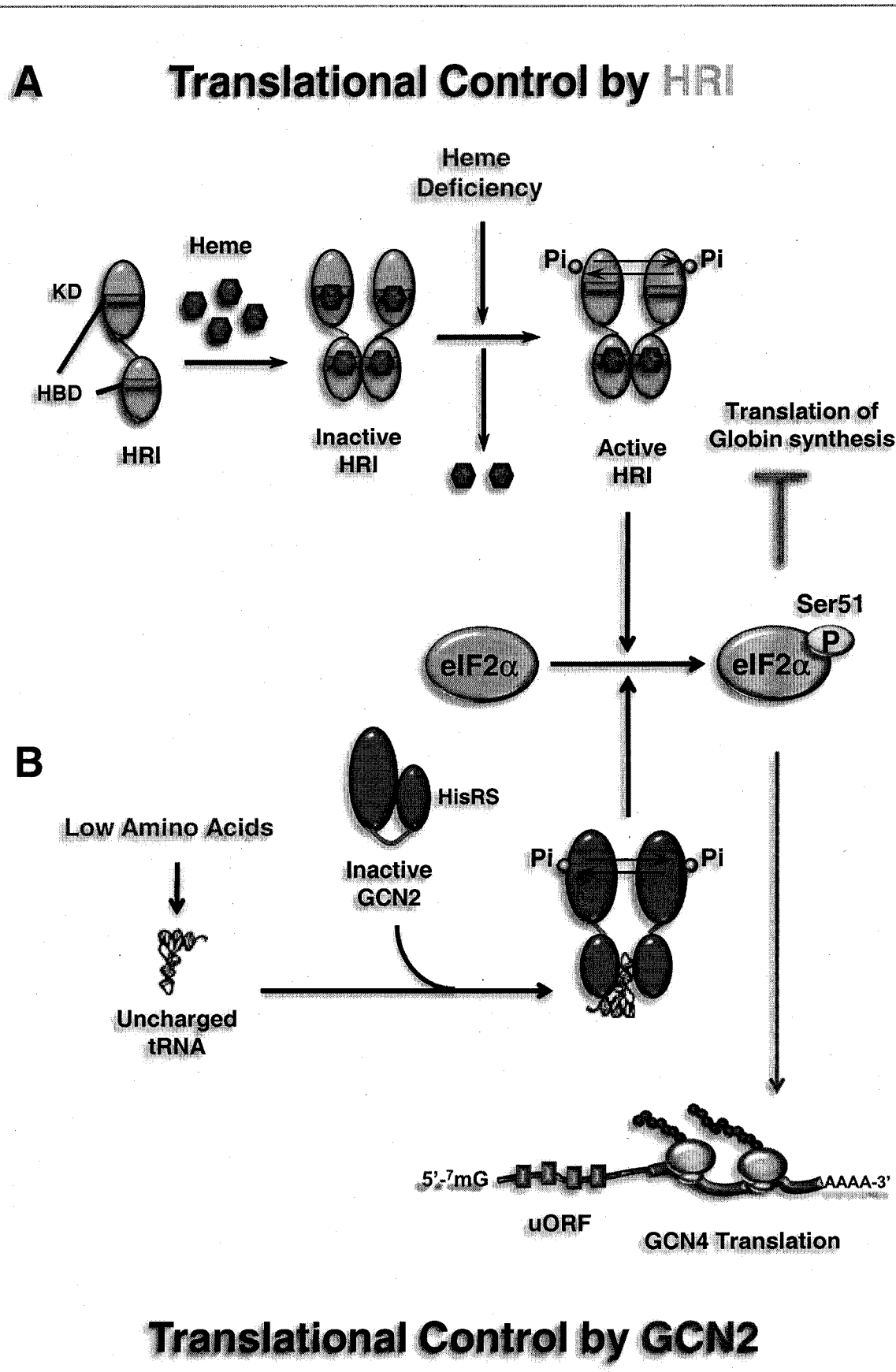
A
Translational Control by HRI
Heme
Deficiency
Heme
KD
HBD
HRI
Inactive
HRI
Pi
Pi
Active
HRI
Translation of
Globin synthesis
Ser51
eIF2α
eIF2α
P
B
Low Amino Acids
HisRS
Inactive
GCN2
Pi
Pi
Uncharged
tRNA
5'-7mG
AAAA-3'
uORF
GCN4 Translation
Translational Control by GCN2

Figure 9

2.2.3 PERK

2.2.3.1 Structure of PERK

The most recently identified eIF2α kinase member is the PKR-like endoplasmic reticulum kinase/pancreatic eIF2α kinase (PERK/PEK) (298,299). PERK is localized in the ER membrane via its signal peptide (SP) within amino acids 1-28. It spans the ER membrane due to its transmembrane domain (TM: aa 514-534). The ER-luminal portion of PERK consists of the N-terminus sensor domain (aa 29-513). This domain is homologous to the IRE1 sensor domain (see section 2.2.3.4) and is responsible for interaction with ER-resident chaperones (128). The C-terminus effector domain is found on the cytosolic side of the ER and consists of the kinase domain (KD: aa 592-1115). Its kinase domain is homologous to the PKR KD (see section 2.2.4) except that it possesses a larger eIF2α insert region (Fig. 10A) (273). PERK phosphorylates eIF2α in response to ER stress in order to shut down protein synthesis of those proteins destined for the secretory pathway in order to relieve the load in the ER. This response is known as the unfolded protein response (UPR) and is discussed in section 2.2.3.4.

2.2.3.2 Regulation & Activation of PERK

PERK is a type I transmembrane ER resident eIF2α kinase that is activated under ER stress-inducing conditions, such as protein misfolding, protein overload in the ER, inhibition of glycosylation, and calcium depletion. PERK contains a luminal domain capable of sensing misfolded proteins, and a cytoplasmic kinase domain. PERK is kept in an inactive state as a monomer by the interaction of its luminal domain with an ER chaperone termed BiP. Upon induction of ER stress, BiP dissociates from the monomeric

PERK protein, and contributes to the proper folding of misfolded proteins. PERK can then oligomerize on the ER membrane and become activated by autophosphorylation. The activated forms of PERK will ultimately reduce the protein overload in the ER by attenuating protein synthesis by phosphorylating eIF2α via its cytoplasmic kinase domain (Fig. 10B) (273).

2.2.3.3 Translational Regulation by PERK

The inhibition of translation by PERK is a transient response in order for cells to recover from ER stress. Late in the ER stress response, the HSP40 co-chaperone $p58^{IPK}$ is activated by ATF6 and binds to the KD to inhibit PERK (335,353). However the inactivation of PERK is not sufficient to recover from its translational block since phosphorylation of eIF2α has already occurred. Several eIF2α phosphatases have been identified that appear to target eIF2α during the late stages of ER stress. Nck-1 was shown to recruit a calyculin A sensitive phosphatase onto eIF2α but its regulation upon ER stress is still unresolved (178). The other is PP1 which is regulated by CreP and GADD34. CreP constitutively regulates PP1 whereas GADD34 is induced by ATF4 late in ER stress where it targets PP1 to the ER and induces eIF2α dephosphorylation (166,181,219,244,245). Thus, the late activation of $p58^{IPK}$ and GADD34 during ER stress serves as a negative feedback loop that restricts protein synthesis inhibition by PERK and eIF2α phosphorylation.

Figure 10. Translational control by PERK.

(A) The ER-resident PKR-like protein kinase (PERK) is a serine/threonine kinase that is embedded in the membrane of the ER and contains 1115 amino acids. The lumenal N-terminus half is composed of the sensor domain (homologous to the sensor domain of IRE1) and binds to BiP in the inactive state. The sensor domain is flanked by a signal peptide (SP) and a transmembrane domain (TM), enabling PERK to localize to the ER membrane. The C-terminus consists of the kinase domain that is homologous to the PKR kinase domain except that PERK has a larger eIF2 insert region.

(B) In unstressed cells PERK is kept inactive via the tight binding of the ER-resident chaperone BiP. Pharmacological and physiological conditions that promote protein misfolding induce an ER stress response. BiP dissociates from PERK to participate in protein folding, and PERK oligomerizes and *trans*-autophosphorylates rendering the kinase active. In turn, PERK induces the phosphorylation of eIF2α thus inhibiting translation and alleviating accumulation of proteins in the ER.

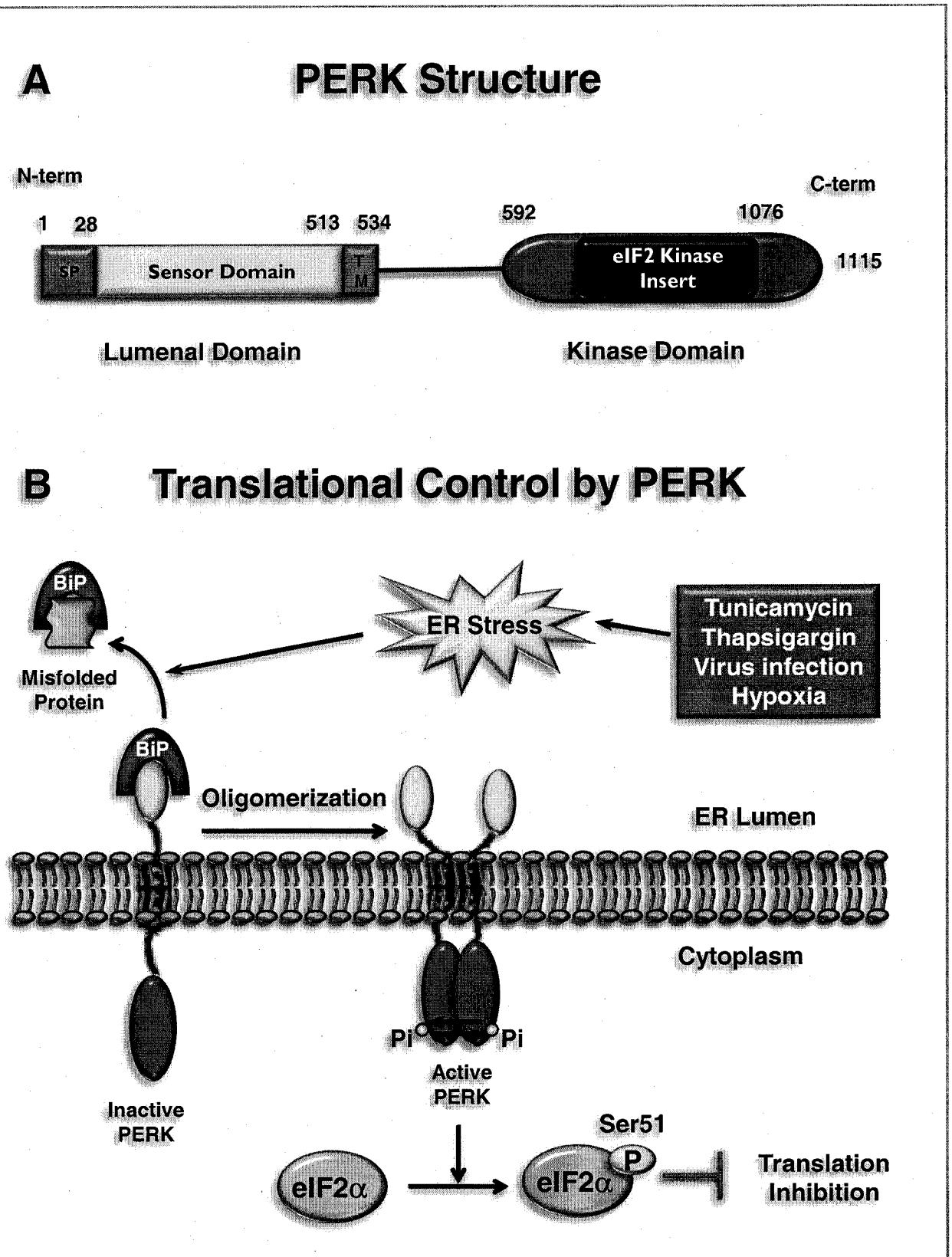
A
PERK Structure
N-term
C-term
1
28
513
534
592
1076
1115
SP
Sensor Domain
T
M
eIF2 Kinase
Insert
Lumenal Domain
Kinase Domain
B
Translational Control by PERK
BiP
Misfolded
Protein
ER Stress
Tunicamycin
Thapsigargin
Virus infection
Hypoxia
BiP
Oligomerization
ER Lumen
Cytoplasm
Pi
Pi
Active
PERK
Inactive
PERK
Ser51
P
eIF2α
eIF2α
Translation
Inhibition

Figure 10

2.2.3.4 Unfolded Protein Response (UPR)

The ER has evolved highly specific signaling pathways termed the unfolded protein response (UPR) to cope with the accumulation of misfolded or unfolded proteins. The UPR consists of several adaptive pathways that are activated upon specific sensors that help reduce the amount of new proteins translocated into the ER lumen, to increase the retro-translocation and degradation of misfolded proteins, and to increase the folding capacity in the ER lumen. The UPR orchestrates the transcriptional activation of genes mediated by IRE1 and ATF6, and the general translational inhibition and selective translation of specific mRNAs mediated by PERK. BiP serves as a common regulator between these three sensors in response to ER stress (30,297).

Under unstressed conditions, BiP binds to IRE1, ATF6 and PERK to prevent their signaling. Upon protein overload or misfolded proteins in the ER lumen, BiP is released from the sensor domains of the three UPR sensors, and helps in the folding of the luminal proteins. This frees IRE1 and PERK to induce homodimerization and autophosphorylation leading to their activation (30). In contrast, release of ATF6 from BiP permits its transport to the Golgi compartment where it is cleaved and discharged to the cytosol and functions as a transcription factor (Fig. 11) (297).

Once IRE1 is activated, it cleaves *XBP1* mRNA to remove a 26-nucleotide intron thus generating a translational frame-shift. Spliced *XBP1* mRNA encodes for a transcriptional activator for many UPR target genes (Fig. 11). Activated cytosolic ATF6 is a UPR transducer that can bind to ER stress response element (ERSE) motifs (359) in the promoters of UPR responsive genes (361). One of the mRNAs induced by

proteolysed ATF6 is *XBP1* mRNA which is ultimately spliced by IRE1 (360). This suggests that IRE1 and ATF6 are involved in parallel pathways that ultimately converge to regulate common targets upon ER stress.

As described earlier, PERK activation upon ER stress leads to translational inhibition in order to relieve the ER lumen from protein overload. Although general protein synthesis is inhibited upon ER stress, eIF2α phosphorylation selectively promotes translation of the transcription factor ATF4 (Fig. 11) (126). ATF4 induces transcription of genes (such as the previously mentioned GADD34) involved in amino acid metabolism, oxidation-reduction reactions, and ER stress-induced apoptosis, such as CHOP/GADD153 (Fig. 11) (129).

When cells are unable to cope or adapt to prolonged ER stress, the UPR signaling pathways induce an apoptotic response to eliminate susceptible cells. CHOP/GADD153 is a transcription factor that has been shown to activate ER stress-induced apoptosis by repressing the expression of the apoptotic repressor Bcl-2 (Fig. 11) (126). Another apoptotic pathway induced by ER stress is the caspase activation cascade mediated by caspase-12 (239). Procaspase-12 is an ER membrane-associated effector caspase that is activated by cleavage by caspase-7 that is recruited to the ER after prolonged ER stress (267). This in turn initiates the caspase cascade leading to the activation of caspase-9 and caspase-3 (Fig. 11) (234).

Although three different UPR sensors have been characterized, the complexity of the UPR signaling pathways suggest that other sensors may be involved or have yet to be discovered. Recently, two novel ER stress transducers have been identified in astrocytes

or damaged neurons. OASIS (182) and BBF2H7 (183) are both transcription factors that are activated during late phase ER stress in a similar matter as ATF6. That is they are imbedded in the ER membrane, cleaved and translocated to the nucleus to induce the UPR response. OASIS mediates the transcription of target genes with ERSE and cyclic AMP-responsive elements (182), whereas BBF2H7 is involved in suppressing ER stress-induced apoptosis (183). These new findings reveal pivotal roles for novel ER stress transducers in modulating the unfolded protein response in various tissues, and the possibility that cell type-specific UPR signaling also exists in all cells.

Figure 11. The unfolded protein response pathway.

The UPR pathway is initiated by conditions that induce ER stress (i.e. protein misfolding). The misfolded proteins are sensed by BiP and in turn BiP dissociates from the three ER-resident sensors of the UPR (ATF6, IRE1, and PERK). ATF6 translocates to the Golgi apparatus where it is cleaved by S1P/S2P peptidases thus generating a nuclear form that acts as a transcriptional activator for ER stress-inducible genes such as BiP and CHOP. ATF6 also induces *XBP-1* mRNA that is spliced via the endonuclease activity of activated IRE1. Spliced XBP-1 induces transcription of ER chaperone genes involved in protein folding or ER-associated degradation response (ERAD). In order to relieve the accumulation of proteins in the ER lumen, PERK activation inhibits overall protein synthesis by eIF2α phosphorylation. However, selective translation can still occur despite protein synthesis inhibition mediated by eIF2α phosphorylation. Such is the case of the transcription factor ATF4. Late in the ER stress response, the adapted cell needs to turn back on translation by inducing GADD34 transcription via ATF4. Together with the PP1 phosphatase, GADD34 promotes eIF2α dephosphorylation thus reinstating translation. However, if the cell has not adapted to the ER stress response, the apoptotic pathway is induced by CHOP. CHOP is a transcriptional repressor of the inhibitor of apoptosis Bcl-2. Also, the ER-resident procaspase-12 is processed by caspase-7 in which the activated caspase-12 initiates the caspase cascade inevitably inducing an apoptotic response.

UPR Pathway

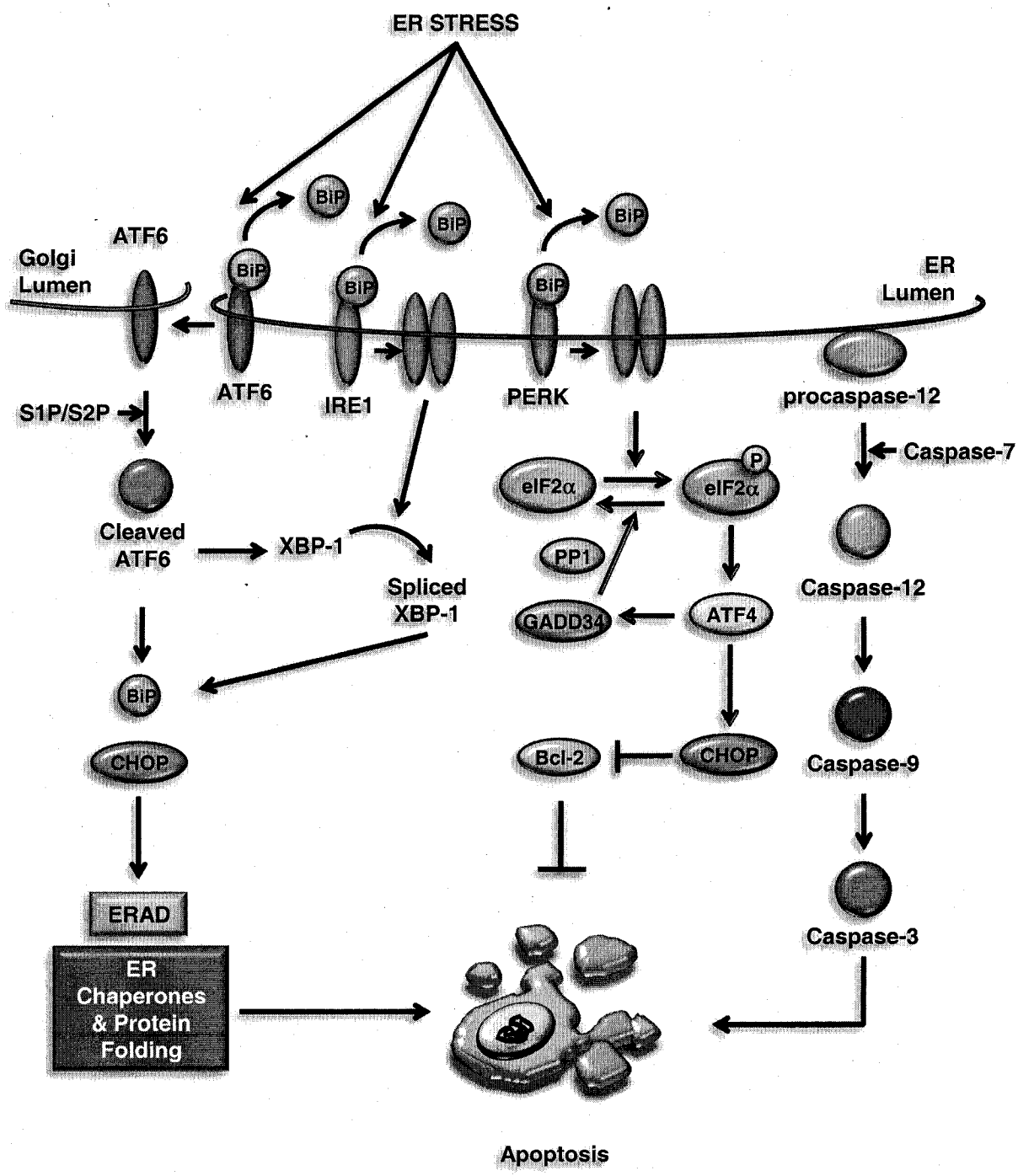

Figure 11

2.2.4 PKR

2.2.4.1 Structure of PKR

The double-stranded (ds)RNA-activated protein kinase, PKR, is an interferon (IFN)-inducible serine/threonine and tyrosine kinase that is activated upon virus infection (14,172,316). Human PKR is encoded on chromosome 2p21-22 (15,308), whereas mouse PKR is located on chromosome 17E2 (15). The human *pkr* gene consists of 17 exons while the mouse gene has 16 exons (188). PKR is a 68 kDa protein containing 551 amino acids in humans and a 65 kDa protein containing 515 amino acids in mice (61). The kinase is divided into two distinct domains: the N-terminus regulatory domain and the C-terminus kinase domain (Fig. 12) (172).

The N-terminus regulatory domain consists of the dsRNA-binding domain (dsRBD) composed of two tandem copies of a conserved dsRNA-binding motif (dsRBMI: aa 11-77 and dsRBMII: aa 101-167) separated by 20 amino acids in between them (Fig. 12). As the name implies, this domain binds to dsRNA or replicative intermediates produced during virus infection inducing the dimerization of PKR (61,172).

The C-terminus kinase domain (KD: aa 228-551) is composed of eleven conserved kinase sub-domains (I-XI) (Fig. 12). The sub-domain II contains the ATP-binding pocket and mutation of Lys296 (K296H or K296R) within this region renders the PKR kinase activity inactive (326,327). The K296H mutant functions as a dominant-negative and prevents PKR activation and eIF2α phosphorylation (326,327). However, the mutant protein can still dimerize and bind to dsRNA but is unable to induce any kinase activity (346). The sub-domain IV spans the eIF2α-insert region and mediates the

substrate recognition function between PKR and eIF2α. Between sub-domains VII and VIII, there are two autophosphorylation sites, Thr446 and Thr451, that are essential for PKR kinase activity (271).

2.2.4.2 Regulation & Activation of PKR

PKR is one of the best-characterized interferon (IFN) inducible proteins (284) that phosphorylates eIF2α on serine 51 in response to stress signals as a result of virus infection (14,85,126,342). This phosphorylation of eIF2α does not only inhibit the infected host cell translation, but it also restrains viral protein synthesis as a anti-viral mechanism (11,198,199,313). Basically, PKR is activated in a 3-step sequential manner: dimerization, autophosphorylation and activation followed by substrate recognition (Fig. 13).

Upon virus infection, dsRNA accumulates in the infected cell and the dsRBD of PKR senses and binds to these viral replicative intermediates. The binding of PKR to dsRNA allows PKR to dimerize and induce *trans*-autophosphorylation on many serine/threonine and tyrosine residues. The phosphorylation of Tyr101/162 and Thr258 influence dsRNA-binding and/or autophosphorylation while Thr446/451 and Tyr293 phosphorylation renders the kinase active and promotes eIF2α phosphorylation (75,88,316,322,323).

Through this capacity PKR exerts its anti-viral activity on a wide range of DNA and RNA viruses, and mediates the biological functions of IFNs (311). In addition to translational control, PKR has been implicated in various signaling pathways leading to gene transcription by modulating the activities of various transcription factors including

NF-κB (189), Stats (278) and the tumor suppressor p53 (72). These transcriptional pathways modulated by PKR are summarized below (section 2.2.4.4) as well as its role in translational regulation (section 2.2.4.3).

2.2.4.3 Translational Regulation by PKR

Since PKR regulates translation, it needs to be in close proximity to the translational machinery in order to target eIF2α for phosphorylation during virus infection. It was previously shown that the dsRBD of PKR facilitates its association with the 40S ribosomal subunit providing PKR access to its substrate (367). Also, the activation of PKR via ribosome-association can be disrupted by the L18 ribosomal protein of the 60S subunit preventing PKR binding to dsRNA and autophosphorylation (191). The ribosome localization of PKR is critical for its local activation in response to virus infection. When infected cells produce and secrete IFNs to stimulate PKR induction of neighboring infected cells, there is a minimal or negligible eIF2α phosphorylation detected in these cells. However, this localized eIF2α phosphorylation is sufficient to inhibit viral RNA translation without affecting overall translation of the host cell. It appears that restricting PKR activation towards locations where viral RNA and protein synthesis occur limits the spread and replication of virion production.

In addition, PKR has been shown to be localized in the nucleus (160). Although there have been some reports about translation occurring in the nucleus (151-153), the role of nuclear PKR remains unclear. However, a recent study suggests that its role may be involved in ER stress-induced apoptosis, since activated PKR migrates to the nucleus in tunicamycin-treated cells and in neurons of Alzheimer's disease patients (248). This

study supports the notion that PKR also regulates gene transcription by modulating transcription factors, and will be discussed in the following section.

2.2.4.4 Transcriptional Regulation by PKR

One of the PKR mechanisms that direct IFN and dsRNA signaling pathways is the modulation of the signal transducers and activators of transcription (Stat). Signaling cascades triggered by IFN and other cytokines are modulated by the Stat transcription factor proteins (76). PKR physically binds to Stat1 via its dsRBD but this interaction is not a kinase-substrate function between the two proteins (Fig. 14). The inactive form of PKR interrupts the DNA-binding activity of Stat1 and is independent of its kinase function (344). This binding is disrupted upon IFN or dsRNA treatment suggesting that both proteins are held together in an inactive state in untreated cells and that activated PKR releases Stat1 to induce its transcriptional activity. However, controversial evidence shows that Stat1 phosphorylation on Ser727 and transactivation is abolished in $PKR^{-/-}$ MEFs (266).

PKR has also been shown to associate with Stat3 and is required for its phosphorylation and activation in response to PDGF treatment by regulating ERK activity (79). Despite these claims, our lab has shown that Stat1 and Stat3 phosphorylation and transactivation are impaired by PKR activation via the phosphatase activity of TC-PTP (339).

Some early evidence suggested that PKR may regulate NF-κB activation. The NF-κB transcription factors regulate gene expression of a number of cellular processes mainly involved in the immune and inflammatory responses (134), and apoptosis (94).

NF-κB is maintained in the inactive state and sequestered in the cytoplasm by IκB proteins. When the IKK complex phosphorylates IκB on Ser32/36 residues, it is targeted for ubiquitination and degradation. This in turn frees NF-κB where it translocates to the nucleus and induces its transcriptional activity (Fig. 14) (269).

Cells depleted of PKR activity were unresponsive to NF-κB activation when treated with dsRNA but not with TNFα (225). Equally, $PKR^{-/-}$ MEFs displayed impaired NF-κB activation in response to the synthetic dsRNA compound poly(rI-rC), and consequentially had defects in type I IFN production compared to their wild type counterparts (190,356). However, when the $PKR^{-/-}$ MEFs were primed with IFNs prior to dsRNA treatment, NF-κB activation was restored, suggesting another IFN-inducible pathway may also regulate NF-κB activity (356).

It was believed that PKR was capable of directly phosphorylating IκB to induce NF-κB activation upon dsRNA (189). However, once again controversial evidence suggested otherwise that PKR appears to have an indirect role regarding NF-κB activation (197). It was later confirmed by our group and others that PKR activates the IKK complex to induce NF-κB activation upon dsRNA or vesicular stomatitis virus (VSV) infection independent of its kinase function (37,111,158,364). Although these studies show that the KD of PKR interacts with the IKK complex in response to dsRNA, the role of PKR catalytic activity in this process is still debatable today. $PKR^{-/-}$ MEFs suggest that PKR kinase activity is indispensable to the full activation of NF-κB (112). In contrast overexpressed catalytically inactive PKR is capable of inducing IKK activation (56,158) suggesting that catalytic activity of PKR is not required. These studies support

the notion that protein-protein interactions are required for IKK activation and not PKR kinase function.

It appears that experimental designs and conditions affect the results between PKR and NF-κB activation, and that they are difficult to interpret. Nevertheless, some NF-κB activation can still be triggered in $PKR^{-/-}$ MEFs despite the huge suppression (356). Due to these discrepancies, the question remains as to whether PKR catalytic activity is required for IKK activation.

Finally, PKR can also modulate some functions of p53 (Fig. 14). The tumor suppressor p53 mounts a transcriptional response resulting to cell cycle arrest and apoptosis upon genotoxic stress (see section 1). PKR has been shown to induce p53-mediated apoptosis upon TNFα treatment in U937 cells (358). Our lab has established a physical interaction between PKR and the C-terminus of p53 resulting in phosphorylation on Ser392 (72). Also, p53 activation upon adriamycin or γ-irradiation is impaired in cells devoid of PKR (71). Furthermore, $PKR^{-/-}$ MEFs display defective phosphorylation of p53 on Ser18 (Ser15 in human p53) as well as an impaired ability to induce cell cycle arrest and p53-target genes (71). The precise mechanism underlying the PKR-p53 pathway remains unknown, and future studies are needed to justify the connection between the two proteins and the tumor suppressor functions of PKR.

Figure 12. Structure of PKR.

Human dsRNA-activated protein kinase (PKR) is a serine/threonine and tyrosine kinase composed of 551 amino acids. The N-terminus comprises the regulatory domain termed dsRNA-binding domain (dsRBD) containing two dsRNA-binding motifs (dsRBM1/2). This domain binds to dsRNA and promotes PKR dimerization. The C-terminus portion is the kinase domain (KD) containing 11 conserved sub-domains (I-XI). The ATP-binding site can be found in sub-domain II, whereas the eIF2 insert region is within sub-domain IV.

PKR Structure

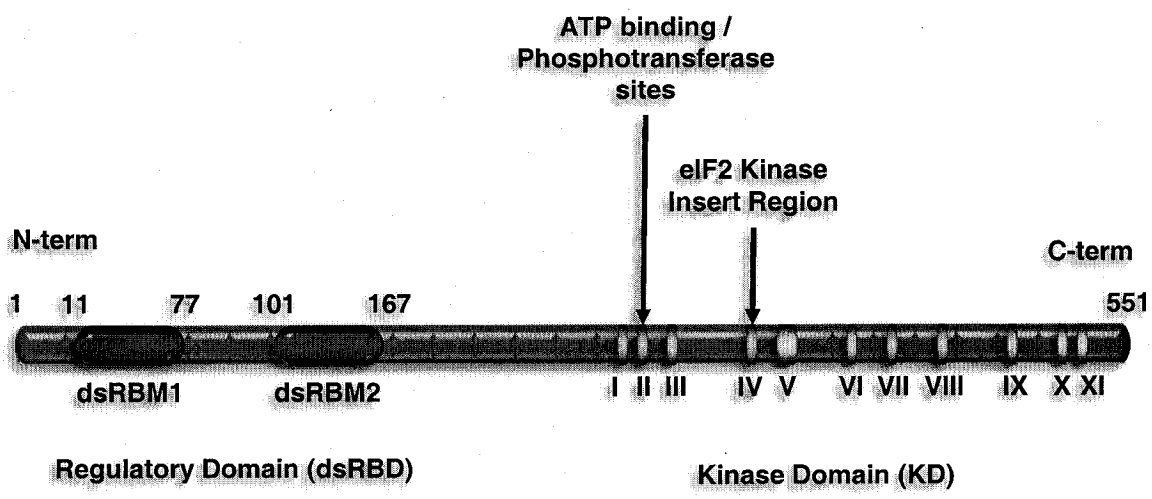

Figure 12

Figure 13. Translational control by PKR.

Virus infection triggers the production of IFNs and subsequent induction of PKR protein levels. When dsRNA is produced during virus replication, the dsRNA-binding domain (dsRBD) of PKR binds to these replicative intermediates and allows the dimerization of PKR. Dimerization induces the catalytic activity of the kinase domain (KD) in which *trans*-autophosphorylation of PKR renders the kinase active. Activated PKR can now target its well studied substrate eIF2α and induce its phosphorylation on Ser51 thus inhibiting protein synthesis.

Translational Control by PKR

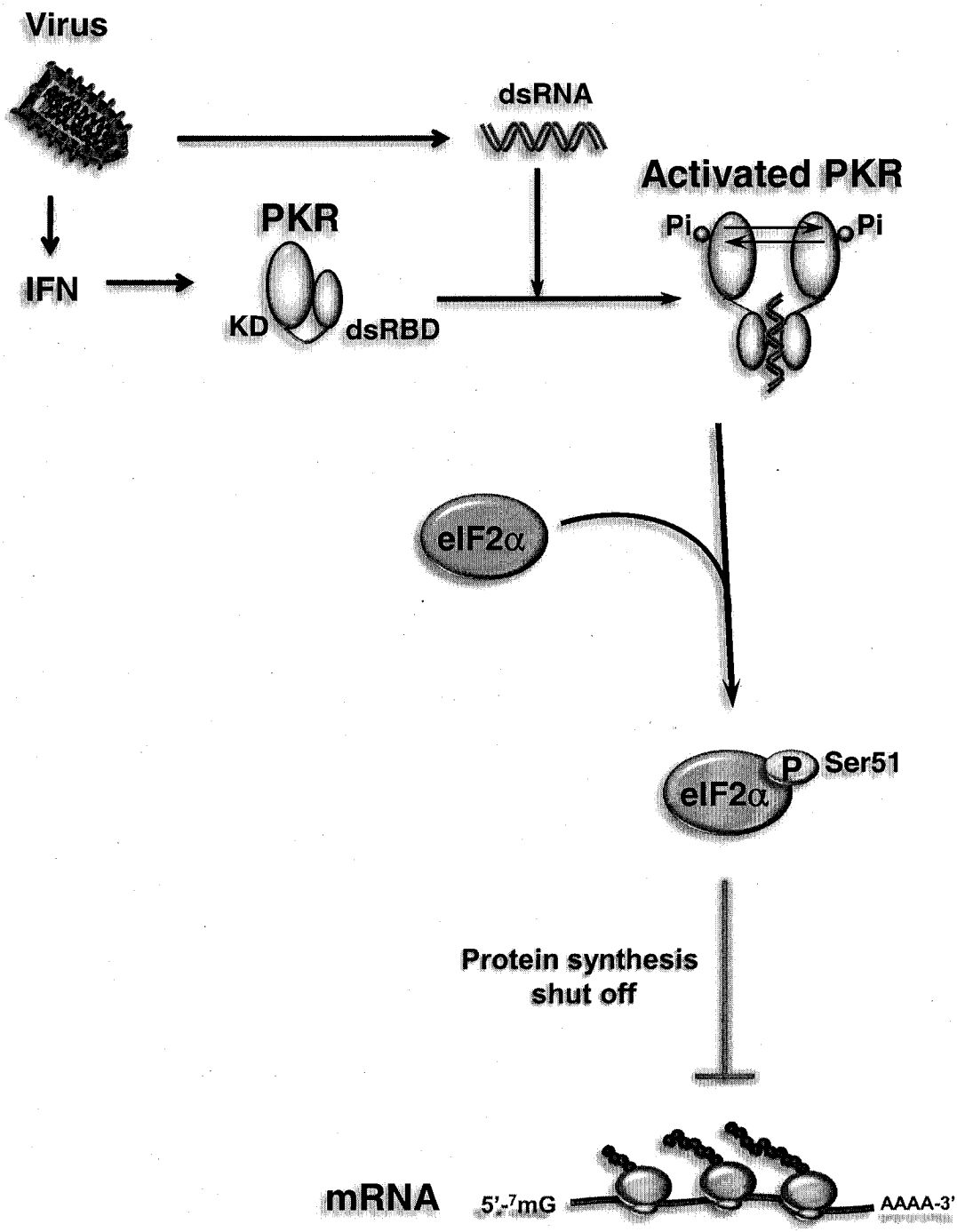

Figure 13

Figure 14. Transcriptional regulation by PKR.

Inactive PKR monomers are bound to unphosphorylated forms of Stat1. Upon IFNα/β stimulation or dsRNA produced during virus infection, the PKR-Stat1 dimers are disrupted and each protein is activated via separate mechanisms. The IFN receptors (IFNAR1/2) induce Stat1 phosphorylation and dimerization with other Stats where the dimers migrate to the nucleus to induce transcription of genes with interferon-sensitive response elements (ISRE). The intracellular dsRNA induces PKR dimerization and activation. PKR has been shown to induce IKK activation, although the role of PKR kinase activity in this process remains debatable. The activated IKK complex phosphorylates IκB that keeps NF-κB in the inactive state. Upon IκB phosphorylation, it dissociates from NF-κB and is targeted for degradation. In turn, NF-κB translocates to the nucleus to induce gene transcription. Furthermore, PKR has been implicated in p53 activation upon DNA damage. However the biological significance or mechanism of activation is still unknown.

Transcriptional Regulation by PKR

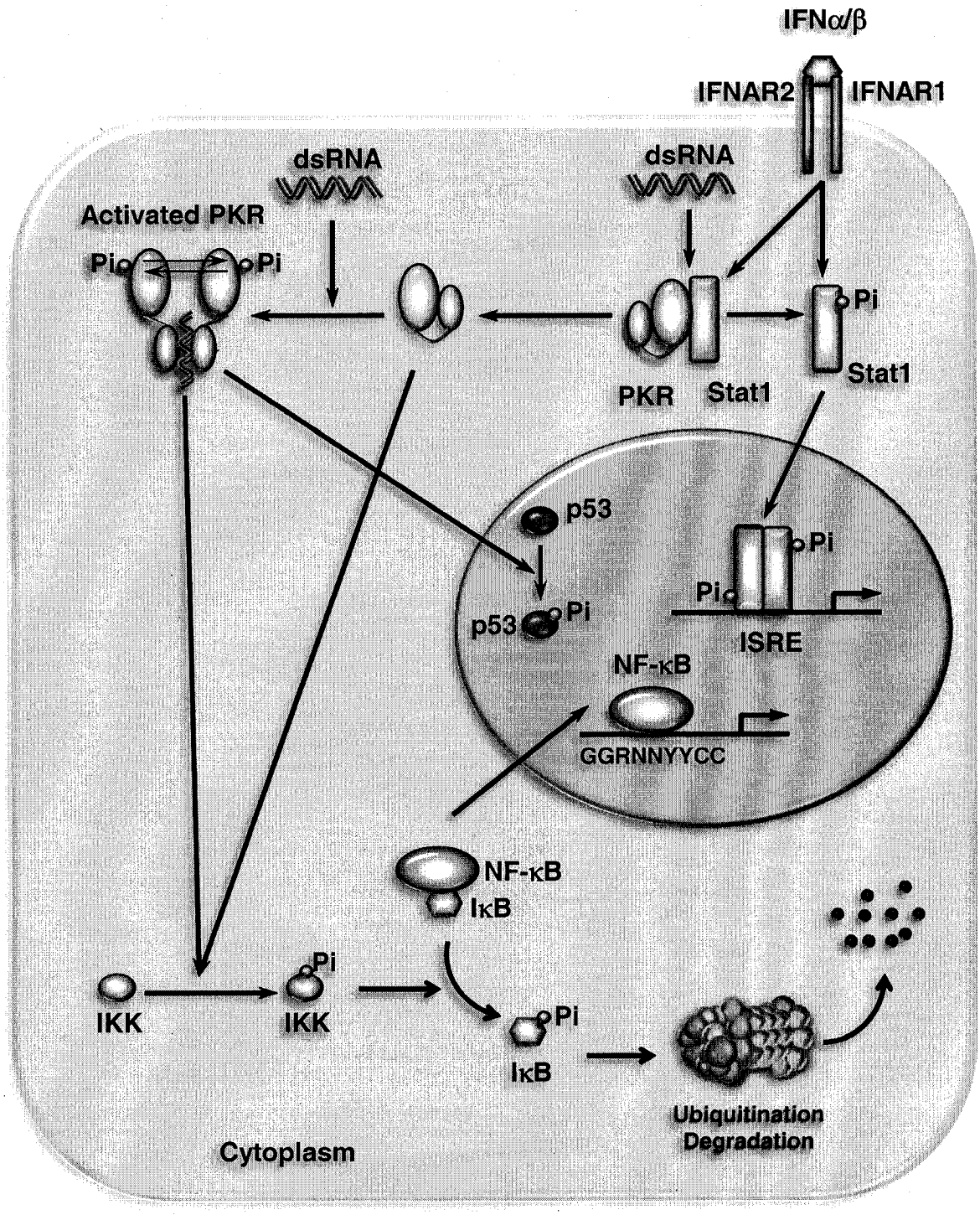

Figure 14

3 VESICULAR STOMATITIS VIRUS

3.1 CLASSIFICATION

Vesicular Stomatitis Virus (VSV) is a member of the Rhabdoviridae family, and grouped into the *Vesiculovirus* genus. The genus contains approximately 35 serologically distinct viruses, most importantly are the Vesicular Stomatitis Virus Indiana and New Jersey strains that are known to cause vesicular disease in horses, cattle, swine, and humans. Although the infection is transmitted directly by the transcutaneous or transmucosal route, VSV has been isolated from sand-flies, mosquitoes, and grasshoppers suggesting that it could be an arbovirus (insect-borne). Natural VSV infections take place in two steps: cytolytic infections of mammalian hosts and transmission by insects through non-cytolytic persistent infections (277).

There is also some evidence that VSV could be a plant virus and that animals are the closing stages of the epidemiological link in which the pathogenesis of the disease is unclear. VSV infectivity is stable in an alkaline environment, but the virus is sensitive to UV irradiation and sunlight. In clinical practice VSV is inactivated easily by detergent-based disinfectants. VSV is a common laboratory virus, and the prototypical virus to study the properties of all Rhabdoviruses and virus evolution (236,277).

3.2 STRUCTURE

Rhabdoviruses are bullet shaped in structure and the virions are approximately 45-100 nm in diameter and 100-400 nm long. They are comprised of two major structural components: the host-derived envelope, which is a lipid bilayer with large peplomers

(glycoprotein projections of the outer viral envelope), and the ribonucleoprotein (RNP) core, which contains the genetic material within a helically coiled cylindrical nucleocapsid. The cylindrical nucleocapsid is what gives the viruses their distinctive bullet shape (Fig. 15A) (277).

3.3 Genome & Viral Proteins

VSV is a member of the Mononegavirales order meaning the genome is a single linear, negative-sense molecule of ssRNA and is about 11-15 kb in size (12,277). The RNA genome encodes five major proteins: glycoprotein (G), matrix protein (M), nucleocapsid protein (N), large protein (L) and phosphoprotein (P) (Fig. 15B). The five genes encoded within the genome are in the order of 3'-N-P-M-G-L-5' (13,62). The N, P, and L proteins encase the viral RNA and are involved in the viral genome transcription and replication. The P protein is the major phosphoprotein (49) and the L protein serves as the RNA-dependent RNA polymerase containing 5' capping and 3' polyadenylation activities (17). Together with the N protein, they serve as the viral transcriptase catalyzing the replication of the mRNA (33,78).

The G and M proteins consist of the membrane-associated proteins. The G protein is oriented externally spanning the membrane and thus comprises the major antigenic determinant of the virus (65,336). It enables viral entry to the cell by mediating both virus attachment to the host cell receptors and fusion of the viral envelope with the endosome following endocytosis (65). The M protein is known as the bridging molecule because it associates with the inner surface of the viral membrane along with the RNP core. This bridge allows the two structures to come together during virion assembly and budding. It

is believed to bind the cytoplasmic tail of the G protein enabling the RNP core to cluster with the G protein prior to budding (54). Therefore the M protein contributes in the final stages of the viral life cycle (Fig. 16) when the virions pinch off from the infected cells (159).

Figure 15. Vesicular stomatitis virus genome & virus particle structure.

(A) Vesicular stomatitis virus (VSV) is composed of five viral proteins that are assembled into a bullet shaped virus particle that is enveloped in a lipid bilayer. Embedded in the membrane are the peplomers (glycoprotein: G) involved in cell adherence. Beneath the membrane is the matrix (M) protein. The M protein is the main structural protein and is involved in the formation of progeny virions and the budding process. Inside the virus is the ribonucleoprotein (RNP) core, which contains the ssRNA genome within a helically coiled cylindrical nucleocapsid (N). The P (phosphoprotein) and the L (large) proteins serve as the viral polymerase.

(B) The negative sense, ssRNA genome of VSV consists of five genes that encode the five major viral proteins: the nucleocapsid protein (N), the phosphoprotein (P), the matrix protein (M), the glycoprotein (G) and the large polymerase protein (L). Transcription of viral genes proceeds from the 3' to 5' end of the negative strand genome thus generating positive sense transcripts beginning with the N gene. Each protein has its own transcribed capped and polyadenylated mRNA.

A

Vesicular Stomatitis Virus

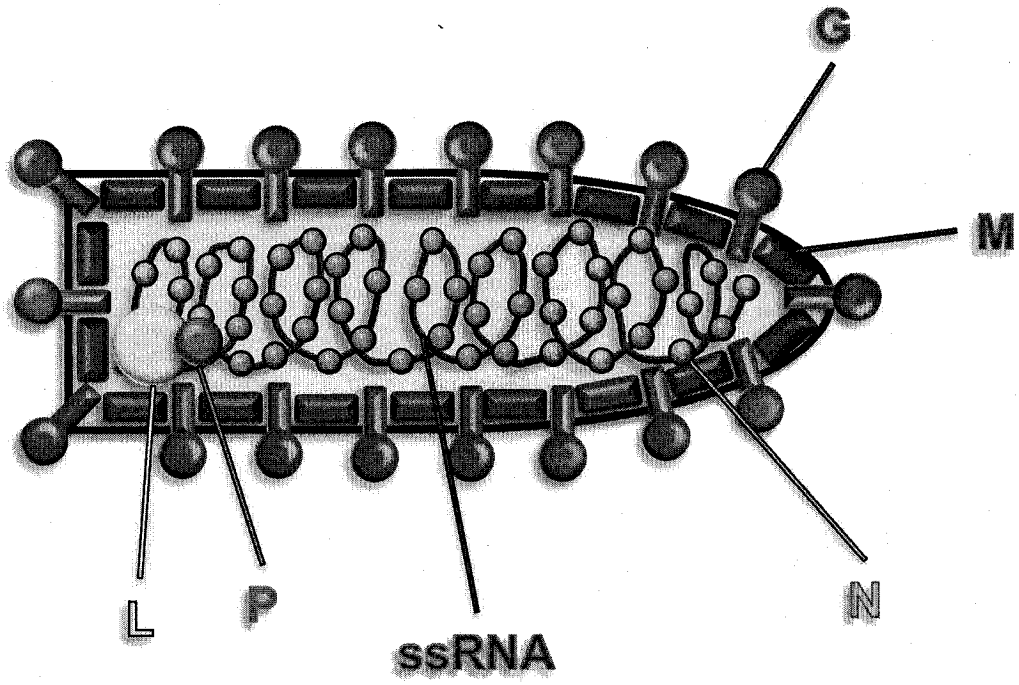

B

VSV Genome & Proteins

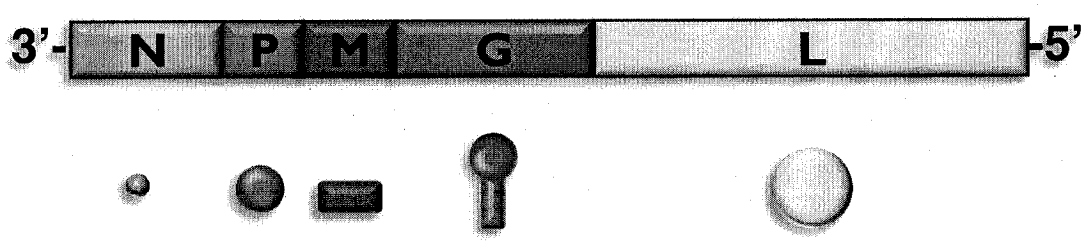

Figure 15

3.4 VSV Life Cycle

VSV is known to infect a wide range of cell types by means of the G protein targeting common cellular receptors that are shared between different cell types (277). However, the receptor has not been identified yet and some speculations indicate that the phosphatidylserines of the cell membrane may contribute to the binding of the G protein and viral endocytosis (Fig. 16) (65,66,68) but it remains questionable (287).

During endocytosis, the pH of the endosome becomes acidic and induces membrane fusion thus releasing the viral RNP core into the cytoplasm (Fig. 16) (34,224). Since the virus brings its own polymerase (L protein) with it during infection, it binds to the 3'-end of the negative strand RNA genome. The viral L polymerase recognizes viral nucleotide sequences at the 3'-end (141) and initiates the sequential transcription of 5 individual positive strand mRNAs encoding the 5 individual proteins (38,258,276). The VSV mRNAs are capped and polyadenylated, and translated with the cellular ribosomal machinery (274,275).

Through an unknown process, the viral polymerase switches from transcription of viral mRNAs to replication of the viral genome possibly via the functions of the P protein (63). This switch only occurs after viral transcription and protein synthesis. Virus replication is restricted to the cytoplasm of the cell (277). The genome is replicated into a full length positive sense RNA which is used as a template to generate more negative sense RNA genomes that will be encapsidated (Fig. 16). During the replication process, dsRNA or replicative intermediates are produced, and are sensed by the dsRBD of PKR as described earlier in order to initiate the anti-viral response. Encapsidation of the RNA

genome is mediated by the N protein forming the RNP core along with the P and L proteins. The RNP core is then condensed with the help of the M protein present on the cell membrane embedded with G proteins. The virions are then formed and bud from the plasma membrane releasing the progeny viruses (Fig. 16) (159,277).

3.5 Regulation of VSV by PKR

The importance of PKR in innate immunity against virus infection has been established by many groups for some time now (2,11,230,231). It is believed that PKR is induced by IFNs produced during virus infection and its activation is required to inhibit virus replication by blocking viral protein synthesis via the phosphorylation of eIF2α (230). Two different strains of $PKR^{-/-}$ mice have been generated (2,356), but they are not particularly sensitive to virus infection suggesting that perhaps other eIF2α kinases may be involved in this redundancy. It was believed that viruses have developed mechanisms of inhibiting PKR activity and this would explain why $PKR^{-/-}$ mice are not more susceptible to viruses as their wild type counterparts. However, this theory does not explain why viruses that do not encode for PKR-inhibitors continue to replicate despite the high levels of PKR activation, as is the case with VSV.

It was shown that $PKR^{-/-}$ mice were susceptible to VSV infection only during intranasal inoculation (11), but it was later determined that this vulnerability is mouse strain dependent (93). This underlines the importance that other host factors or redundant pathways may contribute to the resistance to VSV infection in $PKR^{-/-}$ mice. This claim correlates with the fact that $Stat1^{-/-}$ mice are also susceptible to VSV infection despite the presence of PKR (228). It appears that the role of PKR during VSV infection is to slow

down virus replication by inhibiting protein translation. In turn, this buys time for the cell to initiate an anti-viral response to halt completely VSV replication by inducing IFN-target genes. Thus priming cells with IFNs have been shown to inhibit VSV replication (19), and in some cases PKR was not required for resistance to VSV infection in IFNγ-treated neurons (51). This would explain the fact that VSV has enabled methods to block IFN-inducible gene translation by preventing host mRNA export instead of targeting PKR function (100,103).

VSV has also found mechanisms to inhibit host protein synthesis without affecting its own translation by compromising other initiation factors involved in cap-dependent translation (eIF4E, eIF4G, and eIF4A) (67). However, the mechanisms by which VSV inhibits host cell translation have yet to be determined. Taken together, these data indicate that depending on the cell type or animal strain, the role of PKR in VSV infection appears to be working in synergy with other signaling pathways.

Figure 16. VSV replication cycle.

The attachment of VSV to the host cell is mediated by the glycoprotein (G) embedded in its membrane. Adhered viral particles are engulfed by endocytosis and enter the cellular endosomal trafficking pathway. The endosomes harboring VSV acidify (H^+), and the decrease in pH triggers a conformational change in the G protein that mediates fusion between the viral envelope and the endosomal membrane. The viral RNP core is released into the cytoplasm and initiates viral gene transcription. The viral polymerase first transcribes the individual mRNAs for each viral gene, which are then translated by the host translational machinery. During late stages of infection, the viral polymerase switches from transcription to replication and synthesizes copies of the negative-sense VSV genome using positive-strand intermediates as templates. During this process, dsRNA (replicative intermediates) are produced and can initiate the cellular anti-viral responses. Finally, the viral proteins and genomic RNA are assembled into complete virus particles, and the viral progeny bud from the cell through the plasma membrane.

VSV Life Cycle

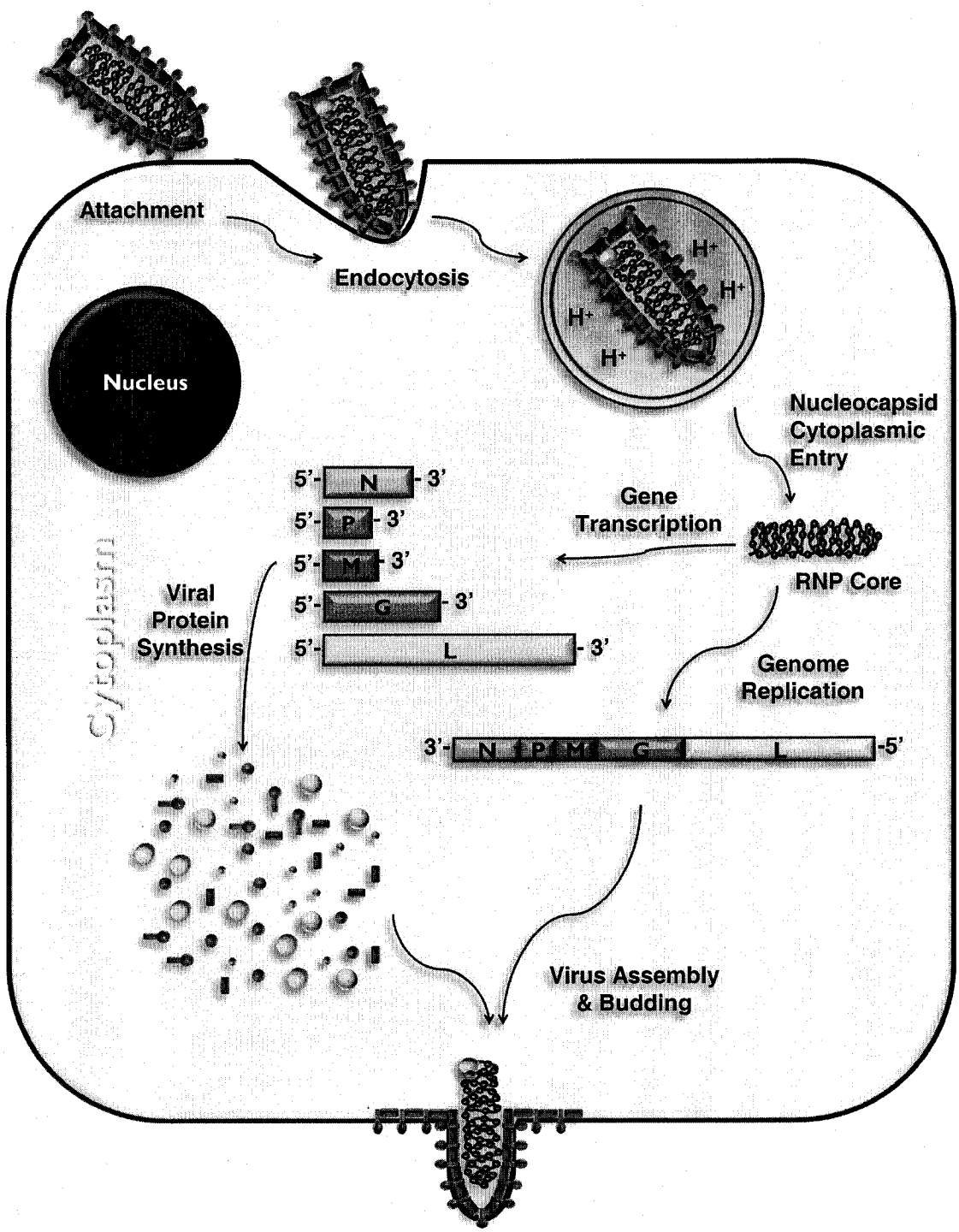

Figure 16

4. HYPOTHESIS & RESEARCH OBJECTIVES

4.1 Aim of Research

The eIF2α kinases, PERK and PKR, have been shown to play important roles in regulating protein synthesis upon ER stress and virus infection, respectively, through their capacity to phosphorylate eIF2α. Although the regulation of translational control by eIF2α kinases has been thoroughly studied, it does not explain the differences between the biological outcomes mediated by the different eIF2α kinases. Modulation of different signaling pathways by each eIF2α kinase could justify these diverse effects. However, little is known about the downstream targets or pathways that may be involved and if eIF2α kinases function individually or in synergy to adapt to various stress conditions.

Since eIF2α kinase activity is induced by various stresses, the aim of this research was first to determine if eIF2α-dependent pathways require a functional interaction between eIF2α kinases during virus infection, and second to verify if the activation of PERK and PKR can modulate other stress sensors, such as p53, through eIF2α-independent pathways.

4.2 Hypothesis

4.2.1 Functional Interaction between PERK and PKR

Work with cultured cells in many laboratories has assigned PKR antiviral, anti-proliferative, and tumor suppressor functions *in vitro*. However, the anti-proliferative and tumor suppressor functions of PKR have not yet been verified *in vivo*. Specifically, the

two distinct PKR knockout mice that have been generated did not exhibit growth abnormalities nor were they tumorigenic. Controversial evidence has been accumulating regarding PKR functions due to discrepancies between the signaling properties of PKR in the two PKR knockout mice. For example, both types of $PKR^{-/-}$ mice have not displayed any significant susceptibility to infections with a variety of viruses with the exception of intranasal VSV infection. However, unlike the mice, $PKR^{-/-}$ MEFs are modestly more permissive to VSV replication indicating that the lack of PKR might be compensated by the expression of another eIF2α kinase, whose activity is induced by VSV infection.

4.2.1.1 Objectives

1. To characterize the proteins involved for the signaling differences and discrepancies observed between the two PKR knockout MEFs.
2. To investigate the possibility that other eIF2α kinases may be implicated in VSV infection considering the modest susceptibility in PKR knockout mice.

4.2.2 Modulation of Stress Sensors by eIF2α Kinases

Stress conditions activate signal transduction pathways leading to the induction of genes encoding for proteins with key roles in damage sensing and apoptosis. Most stress conditions have implicated the tumor suppressor protein p53 as a key sensor that mediates various biological outcomes such as cell growth arrest, and induction of apoptosis. Some stress conditions perturb specific organelles thereby initiating a specific adaptive response. For example, virus infection, energy or nutrient deprivation, or Ca^{2+} depletion from the lumen of the endoplasmic reticulum (ER) can disrupt proper protein

folding in this organelle leading to the accumulation of unfolded proteins. This initiates transcriptional and translational signaling pathways in part through the activation of eIF2α kinases. If these adaptive mechanisms are not sufficient to alleviate ER stress, cells undergo apoptosis. Although a number of cellular stresses induce p53 activation via its stabilization and accumulation, it is unclear if a cross-talk exists between eIF2α kinases and p53, and if it affects the regulation of p53 at the translational or post-translational level.

4.2.2.1 Objectives

1. To determine if the downregulation of p53 upon ER stress is mediated through the induction of eIF2α kinase activity.
2. To investigate if eIF2α phosphorylation-mediated translational control regulates p53 upon ER stress.

CHAPTER II - MATERIALS & METHODS

1. CELL CULTURE & REAGENTS

1.1 CELL LINES

The mouse embryonic fibroblasts (MEFs) from the N-PKR$^{-/-}$ mice were in 129/Sv(ev) X C57BL/6J genetic background (356), whereas the C-PKR$^{-/-}$ mice were in 129/terSv X BALB/c background (2). The strain-matched 129SvEv PKR$^{+/+}$ and C-PKR$^{-/-}$ MEFs were also used, and generated as described (93). The PERK$^{+/+}$ and PERK$^{-/-}$ MEFs were used and generated as described (127). The HT1080 stable cell lines expressing GyrB-PKR WT or the kinase dead GyrB-PKR K296H proteins were generated as described (177). The eIF2α S/S and eIF2α A/A knock-in MEFs were generated as described (286). The GSK3β$^{+/+}$ and GSK3β$^{-/-}$ MEFs were used and generated as described (144). The NIH 3T3-puro and NIH 3T3-shPKR cells were a generous gift from M. Loignon.

1.2 CELL CULTURE

Mouse embryonic fibroblasts (MEFs), NIH3T3 and derived cell lines, HT1080 and derived cell lines, HeLa, VERO, and COS-1 cells were maintained in Dulbecco's Modified Eagle Medium (DMEM, Life Technologies Inc.) supplemented with 10% heat-inactivated calf serum (CS, Life Technologies Inc.), and antibiotics (Penicillin-Streptomycin 100 U/ml, ICN Biomedicals Inc.). Huh7 and U2OS cells were maintained in DMEM supplemented with 10% of heat-inactivated fetal bovine serum (FBS; Life Technologies Inc.), and penicillin-streptomycin (100 U/ml), 0.1 mM of MEM non-essential amino acids (GIBCOBRL). A549 cells were maintained in F12K medium

(Cellgro) supplemented with 10% FBS and penicillin-streptomycin (100 U/ml). HCT116 cells were maintained in McCoy's medium (MultiCell) supplemented with 10% FBS and penicillin-streptomycin (100 U/ml).

1.3 Transfections

Transfections were performed using LipofectAMINE Plus reagents (Invitrogen) according to manufacturer's instructions. Briefly, 5 x 10^5 cells were seeded in 6-cm plates. The day after, cells were incubated with reagents and 2-5 μg of vector DNA or 10 μg/ml of poly(rI-rC) dsRNA in serum-free medium at 37°C for 3-5 h. The medium was then replenished with 10% serum and cells were incubated for an additional 24 or 48 hours (unless specified in figure legends) before proteins were extracted.

1.4 RNA Interference

For siRNA transfection, 1.25 x 10^5 HT1080 cells were seeded onto 6-well plates. The following day, cells were transfected with 200 pmoles of non-specific (GL-2) or human eIF2α or human PERK siRNA (Dharmacon) using 4 μl LipofectAMINE 2000 (Invitrogen) in medium devoid of serum. Six hours post-transfection, the plates were washed with serum-free DMEM and replenished with medium containing 10% serum. Cells were incubated at 37°C for an additional 72 hours before being treated with thapsigargin or coumermycin.

1.5 Biochemical Reagents

Cells were treated with: IFNα/β (1000 IU/ml, Cedarlane), IFNγ (100 IU/ml, Cedarlane), thapsigargin (TG, 1 μM, Sigma), tunicamycin (TM, 10 μg/ml, Sigma),

zVAD-fmk (10 μM), MG132 (10 μM, Biomol), 1-Aza-Kenpaullone (1 μM), Sal003 (75 μM, compound 3, salubrinal derivative, generous gift from J. Pelletier), coumermycin (100 ng/ml, Sigma), adriamycin (ADR, 1 μM).

1.6 VSV Infection & Plaque Assay

Cells were infected with vesicular stomatitis virus (VSV, Indiana serotype) with a multiplicity of infection (MOI) indicated in figures. Cells were plated onto 6 cm plates, and virus was allowed to adhere to cells at room temperature for 1 hour in serum-free medium. After 1 hour, medium was replenished with 10 % CS and cells were incubated at 37°C for indicated period of time post-infection before proteins were extracted.

The VSV plaque assay protocol was previously described (294). Briefly, $PERK^{+/+}$ and $PERK^{-/-}$ MEFs were infected with vesicular stomatitis virus (VSV, MOI 1 or 100). One hour post-infection, the non-adherent virus was removed and plates were washed twice with serum-free DMEM and replenished with complete medium. At different hours post-infection, medium was collected and was serial diluted with serum-free DMEM then used to infect VERO cells (100% confluence). One hour post-infection, medium from the VERO cells was removed and replaced with complete medium containing 0.5% methyl cellulose (Sigma-Aldrich) for 24-36 hours. VERO cells were fixed in 4% formaldehyde and stained with crystal violet. Plaques were counted and titers calculated as plaque forming units (pfu)/ml. Triplicate experiments were performed, and the averages of the viral titers were calculated.

1.7 Recombinant Vaccinia/T7 Virus Expression System

One day before transfection, 0.8 x 10^6 HeLa or Huh7 cells were seeded in 6-cm plates. Cells were infected with recombinant vaccinia virus containing the bacterial T7 RNA polymerase gene (106) for an hour followed by transfection with LipofectAMINE Plus reagents (Invitrogen) and 2 μg of DNA containing the gene of interest in expression vector under the control of T7 promoter. Cells were incubated in serum-free medium at 37°C for 6 hours followed by the addition of complete medium and incubation for an additional 18 hours before protein extraction.

2. PLASMIDS

The plasmids used were previously described: GFP-p53 WT cDNA in the pEGFP/N1 vector (40), pcDNA3 plasmids containing wild type PERK or mutant PERK K618A (128), and wild type PKR or dominant-negative PKRΔ6 (91). Plasmids containing BiP/Grp78, XBP-1 or CHOP/GADD153 were generous gifts from D. Ron.

3. PROTEIN ANALYSIS

3.1 Protein Extraction

Cells were washed twice with ice-cold phosphate-buffered saline (PBS) and proteins were extracted in ice-cold lysis buffer containing 10 mM Tris-HCl, pH 7.5, 50 mM KCl, 2 mM $MgCl_2$, 1% Triton X-100, 3 μg/ml aprotinin, 1 μg/ml pepstatin, 1 μg/ml

leupeptin, 1 mM dithiothreitol, 0.1 mM Na_3VO_4, and 1 mM phenylmethylsulfonyl fluoride. Extracts were kept on ice for 15 min, centrifuged at 10,000 × *g* for 15 min (4 °C), and supernatants were stored at -80 °C. Proteins were quantified by Bradford assay (BioRad).

3.2 SDS-PAGE

Protein extracts were subjected to sodium dodecyl sulfate-polyacrylamide gel electrophoresis (SDS-PAGE) as described (283). Proteins were then electroblotted onto PVDF membranes (Immobilon P, Millipore).

3.3 Two-Dimensional (2D) Gel Electrophoresis

$PERK^{+/+}$ and $PERK^{-/-}$ MEFs were infected with VSV or treated with thapsigargin before being lysed with 8 M urea, 4% (w/v) CHAPS, 65 mM DTT, 0.5% (v/v) IPG buffer pH 4-7 or pH 6-11 (Bio-Rad). Isoelectric focusing (IEF) step was performed using the Ettan IPGphor Isoelectric Focusing unit (Amersham) and 7 cm strips pH 4-7 or pH 6-11 (Bio-Rad). The strips were passively rehydrated with 125 µl of rehydration buffer containing 80 µg of the protein extracts, 8 M urea, 2% (w/v) CHAPS, 10 mM DTT, 0.5% (v/v) IPG buffer pH 4-7 or pH 6-11, and trace amount of bromophenol blue for 10 hours. IEF was performed at 150 V for 40 minutes, 500 V for 40 minutes, 1000 V for 40 minutes, and 5000 V for 2.5 hours. The strips were then equilibrated for 12 minutes in 50 mM Tris-HCl pH 8.8, 6 M urea, 30% glycerol, 2% SDS, 1% (w/v) DTT, and trace amount of bromophenol blue. The strips were then incubated for 5 minutes in 50 mM Tris-HCl pH 8.8, 6 M urea, 30% glycerol, 2% SDS, 2.5% (w/v) iodoacetamide, and trace

amount of bromophenol blue. The equilibrated strips were then subjected to second dimension with SDS-10%PAGE followed by immunoblot analysis.

3.4 Immunoblot Analysis

3.4.1 Western Blot

Following SDS-PAGE and protein transfer onto PVDF membranes, the membranes were blocked in phosphate buffered saline with 0.5% Triton-X100 (PBST) containing 5% non-fat milk for one hour at room temperature. Primary antibodies (1:1000 dilution) were all prepared in PBST containing 5% BSA and incubated overnight at 4°C. The following day, membranes were washed 6 times with 5 minute incubation periods with PBST at room temperature. Then the corresponding secondary antibody was incubated for one hour at room temperature. All secondary antibodies (1:1000 dilution) were prepared in PBST containing 5% non-fat milk. The membranes were then washed 6 times for 5 minutes with PBST and proteins were visualized by enhanced chemiluminescence (ECL). Quantification of bands was performed by densitometry using the NIH Image 1.54 software.

3.4.2 Primary Antibodies

The primary antibodies used were as follows: goat polyclonal antibody to PERK (T-19, Santa Cruz), rabbit polyclonal antibody to phosphothreonine 980 of PERK (Cell Signaling), rabbit polyclonal antibody to PERK (this antibody detects a shift in the migration of PERK when activated, generous gift from D. Ron), rabbit polyclonal antibody to PERK (Cell Signaling), rabbit polyclonal antibody to phosphoserine 51 of

eIF2α (1:5000 dilution, BioSource), mouse monoclonal antibody to mouse eIF2α, rabbit polyclonal anti-human eIF2α (sc-11386, Santa Cruz, CA), rabbit antiserum to TrpE-yeast eIF2α fusion protein (CM-217), rabbit polyclonal antibody to Caspase-12 (Cell Signaling), mouse monoclonal antibody to myc epitope (9E10, Santa Cruz), rabbit polyclonal antibody to phospho-JNK-1 (Cell Signaling), rabbit polyclonal antibody to JNK-1 (Cell Signaling), rabbit polyclonal antibody to phospho-p38 MAPK (Cell Signaling), rabbit polyclonal antibody to p38 MAPK (Cell Signaling), mouse monoclonal antibody to PKR (B-10, sc-6282, Santa Cruz), rabbit polyclonal antibody to PKR (D-20, sc-708, Santa Cruz), rabbit polyclonal antibody to phosphothreonine 446 of PKR (UBI), rabbit antiserum to residues 101-112 within the N-terminus of mouse PKR (1), rabbit antiserum to human PKR (first 80 amino acids of hPKR), rabbit polyclonal antibody to VSV (1:5000 dilution, manufactured by Dr. Earl Brown), rabbit polyclonal antibody to PARP (Cell Signaling), mouse monoclonal antibody to Actin (1:5000 dilution, Clone C4, ICN Biomedicals Inc.), rabbit polyclonal anti-histidine antibodies (sc-803, Santa Cruz), rabbit antiserum to phosphoserine 32 of IκBα (9241S, New England Biolabs), rabbit antiserum to IκBα (06-494, Upstate Biotechnology Inc.), rabbit polyclonal antibody to mouse p53 (FL-393, Santa Cruz), mouse monoclonal antibody to human p53 (DO-1, Ab-6, Oncogene Science), a rabbit polyclonal antibody to mouse p53 (CM-5, Novocastra), rabbit polyclonal antibody to GSK3β (Cell Signaling), rabbit polyclonal antibody to phosphoserine 641/645 of glycogen synthase (Upstate), mouse monoclonal antibody to glycogen synthase (Cell Signaling), rabbit polyclonal antibody to PUMA (3041, ProSci Inc.), rabbit polyclonal antibody to NOXA (2437, ProSci Inc.).

3.4.3 Secondary Antibodies

Anti-mouse IgG-HRP or anti-goat IgG-HRP or anti-rabbit IgG-HRP conjugated antibodies were used as secondary antibodies (1:1000 dilution). Proteins were visualized by enhanced chemiluminescence (ECL) according to manufacturer's specification (Amersham Life Science Inc., Cleveland, OH).

3.5 Pulldown Assays

3.5.1 Immunoprecipitation

Equal amounts of protein extracts were incubated with 2 μg of the specified antibody for 2 hours in 4°C with rotation. Proteins were then immunoprecipitated using 50 μl of a 50% suspension of anti-mouse IgG (whole molecule) agarose beads (Sigma) or protein A-agarose beads (Pharmacia). The samples were then rotated for additional 2 hours at 4°C. The immunoprecipitates were washed three times in the lysis buffer, and subjected to SDS-PAGE and immunoblot analysis.

3.5.2 Poly(rI-rC) Pulldown

Equal amount of protein extracts were used for a pulldown with poly(rI-rC) dsRNA coupled to agarose beads (Type 6, Amersham Pharmacia Biotech). The samples were rotated for 2 hours at 4°C before being washed 3 times with lysis buffer. The dsRNA-bound proteins were subjected to SDS-PAGE followed by immunoblot analysis.

4. KINASE ASSAYS

4.1 PKR AUTOPHOSPHORYLATION KINASE ASSAY

Whole cell extracts (200-500 μg of protein) were used for a pulldown with poly(rI-rC) dsRNA coupled to agarose beads (Type 6, Amersham Biosciences) or for an immunoprecipitation with the anti-mPKR antibody (D-20). The bound proteins were equilibrated in kinase buffer (10 mM Tris-HCl pH 7.7, 50 mM KCl, 2 mM $MgCl_2$, 3 μg/ml aprotinin, 1 μg/ml pepstatin, 1 μg/ml leupeptin, 1 mM DTT, and 1 mM PMSF) and incubated in the presence of 1 μCi of [γ-^{32}P]ATP. The reactions were incubated at 30°C for 30 min and subjected to SDS-10%PAGE followed by either immunoblot analysis or autoradiography.

4.2 GSK3β KINASE ASSAY

For measuring GSK3 activity, 100 μg whole cell extracts were used for immunoprecipitation with anti-GSK3β antibody (Cell Signaling) and protein A-agarose beads (Pharmacia). Bound proteins (15 μl) was mixed with 15 μl of kinase buffer (50 mM HEPES (pH 7.2), 0.1 mM EDTA, 0.1 mM DTT, 1 μCi [γ^{32}P]ATP, 10 mM $MgCl_2$, and 5 mg/ml synthetic phospho-CREB substrate peptide (KRREILSRRP[pS]YR) with or without 1-Aza-kenpaullone (1 μM). After 30 min of incubation at 30°C, 10 μl of TCA was added and the reaction mixtures were centrifuged, and 20 μl of the supernatant was spotted onto Whatman P10 phosphocellulose paper. Filters were washed in three changes of 0.85% phosphoric acid, dried and subjected to liquid scintillation counting.

4.3 PKR-eIF2α Kinase Assay

Protein extracts were immunoprecipitated with rabbit polyclonal antibody to mouse PKR (D-20, Santa Cruz) and protein A-agarose beads (Pharmacia). The immunoprecipitates were equilibrated in 1 X PKR kinase buffer containing 10 mM Tris-HCl pH 7.7, 50 mM KCl, 2 mM $MgCl_2$, 3 μg/ml aprotinin, 1 μg/ml pepstatin, 1 μg/ml leupeptin, 1 mM DTT, and 1 mM PMSF. Activator reovirus dsRNA was then added to the final concentration of 0.1 μg/ml in the presence of 1 μg of bacteria purified histidine-tagged eIF2α (368) and 1 μM ATP. After incubation at 30°C for 30 min, the reactions were subjected to SDS-PAGE and immunoblotting with rabbit antiserum to phosphoserine 51 of eIF2α followed by immunoblotting with rabbit polyclonal anti-histidine antibodies.

5. FLUORESCENCE MICROSCOPY

GFP-positive and live cells were scored and classified into two groups; the first group with fluorescence predominantly in the nucleus and the second with fluorescence in both nucleus and cytoplasm. Total green fluorescence in the nucleus and whole cell were quantified with AxioVision 4.5 software from 100 randomly selected GFP-positive and live cells.

For immunofluorescence, cells were stained with a 1:200 dilution for mouse monoclonal antibody to p53 (DO-1, Oncogene Science) or a 1:100 dilution for rabbit polyclonal antibody to GSK3β (Cell signaling). Cells were incubated with primary

antibodies for 16 h at 4°C, washed with PBS, and incubated for 1 h with Alexa Fluro-488-conjugated secondary antibody or Alexa Fluro-546-conjugated secondary antibody (Molecular Probes). The nucleus was visualized after staining with 0.05 μg/mL of 4,6-diamidino-2-phenylindole (DAPI; Sigma). Images were captured on a Zeiss microscope using equal exposure times. Nuclear/cytoplasmic ratios were determined by calculating total pixel intensity in a circle of 4 μm in diameter in the nucleus and the cytoplasm using AxioVision 4.5 software. The background was determined by calculating pixel intensity in a 4 μm diameter cell-free area. This area was then subtracted from the nuclear and cytoplasmic measurements for each cell within the microscopy field.

6. YEAST

6.1 YEAST STRAINS

The yeast strain used was J110 (*Mata ura3-52 leu2-3, 2-112 trp*1-Δ*63 gcn2*Δ<LEU2>*@leu2)* (206).

6.2 YEAST PLASMIDS

Wild type mouse PKR (mPKR) and human PKR (hPKR) were inserted in pYES3/CT vector (Invitrogen) whereas the exon-skipped form of mPKR (ES-mPKR; aa 136 to 518) was subcloned into pYES2 vector (Invitrogen).

6.3 Yeast Transformation

J110 yeast cells were transformed with DNA using the LiAc method (3). Transformed strains were grown in SGAL liquid medium overnight at $30^{O}C$.

6.4 Yeast Protein Extraction

Yeast protein extracts were prepared as described (3). Immunoblot analysis was performed as described above.

7. CLONING

7.1 List of Primers

Table 1: PCR Primers used in Cloning

	Primers		Sequence	Tm (°C)	PCR cycles
mPKR	**T502**	*Forward*	5′-CAGCACCTGGAAGTTTTTCC-3′	58	35
	T302	*Reverse*	5′-TCATTTTCCAGGGCTGTTGC-3′		
	T503	*Forward*	5′-TTCAGGTGTCACCAAACAGG-3′	58	35
	T303	*Reverse*	5′-GTTCAGCTAGAATAAGGCCC-3′		

7.2 RT-PCR

Exon-skipped *mPKR* cDNA from N-PKR$^{-/-}$ cells was cloned as described (356) and subcloned into BamHI/XbaI sites of pYES2 expression vector (Invitrogen). Table 1 summarizes all the primers used for RT-PCR analysis of RNA from C-PKR$^{-/-}$ cells. The primers were designed according to the mouse PKR sequence [accession number:

M65029; locus: MUSSTKINA (154)]. Total RNA isolation was established using TRIZOL (GIBCOBRL) according to the protocol provided by the manufacturer. One μg of RNA was used for reverse transcription (RT) with the Moloney Murine Leukemia Virus (M-MLV) reverse transcriptase (GIBCOBRL) using the oligo-$(dT)_{18}$ primer (RT was performed as described by manufacturer).

The single-stranded cDNA was amplified by PCR using the T502/T302 or T503/T303 set of primers (see Table 1) and *Taq* DNA polymerase (cat.#1146 165, Roche Diagnostics) with 35 PCR cycles to generate the final product: 1 minute at 94°C for the denaturing step, 1.5 minutes at 58°C for the annealing step, 2 minutes at 72°C for the elongation step. PCR products were visualized by ethidium bromide staining under a UV light source. The PCR products generated by the T503/T303 primer set were subcloned into the pCR2.1 vector provided by the TA cloning kit (K2000-01, Invitrogen) and subjected to DNA sequencing.

7.3 EXPRESSION OF MPKR ISOFORMS IN MOUSE TISSUE

Normalized cDNA from 12 different mouse tissues (mouse MTC Panel I, K1423-1, Clontech) were subjected to 35 cycles of PCR using the T502/T302 set of primers (Table1) with 1 minute at 94°C for the denaturing step, 1.5 minutes at 58°C for the annealing step, 2 minutes at 72°C for the elongation step. PCR products were separated in agarose gels and subjected to Southern blot analysis using as a probe the entire wild type *mPKR* cDNA labeled with [^{32}P–α]dCTP, as previously described (302).

8. POLYSOME PROFILING

8.1 Polysome Extraction & Fractionation

Approximately 2 X 10^7 cells (two 15 cm plates/gradient) were used for each sucrose gradient. Prior to harvest, 100 μg/ml of cycloheximide was added to the medium and then removed immediately. Plates were then washed 3 times with 10 ml ice cold 1 X PBS containing 100 μg/ml cycloheximide, and the plates were placed on ice. The cells were lysed directly on plates with 500 μl of polysome lysis buffer (15 mM Tris-HCl, pH 8.0, 5 mM $MgCl_2$, 0.3 M NaCl, 0.5 mM DTT, 100 μg/ml cycloheximide, and 1% Triton X-100). Extracts were transferred into a 1.5 ml Eppendorf tubes, and placed on ice for 10 minutes. Tubes were centrifuged at 13 000 X g for 10 minutes. Supernatants were recovered and layered onto 10 ml 10-55% sucrose gradients (10-55% sucrose, 20 mM Tris-HCl, pH 8.0, 140 mM KCl, 5 mM $MgCl_2$, 0.5 mM DTT, and 100 μg/ml cycloheximide). The gradients were prepared with the ISCO Model 160 Gradient Former. The lysate was sedimented at 40,000 rpm for 2h35m in a SW40Ti rotor at 4°C.

The gradients were fractionated into 20 fractions of 500 μl using the ISCO Density Gradient Fractionation System-Foxy Jr. Fraction Collector while measuring the absorbance at 254 nm. Samples were collected into 1.5 ml Eppendorf tubes and stored at -80°C.

8.2 RNA Isolation of Polysome Fractions

The RNA was isolated from each fraction (500 μl) using equal amount of volume of TRIzol (GibcoBRL). Fractions were centrifuged for 15 minutes at 13 000 X g after a

volume of 100 µl of chloroform was added in order to separate aqueous phase from the organic phase. The aqueous (supernatant) phase was transferred to a new tube containing 500 µl of isopropanol and RNA was precipitated overnight at -20°C. The following day, tubes were centrifuged at 13 000 X g for 30 minutes. RNA pellet was washed with 400 µl of 75% ethanol (-20°C) and air-dried for 5-10 minutes before being dissolved in 10 µl dH_2O. Samples were stored at -80°C.

8.3 RT-PCR of Polysome Fractions

8.3.1 List of Primers

Table 2: PCR Primers used in Polysome Profile Analysis

Primers		Sequence	Tm (°C)	PCR cycles
p53	*Forward*	5′-AACCTACCAGGGCAGCTACG-3′	58.5	28
	Reverse	5′-TTCCTCTGTGCGCCGGTCTC-3′		
ATF4	*Forward*	5′-CTGGCTGTGGATGGGTTGGT-3′	58	23
	Reverse	5′-GAGGGGCTGTGCTGCGGAGA-3′		
GAPDH	*Forward*	5′-CATCATCTCTGCCCCCTCTGCT-3′	60	23
	Reverse	5′-GACGCCTGCTTCACCACCTTCT-3′		

8.3.2 RT-PCR

A volume of 3 µL of the extracted RNA (from each fraction) was used for reverse transcription using the SuperScript II RNase H- Reverse Transcriptase (200U/µL, 18064-014, Invitrogen) and 100 µM oligo-dT primer ($dT_{20}VN$) according to the manufacturer's instructions. Once reaction was completed, the final volume of the 20 µl reaction was adjusted to 100 µl with dH_2O, and 2 µl of the diluted cDNA was used for polymerase

chain reaction. The TaqPlus Precision Polymerase (1000 U, 600212, Stratagene) was used for PCR according to the manufacturer's specifications. Table 2 summarizes the primers used for PCR, including the number of cycles and corresponding annealing temperature for each set of primers. PCR program: (94°C, 1 min; annealing temperature, 1 min; 72°C, 1 min) X number of cycles.

9. FLOW CYTOMETRY

Apoptotic assays were carried out by surface staining with the Annexin-V FITC apoptosis kit (BioSource) following the manufacturer's instructions. The stained cells were analyzed by flow cytometry using FACScan (Becton Dickinson), and data was analyzed using the WinMDI 2.8 software (Scripp Institute). Samples were gated on a dot-plot showing forward scatter and side scatter in order to exclude cell debris not within normal cell size. Gated cells were plotted on a dot-plot showing Annexin-V staining (FL1-H) and Propidium Iodide (PI) staining (FL2-H).

CHAPTER III - RESULTS

1. CHARACTERIZATION OF PKR GENE PRODUCTS IN PKR$^{-/-}$ MEFS

1.1 N-TERMINAL PKR KNOCKOUT MEFS

1.1.1 Detection of the Exon-skipped Mouse PKR Product in N-PKR$^{-/-}$ MEFs

The striking signaling differences between the two types of PKR$^{-/-}$ cells prompted us to investigate the possible expression of truncated PKR proteins as a result from incomplete disruption of the *pkr* gene. Specifically, Yang *et al.* (356) initially hypothesized that the N-PKR$^{-/-}$ mice might express a truncated PKR, which is the product of translation of a *PKR* mRNA devoid of exons 2 and 3. Translation of this exon-skipped mRNA could initiate from an AUG that corresponds to methionine 136 producing a 382 amino acid (aa) C-terminal fragment of mPKR (356). In fact, the 42-44 kDa exon-skipped mouse PKR (ES-mPKR) protein was detected in reticulocyte lysates programmed to translate the *ES-mPKR* mRNA from N-PKR$^{-/-}$ cells (356). However, Yang *et al.* were not able to detect ES-mPKR expression in extracts from N-PKR$^{-/-}$ cells due to the unavailability of antibodies against the C-terminus part of mPKR (356).

To test whether N-PKR$^{-/-}$ cells express the PKR fragment produced from the translation of exon-skipped mouse *PKR* mRNA (Fig. 17A) (356), we performed western blot analysis with protein extracts from strain matched PKR$^{+/+}$ and N-PKR$^{-/-}$ MEFs (Fig. 17B). To induce PKR protein expression, MEFs were treated with mouse IFNα/β. Immunoblot analysis with an anti-PKR monoclonal antibody (mAb) specific for an epitope within the C-terminus half of the kinase (clone B-10, top panel) detected the expression of full-length PKR in PKR$^{+/+}$ cells (lanes 1 and 2) and the presence of a 45 kDa protein in isogenic N-PKR$^{-/-}$ MEFs (lane 3), which was highly induced by IFN

treatment (lane 4). To further substantiate this finding, we performed a western blot analysis with protein extracts from isogenic $PKR^{+/+}$ and N-$PKR^{-/-}$ MEFs using a rabbit polyclonal anti-PKR Ab (clone D-20) specific for an epitope at the very C-terminus end of the kinase (Fig. 1B, bottom panel). Similarly, we observed the presence of the 45 kDa protein in N-$PKR^{-/-}$ cells (lane 3), which was significantly induced after IFN treatment (lane 4). Note that this protein was undetectable in protein extracts from isogenic $PKR^{+/+}$ cells (lanes 1 and 2). To confirm that the 45 kDa protein is specifically expressed in N-$PKR^{-/-}$ cells, we performed an immunoprecipitation with the rabbit polyclonal anti-mouse PKR Ab (clone D-20) followed by immunoblotting with the monoclonal anti-mouse PKR Ab (clone B-10; Fig. 17C). This assay demonstrated the expression of the 45 kDa exon-skipped mPKR (ES-mPKR) protein in the N-$PKR^{-/-}$ cells.

Figure 17. Immunodetection of exon-skipped mouse PKR in N-PKR$^{-/-}$ MEFs.

(A) ***Schematic representation of ES-mPKR.*** ES-mPKR is translated from an alternative start site at position 553 within exon 5 of the *PKR* mRNA (Met 136). The primary initiator AUG within exon 2 was disrupted by the neomycin resistance gene (neo^r) to generate the N-PKR$^{-/-}$ mouse. ES-mPKR is a 382 aa, 45 kDa protein, which contains part of the dsRNA binding-motif 2 (dsRBM2), and an intact kinase domain (KD).

(B) ***ES-mPKR is recognized by two different PKR antibodies.*** Protein extracts from isogenic (i.e. genetic background 129Sv(ev) x C57BL/6J) PKR$^{+/+}$ and N-PKR$^{-/-}$ MEFs before (lanes 1 and 3) or after stimulation with mIFNα/β (1000 IU/ml for 18 hours; lanes 2 and 4) were subjected to immunoblot analysis with a anti-mPKR mAb (B-10; top panel) or with a rabbit polyclonal anti-mPKR antibody (D-20; bottom panel) both specific for the C-terminus domain of mPKR. The positions of mPKR and ES-mPKR protein are indicated.

(C) ***Immunoprecipitation of ES-mPKR from N-PKR$^{-/-}$ MEFs.*** Protein extracts (500 μg) of PKR$^{+/+}$ and N-PKR$^{-/-}$ MEFs before (lanes 1 and 3) and after stimulation with mIFNα/β (1000 IU/ml, 18 hours; lanes 2 and 4) were subjected to immunoprecipitation with 2 μg of the rabbit polyclonal anti-mPKR Ab (D-20). Immunoprecipitates were then subjected to SDS-10%PAGE and immunoblotted with the anti-mPKR mAb (B-10, Santa Cruz). The positions of mPKR and ES-mPKR proteins are indicated.

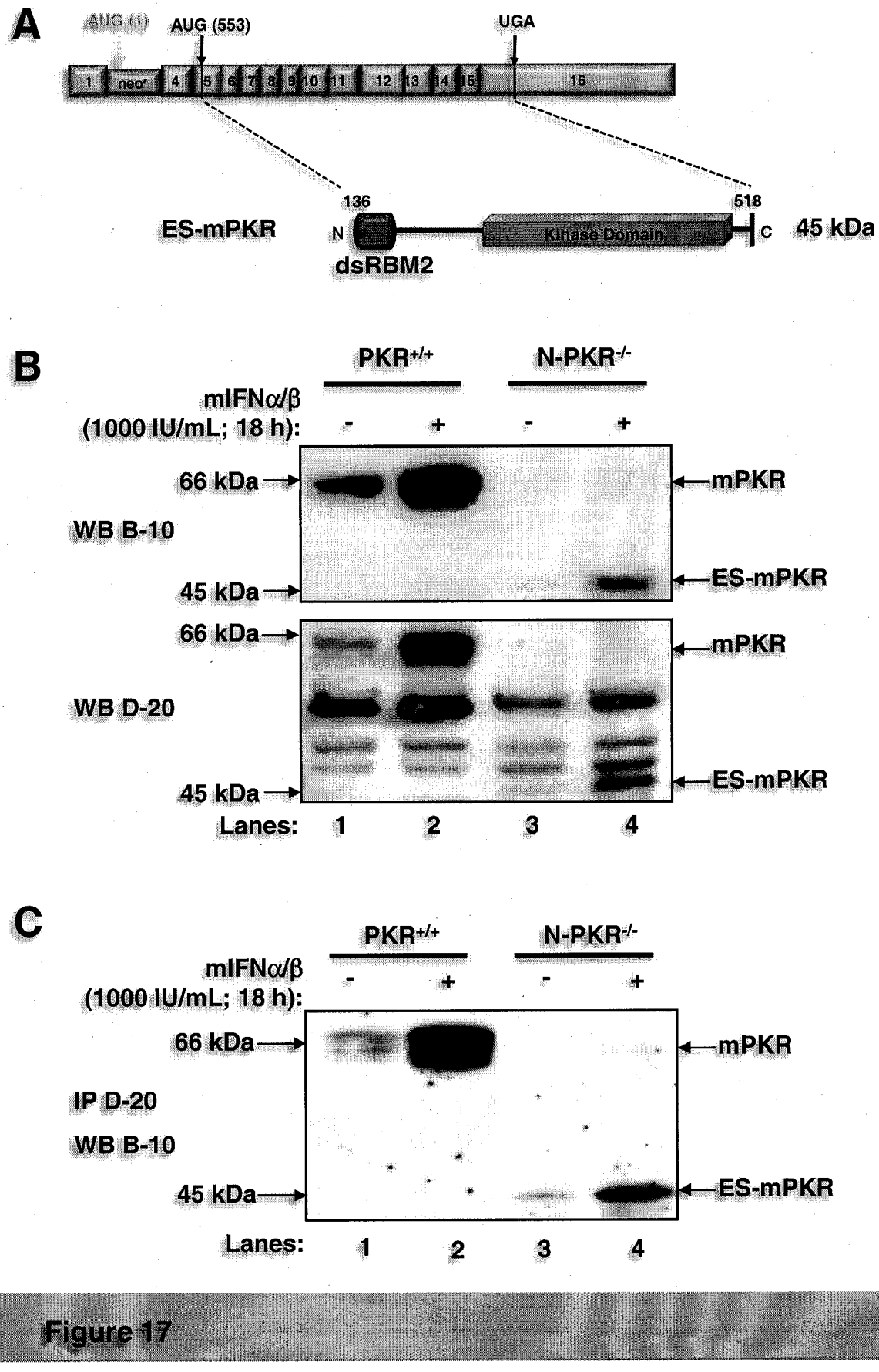
A
AUG (1)
AUG (553)
UGA
1
neo
4
5
6
7
8
9
10
11
12
13
14
15
16
136
518
ES-mPKR
N
Kinase Domain
C
45 kDa
dsRBM2
B
PKR+/+
N-PKR-/-
mIFNα/β
(1000 IU/mL; 18 h):
-
+
-
+
66 kDa
mPKR
WB B-10
45 kDa
ES-mPKR
66 kDa
mPKR
WB D-20
45 kDa
ES-mPKR
Lanes:
1
2
3
4
C
PKR+/+
N-PKR-/-
mIFNα/β
(1000 IU/mL; 18 h):
-
+
-
+
66 kDa
mPKR
IP D-20
WB B-10
45 kDa
ES-mPKR
Lanes:
1
2
3
4

Figure 17

1.1.2 ES-mPKR Contains eIF2α Kinase Activity *In Vivo* and *In Vivo*

Since ES-mPKR possesses an intact kinase domain, we examined whether ES-mPKR retains the catalytic activity of PKR. To this end, protein extracts from isogenic $PKR^{+/+}$ and $N\text{-}PKR^{-/-}$ cells were subjected to immunoprecipitation with the rabbit polyclonal anti-mouse PKR antibody (clone D-20) followed by *in vitro* kinase assay in the presence of recombinant histidine-tagged eIF2α, dsRNA and ATP (Fig. 18A). Phosphorylation of eIF2α was then detected by immunoblot analysis using a phosphoserine 51 specific anti-eIF2α antibody (top panel). The levels of recombinant eIF2α in the kinase reactions were measured by immunoblot analysis with anti-histidine antibodies (bottom panel). These assays showed that eIF2α is phosphorylated on serine 51 in $N\text{-}PKR^{+/+}$ cells (lane 1), and this phosphorylation was more highly induced after IFN treatment (lane 2). On the other hand, eIF2α phosphorylation in the PKR immunoprecipitates from $N\text{-}PKR^{-/-}$ MEFs (lane 3) was lower than in $PKR^{+/+}$ MEFs (lane 1) and detectable only after IFN treatment (lane 4). These differences most likely reflected the different levels of expression of full-length mPKR and ES-mPKR in $PKR^{+/+}$ and $N\text{-}PKR^{-/-}$ cells, respectively (Fig. 17B).

We tested the ability of ES-mPKR to induce the phosphorylation of eIF2α *in vivo*. For this, we used the human hepatocarcinoma Huh7 cells, which exhibit 80-90% transfection efficiency as judged by the expression of the green fluorescence protein (GFP, data not shown). That is, WT-mPKR and ES-mPKR were transiently expressed in Huh7 cells using the vaccinia/T7 virus system (Fig. 18B). Protein extracts were subjected to immunoblot analysis for mPKR (top panel), eIF2α serine 51 phosphorylation (middle

panel), or total eIF2α levels (bottom panel). We found that expression of both WT-mPKR and ES-mPKR was able to induce the phosphorylation of endogenous eIF2α (lanes 2 and 3) demonstrating that ES-mPKR indeed acts as an eIF2α kinase *in vivo*. In these experiments, we noticed that ES-mPKR migrated higher than the 45 kDa protein marker (Fig. 18B, lane 3; Fig. 19A, lane 3) probably due to its phosphorylation caused by overexpression.

1.1.3 ES-mPKR has no dsRNA Binding Activity

We also examined whether ES-mPKR retains its capacity to bind dsRNA and autophosphorylate. To this end, we used HeLa cells to express transiently wild type (WT) mPKR or ES-mPKR using the recombinant vaccinia/T7 virus method. In this method, transfected genes under the control of bacteriophage T7 promoter are efficiently transcribed in the cytoplasm by the T7 RNA polymerase delivered into the cells by infection with recombinant vaccinia viruses (106). This method is suitable for expressing PKR and studying the translational functions of the kinase (206).

First, we tested the dsRNA-binding capacity of ES-mPKR. Protein extracts from HeLa cells expressing WT-mPKR and ES-mPKR were incubated with poly(rI-rC)-agarose beads, and proteins bound to dsRNA were detected by immunoblotting (Fig. 19A). We found that WT-mPKR was capable of binding to dsRNA (lane 5) unlike ES-mPKR (lane 6).

When the dsRNA-bound proteins were subjected to *in vitro* autophosphorylation assay in the presence of [^{32}P-γ]ATP (Fig. 19B), we found that WT-mPKR was highly autophosphorylated (lane 2) whereas no kinase activity was detected for ES-mPKR (lane

3). The high MW band (~110 kDa) phosphoprotein was non-specific. These data suggested that ES-mPKR lacks the ability to bind dsRNA and conceivably the capacity to autophosphorylate in the presence of dsRNA.

Figure 18. Functional analysis of the kinase activity of ES-mPKR.

(A) ***ES-mPKR exhibits eIF2α kinase activity in vitro.*** Protein extracts (500 μg) of $PKR^{+/+}$ and N-$PKR^{-/-}$ MEFs before (lanes 1 and 3) and after stimulation with mIFNα/β (1000 IU/ml, 18 hours; lanes 2 and 4) were subjected to immunoprecipitation with 2 μg of the rabbit polyclonal anti-mPKR Ab (D-20, Santa Cruz). Immunoprecipitates were incubated with 1 μg of recombinant histidine-tagged eIF2α in the presence of 0.1 μg/ml activator reovirus dsRNA and 1 μM ATP. After incubation at 30ºC for 30 min, the reactions were subjected to SDS-12%PAGE and immunoblot analysis using a rabbit polyclonal anti-phosphoserine 51 eIF2α specific Ab (top panel) followed by immunoblot analysis with anti-histidine tag Ab (bottom panel).

(B) ***ES-mPKR exhibits eIF2α kinase activity in vivo.*** Huh7 cells were infected with vaccinia virus/T7, and transfected with either pYES2 vector DNA (mock; lane 1), WT-mPKR in pYES3/CT vector (lane 2), ES-mPKR in pYES2 vector (lane 3). Ten μg of protein extracts were subjected to a SDS-12%PAGE followed by immunoblot analysis with either rabbit polyclonal anti-mPKR Ab (D-20; top panel), rabbit polyclonal anti-phosphoserine 51 eIF2α Ab (second panel) or rabbit polyclonal anti-human eIF2α Ab (bottom panel).

A

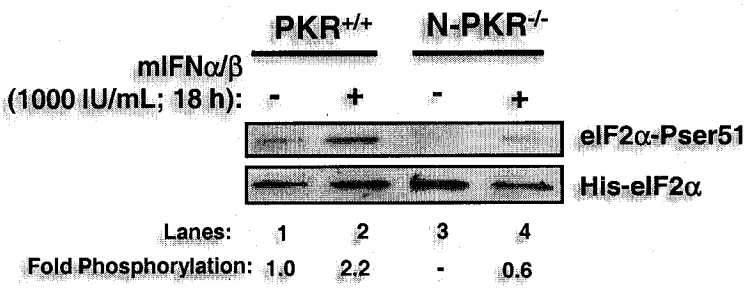
PKR+/+
N-PKR-/-
mIFNα/β
(1000 IU/mL; 18 h):
- + - +
eIF2α-Pser51
His-eIF2α
Lanes: 1 2 3 4
Fold Phosphorylation: 1.0 2.2 - 0.6

B

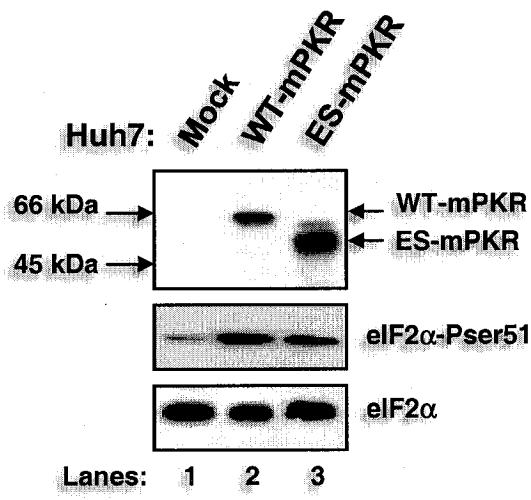
Huh7:
Mock
WT-mPKR
ES-mPKR
66 kDa
45 kDa
WT-mPKR
ES-mPKR
eIF2α-Pser51
eIF2α
Lanes: 1 2 3

Figure 18

Figure 19. Functional analysis of the dsRNA-binding activity of ES-mPKR.

(A, B) ***ES-mPKR does not bind dsRNA.*** HeLa cells were infected with recombinant vaccinia /T7 virus, and transfected with either pYES2 vector DNA alone (mock; lane 1), WT-mPKR in pYES3/CT vector (lane 2), or ES-mPKR in pYES2 vector (lane 3). Whole cell extracts (WCE) containing 10 μg of protein used to detect the expression of PKR proteins by immunoblotting with the rabbit polyclonal anti-mPKR Ab (D-20) (B, lanes 1-3). For the dsRNA pull-down assays, 200 μg of protein extracts were incubated with poly(rI-rC)-agarose beads, and the dsRNA-bound proteins were subjected to immunoblotting with rabbit polyclonal anti-mPKR Ab (D-20; **A**, lanes 4-6) or kinase assay in the presence of [^{32}P-γ]ATP (**B**, lanes 1-3).

A

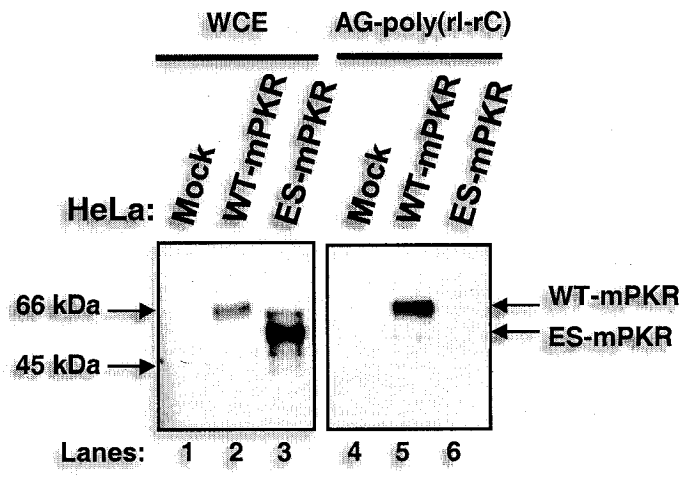
WCE
AG-poly(rI-rC)
HeLa:
Mock
WT-mPKR
ES-mPKR
Mock
WT-mPKR
ES-mPKR
66 kDa
45 kDa
WT-mPKR
ES-mPKR
Lanes: 1 2 3 4 5 6

B

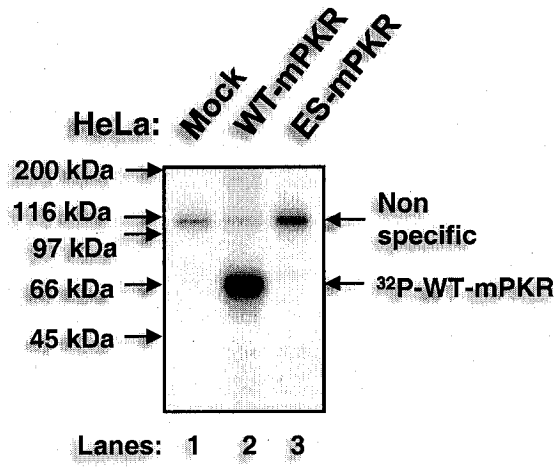
HeLa:
Mock
WT-mPKR
ES-mPKR
200 kDa
116 kDa
97 kDa
66 kDa
45 kDa
Non specific
32P-WT-mPKR
Lanes: 1 2 3

Figure 19

1.1.4 ES-mPKR is Catalytically Active in Yeast Cells

It has been demonstrated that hPKR substitutes the function for GCN2 (86), the only eIF2α kinase in *Saccharomyces cerevisiae* (87). Since expression of PKR in yeast induces endogenous eIF2α phosphorylation (86), we examined whether expression of ES-mPKR in the yeast strain J110, which lacks GCN2 (*gcn2Δ*) (272), was also capable of inducing eIF2α phosphorylation *in vivo* (Fig. 20).

To do so, ES-mPKR cDNA from N-PKR$^{-/-}$ MEFs was subcloned into pYES2 expression vector that allows expression under the galactose-inducible promoter (206). J110 cells were transformed with pYES2 vector DNA (mock, lane 1), pYES3/CT *mPKR* cDNA (lane 2), pYES2 *ES-mPKR* cDNA (lane 3) or pYES3/CT *hPKR* DNA (lane 4). The expression of the PKR forms was induced after growth of yeast cells in galactose-rich medium. Yeast protein extracts were subjected to immunoblot analysis with antibodies against mPKR (first and second from the top panels), hPKR (third from the top panel), phosphoserine 51 of eIF2α (fourth from the top panel), and endogenous eIF2α (bottom panel).

We found that the two different anti-mPKR antibodies (B-10, top panel; D-20, second from the top panel) recognized mPKR and ES-mPKR in lanes 2 and 3 respectively, but not hPKR (lane 4, third panel). We noticed that the D-20 Ab recognized full-length mPKR better than the B-10 mAb (lane 2) for reasons that are not immediately clear. We also noticed a couple of slower migrating band(s) with the anti-mPKR antibodies in lane 3, which may represent phosphorylated forms of ES-mPKR. More importantly, however, we observed that phosphorylation of endogenous eIF2α was

induced in cells expressing ES-mPKR (fourth from the top panel, lane 3) and that eIF2α phosphorylation levels were proportional to the amounts of mPKR and ES-mPKR expressed in yeast cells. These findings clearly demonstrate that ES-mPKR is catalytically active in yeast cell *in vivo*.

Figure 20. ES-mPKR exhibits eIF2α kinase activity in yeast.

The yeast strain J110 was transformed with pYES2 vector DNA (mock; lane 1), WT-mPKR in pYES3/CT vector (lane 2), ES-mPKR in pYES2 vector (lane 3) or WT-hPKR in pYES3/CT vector (lane 4). Fifty μg of protein extracts from galactose-induced cells were subjected to a SDS-12%PAGE followed by immunoblot analysis with either an anti-mPKR mAb (B-10; top panel), a rabbit polyclonal anti-mPKR Ab (D-20; second panel), a rabbit polyclonal anti-hPKR Ab (third panel), a rabbit polyclonal anti-phosphoserine 51 eIF2α Ab (fourth panel) or a rabbit polyclonal anti-yeast eIF2α Ab (bottom panel).

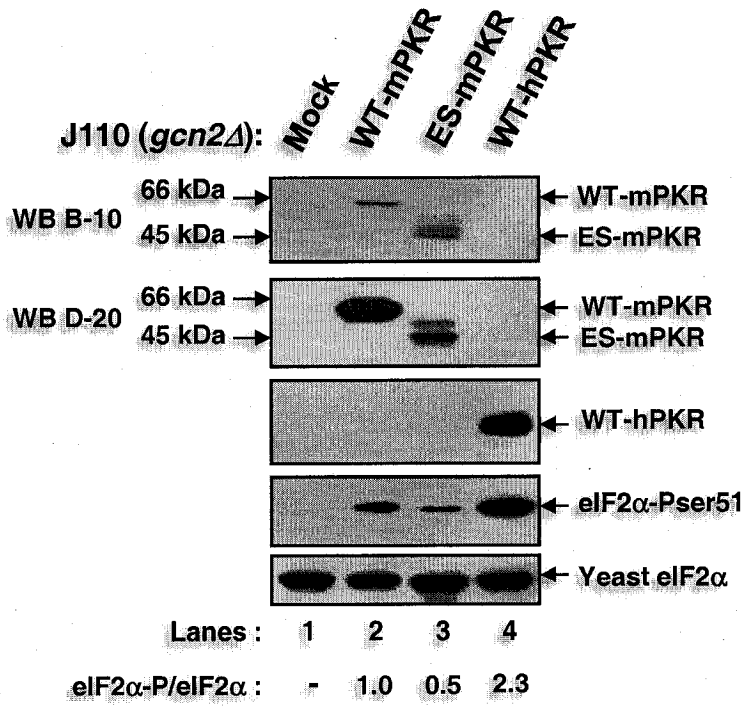
J110 (gcn2Δ):
Mock
WT-mPKR
ES-mPKR
WT-hPKR
WB B-10
66 kDa
45 kDa
WT-mPKR
ES-mPKR
WB D-20
66 kDa
45 kDa
WT-mPKR
ES-mPKR
WT-hPKR
eIF2α-Pser51
Yeast eIF2α
Lanes : 1 2 3 4
eIF2α-P/eIF2α : - 1.0 0.5 2.3

Figure 20

1.2 C-Terminal PKR Knockout MEFs

1.2.1 C-PKR$^{-/-}$ MEFs Express a 40 kDa PKR-like Protein

The above findings prompted us to perform similar experiments with MEFs from the C-PKR$^{-/-}$ mouse (2). We performed immunoblot analysis of protein extracts from untreated and IFNα/β-treated cells with either the anti-PKR B-10 mAb (Fig. 21A, top panel) or a rabbit polyclonal anti-PKR Ab specific for the dsRBM1 within the N-terminus domain of mouse PKR (Fig. 21A, middle panel) (1). Both antibodies detected the expression of a ~40 kDa protein in C-PKR$^{-/-}$ MEFs, which was more highly induced after IFN treatment (lane 4). This PKR-like protein, herein designated as mPKR*, was also detected by immunoprecipitation and immunoblotting with the anti-mPKR B10 mAb (Fig. 21B, lanes 5 to 8). The molecular size of mPKR* was better assessed by comparing its migration on SDS-PAGE to that of the 38 kDa eIF2α phosphoprotein (Fig. 21C) by immunoblotting of the same membrane with anti-mPKR B-10 mAb (lane 1) or anti-phosphoserine 51 of eIF2α (lane 2). This experiment showed that the size of mPKR* is higher than 38 kDa. In addition, since ES-mPKR is not recognized by the anti-N-terminus mPKR Ab (data not shown), we conclude that mPKR* and ES-mPKR proteins are different (see also below).

1.2.2 mPKR* Possesses dsRNA-binding Activity but is Catalytically Inactive

Next, we examined the functionality of mPKR*. In this, we performed dsRNA-binding assays with protein extracts from isogenic PKR$^{+/+}$ and C-PKR$^{-/-}$ cells (2) or isogenic PKR$^{+/+}$ and N-PKR$^{-/-}$ cells (356) using poly(rI-rC) coupled to agarose beads. The identity of the pulled-down dsRNA-bound proteins was revealed by immunoblot analysis

using the anti-PKR B-10 mAb (Fig. 22A). We found that full-length mPKR was efficiently bound to dsRNA as expected (lanes 1, 2, 5 and 6). Interestingly, mPKR* in C-PKR$^{-/-}$ cells was also bound to dsRNA efficiently (lanes 3 and 4). However, mPKR* was not present in N-PKR$^{-/-}$ cells (lanes 7 and 8). In these assays, we noticed the presence of a protein of 65 kDa in both N-PKR$^{-/-}$ and C-PKR$^{-/-}$ cells that was recognized by the anti-PKR B-10 mAb. This 65 kDa protein was not full length mPKR in C-PKR$^{-/-}$ or N-PKR$^{-/-}$ cell extracts that were contaminated with PKR$^{+/+}$ cell extracts since its expression was not induced after IFN treatment (lanes 4 and 8). Most likely, the 65 kDa protein represents an unknown dsRNA-binding protein, which is recognized by the anti-mPKR B-10 mAb (see also below).

Then, we tested whether mPKR* possesses kinase activity. To do so, protein extracts from isogenic PKR$^{+/+}$ and C-PKR$^{-/-}$ MEFs were incubated with poly(rI-rC) dsRNA-agarose beads (Fig. 22B), and phosphorylation of dsRNA-bound proteins on the pulled down beads was tested in the presence of [^{32}P-γ]ATP. The 65 kDa dsRNA-bound phosphoprotein in PKR$^{+/+}$ extracts (lane 1), whose phosphorylation was more highly induced after treatment with IFN (lane 2) was mPKR. Contrary to PKR$^{+/+}$ extracts, C-PKR$^{-/-}$ protein extracts were free of kinase activity (lanes 3, 4) demonstrating that mPKR* is catalytically inactive. Note that the 65 kDa protein recognized by the anti-PKR B-10 mAb in C-PKR$^{-/-}$ cells (Fig. 22A, lanes 3 and 4) was not phosphorylated in these assays (Fig. 22B, lanes 3 and 4) and therefore, it is unlikely to be a PKR-related protein.

Figure 21. Immunodetection of a 40 kDa PKR-like protein in C-PKR$^{-/-}$ MEFs.

(A) ***A PKR-like protein (mPKR*) is recognized by two different PKR antibodies.*** Protein extracts from isogenic PKR$^{+/+}$ and C-PKR$^{-/-}$ MEFs (i.e. genetic background 129/terSv X BALB/c) before (lanes 1 and 3) or after stimulation with mIFNα/β (1000 IU/ml for 18 hours; lanes 2 and 4) were subjected to immunoblot analysis with anti-mPKR mAb (B-10; top panel), rabbit polyclonal anti-mPKR Ab specific for the N-terminus domain of the kinase (middle panel) or anti-actin antibody mAb (bottom panel). The PKR-like protein is indicated as mPKR* (lanes 3 and 4).

(B) ***Immunoprecipitation of mPKR*.*** Protein extracts from PKR$^{+/+}$ and C-PKR$^{-/-}$ MEFs stimulated with mIFNα/β (1000 IU/ml, 18 hours) were subjected to immunoprecipitation with 1μg of anti-mPKR B-10 mAb. Immunoprecipitates were then subjected to SDS-12%PAGE and immunoblotted with anti-mPKR B-10 mAb. Lanes 1 to 4 are 50 μg of whole protein extracts (WPE) from PKR$^{+/+}$ and C-PKR$^{-/-}$ MEFs before (lanes 1 and 3) or after mIFNα/β stimulation (lanes 2 and 4).

(C) ***mPKR* is a 40 kDa protein.*** Protein extracts from C-PKR$^{-/-}$ MEFs after stimulation with mIFNα/β (1000 IU/ml, 18 hours; lanes 1) was immunoblotted with anti-mPKR B-10 mAb. The same blot was stripped and re-probed with rabbit polyclonal anti-phosphoserine51-eIF2α Ab (lanes 2), which recognizes the 38 kDa eIF2α phosphoprotein.

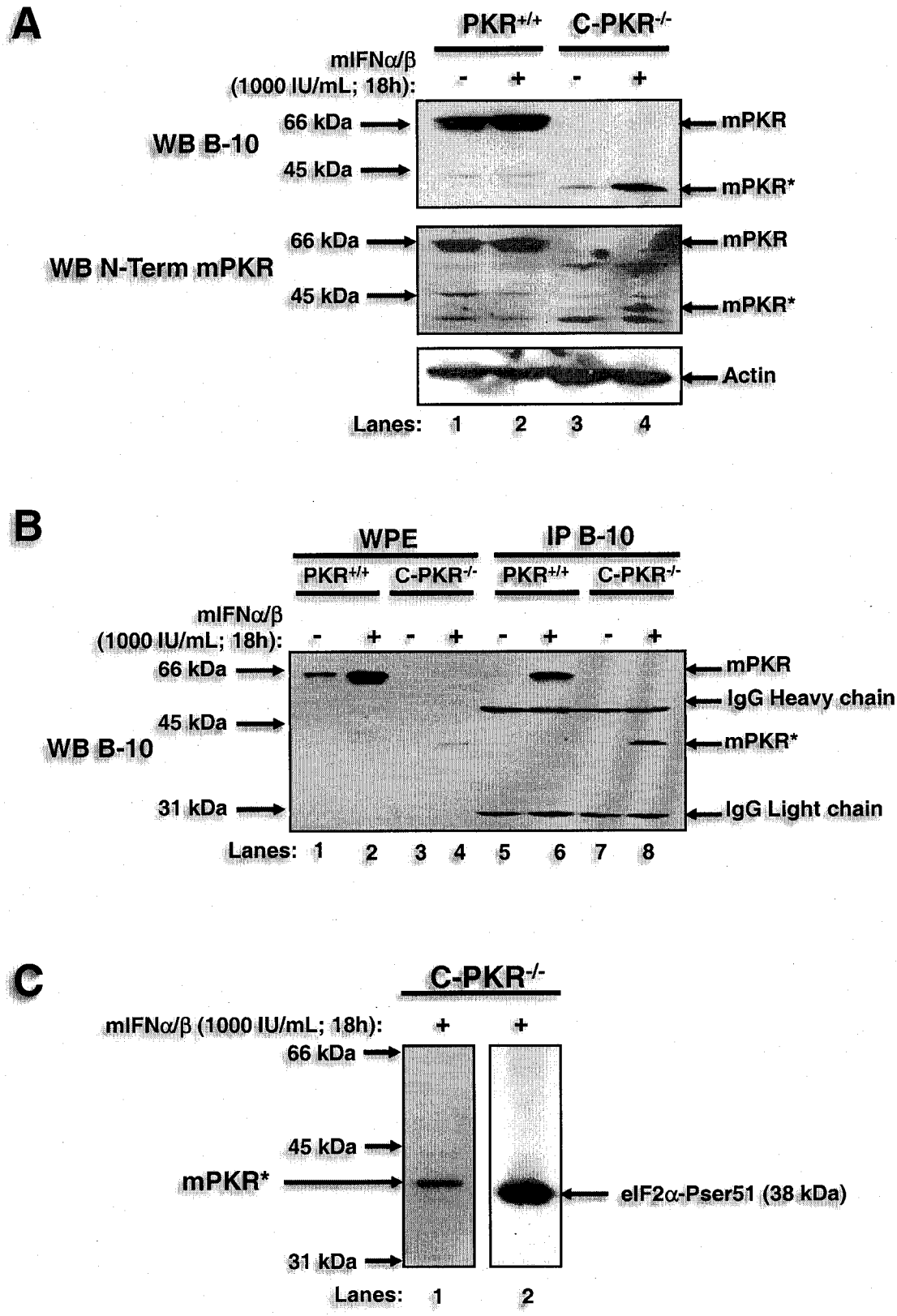
A
PKR+/+
C-PKR-/-
mIFNα/β
(1000 IU/mL; 18h):
- + - +
WB B-10
66 kDa
45 kDa
mPKR
mPKR*
WB N-Term mPKR
66 kDa
45 kDa
mPKR
mPKR*
Actin
Lanes: 1 2 3 4
B
WPE
IP B-10
PKR+/+
C-PKR-/-
PKR+/+
C-PKR-/-
mIFNα/β
(1000 IU/mL; 18h):
- + - + - + - +
66 kDa
45 kDa
31 kDa
WB B-10
mPKR
IgG Heavy chain
mPKR*
IgG Light chain
Lanes: 1 2 3 4 5 6 7 8
C
C-PKR-/-
mIFNα/β (1000 IU/mL; 18h):
+ +
66 kDa
45 kDa
mPKR*
31 kDa
eIF2α-Pser51 (38 kDa)
Lanes: 1 2

Figure 21

Figure 22. Functional analysis of mPKR*.

(A) ***mPKR* is a dsRNA-binding protein.*** Isogenic (i.e. genetic background 129/terSv X BALB/c) $PKR^{+/+}$ (lanes 1 and 2), C-$PKR^{-/-}$ MEFs (lanes 3 and 4), and isogenic (i.e. genetic background 129Sv(ev) x C57BL/6J) $PKR^{+/+}$ (lanes 5 and 6) and N-$PKR^{-/-}$ MEFs (lanes 7 and 8) were left untreated (lanes 1, 3, 5 and 7) or treated with mIFNα/β (1000 IU/ml, 18 hours; lanes 2, 4, 6 and 8). Protein extracts (200 μg) were used for the pull-down assays with poly(rI-rC) coupled to agarose beads. The bound proteins were subjected to a SDS-12%PAGE followed by immunoblot analysis with the anti-mPKR B-10 mAb. The positions of full-length mPKR and mPKR* proteins are indicated. The band of 65 kDa that was pulled down by dsRNA in both $PKR^{-/-}$ MEFs is not mPKR (see Results).

(B) ***mPKR* is catalytically inactive.*** Protein extracts (200 μg) from $PKR^{+/+}$ and C-$PKR^{-/-}$ MEFs before (lanes 1 and 3) and after stimulation with mIFNα/β (1000 IU/ml, 18 hours; lanes 2 and 4) were used for a pull-down with poly(rI-rC) coupled to agarose beads. The dsRNA-bound proteins were subjected to an autophosphorylation assay with [^{32}P-γ]ATP. Proteins were fractionated by SDS-12%PAGE and radioactive bands were visualized by autoradiography.

A

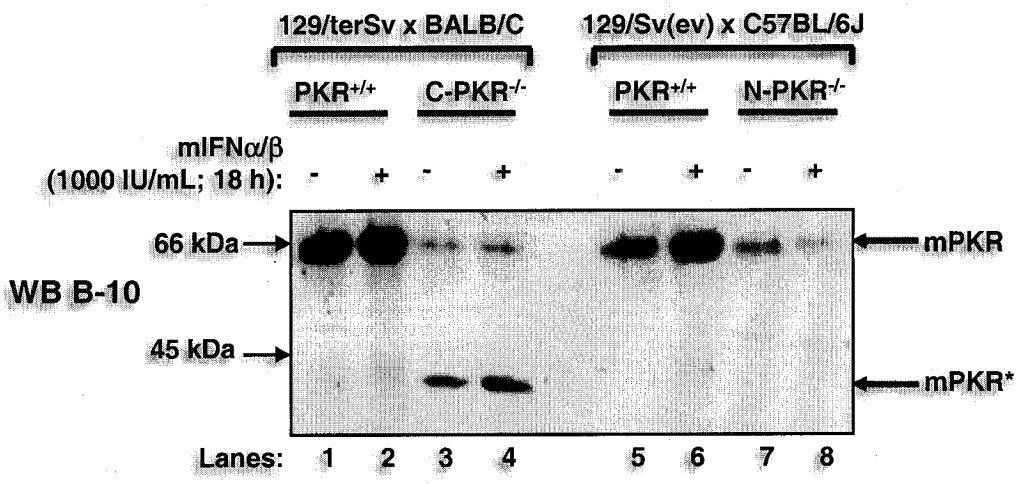
129/terSv x BALB/C
129/Sv(ev) x C57BL/6J
PKR+/+
C-PKR-/-
PKR+/+
N-PKR-/-
mIFNα/β
(1000 IU/mL; 18 h): - + - + - + - +
66 kDa
WB B-10
45 kDa
mPKR
mPKR*
Lanes: 1 2 3 4 5 6 7 8

B

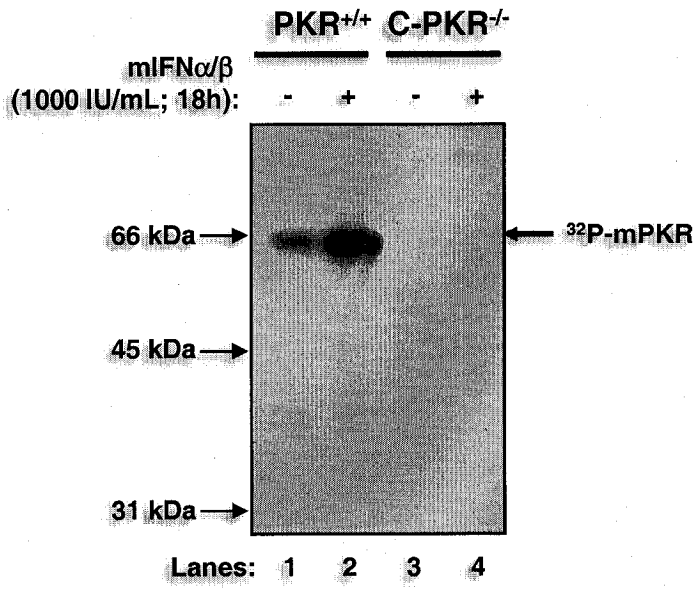
PKR+/+
C-PKR-/-
mIFNα/β
(1000 IU/mL; 18h): - + - +
66 kDa
45 kDa
31 kDa
32P-mPKR
Lanes: 1 2 3 4

Figure 22

1.2.3 mPKR* is an Alternative Spliced Form of mPKR

Next, we sought to explain the presence of mPKR* in C-PKR$^{-/-}$ cells. We speculated that mPKR* might be a product of alternative splicing based on our previous findings that spliced forms of PKR are expressed in human cells (206). To test this hypothesis, RNA from PKR$^{+/+}$ and C-PKR$^{-/-}$ MEFs was subjected to RT-PCR analysis using two sets of primers, one that amplifies the region of *mpkr* cDNA between exons 5 and 14 (Fig. 23A), and the other the region between exons 7 and 13 (Fig. 23B). We found that full length PKR was not amplified in RNA samples from C-PKR$^{-/-}$ cells providing further evidence that the 65 kDa protein recognized by the anti-PKR B-10 mAb in C-PKR$^{-/-}$ cells (Fig. 22A) was not a contamination with PKR$^{+/+}$ cells. Instead, we observed the presence of two smaller amplified bands (herein designated as *SF1-mPKR* and *SF2-mPKR*), which were subsequently identified as spliced forms (SF) of the *pkr* gene.

Sequencing of the cloned PCR products using the primers indicated in Table 1 demonstrated that SF1-mPKR is a product of alternative splicing that occurs between exons 11 and 13 (Fig. 24, middle panel), whereas SF2-mPKR is made by alternative splicing between exons 10 and 13 (Fig. 24, bottom panel). Thus, both SF-mPKR products bypass exon 12, which contains the neomycin resistance gene used for the generation of the C-PKR$^{-/-}$ mouse (2). Analysis of the sequencing data also showed that the alternative splicing mechanisms generated non-sense mutations for both alternatively spliced products with a stop codon a few nucleotides downstream of the splicing site. Thus, SF1-mPKR consists of 323 residues with a predicted molecular size of 40 kDa, whereas SF2-mPKR generates a protein of 283 residues with a molecular size of 35 kDa (Fig. 24).

However, the immunoblot analysis in Fig. 21C clearly identified mPKR* as a 40 kDa protein suggesting that mPKR* is identical to SF1-mPKR product. Detection of SF2-mPKR protein in C-PKR$^{-/-}$ cells was not possible.

1.2.4 Tissue Distribution of *SF1-mPKR* mRNA

The lack of any detectable levels of SF-mPKR proteins in PKR$^{+/+}$ cells prompted us to examine whether these PKR forms are expressed in normal mouse tissue at low levels and whether their expression is tissue specific. To this end, we performed PCR analysis of normalized single-stranded cDNA prepared from 12 different normal mouse tissues using the T502/T302 set of primers. To increase the sensitivity of the screening, the PCR products were detected by Southern blotting (Fig. 25). These experiments showed that expression of full-length *mPKR* did not significantly vary between the mouse tissues whereas *SF1-mPKR* was expressed at very low levels in brain, spleen, lung, kidney and testis (Fig. 25). Interestingly, *SF1-mPKR* was also detected in tissues from 7-, 11- and 17-day mouse embryo but not in tissue from 15-day mouse embryo indicating that its expression could be under developmental control. Detection of *SF2-mPKR* mRNA in these assays was not possible suggesting that its expression is probably unique for C-PKR$^{-/-}$ MEFs.

Figure 23. Cloning and sequencing of two alternatively spliced forms (SF) of *mPKR* in C-PKR$^{-/-}$ MEFs.

(A, B) *RT-PCR analysis of C-PKR$^{-/-}$ MEFs.* Exponentially grown PKR$^{+/+}$ and C-PKR$^{-/-}$ MEFs both with genetic background 129/terSv X BALB/c were treated with 1000 IU/ml of mIFNα/β for 18 hours. Reverse transcription (RT) was performed using 1 μg of total RNA, oligo-dT_{18} primer, and Moloney murine leukemia virus (M-MLV) reverse transcriptase followed by PCR with either the T503/T303 set of primers **(A)** or with the T502/T302 set of primers **(B).** Amplified DNA was subjected to 1.5% agarose electrophoresis and bands were visualized by EtBr staining. Lane 1, Marker DNA (ΦX174 DNA digested with Hae III). Lane 4, negative control (dH_2O). Lane 5, *mpkr* gene in pcDNA3.1/zeo.

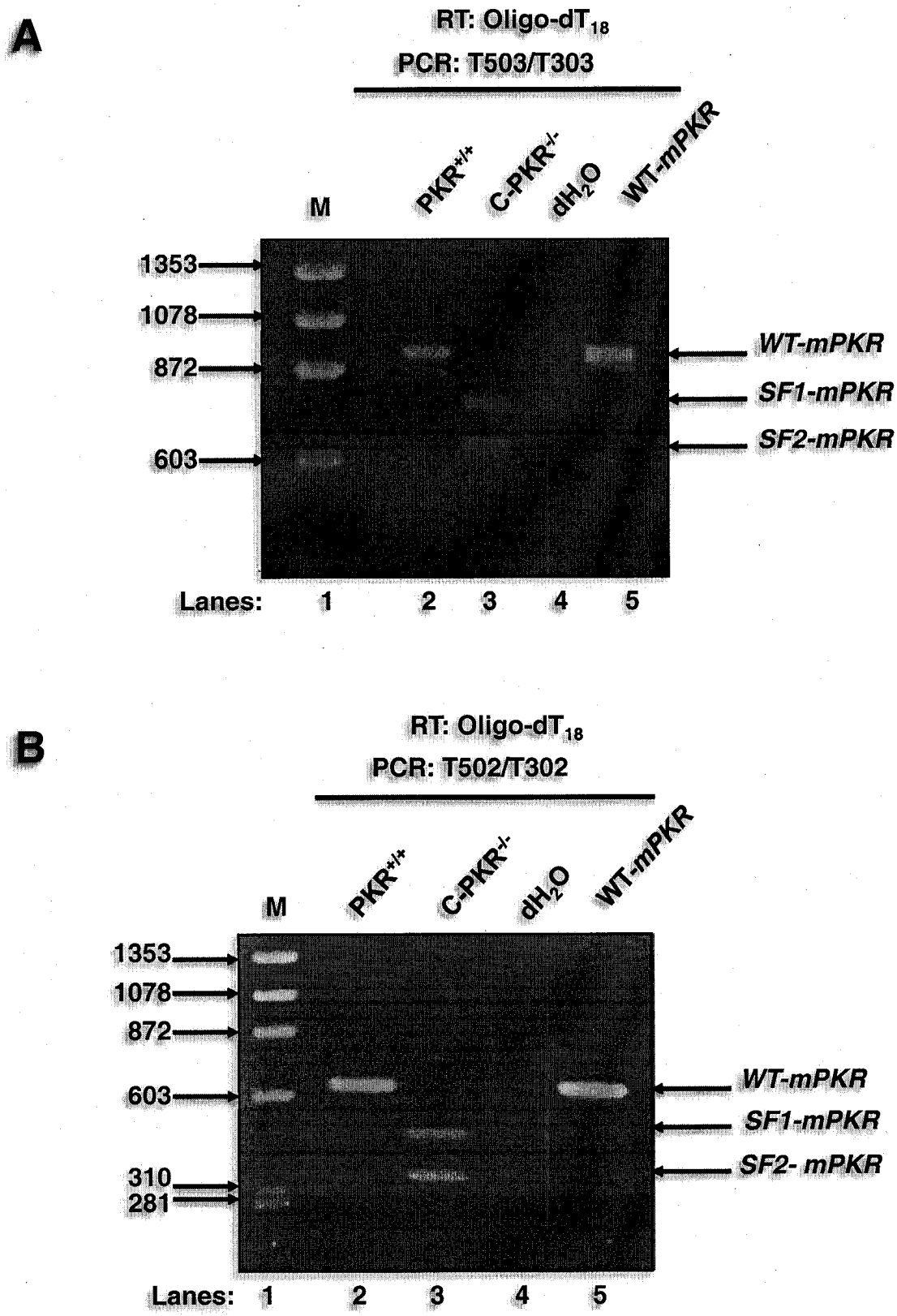
A
RT: Oligo-dT18
PCR: T503/T303
M
PKR+/+
C-PKR-/-
dH2O
WT-mPKR
1353
1078
872
603
WT-mPKR
SF1-mPKR
SF2-mPKR
Lanes: 1 2 3 4 5
B
RT: Oligo-dT18
PCR: T502/T302
M
PKR+/+
C-PKR-/-
dH2O
WT-mPKR
1353
1078
872
603
310
281
WT-mPKR
SF1-mPKR
SF2- mPKR
Lanes: 1 2 3 4 5

Figure 23

Figure 24. DNA sequence and schematic representation of SF-mPKR.

The DNA sequence around the junctions between exon10/exon11, exon 11/exon 12, exon 12/exon 13 of wild type *mPKR*, exon 10/exon 11 and exon 11/exon 13 of *SF1-mPKR*, and exon 10/exon 13 of *SF2-mPKR* are shown (top panels). The predicted structures and molecular sizes of SF1-mPKR and SF2-mPKR (middle and bottom panels) are shown and compared to full-length mPKR (top panel).

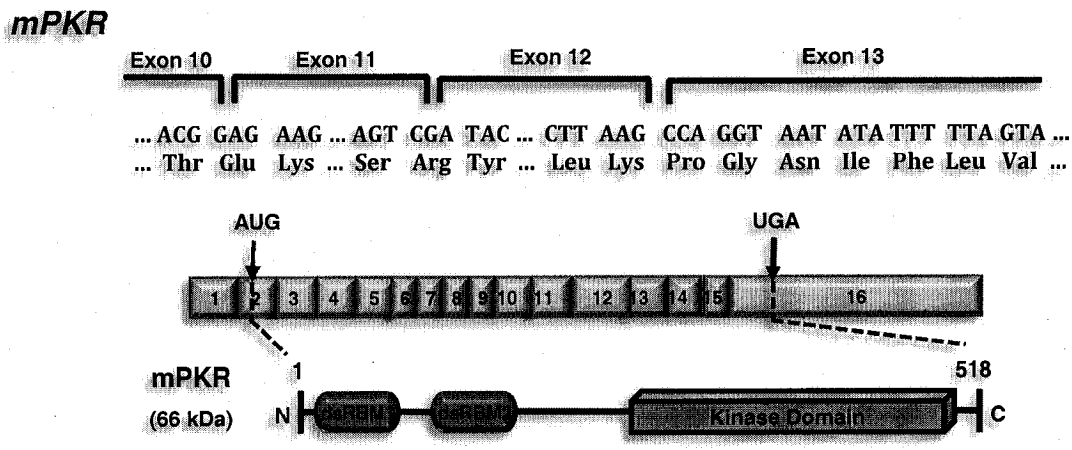
mPKR
Exon 10
Exon 11
Exon 12
Exon 13
... ACG GAG AAG ... AGT CGA TAC ... CTT AAG CCA GGT AAT ATA TTT TTA GTA ...
... Thr Glu Lys ... Ser Arg Tyr ... Leu Lys Pro Gly Asn Ile Phe Leu Val ...
AUG
UGA
1 2 3 4 5 6 7 8 9 10 11 12 13 14 15 16
mPKR
(66 kDa)
1
518
N
Kinase Domain
C

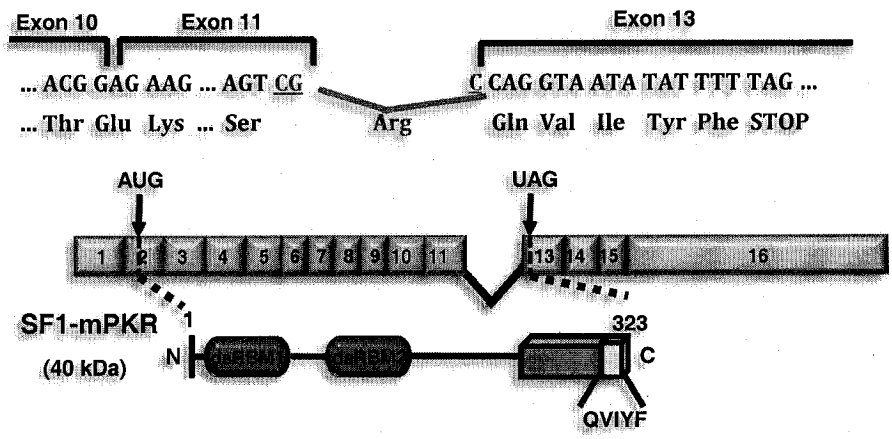
SF1-mPKR: Splicing of Exon 12
Exon 10
Exon 11
Exon 13
... ACG GAG AAG ... AGT CG
C CAG GTA ATA TAT TTT TAG ...
... Thr Glu Lys ... Ser
Arg
Gln Val Ile Tyr Phe STOP
AUG
UAG
1 2 3 4 5 6 7 8 9 10 11 13 14 15 16
SF1-mPKR
(40 kDa)
1
323
N
C
QVIYF

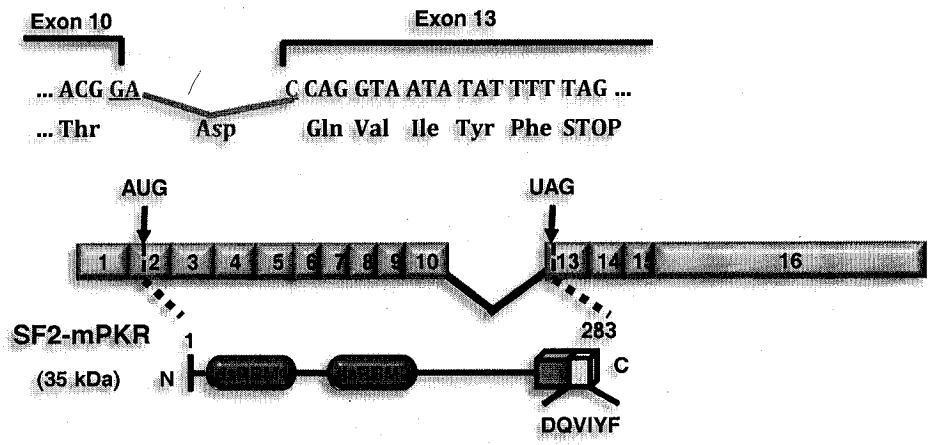
SF2-mPKR: Splicing of Exons 11 and 12
Exon 10
Exon 13
... ACG GA
C CAG GTA ATA TAT TTT TAG ...
... Thr
Asp
Gln Val Ile Tyr Phe STOP
AUG
UAG
1 2 3 4 5 6 7 8 9 10 13 14 15 16
SF2-mPKR
(35 kDa)
1
283
N
C
DQVIYF

Figure 24

Figure 25. Tissue distribution of *SF1-mPKR* mRNA.

Normalized cDNAs from mouse multiple tissue panel (mouse MTC Panel I; K1423-1; Clontech) was used as templates for PCR amplification with T502/T302 set of primers. The PCR products were subjected to a 1.5% agarose gel electrophoresis followed by a Southern blot analysis using ^{32}P-labeled full-length *mPKR* cDNA as a probe. The radioactive bands were visualized by autoradiography. The top panel corresponds to a long film exposure of the membrane (24 hours), whereas a shorter film exposure (8 hours) is shown in the bottom panel.

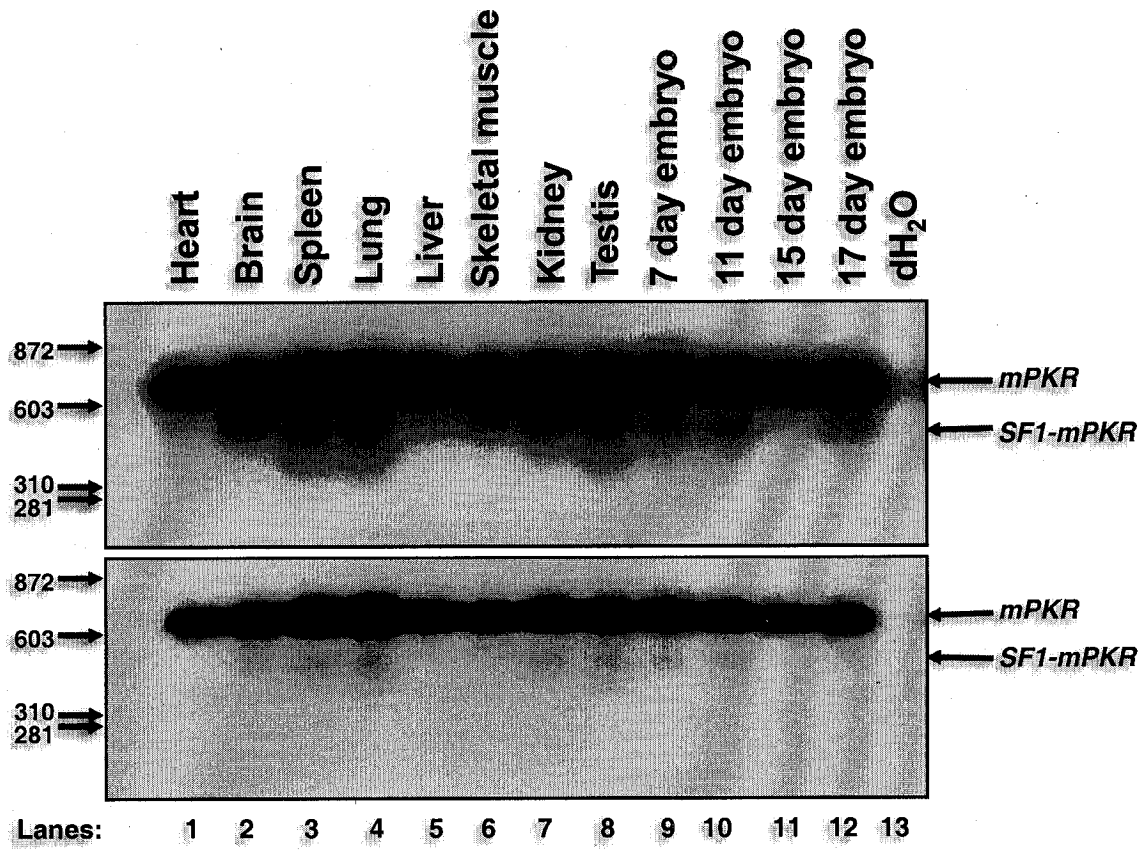
Heart
Brain
Spleen
Lung
Liver
Skeletal muscle
Kidney
Testis
7 day embryo
11 day embryo
15 day embryo
17 day embryo
dH2O
872
603
310
281
mPKR
SF1-mPKR
872
603
310
281
mPKR
SF1-mPKR
Lanes:
1 2 3 4 5 6 7 8 9 10 11 12 13

Figure 25

1.2.5 Control of IκBα and eIF2α Phosphorylation in C-PKR$^{-/-}$ MEFs

The partial inactivation of PKR in both PKR$^{-/-}$ mice may account, at least in part, for the signaling differences between the two PKR$^{-/-}$ cell types. For example, previous work with N-PKR$^{-/-}$ cells showed an impaired IκBα phosphorylation and NF-κB activation in response to dsRNA treatment (56,356,364). Contrary to this, NF-κB activation by dsRNA is normal in C-PKR$^{-/-}$ cells compared to isogenic PKR$^{+/+}$ cells (157). We further confirmed this finding by assessing IκBα phosphorylation levels in PKR$^{+/+}$ and C-PKR$^{-/-}$ cells in response to dsRNA (Fig. 26A). We found that IκBα phosphorylation *in vivo* was induced at equal levels in both PKR$^{+/+}$ and C-PKR$^{-/-}$ cells (Fig. 26A, top panel). This finding demonstrates that the catalytic activity of mPKR plays no role in dsRNA-mediated signaling to NF-κB-dependent transcription. This is in agreement with recent findings from us and others showing that the catalytic activity of hPKR is dispensable for NF-κB-mediated gene transcription (37,158).

We also examined the eIF2α phosphorylation levels in virus infected C-PKR$^{-/-}$ MEFs. To this end, cells derived from isogenic PKR$^{+/+}$ and C-PKR$^{-/-}$ mice bred onto 129SvEv background (93) were infected with vesicular stomatitis virus (VSV) (Fig. 26B). Immunoblot analysis with anti-eIF2α phosphoserine 51 antibodies (Fig. 26B, top panel) followed by immunoblotting with anti-mouse eIF2α mAb (bottom panels) showed no significant differences in eIF2α phosphorylation between PKR$^{+/+}$ and C-PKR$^{-/-}$ cells. These data show the redundancy of PKR in eIF2α phosphorylation in response to VSV infection.

Figure 26. Signaling properties of C-PKR$^{-/-}$ MEFs.

(A) ***Induction of IκBα phosphorylation by dsRNA in vivo in C-PKR$^{-/-}$ MEFs.*** Exponentially grown PKR$^{+/+}$ and C-PKR$^{-/-}$ MEFs of 129/terSv X BALB/c genetic background were untreated (lanes 1 and 6) or treated with 0.1 mg/mL poly(rI-rC) for the indicated time (lanes 2-5 and 7-10). Protein extracts (50 μg) were subjected to SDS-10%PAGE, transferred onto Immobilon P membrane (Millipore). Phosphorylation of IκBα was detected after immunoblot analysis with rabbit polyclonal anti-phosphoserine 32 IκBα Ab (top panel) and normalized to IκBα protein levels by immunoblotting with a rabbit polyclonal to anti-IκBα Ab (bottom panel). The ratio of phosphorylated to total IκBα for each lane is indicated.

(B) ***Phosphorylation of eIF2α in virus infected C-PKR$^{-/-}$ MEFs.*** PKR$^{+/+}$ and C-PKR$^{-/-}$ MEFs from mice bred onto 129SvEv genetic background were infected with vesicular stomatitis virus (VSV, MOI 10) for the indicated time. Protein extracts (50 μg) were subjected onto SDS-12%PAGE, transferred onto Immobilon P membrane (Millipore) and immunoblotted with a rabbit polyclonal anti-phosphoserine 51 eIF2α Ab (top panels) followed by immunoblotting with an anti-eIF2α mAb (bottom panels). The ratio of phosphorylated to total eIF2α protein is indicated below each lane.

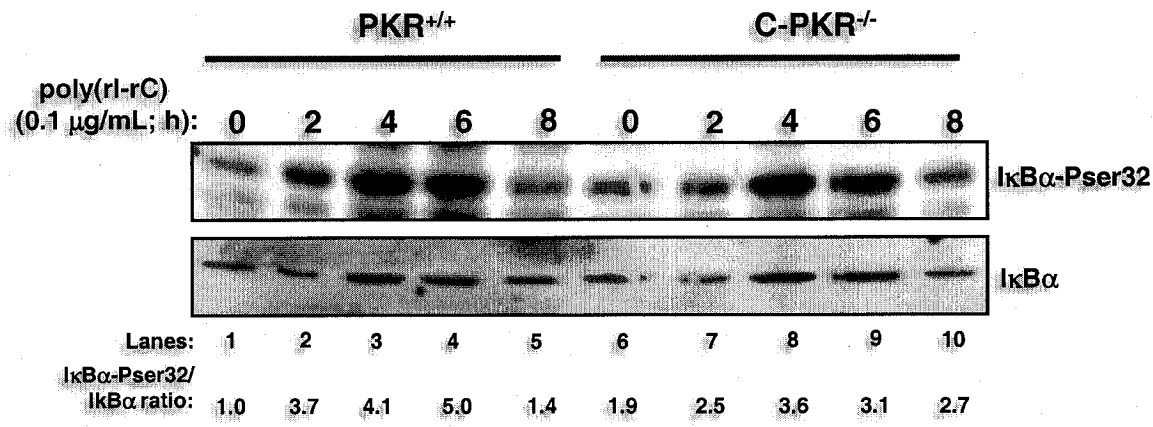
A
PKR+/+
C-PKR-/-
poly(rI-rC)
(0.1 μg/mL; h):
0 2 4 6 8 0 2 4 6 8
IκBα-Pser32
IκBα
Lanes: 1 2 3 4 5 6 7 8 9 10
IκBα-Pser32/
IκBα ratio:
1.0 3.7 4.1 5.0 1.4 1.9 2.5 3.6 3.1 2.7

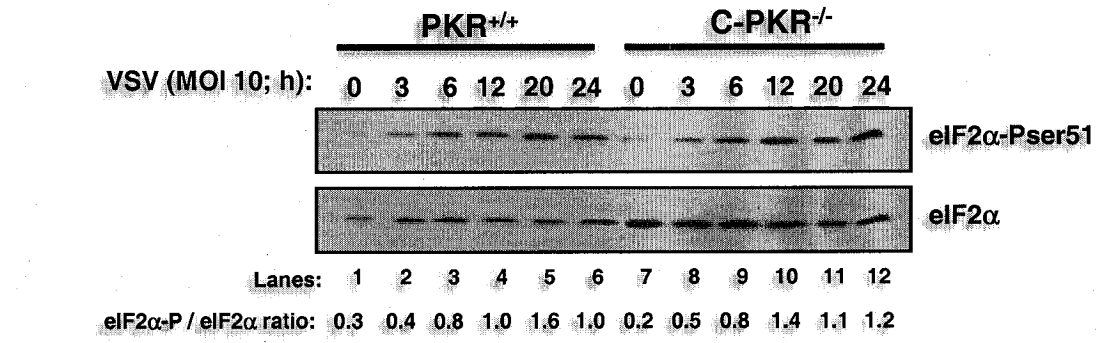
B
PKR+/+
C-PKR-/-
VSV (MOI 10; h):
0 3 6 12 20 24 0 3 6 12 20 24
eIF2α-Pser51
eIF2α
Lanes: 1 2 3 4 5 6 7 8 9 10 11 12
eIF2α-P / eIF2α ratio:
0.3 0.4 0.8 1.0 1.6 1.0 0.2 0.5 0.8 1.4 1.1 1.2

Figure 26

2. RESISTANCE TO VSV INFECTION REQUIRES A CROSS-TALK BETWEEN PERK & PKR

2.1 VSV INFECTION INDUCES PERK ACTIVATION

2.1.1 Susceptibility of PERK$^{-/-}$ MEFs to VSV-mediated Apoptosis

The redundancy of PKR in eIF2α phosphorylation in response to VSV infection (Fig. 26B), and the recent finding implicating PERK in Hepatitis C virus (HCV) replication (256) prompted us to examine whether PERK plays a role in VSV replication. To do so, we first assessed the susceptibility of PERK$^{+/+}$ and PERK$^{-/-}$ MEFs to VSV-mediated apoptosis. That is, we tested the viability of non-infected or VSV infected (MOI 1) MEFs at different hours-post-infection (h.p.i.) (Fig. 27A). We noticed that a higher number of PERK$^{-/-}$ than PERK$^{+/+}$ MEFs were susceptible to cytopathic effects of VSV (Fig 27A). Pre-treatment with IFNα/β completely protected both PERK$^{+/+}$ and PERK$^{-/-}$ MEFs against VSV infection (Fig. 27B). To establish whether PERK$^{-/-}$ MEFs were indeed undergoing apoptosis, PERK$^{+/+}$ and PERK$^{-/-}$ MEFs infected with VSV were analyzed for staining with Annexin-V, an indicator of early apoptosis (Fig. 28). We found that at 24 h.p.i almost 30% of PERK$^{-/-}$ MEFs were apoptotic compared to 10% of PERK$^{+/+}$ MEFs whereas at 36 h.p.i, the population of apoptotic PERK$^{-/-}$ MEFs reached 60% compared to 20% of the PERK$^{+/+}$ MEFs (Fig. 28).

We also examined whether the increased susceptibility of PERK$^{-/-}$ MEFs to VSV infection is affected by treatment with either IFNα/β (Fig. 28, middle rows) or IFNγ (Fig. 28, bottom rows). Pre-treatment with either type of IFNs eliminated the apoptotic effects of VSV infection in both PERK$^{+/+}$ and PERK$^{-/-}$ MEFs indicating that IFN-signaling

remains intact in PERK$^{-/-}$ MEFs, and expression of one or more IFN-induced genes can compensate for the loss of PERK in these cells.

We then performed viral plaque assays in order to determine if the susceptibility of PERK$^{-/-}$ MEFS to VSV infection was due to a higher virus production. We determined that VSV production increased exponentially in PERK$^{-/-}$ MEFs (MOI 1, Fig. 29A, left panel) with a 3 log higher titer than PERK$^{+/+}$ MEFs at 12 h.p.i., and 4 log and 8 log higher at 24 and 36 h.p.i., respectively. Immunoblot analysis with an anti-VSV antibody revealed that VSV protein production was only detectable in PERK$^{-/-}$ MEFs infected with MOI 1 (Fig. 29A, right panel). Despite the fact that the VSV titer increased in PERK$^{+/+}$ infected at MOI 100 (Fig. 29B, left panel), it remains relatively lower than in PERK$^{-/-}$ MEFs (2-fold lower at 4 h.p.i.) throughout the growth curve and viral production reached a plateau after 8 h.p.i. The right panel of Fig. 29B clearly shows that VSV replication was significantly higher in infected PERK$^{-/-}$ MEFs due to robust viral protein production. These results explain that the susceptibility of PERK$^{-/-}$ MEFs to VSV-mediated apoptosis is due to higher viral protein production and release of progeny virions.

Figure 27. Increased susceptibility of PERK$^{-/-}$ MEFs to VSV infection.

PERK$^{+/+}$ and PERK$^{-/-}$ MEFs were untreated **(A)** or treated **(B)** with mouse IFNα/β (1000 IU/ml) for 18 hours in the absence (**A** & **B**, left panels) or presence (**A** & **B**, right panels) of VSV infection at a MOI of 1. Cells were photographed at 100x magnification at indicated hours after infection.

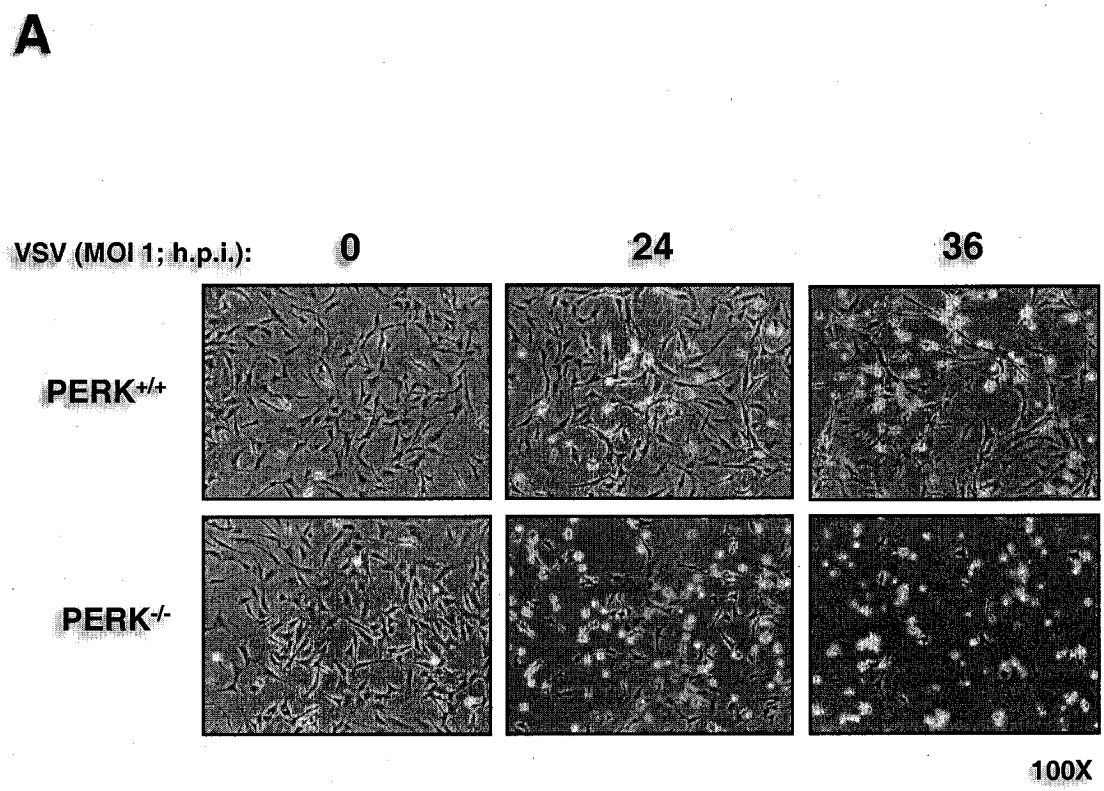
A
VSV (MOI 1; h.p.i.):
0
24
36
PERK+/+
PERK-/-
100X

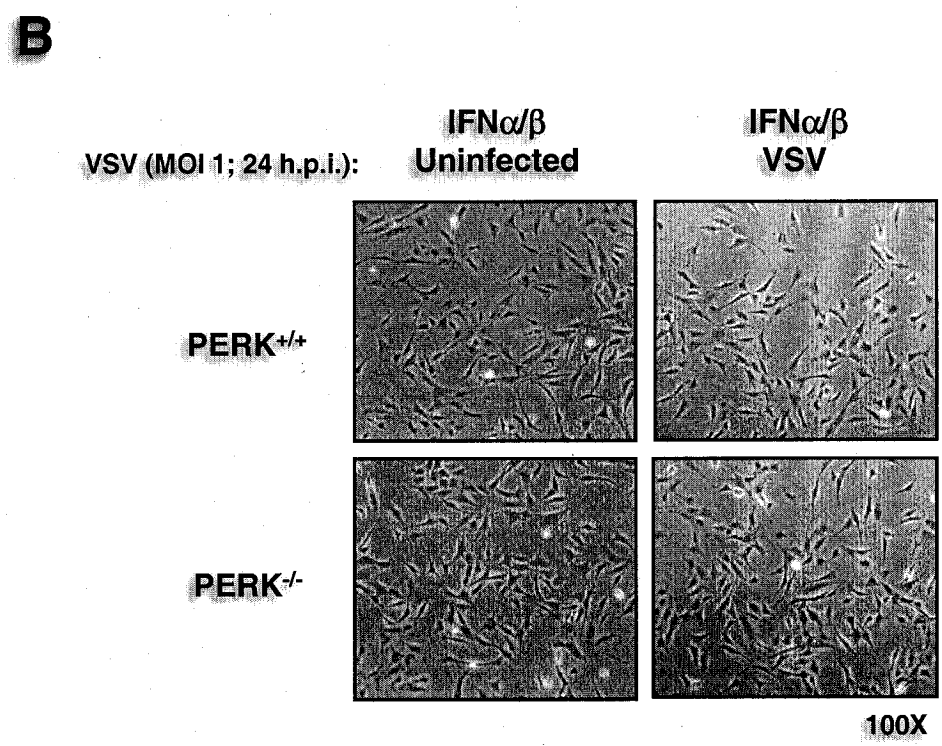
B
VSV (MOI 1; 24 h.p.i.):
IFNα/β
Uninfected
IFNα/β
VSV
PERK+/+
PERK-/-
100X

Figure 27

Figure 28. A higher induction of VSV-mediated apoptosis in PERK$^{-/-}$ MEFs.

PERK$^{+/+}$ (**A**) and PERK$^{-/-}$ MEFs (**B**) were untreated or treated with either mouse IFNα/β (1000 IU/ml) or IFNγ (100 IU/ml) for 20 h followed by infection with VSV at MOI of 1. Cells were harvested at 24 or 36 hours post infection (h.p.i.) and subjected to Annexin-V/PI staining (BioSource) according to manufacturer's specifications. Cells were then subjected to flow cytometry analysis using FACScan (Becton Dickinson), and data was analyzed using WinMDI version 2.8 software (Scripp Institute). Cells were gated on a dot-plot showing forward and side scatter in order to exclude debris not within the normal size. Gated cells were plotted on a dot-plot showing annexin-V staining (FL1-H) and propidium iodide (PI) straining (FL2-H). The numbers represent the percentage of gated cells counted for their corresponding quadrant. These are data of one out of three reproducible experiments.

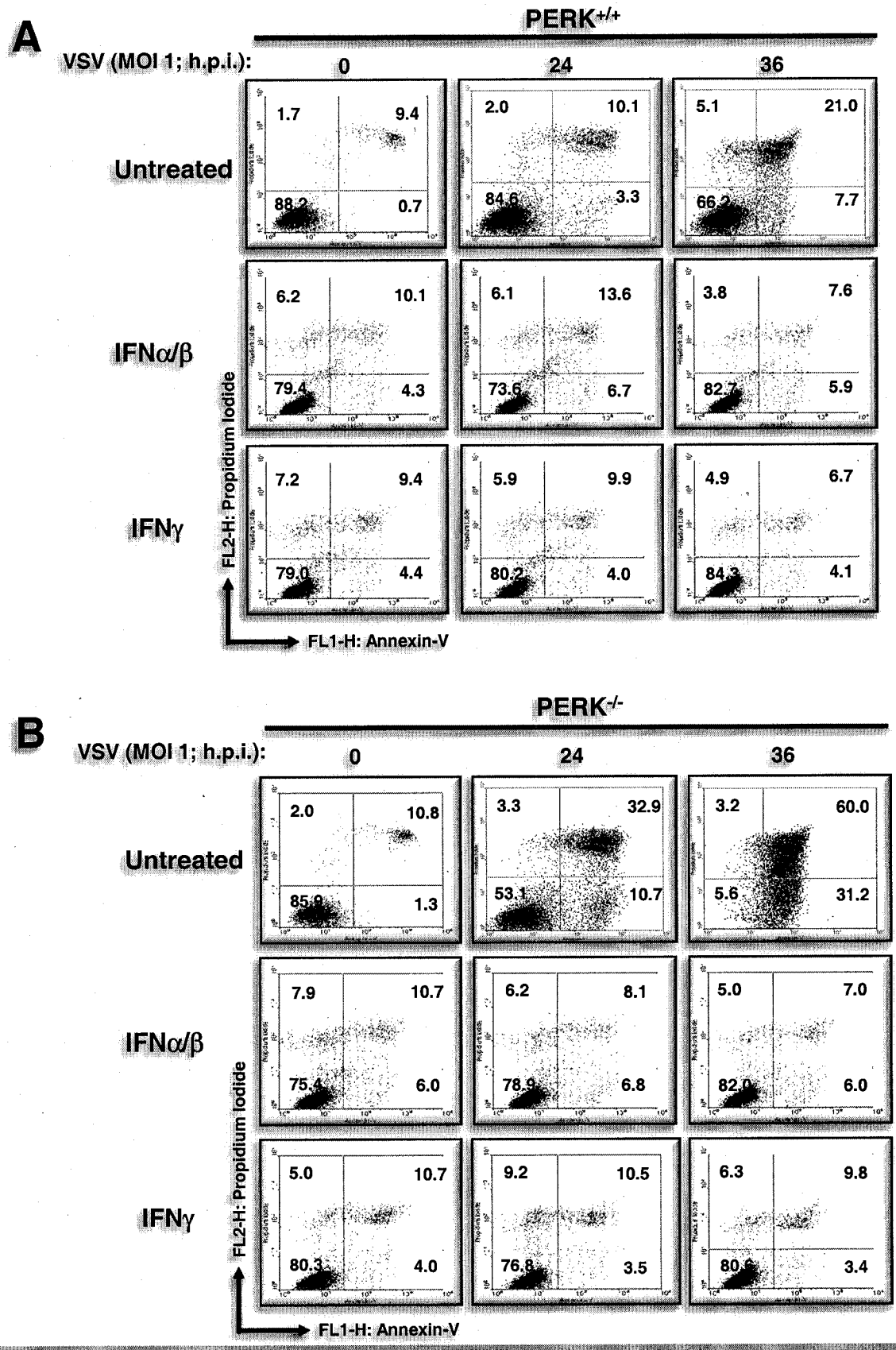
A
PERK+/+
VSV (MOI 1; h.p.i.):
0
24
36
Untreated
IFNα/β
IFNγ
1.7
9.4
88.2
0.7
2.0
10.1
84.6
3.3
5.1
21.0
66.2
7.7
6.2
10.1
79.4
4.3
6.1
13.6
73.6
6.7
3.8
7.6
82.7
5.9
7.2
9.4
79.0
4.4
5.9
9.9
80.2
4.0
4.9
6.7
84.3
4.1
FL2-H: Propidium Iodide
FL1-H: Annexin-V
B
PERK-/-
VSV (MOI 1; h.p.i.):
0
24
36
Untreated
IFNα/β
IFNγ
2.0
10.8
85.9
1.3
3.3
32.9
53.1
10.7
3.2
60.0
5.6
31.2
7.9
10.7
75.4
6.0
6.2
8.1
78.9
6.8
5.0
7.0
82.0
6.0
5.0
10.7
80.3
4.0
9.2
10.5
76.8
3.5
6.3
9.8
80.6
3.4
FL2-H: Propidium Iodide
FL1-H: Annexin-V

Figure 28

Figure 29. A higher induction of VSV replication in PERK$^{-/-}$ MEFs.

(A, B) PERK$^{+/+}$ and PERK$^{-/-}$ MEFs were left uninfected or infected with VSV MOI 1 **(A)** or VSV MOI 100 **(B),** and protein extracts were subjected to immunoblot analysis with an anti-VSV antibody (right panels) or viral titers were measured by harvesting medium at indicated hours post-infection followed by plaque assay analysis (left panels). The triangle (▲) represents viral titers from PERK$^{+/+}$ MEFs, and the square (■) represents viral titers from PERK$^{-/-}$ MEFs.

A

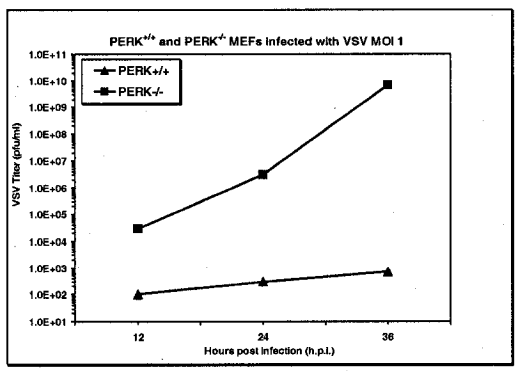
PERK+/+ and PERK-/- MEFs infected with VSV MOI 1
PERK+/+
PERK-/-
VSV Titer (pfu/ml)
1.0E+11
1.0E+10
1.0E+09
1.0E+08
1.0E+07
1.0E+06
1.0E+05
1.0E+04
1.0E+03
1.0E+02
1.0E+01
12
24
36
Hours post infection (h.p.i.)

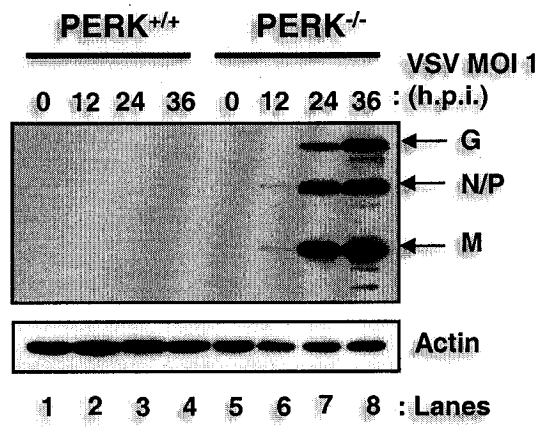
PERK+/+
PERK-/-
VSV MOI 1
0 12 24 36 0 12 24 36 : (h.p.i.)
G
N/P
M
Actin
1 2 3 4 5 6 7 8 : Lanes

B

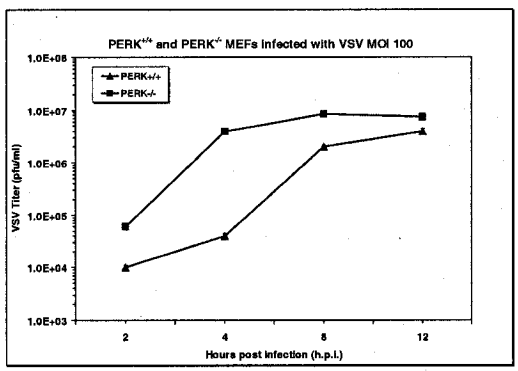
PERK+/+ and PERK-/- MEFs infected with VSV MOI 100
PERK+/+
PERK-/-
VSV Titer (pfu/ml)
1.0E+08
1.0E+07
1.0E+06
1.0E+05
1.0E+04
1.0E+03
2
4
8
12
Hours post infection (h.p.i.)

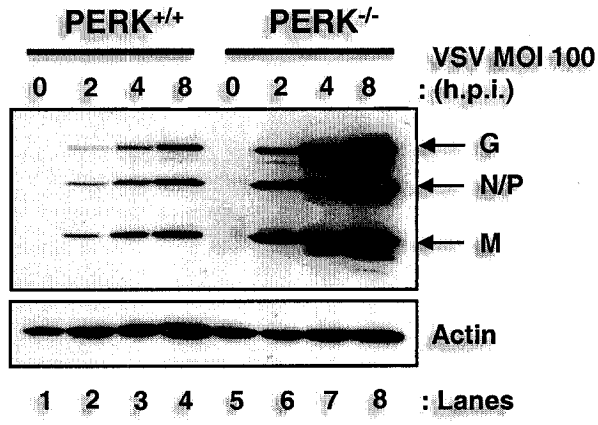
PERK+/+
PERK-/-
VSV MOI 100
0 2 4 8 0 2 4 8 : (h.p.i.)
G
N/P
M
Actin
1 2 3 4 5 6 7 8 : Lanes

Figure 29

2.1.2 Impaired eIF2α Phosphorylation in VSV infected PERK$^{-/-}$ MEFs

To further characterize the PERK$^{-/-}$ MEFs, we next assessed the eIF2α phosphorylation levels in response to VSV infection with different multiplicity of infections (MOI 1, 10 and 50). We reasoned that VSV replication might activate intracellular pathways leading to PERK-mediated eIF2α phosphorylation. VSV infection induced eIF2α phosphorylation levels in both types of MEFs, however eIF2α phosphorylation was induced at higher levels in PERK$^{+/+}$ than PERK$^{-/-}$ MEFs (Fig. 30A, B and C, top panels). To further verify this observation, we measured the eIF2α phosphorylation levels in VSV-infected MEFs using 2D gel electrophoresis (Fig. 30D). We noticed that phosphorylation of eIF2α was increased in PERK$^{+/+}$ than in PERK$^{-/-}$ MEFs after infection with VSV or treatment with ER stress inducer thapsigargin (compare top panels with middle or bottom panels). These data suggested that the higher levels of eIF2α phosphorylation are capable of limiting VSV replication in PERK$^{+/+}$ MEFs as opposed to PERK$^{-/-}$ MEFs, in which eIF2α phosphorylation was diminished.

2.1.3 VSV Induces PERK-mediated eIF2α Phosphorylation

Next, we performed immunoblot analysis with a phosphospecific antibody against the Thr980-phosphorylation site of PERK, a site that serves as a marker for activation, using VSV-infected HeLa cells to detect endogenous PERK phosphorylation (Fig. 31A). PERK phosphorylation was induced as early as 2 h.p.i. Thapsigargin (TG) treatment for 1 hour was used as a positive control. A shift in PERK migration was observed in TG-treated cells as opposed to VSV infected cells, indicating that TG induces a higher phosphorylation pattern of PERK than VSV infection.

To further substantiate the above findings, we performed transient transfections of plasmids that express either wild type mouse PERK (WT) or the kinase inactive mouse PERK bearing the K618A mutation in COS-1 cells (Fig. 31B). We reasoned that if PERK is activated by VSV infection, then eIF2α phosphorylation should be induced in cells transfected with the wild type kinase as opposed to cells expressing the catalytically inactive kinase. The expression of both proteins was detected by immunoblotting with either an anti-Myc tag antibody (second panel) or with an anti-PERK antibody (third panel). In the absence of VSV infection, we noticed that WT-PERK migrated slower than the PERK K618A due to the autophosphorylation of the active kinase (Fig. 31B, lanes 2 and 3, second and third panels) (128).

On the other hand, in cells infected with VSV we noticed a slight shift in the mobility of WT-PERK after immunoblotting with both antibodies (second and third panels, compare lane 2 and 5) indicating PERK activation during virus replication. Activation of PERK became more evident after immunoblotting with the phosphothreonine 980 antibody (top panel). We detected an induction in PERK phosphorylation upon VSV infection (lane 5, top panel) and in cells treated with thapsigargin (lane 8, top panel) when compared to uninfected or untreated cells (lane 2, top panel). As expected, this phosphospecific antibody was unable to detect the PERK K618A mutant since the latter mutation renders the kinase inactive (lanes 3, 6, 9, top panel).

The induction of phosphorylation and activation of PERK upon VSV infection correlated with the eIF2α phosphorylation pattern we observed (fourth panel). We noticed that VSV infection induced eIF2α phosphorylation is cells transfected with WT-

PERK compared to cells transfected with PERK-K618A mutant (compare lanes 5 and 6). In addition, eIF2α phosphorylation was significantly increased in VSV infected cells than in uninfected cells expressing WT-PERK (compare lane 2 and 5). Activation of WT-PERK and induction of eIF2α phosphorylation in transiently transfected COS-1 cells was also observed after treatment with thapsigargin, which served as a positive control in these assays (lanes 7-9). Based on these results, we concluded that VSV-infection results in the induction of PERK activity and eIF2α phosphorylation.

Figure 30. Enhanced VSV replication in PERK$^{-/-}$ MEFs as a result of impaired eIF2α phosphorylation.

PERK$^{+/+}$ and PERK$^{-/-}$ MEFs were infected (lanes 2-4 and 6-8) or not (lanes 1 and 5) with VSV at MOI of 1 **(A)**, 10 **(B)** or 50 **(C)**. Proteins extracts were harvested at indicated hours post-infection (h.p.i.) and subjected to immunoblot analysis using the rabbit polyclonal anti-phosphoserine 51-eIF2α antibody (top panels) or with the eIF2α antibody (lower panels). The ratio of phosphorylated to total eIF2α protein for each lane is indicated.

(D) PERK$^{+/+}$ and PERK$^{-/-}$ MEFs were either treated with 1 μM of thapsigargin for 2 hours (bottom panels), infected (middle panels) or uninfected (top panels) with VSV at MOI of 10 and harvested at 12 hours post infection. Protein extracts were subjected to 2D electrophoresis and immunoblot analysis with a rabbit polyclonal anti-phosphoserine51-eIF2α antibody.

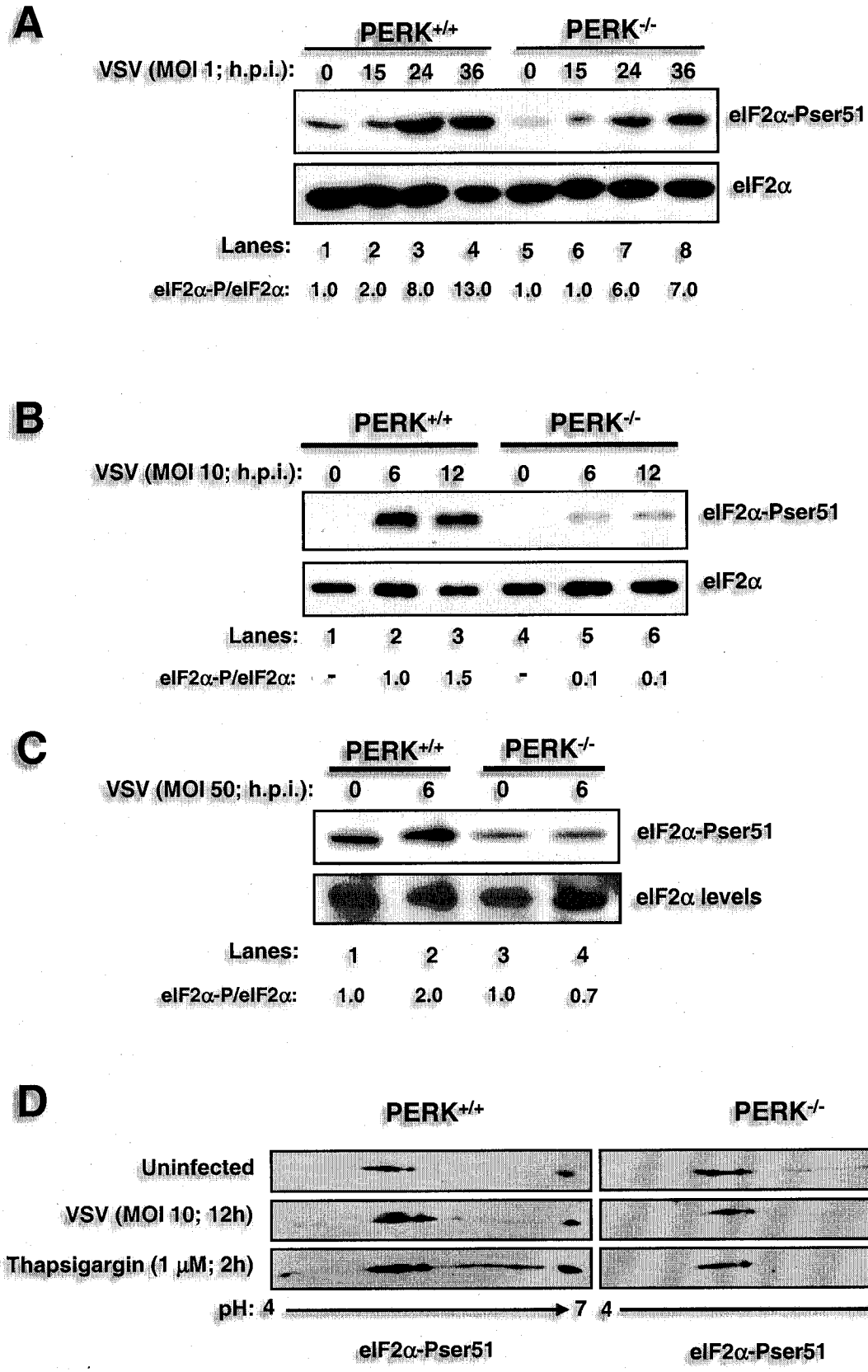
A
PERK+/+
PERK-/-
VSV (MOI 1; h.p.i.): 0 15 24 36 0 15 24 36
eIF2α-Pser51
eIF2α
Lanes: 1 2 3 4 5 6 7 8
eIF2α-P/eIF2α: 1.0 2.0 8.0 13.0 1.0 1.0 6.0 7.0
B
PERK+/+
PERK-/-
VSV (MOI 10; h.p.i.): 0 6 12 0 6 12
eIF2α-Pser51
eIF2α
Lanes: 1 2 3 4 5 6
eIF2α-P/eIF2α: - 1.0 1.5 - 0.1 0.1
C
PERK+/+
PERK-/-
VSV (MOI 50; h.p.i.): 0 6 0 6
eIF2α-Pser51
eIF2α levels
Lanes: 1 2 3 4
eIF2α-P/eIF2α: 1.0 2.0 1.0 0.7
D
PERK+/+
PERK-/-
Uninfected
VSV (MOI 10; 12h)
Thapsigargin (1 μM; 2h)
pH: 4 7 4 7
eIF2α-Pser51
eIF2α-Pser51

Figure 30

Figure 31. VSV induces PERK-mediated eIF2α phosphorylation.

(A) Protein extracts from HeLa cells infected with VSV (MOI 100) were collected at different hours post infection (h.p.i.), and subjected to immunoblot analysis with a rabbit polyclonal phosphothreonine 980 PERK antibody (top panel) or a rabbit polyclonal anti-PERK antibody (H-300; bottom panel).

(B) COS-1 cells were transfected with either myc-tagged wild-type (WT) mouse PERK or the K618A catalytic mutant of mouse PERK (5 μg of plasmid DNA) followed by VSV infection or thapsigargin treatment. Protein extracts were subjected to immunoblot analysis with a rabbit polyclonal phosphothreonine 980 PERK antibody (top panel), a mouse monoclonal myc-tag antibody (second panel), a goat polyclonal anti-PERK antibody (third panel), a rabbit polyclonal phosphoserine 51 eIF2α antibody (fourth panel) or with a mouse monoclonal eIF2α antibody (fifth panel). A non-specific (N.S.) band was used to determine the amount of protein loaded (bottom panel).

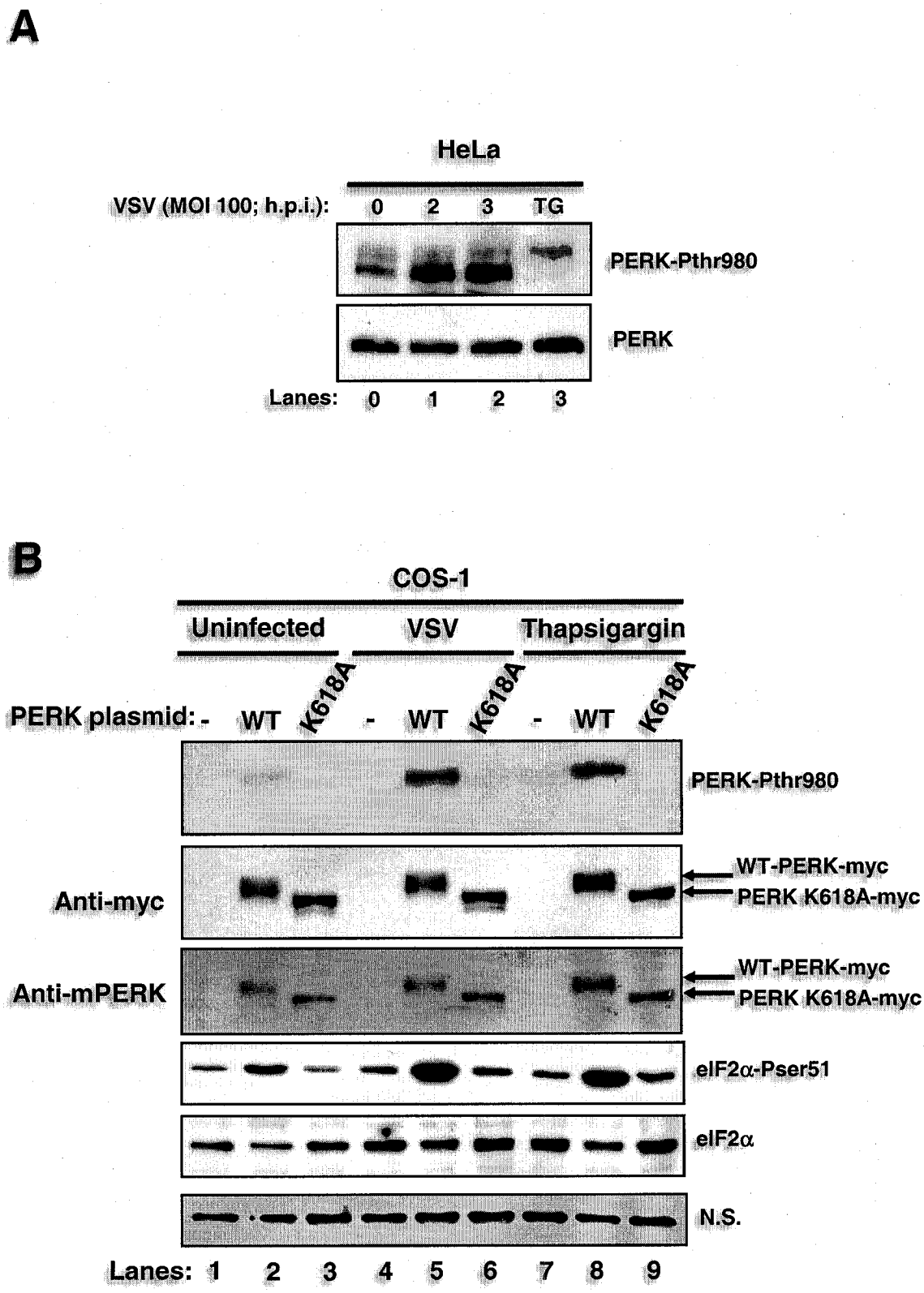
A
HeLa
VSV (MOI 100; h.p.i.):
0
2
3
TG
PERK-Pthr980
PERK
Lanes:
0
1
2
3
B
COS-1
Uninfected
VSV
Thapsigargin
PERK plasmid:
-
WT
K618A
-
WT
K618A
-
WT
K618A
PERK-Pthr980
Anti-myc
WT-PERK-myc
PERK K618A-myc
Anti-mPERK
WT-PERK-myc
PERK K618A-myc
eIF2α-Pser51
eIF2α
N.S.
Lanes:
1
2
3
4
5
6
7
8
9

Figure 31

2.1.4 Caspase-12 Induction in VSV-mediated Apoptosis

In order to elucidate the mechanisms of VSV-mediated apoptosis, we measured caspase-12 activation in $PERK^{+/+}$ and $PERK^{-/-}$ MEFs in response to infection. Caspase-12 is an ER-membrane associated cysteine protease activated by ER stress (239). This protease is also induced in cells infected with the respiratory syncytial virus (RSV) (32) or bovine viral diarrhoea virus (BVDV) (165). Immunoblot analysis with an antibody that recognizes the inactive and active (i.e. cleaved) forms of caspase-12 demonstrated a higher activity of the protease in $PERK^{-/-}$ than in $PERK^{+/+}$ MEFs (Fig. 32A, compare lane 2 with 5, and lane 3 with 6). Thus, it appears that caspase-12 activation can account, at least in part, for the higher induction of VSV-mediated apoptosis in $PERK^{-/-}$ MEFs.

It was previously shown that broad-spectrum caspase inhibitors effectively prevented the activation of programmed cell death pathways in VSV-infected cells (84). In order to get a better understanding on VSV-mediated apoptosis, we treated $PERK^{+/+}$ and $PERK^{-/-}$ MEFs with a general caspase inhibitor (zVAD-fmk) prior to VSV infection. We noticed that caspase inhibitors protected $PERK^{+/+}$ from VSV infection (Fig. 32B, compare row 1 column 4 with row 1 column 2). However, the cell rounding phenotype associated with VSV infection was not prevented in $PERK^{-/-}$ MEFs treated with caspase inhibitors (Fig. 32B, compare row 2 column 4 with row 2 column 2) indicating their inability to be rescued from VSV-mediated apoptosis.

This was further verified by immunoblot analysis of the poly(ADP ribose) polymerase (PARP), a common marker of apoptosis, where its cleavage is induced in VSV infected cells (Fig. 32C) (143). VSV-infected $PERK^{-/-}$ MEFs had a higher PARP cleavage capacity than $PERK^{+/+}$ cells (Fig. 32C, compare lane 6 with lane 2). When cells

were treated with caspase inhibitors prior to VSV infection, PARP cleavage was abolished in $PERK^{+/+}$ cells indicating apoptotic rescue (Fig. 32C, lane 4), whereas such inhibitors were unable to prevent PARP cleavage in $PERK^{-/-}$ MEFs (lane 8). This suggested that caspases play a critical role in VSV-mediated apoptosis in the presence of PERK. Conversely, in the absence of PERK, inactivation of caspases is not sufficient to abolish apoptosis suggesting that the lack of PERK can induce caspase-independent apoptotic pathways.

ER-mediated apoptosis also proceeds through the activation of c-Jun NH_2-terminal kinase (JNK) (252). On the other hand, virus infection results in the activation of JNK-1 and p38 mitogen activated protein kinase (p38 MAPK), both of which have been implicated in virus-mediated apoptosis (56,156). Taken together, we sought to determine the expression and activity of these pro-apoptotic proteins in VSV-infected $PERK^{+/+}$ and $PERK^{-/-}$ MEFs. Immunoblot analysis with phosphospecific antibodies to either JNK-1 or p38 MAPK showed equal levels of expression and activation of these kinases in both types of MEFs (Fig. 33). This indicated that the higher induction of VSV-mediated apoptosis in $PERK^{-/-}$ MEFs is independent of JNK-1 and p38 MAPK activation.

Figure 32. VSV-induced apoptosis of PERK$^{-/-}$ MEFs proceeds through caspase-12 activation.

(A) Protein extracts from PERK$^{+/+}$ and PERK$^{-/-}$ MEFs infected with VSV (MOI 1) were collected at different hours post infection (h.p.i.) and subjected to immunoblot analysis with a rabbit polyclonal antibody against caspase-12. The upper band represents the inactive protease (procaspase-12) whereas the lower band represents the cleaved and active enzyme (caspase-12).

(B, C) PERK$^{+/+}$ and PERK$^{-/-}$ MEFs were treated with or without caspase inhibitors (zVAD-fmk; 10 μM) 2h before infection with VSV (MOI 2) for 24 hours. Cells were photographed at 100x magnification **(B)** or protein extracts were subjected to immunoblot analysis with a rabbit polyclonal antibody against PARP **(C).** The upper band represents the full length 116 kDa PARP protein and the lower band represents the cleaved 89 kDa PARP.

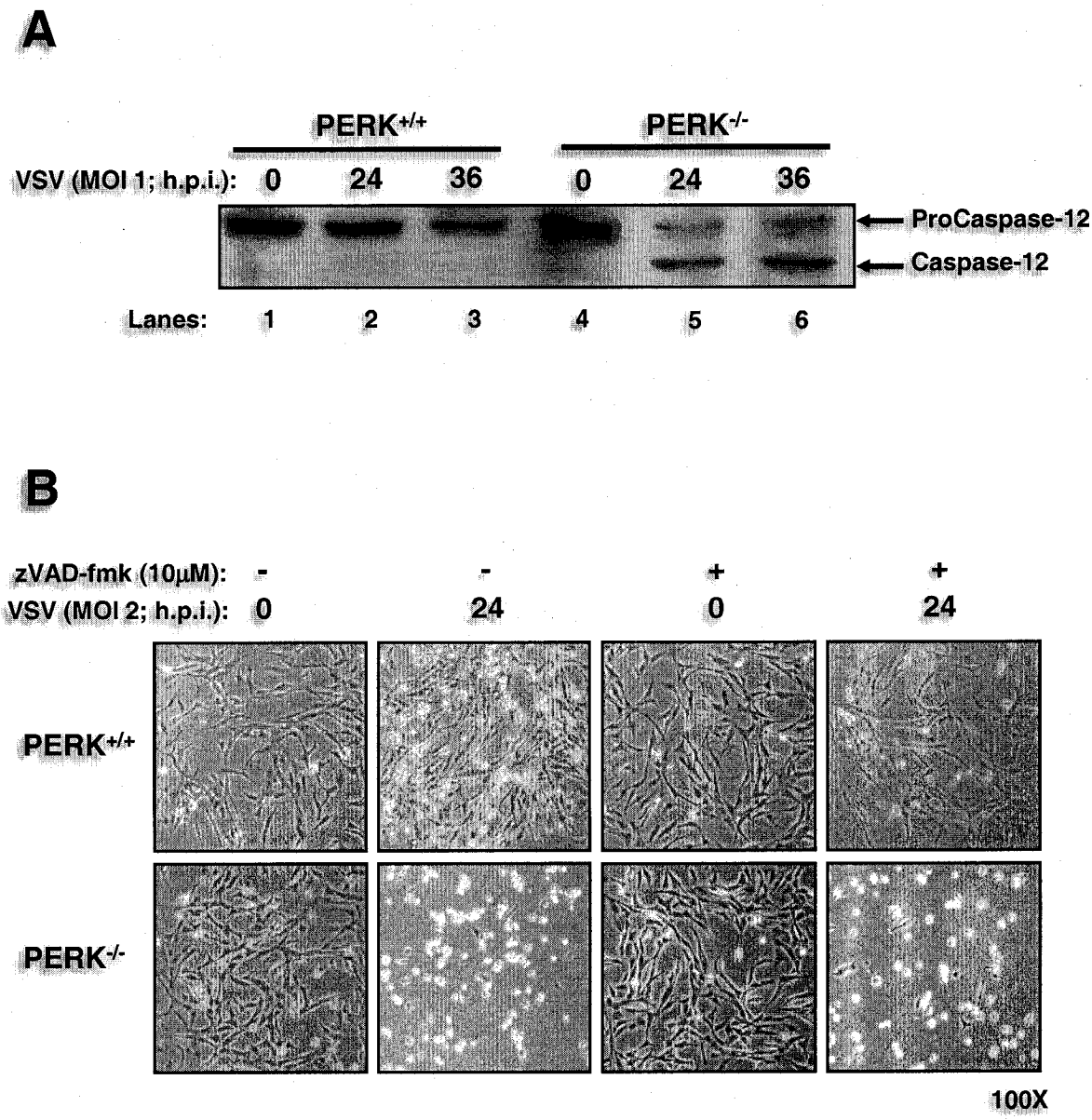
A
PERK+/+
PERK-/-
VSV (MOI 1; h.p.i.): 0 24 36 0 24 36
ProCaspase-12
Caspase-12
Lanes: 1 2 3 4 5 6
B
zVAD-fmk (10μM): - - + +
VSV (MOI 2; h.p.i.): 0 24 0 24
PERK+/+
PERK-/-
100X
C
PERK+/+
PERK-/-
zVAD-fmk (10μM): - - + + - - + +
VSV (MOI 2; h.p.i.): 0 24 0 24 0 24 0 24
PARP (Full length)
PARP (89 kDa)
Lanes: 1 2 3 4 5 6 7 8

Figure 32

Figure 33. VSV-mediated apoptosis is independent of the JNK/p38 MAPK pathway.

Protein extracts from $PERK^{+/+}$ and $PERK^{-/-}$ MEFs infected with VSV (MOI 1) were collected at different hours post infection (h.p.i.) and were used for immunoblot analysis with a rabbit polyclonal anti-phospho JNK-1 antibody (top panel), a rabbit polyclonal anti-JNK-1 antibody (second panel), a rabbit polyclonal anti-phospho p38 MAPK antibody (third panel), a rabbit polyclonal anti-p38 MAPK antibody (fourth panel). The protein load was normalized to Actin after immunoblotting with an anti-Actin monoclonal antibody (bottom panel).

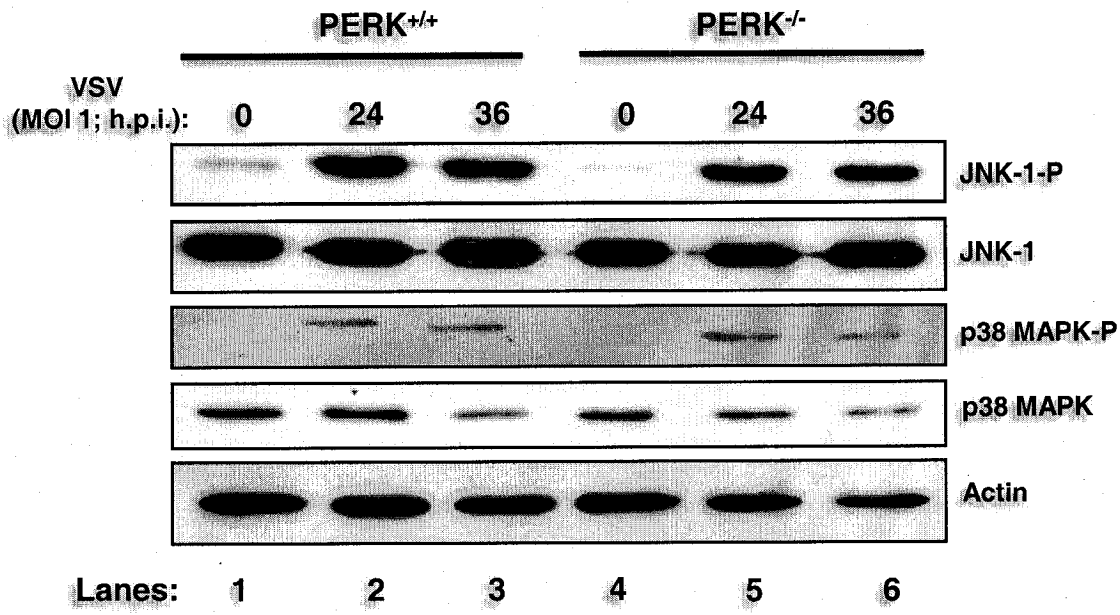
PERK+/+
PERK-/-
VSV
(MOI 1; h.p.i.):
0
24
36
0
24
36
JNK-1-P
JNK-1
p38 MAPK-P
p38 MAPK
Actin
Lanes:
1
2
3
4
5
6

Figure 33

2.2 Cross-Talk between PERK and PKR During VSV Infection

2.2.1 Impaired PKR Activation in VSV Infected PERK$^{-/-}$ MEFs

Given the demonstrated role for PKR in halting VSV replication (11,93,313), we wished to examine whether induction of VSV replication and apoptosis in PERK$^{-/-}$ MEFs was due to defective activation of PKR. When protein extracts from VSV-infected cells were subjected to pull down with poly(rI-rC)-agarose (Fig. 34A) or immunoprecipitation with PKR antibodies (Fig. 34B) followed by kinase autophosphorylation, we found that PKR kinase activity was severely diminished in PERK$^{-/-}$ MEFs as opposed to their wild type counterparts after virus infection (Fig. 34A and B). This indicated that the higher replication and apoptotic capacity of VSV in PERK$^{-/-}$ MEFs is caused, at least in part, due to defective PKR activation. We further verified this finding by assessing the activation of PKR *in vivo* by 2D gel electrophoresis and immunoblot analysis (Fig. 34C). We observed an increase in PKR protein towards the acidic side (pH 6; bottom left panel, arrow) in VSV-infected PERK$^{+/+}$ MEFs as opposed to the VSV-infected PERK$^{-/-}$ MEFs (bottom right panel). This acidic fraction of PKR was present only in PERK$^{+/+}$ cells indicating an induction of PKR activity in cells containing PERK as opposed to cells lacking it.

This finding prompted us to examine whether PKR activity is induced by ER stress and, if so, whether its activation is mediated by PERK. To do so, we treated PERK$^{+/+}$ and PERK$^{-/-}$ MEFs with tunicamycin, an inhibitor of protein glycosylation and an ER stress inducer, followed by autophosphorylation of immunoprecipitated PKR (Fig. 35A). We noticed that PKR kinase activity was induced in PERK$^{+/+}$ MEFs upon

tunicamycin treatment (lanes 1-4) as opposed to $PERK^{-/-}$ MEFs, which failed to activate PKR (lanes 5-8). Interestingly, PKR autophosphorylation was significantly diminished after 4h of tunicamycin treatment (lane 8) indicating that prolonged ER stress may lead to the inactivation of PKR. This data provided evidence for a cross-talk between the two eIF2α kinases with PKR functioning downstream of PERK in response to ER stress or VSV infection.

These data suggested that PERK is capable of modulating PKR autophosphorylation and its full scale activation. To further substantiate this, we co-transfected COS-1 cells with PERK or PKR in the presence or absence of a dominant negative PKR mutant (PKRΔ6) (91) (Fig. 35B). PERK and PKR were able to induce eIF2α phosphorylation upon VSV infection (third panel, compare lanes 9 and 13 to lanes 2 and 6, respectively), whereas PKRΔ6 showed no kinase activity (third panel, compare lane 3 with lane 10). Also, PKRΔ6 was able to prevent PKR-mediated eIF2α phosphorylation before and after VSV infection (third panel, compare lane 7 with lane 14). To this extent, PKRΔ6 was capable of inhibiting PERK-mediated eIF2α phosphorylation (third panel, compare lane 4 with lane 11, and lane 5 with lane 12). Also, PKRΔ6 did not affect PERK phosphorylation on Thr980 (top panel). These data further substantiate the notion that eIF2α phosphorylation is mediated by both PERK and PKR upon VSV infection, and that a cross-talk between both kinases is necessary to inhibit viral replication.

Figure 34. PKR activation is impaired in VSV infected $PERK^{-/-}$ MEFs.

Protein extracts from VSV infected (MOI 10) $PERK^{+/+}$ and $PERK^{-/-}$ MEFs were pulled down with either **(A)** poly(rI-rC)-agarose beads (Amersham-Pharmacia) or **(B)** immunoprecipitated with a rabbit polyclonal anti-mPKR antibody (D-20), and subjected to *in vitro* phosphorylation in the presence of [^{32}P]-γATP. Half of the dsRNA-bound PKR was subjected to SDS-10%PAGE and autoradiography (top panel) whereas the other half to immunoblot analysis with an antibody against mouse PKR (bottom panel, B-10).

(C) $PERK^{+/+}$ and $PERK^{-/-}$ MEFs were either infected (bottom panels) or uninfected (top panels) with VSV at MOI of 10 and harvested at 12 hours post infection. Protein extracts were subjected to 2D electrophoresis and immunoblot analysis with a rabbit polyclonal anti-mPKR antibody (D-20).

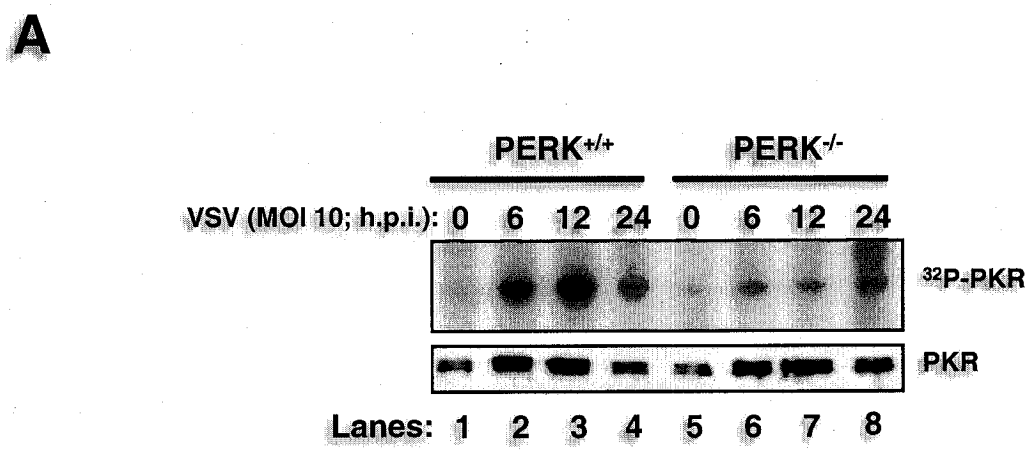
A
PERK+/+
PERK-/-
VSV (MOI 10; h.p.i.): 0 6 12 24 0 6 12 24
32P-PKR
PKR
Lanes: 1 2 3 4 5 6 7 8

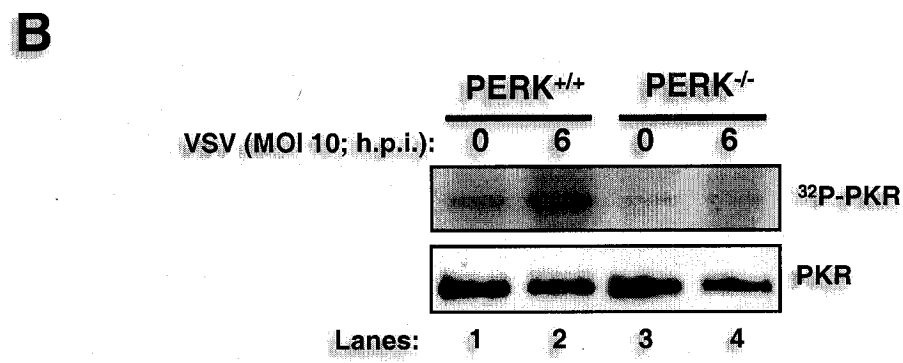
B
PERK+/+
PERK-/-
VSV (MOI 10; h.p.i.): 0 6 0 6
32P-PKR
PKR
Lanes: 1 2 3 4

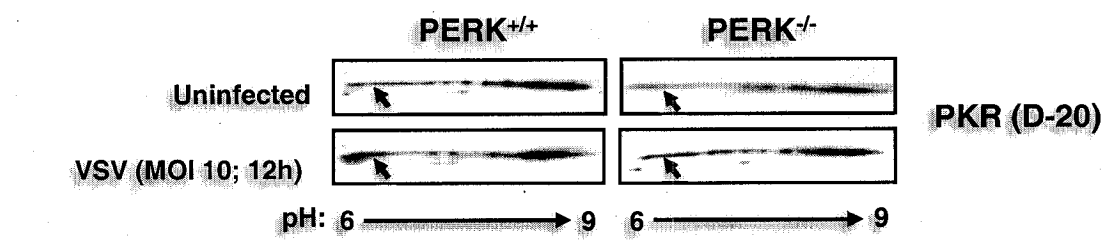
C
PERK+/+
PERK-/-
Uninfected
VSV (MOI 10; 12h)
PKR (D-20)
pH: 6 9 6 9

Figure 34

Figure 35. PERK functions upstream to PKR upon ER stress and VSV infection.

(A) $PERK^{+/+}$ and $PERK^{-/-}$ MEFs were either treated or not with 10 μg/ml of tunicamycin for indicated period of time. Protein extracts were subjected to a similar kinase assay as in Fig. 34.

(B) COS-1 cells were mock transfected (lanes 1 and 8) or transfected with either WT PERK (5 μg of plasmid DNA, lanes 2, 4, 5, 9, 11 and 12) or WT PKR with (5 μg of plasmid DNA, lanes 6, 7, 13 and 14) or without PKRΔ6 (2 μg of plasmid DNA, lane 4 and 11 or 5 μg of plasmid DNA, lanes 3, 5, 7, 10, 12 and 14) followed by VSV infection. Protein extracts were subjected to immunoblot analysis with either with a rabbit polyclonal phosphothreonine 980 PERK antibody (top panel), a mouse monoclonal myc-tag antibody (second panel), a rabbit polyclonal phosphoserine 51 eIF2α antibody (third panel) or with a mouse monoclonal eIF2α antibody (bottom panel).

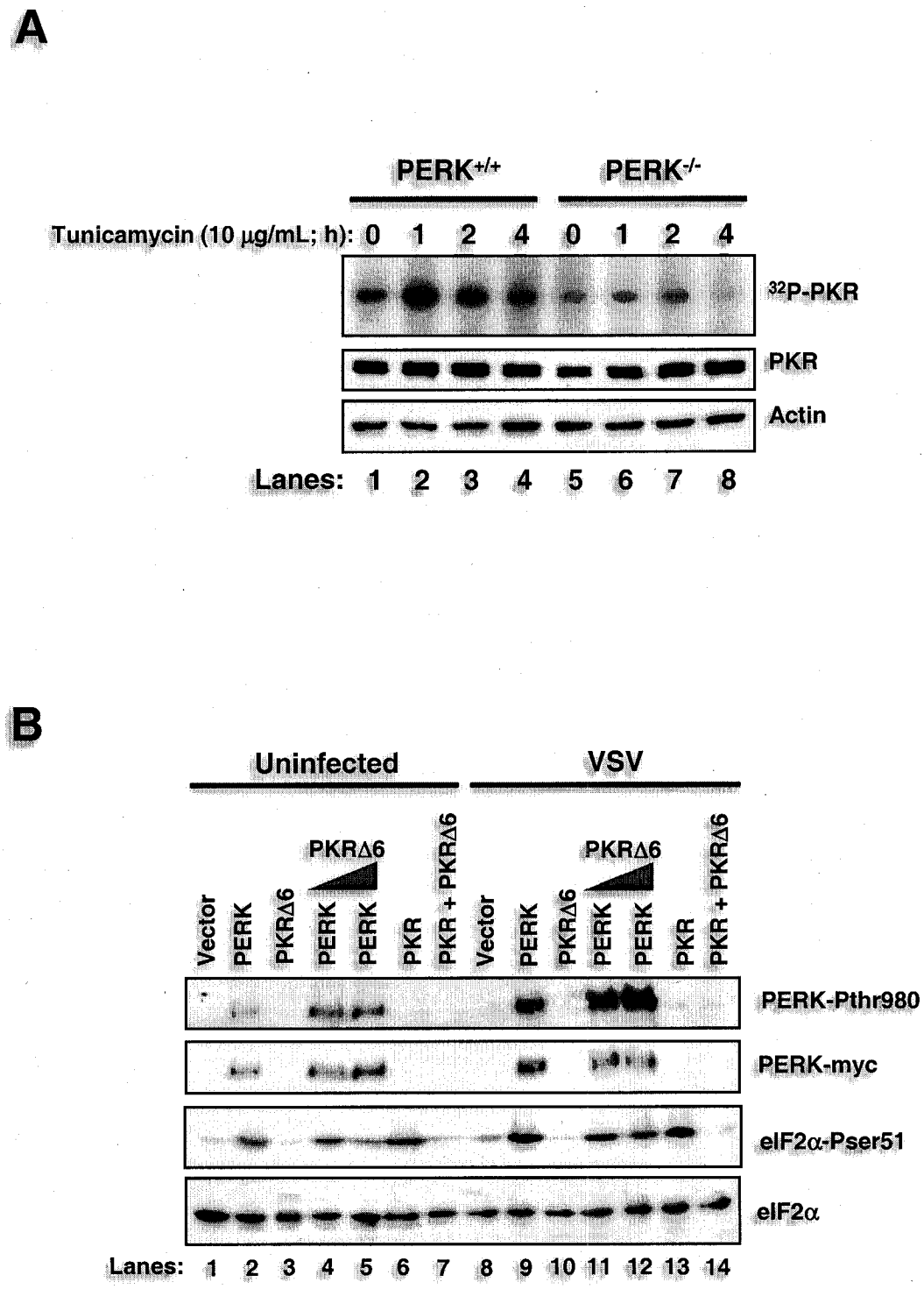
A
PERK+/+
PERK-/-
Tunicamycin (10 μg/mL; h): 0 1 2 4 0 1 2 4
32P-PKR
PKR
Actin
Lanes: 1 2 3 4 5 6 7 8
B
Uninfected
VSV
PKRΔ6
Vector
PERK
PKRΔ6
PERK
PERK
PKR
PKR + PKRΔ6
PERK-Pthr980
PERK-myc
eIF2α-Pser51
eIF2α
Lanes: 1 2 3 4 5 6 7 8 9 10 11 12 13 14

Figure 35

2.2.2 PERK Modulates dsRNA-mediated PKR Activation

One of the mechanisms proposed to activate PKR during virus infection is the dimerization of the kinase upon dsRNA binding (172). Since dsRNA is generated throughout the life cycle of VSV (338), we wanted to investigate if PERK was capable of modulating PKR activation in cells transfected with dsRNA (Fig. 36). We noticed that the induction of eIF2α phosphorylation was impaired in $PERK^{-/-}$ MEFs upon dsRNA treatment as opposed to $PERK^{+/+}$ cells (Fig. 36A, compare lane 4 with lane2). The same was observed regarding PKR activation (Fig. 36B). We performed a PKR immunoprecipitation followed by an *in vitro* kinase assay thus revealing that $PERK^{-/-}$ MEFs were incapable of fully activating PKR (Fig. 36B, top panel). To the same extent, phosphorylation of PKR on Thr446 was impaired in the $PERK^{-/-}$ cells (Fig. 36B, middle panel). These results suggested that the efficient activation of PKR by dsRNA required PERK.

2.2.3 VSV does not Induce ER stress

PERK plays an essential role in the unfolded protein response (UPR) (273), and as such, its activation in VSV infection initially indicated an ability of the virus to elicit the UPR. This was consistent with the notion that viruses that use the ER as an integral part of their replication strategy are likely able to induce an ER stress response (5). In fact, previous studies showed that the VSV glycoprotein (G) oligomerizes in the ER prior to its transport to the cell surface (363). Misfolded and unassembled VSV-G is retained in the ER (77) whereas the interactions of the viral protein with two chaperones, BiP and calnexin, are essential for efficient folding and for retention of partially folded G protein

forms in the ER (124). Thus, an overload of VSV-G in the ER during virus replication might have been one of the mechanisms eliciting an ER stress response in infected cells. Contrary to this, we found that expression of various ER stress markers including CHOP, BiP, or XBP-1 was not induced in infected cells nor was their expression impaired in $PERK^{-/-}$ MEFs (Fig. 37). As such, we concluded that VSV utilizes a novel pathway to activate PERK. Although this pathway is not currently known, we hypothesize that virus infection might induce protein phosphorylation cascades leading to the activation of PERK in the ER.

Figure 36. PKR activation is impaired in dsRNA treated PERK$^{-/-}$ MEFs.

(A) PERK$^{+/+}$ and PERK$^{-/-}$ MEFs were transfected with dsRNA (10 μg/ml, lanes 2 and 4) or mock transfected (lanes 1 and 3) or treated with thapsigargin (1 μM, 2h; lanes 5, 6). Proteins extracts were harvested at indicated hours and subjected to immunoblot analysis using the serine 51 phosphospecific eIF2α antibody (top panel) or with the eIF2α antibody (lower panel).

(B) Protein extracts from dsRNA transfected PERK$^{+/+}$ and PERK$^{-/-}$ MEFs were immunoprecipitated with a rabbit polyclonal anti-mPKR antibody (D-20), and subjected to phosphorylation *in vitro* in the presence of [^{32}P]-γATP. The immunoprecipitated PKR was subjected to SDS-10%PAGE and autoradiography (top panel). Protein extracts were subjected to immunoblot analysis with a rabbit polyclonal phosphothreonine 446 PKR antibody (second panel) or a mouse monoclonal Actin antibody (bottom panel).

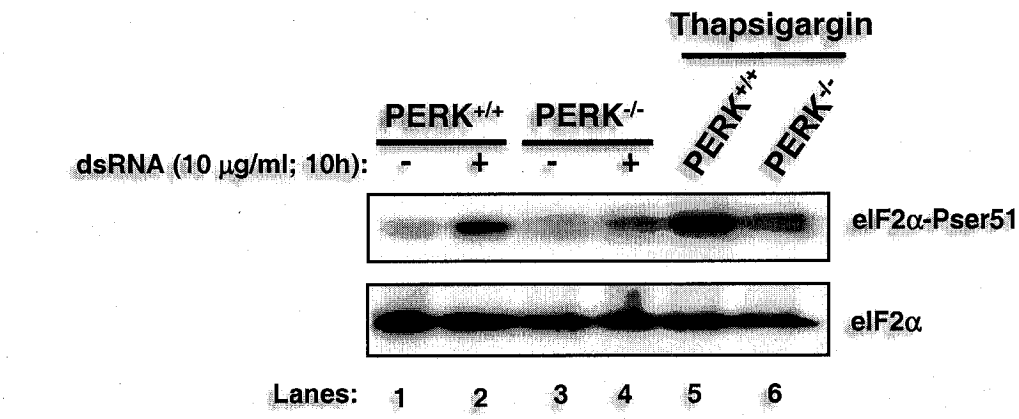
A
Thapsigargin
PERK+/+
PERK-/-
PERK+/+
PERK-/-
dsRNA (10 μg/ml; 10h):
-
+
-
+
eIF2α-Pser51
eIF2α
Lanes:
1
2
3
4
5
6

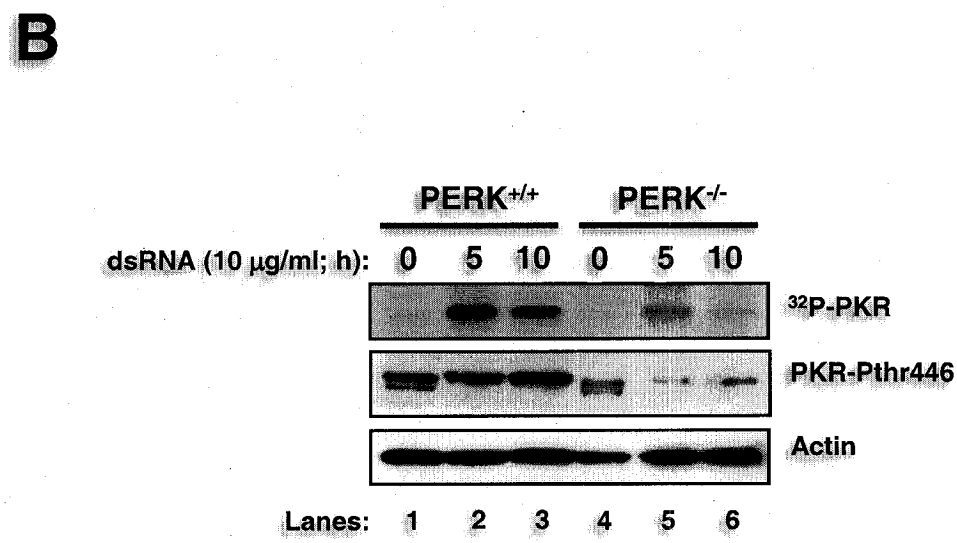
B
PERK+/+
PERK-/-
dsRNA (10 μg/ml; h):
0
5
10
0
5
10
32P-PKR
PKR-Pthr446
Actin
Lanes:
1
2
3
4
5
6

Figure 36

Figure 37. VSV infection does not elicit an ER stress response.

Total RNA was isolated from VSV infected (MOI 10) $PERK^{+/+}$ and $PERK^{-/-}$ MEFs (lanes 1-12) or from thapsigargin treated cells (1 μM, 5h; lanes 13 and 14). 10 μg of RNA was used for northern blot analysis. The membrane-bound RNA was probed with radio-labeled cDNA corresponding to *BiP/Grp78* (top panel), *XBP-1* (second panel) or *CHOP/GADD153* (third panel). The bottom panel is a picture of the ethidium bromide stained gel depicting the 28S and 18S rRNA as an indication for equal loading.

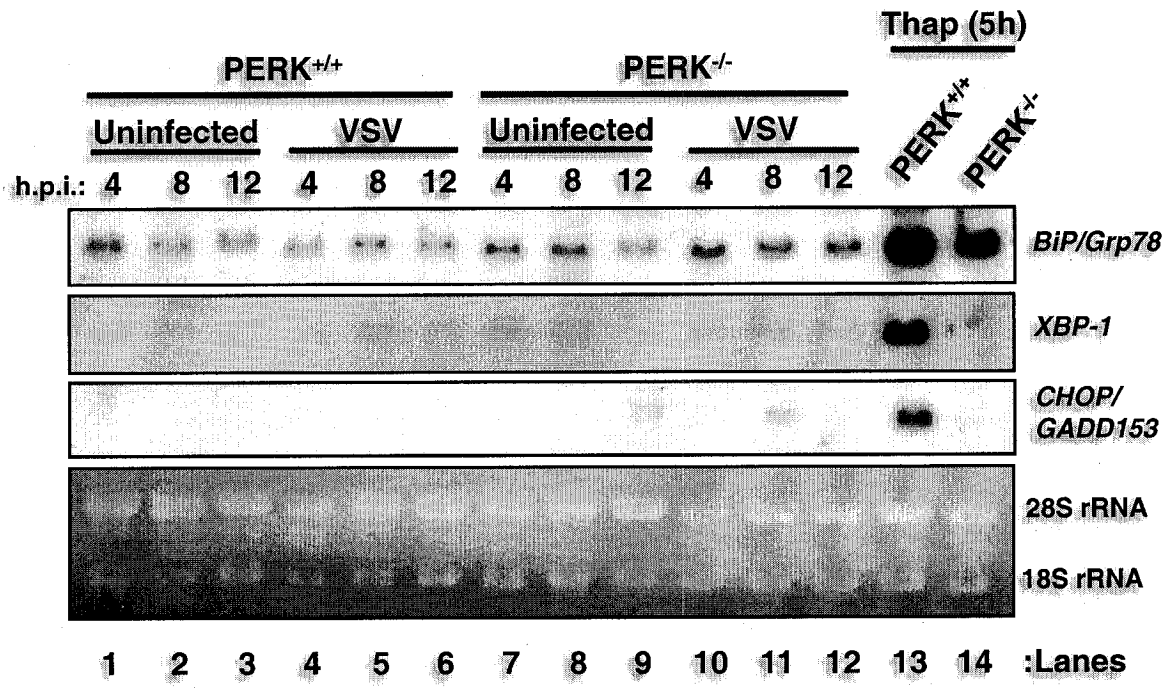
Thap (5h)
PERK+/+
PERK-/-
Uninfected
VSV
Uninfected
VSV
PERK+/+
PERK-/-
h.p.i.: 4 8 12 4 8 12 4 8 12 4 8 12
BiP/Grp78
XBP-1
CHOP/
GADD153
28S rRNA
18S rRNA
1 2 3 4 5 6 7 8 9 10 11 12 13 14 :Lanes

Figure 37

3. ROLE OF EIF2α KINASES IN THE REGULATION OF P53

3.1 eIF2α Kinases Downregulate p53 Independent of Translation Control

3.1.1 ER Stress Response Downregulates p53

We have previously observed that pharmacological and physiological inducers of ER stress target p53 to the cytoplasm where it is degraded (263). Given the ability of ER stress to trigger the activation of eIF2α kinases, we hypothesized that eIF2α kinases may be involved in the downregulation of p53 mediated by ER stress. We first examined the expression levels of p53 and the phosphorylation of eIF2α on Ser51 in response to prolonged (16 hours) ER stress in different human tumor cell lines harboring wild type p53. We employed the fibrosarcoma cell line HT1080, the lung carcinoma epithelial cell line A549, the osteosarcoma cell line U2OS, and the colon carcinoma cell line HCT116 (Fig. 38A). All four human cell lines responded to both ER stress inducing agents tunicamycin (TM), and thapsigargin (TG) as indicated by the induction of eIF2α phosphorylation on Ser51 (Fig. 38A).

In relation to our previous observations (263), the p53 protein levels decreased upon treatment with TM or TG (Fig. 38A). Short term ER stress led to the same conclusions when HT1080 cells were treated with TG for 4 hours (Fig. 38B, lanes 1 and 2). Both, the induction of eIF2α phosphorylation and the downregulation of p53 were observed in HT1080 cells (Fig. 38B) and in the other human cancer cell lines previously

mentioned (data not shown). For practical reasons, the remaining experiments were done with short term ER stress response between 2-4 hours.

Next we investigated whether similar results can be obtained in the mouse fibroblast cell line NIH 3T3 treated with TG for 4 hours. As expected, ER stress induced eIF2α phosphorylation in conjunction with p53 downregulation in NIH 3T3 cells (Fig. 38C, lanes 1-2). These experiments suggest that both human and mouse cells may utilize a similar pathway to downregulate p53 upon ER stress. We previously showed that this ER stress-induced downregulation of p53 was due to the accelerated Mdm2-p53 degradation pathway (260,263). Also, this downregulation can be rescued if the proteasome pathway is chemically inhibited with MG132. We observed a recovery of p53 protein levels with MG132 above the basal levels in HT1080 (Fig. 38B, lanes 3-4) and NIH 3T3 (Fig. 38C, lanes 3-4) cells despite the induction of ER stress. These results support our previous claim that ER stress induces the degradation of p53 (263).

Figure 38. Downregulation of p53 upon ER stress in different cell lines.

(A) A549, HCT116, U2OS, HT1080 cells harboring wild type p53 were treated for 16h with tunicamycin (TM; 10 μg/ml) or thapsigargin (TG; 1 μM). Total protein extracts were used to determine the protein levels of p53, phospho-ser51 of eIF2α, total eIF2α, PUMA, NOXA, phospho-Ser641/645-glycogen synthase, total glycogen synthase by immunoblot analysis.

(B, C) HT1080 cells **(B)** or NIH 3T3 cells **(C)** were treated with 1 μM TG for 4h in the presence or absence of MG132 (10 μM). Cell extracts were subjected to immunoblot analysis with anti-p53, anti-phospho-Ser51-eIF2α and anti-eIF2α antibodies.

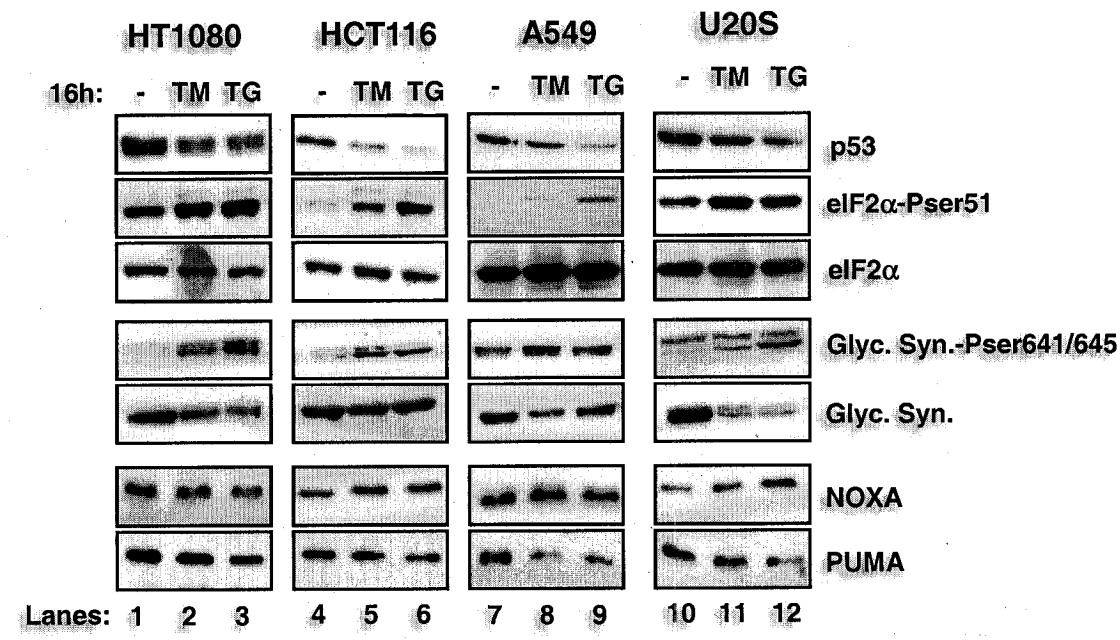
A
HT1080
HCT116
A549
U20S
16h: - TM TG - TM TG - TM TG - TM TG
p53
eIF2α-Pser51
eIF2α
Glyc. Syn.-Pser641/645
Glyc. Syn.
NOXA
PUMA
Lanes: 1 2 3 4 5 6 7 8 9 10 11 12

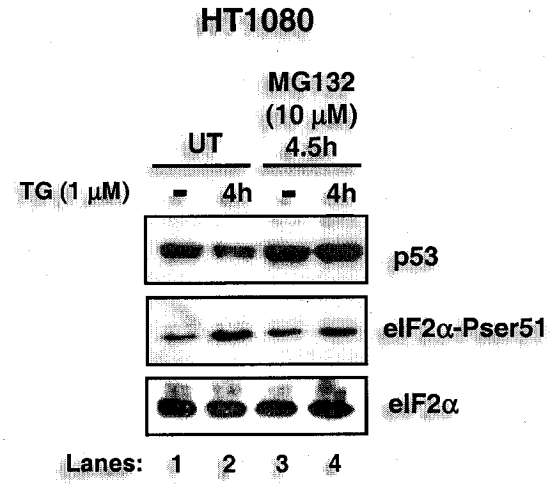
B
HT1080
MG132 (10 μM) 4.5h
UT
TG (1 μM) - 4h - 4h
p53
eIF2α-Pser51
eIF2α
Lanes: 1 2 3 4

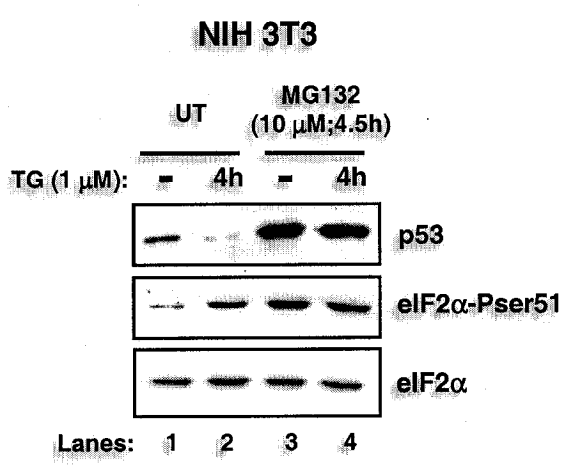
C
NIH 3T3
UT
MG132 (10 μM;4.5h)
TG (1 μM): - 4h - 4h
p53
eIF2α-Pser51
eIF2α
Lanes: 1 2 3 4

Figure 38

3.1.2 eIF2α Kinase Activity Downregulates p53

It has been demonstrated that PERK activation is induced upon ER stress, and it is the main eIF2α kinase that mediates the shutdown of protein synthesis (128). In order to assess the role that PERK plays in the downregulation of p53, $PERK^{+/+}$ and $PERK^{-/-}$ primary MEFs were treated with TG, and p53 levels were detected by immunoblot analysis. Thapsigargin treatment mediated the downregulation of p53 protein levels in $PERK^{+/+}$ MEFs, however this decrease was not observed in the $PERK^{-/-}$ MEFs (Fig. 39A). To further confirm the involvement of PERK in human cells, we knocked down PERK using the RNA interference (RNAi) approach (97) in HT1080 cells (Fig. 39B). We observed a dramatic decrease in PERK protein levels in the PERK RNAi cells (Fig. 39B, fourth panel, lanes 3-4 compared to lanes 1-2), and a failure to induce eIF2α phosphorylation (Fig. 39B, second panel) upon TG treatment indicating that PERK activation was impaired in these cells. This impairment of PERK was sufficient to rescue p53 protein levels even in the presence of TG (Fig. 39B, first panel). Both experiments suggest that PERK activation mediates p53 downregulation in response to ER stress.

We next investigated whether other forms of stress that induce eIF2α phosphorylation are capable to downregulate p53. To this extent we decided to study if another eIF2α kinase such as PKR can lead to the same conclusions. PKR dimerizes and autophosphorylates in the presence of dsRNA produced during virus infection (59). To confirm the role of PKR in p53 downregulation upon dsRNA, we used the knockdown approach. Specifically, we used a stable NIH3T3 cell line expressing a short-hairpin RNA targeted against *PKR* mRNA (shPKR) in order to knockdown PKR protein levels

(Fig. 40A, second panel). We observed an induction of eIF2α phosphorylation after transfection of dsRNA in control cells but not in shPKR cells due to the lack of PKR expression (Fig. 40A, third panel). We found that by stably knocking down PKR, we were able to rescue the endogenous wild type p53 from the inhibitory effects of dsRNA transfection (Fig. 40A, top panel) providing evidence for a role of PKR in this process.

Similar to TG treatment, dsRNA transfection was able to downregulate p53 and induce eIF2α phosphorylation in HT1080 cells (Fig. 40B, lane 3) but not when dsRNA was added to the medium (Fig. 40B, lane 2). This confirms that intracellular or cytoplasmic dsRNA was required to induce PKR activation and promote p53 downregulation. More so, the downregulation of p53 was rescued in the presence of MG132 (Fig. 40B, lane 6) further suggesting that the proteasome pathway is responsible for the p53 downregulation upon dsRNA transfection. Together these data suggest that eIF2α kinase activity induced by thapsigargin (PERK) or dsRNA (PKR) is sufficient to inhibit the expression of p53.

Figure 39. Activation of PERK triggers the downregulation of p53 upon ER stress.

(A) Primary $PERK^{-/-}$ and $PERK^{+/+}$ MEFs were treated with TG (1 μM) for 4 h and total cell extracts were used to determine p53 and actin levels by immunoblot analysis.

(B) HT1080 cells were transiently transfected with non-specific siRNA (GL-2) or PERK siRNA (PERKi) and then treated with TG (1 μM) for 4 h. Cell extracts were subjected to immunoblot analysis with anti-p53, anti-phospho-Ser51-eIF2α, anti-eIF2α, and anti-PERK antibodies.

A

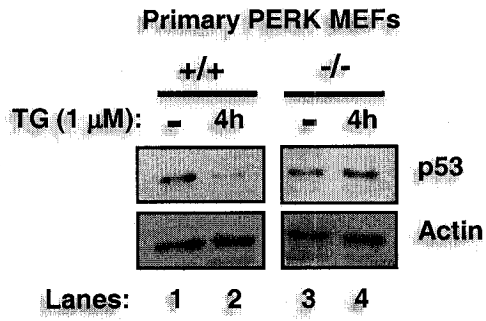
Primary PERK MEFs
+/+
-/-
TG (1 μM): - 4h - 4h
p53
Actin
Lanes: 1 2 3 4

B

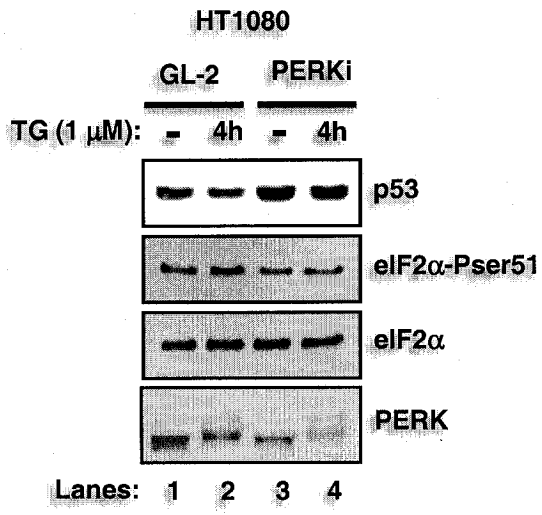
HT1080
GL-2
PERKi
TG (1 μM): - 4h - 4h
p53
eIF2α-Pser51
eIF2α
PERK
Lanes: 1 2 3 4

Figure 39

Figure 40. Activation of PKR by dsRNA triggers the downregulation of p53.

(A) NIH 3T3 cells were stably transfected with non-specific shRNA (CON) or with shRNA against *PKR* (shPKR) followed by transfection with dsRNA (10 μg/ml) for 3h. Cell extracts were subjected to immunoblot analysis with anti-p53, anti phospho-Ser51-eIF2α, anti-eIF2α, and anti-PKR antibodies.

(B) HT1080 cells were either transfected with LipofectAMINE and dsRNA (10 μg/ml) or incubated with dsRNA (10 μg/ml) alone and pre-treated (30 min) with or without MG132 (10 μM) for 4h. Cell extracts were subjected to immunoblot analysis with anti-p53, anti-phospho-Ser51-eIF2α, anti-eIF2α antibodies.

A

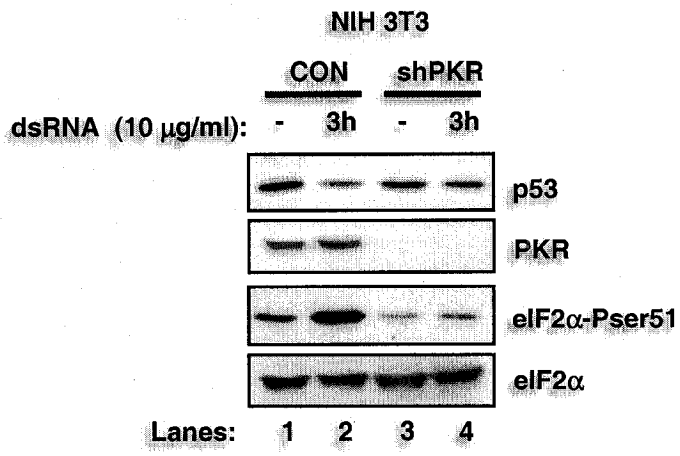
NIH 3T3
CON
shPKR
dsRNA (10 μg/ml): - 3h - 3h
p53
PKR
eIF2α-Pser51
eIF2α
Lanes: 1 2 3 4

B

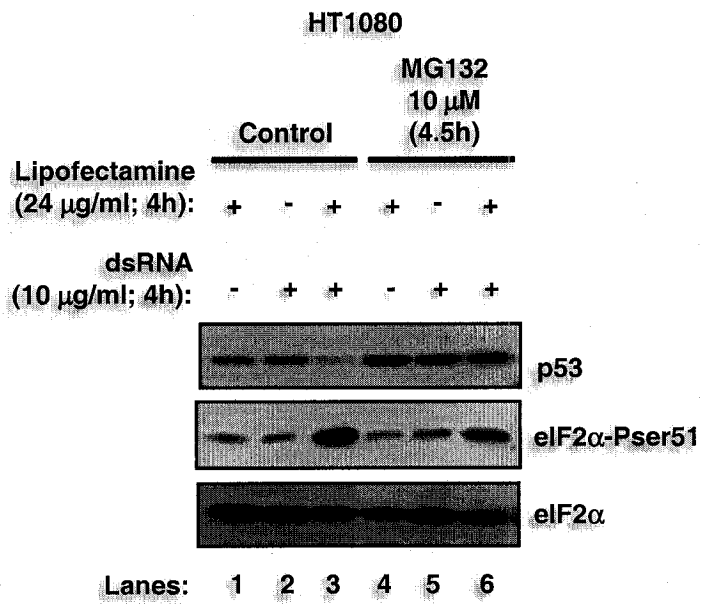
HT1080
MG132
10 μM
(4.5h)
Control
Lipofectamine
(24 μg/ml; 4h): + - + + - +
dsRNA
(10 μg/ml; 4h): - + + - + +
p53
eIF2α-Pser51
eIF2α
Lanes: 1 2 3 4 5 6

Figure 40

3.1.3 dsRNA Promotes p53 Cytoplasmic Localization

We previously reported that the ER stress response induces the nucleocytoplasmic transport and degradation of p53 (263). Since similar results were obtained between TG treatment and dsRNA transfection regarding p53 downregulation, we tested whether dsRNA also controls p53 localization. Immunohistochemistry analysis of untreated HT1080 cells show high levels of p53 localized in the nucleus (Fig. 41, top panel). Treatment with dsRNA had no effect on p53 localization (Fig. 41, second panel), whereas transfected dsRNA induced cytoplasmic localization of p53 (Fig. 41, third panel). The addition of MG132 was able to recover nuclear p53 (Fig. 41, panels 4-6) despite the activation of PKR mediated by transfected dsRNA as indicated by the phosphorylation of eIF2α (Fig. 40B, second panel).

We also observed that the induction of eIF2α phosphorylation was lower in HT1080 cells transfected with dsRNA in the presence of MG132 as opposed to dsRNA alone (Fig. 40B, second panel, lanes 6 compared to lane 3) for reasons not yet understood. This observation was not observed in NIH 3T3 cells treated with TG and/or MG132 (Fig. 38C) indicating that MG132 may have different effects on human cells than on mouse cells. It was previously shown that MG132 induces eIF2α phosphorylation via GCN2 activation in mouse fibroblast cells (163). We also had a similar induction of eIF2α phosphorylation in NIH 3T3 cells treated with MG132 (Fig. 38C, second panel, lane 3). However, this induction failed to downregulate p53 despite any translational shutdown mediated by eIF2α phosphorylation. These data support our previous observations that p53 is subjected to proteasome mediated degradation since MG132 was

sufficient to recover and stabilize p53 protein above basal levels. Taken together, PKR activation induced by intracellular dsRNA promotes the nuclear export and degradation of p53, and that the translation control mediated by eIF2α kinases may not be involved in this process.

Figure 41. dsRNA transfection induces the cytoplasmic localization of p53.

HT1080 cells were treated (dsRNA) or transfected (Lipo + dsRNA) with 10 μg/ml dsRNA for 4h in presence or absence of MG132 (10 μM). The localization of endogenous p53 was examined by immunofluorescence. Cell nuclei were visualized by staining with DAPI.

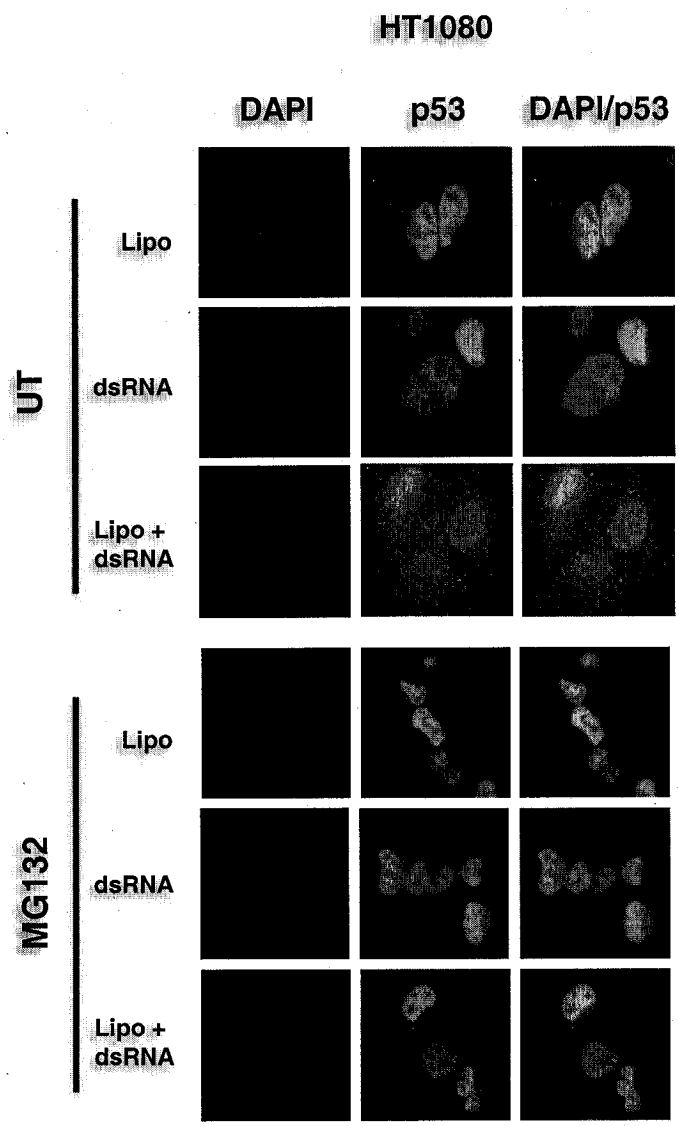
HT1080
DAPI
p53
DAPI/p53
UT
Lipo
dsRNA
Lipo +
dsRNA
MG132
Lipo
dsRNA
Lipo +
dsRNA

Figure 41

3.1.4 Downregulation of p53 is Independent of eIF2α Phosphorylation

To determine whether the phosphorylation of eIF2α plays a role in the downregulation of p53 upon ER stress, we treated HT1080 cells with compound 3 (Sal003), a derivative of salubrinal (39). Salubrinal is a drug that acts as a potent inhibitor of the PP1 phosphatase thus preventing eIF2α dephosphorylation, and ultimately prevents protein synthesis independently of eIF2α kinase activity (39). We noticed that Sal003 treatment was capable of inducing eIF2α phosphorylation to the same extent as dsRNA transfection in HT1080 cells (Fig. 42A). Despite the robust accumulation of eIF2α phosphorylation, Sal003 treatment did not inhibit p53 levels (Fig. 42A) nor did it induce the cytoplasmic localization of p53 (Fig. 42B) in HT1080 cells as opposed to dsRNA transfection. This suggests that eIF2α phosphorylation in the absence of eIF2α kinase activity is not sufficient to decrease p53 levels or mediate its cytoplasmic localization.

We further investigated whether the phosphorylation of eIF2α is responsible for p53 nuclear export upon ER stress. To this end, we used immortalized MEFs bearing a homozygous Ser51Ala knock-in mutation of eIF2α (eIF2α A/A) (286). Isogenic wild type (eIF2α S/S) and eIF2αS51A knock-in (eIF2α A/A) MEFs were treated with tunicamycin (TM) and/or with a genotoxic drug adriamycin (ADR) to determine if eIF2α MEFs respond to ER stress and DNA damage. As expected, TM induced eIF2α phosphorylation on ser51 in the eIF2α S/S MEFs whereas no detectable phosphorylation was observed in the eIF2α A/A MEFs (Fig. 43A). Due to the immortalization of the eIF2α MEFs, p53 was undetectable in the eIF2α S/S MEFs despite the treatment with

ADR, and appeared to be mutated or already stabilized in the eIF2α A/A MEFs since neither treatment affected p53 protein levels. To bypass this limitation, we transfected the eIF2α MEFs with a chimeric protein consisting of the human wild type p53, and the green fluorescent protein (GFP-p53). The cells were then subjected to TM or TG (Fig. 43B). It was previously reported that the fluorescent GFP-p53 protein and the wild type p53 protein are recognized equally by several monoclonal p53-specific antibodies, have similar half-lives, and function comparably in transactivating a p53-responsive element as well as in suppressing the growth of tumor cells (243). In untreated conditions, GFP-p53 was localized in the nucleus in both cell lines (Fig. 43B). Upon ER stress, localization of GFP-p53 was both nuclear and cytoplasmic despite conditions in which eIF2α phosphorylation is not possible such as the case of the eIF2α A/A MEFs (Fig. 43B). Together these results confirmed that although eIF2α kinases are activated upon ER stress or dsRNA, the phosphorylation of eIF2α played no role in the nuclear export or downregulation of p53.

Figure 42. Salubrinal does not promote the downregulation or cytoplasmic localization of p53.

(A) HT1080 cells were treated with Sal003 (75 μM) or transfected with dsRNA (10 μg/ml). Cell extracts were subjected to immunoblot analysis with anti-p53, anti-phospho-Ser51-eIF2α, and anti-eIF2α antibodies.

(B) HT1080 cells were treated with Sal003 (75 μM) or transfected with dsRNA (10 μg/ml) for 6h. The localization of endogenous p53 was examined by immunofluorescence. Cell nuclei were visualized by staining with DAPI.

A

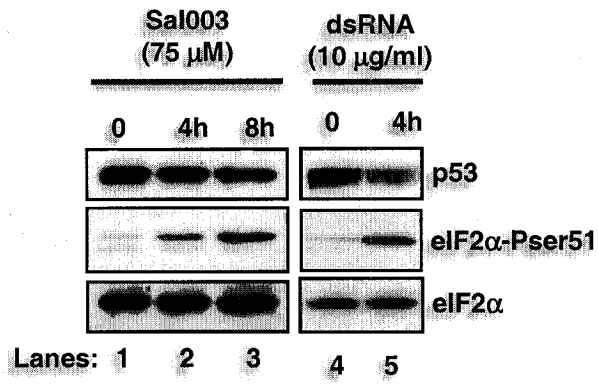
Sal003
(75 μM)
dsRNA
(10 μg/ml)
0
4h
8h
0
4h
p53
eIF2α-Pser51
eIF2α
Lanes: 1
2
3
4
5

B

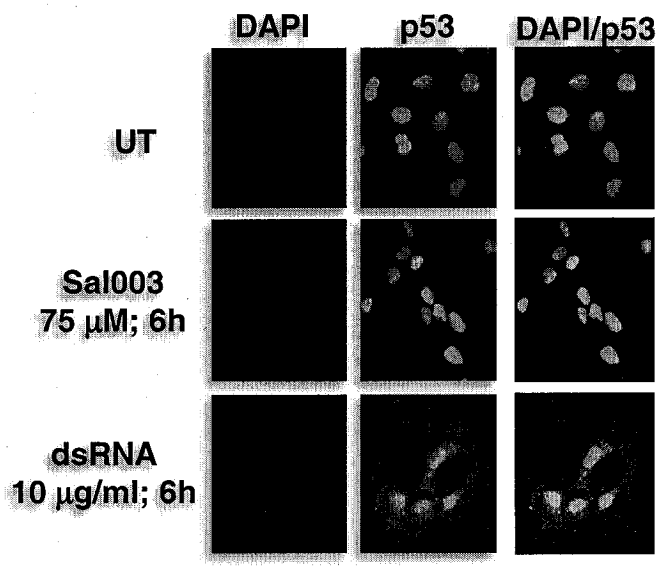
DAPI
p53
DAPI/p53
UT
Sal003
75 μM; 6h
dsRNA
10 μg/ml; 6h

Figure 42

Figure 43. The phosphorylation of eIF2α does not control the downregulation of p53.

(A) eIF2α S/S and eIF2α A/A MEFs were untreated or treated with tunicamycin (10 μg/ml) and/or adriamycin (1 μM) for 4h. Cell extracts were subjected to immunoblot analysis with anti-p53, and anti-phospho-Ser51-eIF2α antibodies.

(B) GFP-p53 WT (0.5 μg) was transiently transfected into eIF2α S/S and eIF2α A/A MEFs. Twenty-four hours later, cells were left untreated or treated with TM (10 μg/ml) or TG (1 μM) for 2h, and then examined for GFP-p53 fluorescence. Cell nuclei were visualized by DAPI staining.

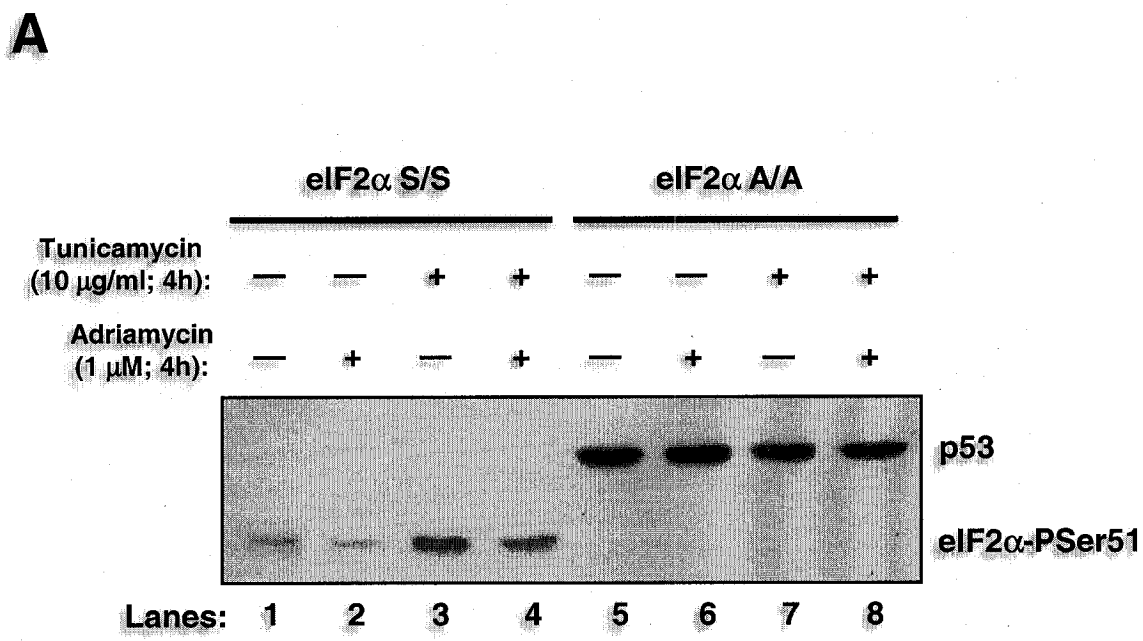
A
eIF2α S/S
eIF2α A/A
Tunicamycin
(10 μg/ml; 4h):
— — + + — — + +
Adriamycin
(1 μM; 4h):
— + — + — + — +
p53
eIF2α-PSer51
Lanes: 1 2 3 4 5 6 7 8

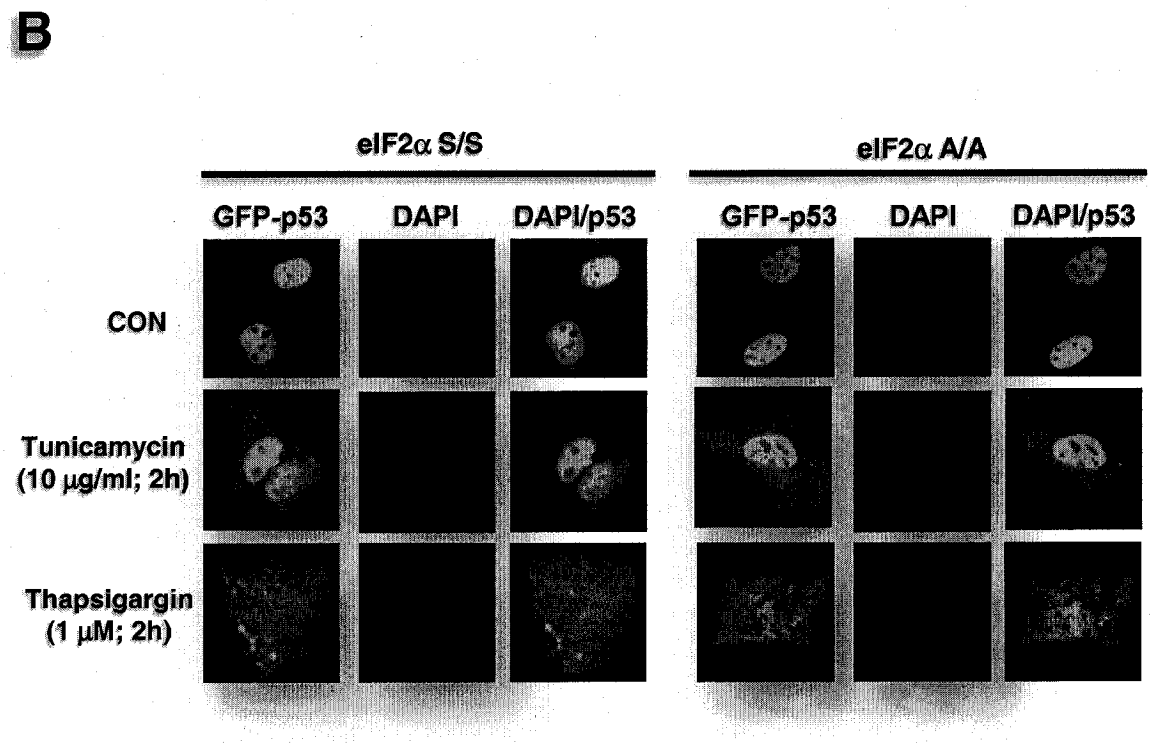
B
eIF2α S/S
eIF2α A/A
GFP-p53
DAPI
DAPI/p53
GFP-p53
DAPI
DAPI/p53
CON
Tunicamycin
(10 μg/ml; 2h)
Thapsigargin
(1 μM; 2h)

Figure 43

3.1.5 Inhibition of Protein Synthesis does not Alter *p53* mRNA Translation

The lack of eIF2α phosphorylation in the involvement of the downregulation of p53 led us to question whether the inhibition of protein synthesis affected *p53* mRNA translation. One of the most common methods to study translation mechanisms and regulation is polysome profiling using sucrose gradients (4). The method involves size separation of large cellular components on a sucrose gradient and monitoring the A_{254} across the gradient. The A_{254} profile of the separated complexes contains information not only about polyribosomes (two or more ribosomes), but also about other translational machinery components, including the small ribosomal subunit (40S), large ribosomal subunit (60S), and single ribosome (80S). Changes in this profile are indicative of changes in translation.

To study the behavior of specific mRNAs, the gradient is fractionated and the different fractions are analyzed by RT-PCR. Important information regarding translation of these mRNAs is obtained. The fraction of translationally active messages (those associated with ribosomes) can be deduced from the ratio between messages that sediment in the polysomal fractions versus those that sediment in the non-polysomal fractions. Changes in this ratio indicate changes in translation efficiency.

We performed polysome profiling analysis of HT1080 cells to study the translation of the *p53* mRNA (*TP53*) after TG, Sal003 treatment (Fig. 44A) or dsRNA transfection (Fig. 44B). Total RNA was isolated and sedimented through a linear sucrose gradient followed by fractionation. The distribution of RNA in the gradient fractions was determined by UV-spectroscopy (A_{254}) and the RNA from each fraction was isolated

followed by RT-PCR analysis using specific primers (Table 2) targeted against specific mRNA indicated in Figure 44. In each gradient, fractions 1 to 4 represent free mRNAs, whereas fractions 5 to 11 represent the ribosomal subunits (40S and 60S) and the single associated ribosome (80S or monosome). Fractions 12 to 20 represent the mRNAs associated with polysomes (2 or more ribosomes).

After TG or Sal003 treatment, we show a significant inhibition in protein translation indicated by the peak increase of ribosomal subunits (fractions 5-11) and by a disruption of polysome peaks in fractions 12 to 20 (Fig. 44A). We analyzed the distribution of *ATF4* mRNA as a control since it was previously shown to be translated under conditions that induce eIF2α phosphorylation (39,126,244,286). In untreated cells, the distribution of *ATF4* mRNA is mainly associated with one or two ribosomes (Fig. 44A, fractions 9-14, *ATF4* panel). Treatment with TG or Sal003 clearly shows a shift of *ATF4* mRNA associated with large polyribosomes (Fig. 44A, fractions 15-20, *ATF4* panels) indicating more efficient translation.

Unlike the *ATF4* mRNA, *p53* transcripts exhibited similar mRNA sedimentation patterns as the one found in untreated cells (Fig. 44A, *TP53* panels). We observed 1 or 2 fraction changes in the distribution of *p53* mRNA possibly due to the extensive disruption of the polysomes during translation inhibition. However this change appears to be negligible since all *p53* transcripts were localized above fraction 15 where most polyribosomes are in conjunction with the enhanced translation of *ATF4*. This suggests that *p53* mRNA is translated despite the shutdown of protein synthesis. In the case of *GAPDH*, TG and Sal003 treatment appear to induce changes in the distribution of its mRNAs towards monosomes (Fig. 44A, *GAPDH* panels). Although most of the *GAPDH*

mRNA appears in the polysome fractions, inhibition of protein synthesis shows some transcripts in the monosome portion of the profile (Fig. 44A, fractions 9-12, *GAPDH* panels), where the non-translated *ATF4* mRNAs are located.

Next, we inhibited protein synthesis by transfecting HT1080 cells with dsRNA (Fig. 44B) indicated by the increase of the 60S/80S peaks and the disruption of the polyribosome peaks. As expected, we observed a small shift of *ATF4* mRNA towards the polyribosome fractions (Fig. 44B, *ATF4* panels). Due to a larger polyribosome disruption upon dsRNA transfection, the *p53* transcripts shifted more so towards the lower end of the polysome fractions as opposed to the other two treatments (compare *TP53* panels of Fig. 44A with 44B). However, the lack of *p53* mRNA in the ribosome/monosome fractions indicated that these mRNAs were still efficiently translated. The *GAPDH* mRNA also shifted towards the lower end of the polysome fractions and towards the free mRNA fractions suggesting that translation of GAPDH was affected upon dsRNA transfection (Fig. 44B, *GAPDH* panels).

These results confirmed that p53 downregulation in response to various treatments that induce eIF2α kinase activity was not due to their ability to regulate *p53* mRNA translation. Together, our data suggest that the downregulation of p53 involved another pathway that requires eIF2α kinase activity independent of eIF2α phosphorylation.

Figure 44. The downregulation of p53 is not controlled by translation.

(A, B) HT1080 cells were treated with TG (A; 1 μM) for 2h or Sal003 (**A**; 75 μM) for 5h or transfected with dsRNA (**B**; 10 μg/ml) for 3h. Cell lysates were separated on a sucrose gradient and subjected to polysome profile analysis followed by fractionation and RNA extraction as described in materials and methods. The positions of the polysomes and ribosomal subunits (40S, 60S, and 80S) are indicated above each corresponding peaks. Translation efficiency of *ATF4* mRNA, *TP53* mRNA, and *GAPDH* mRNA were determined by RT-PCR using specific primers and the RNA isolated from each polysome fractions.

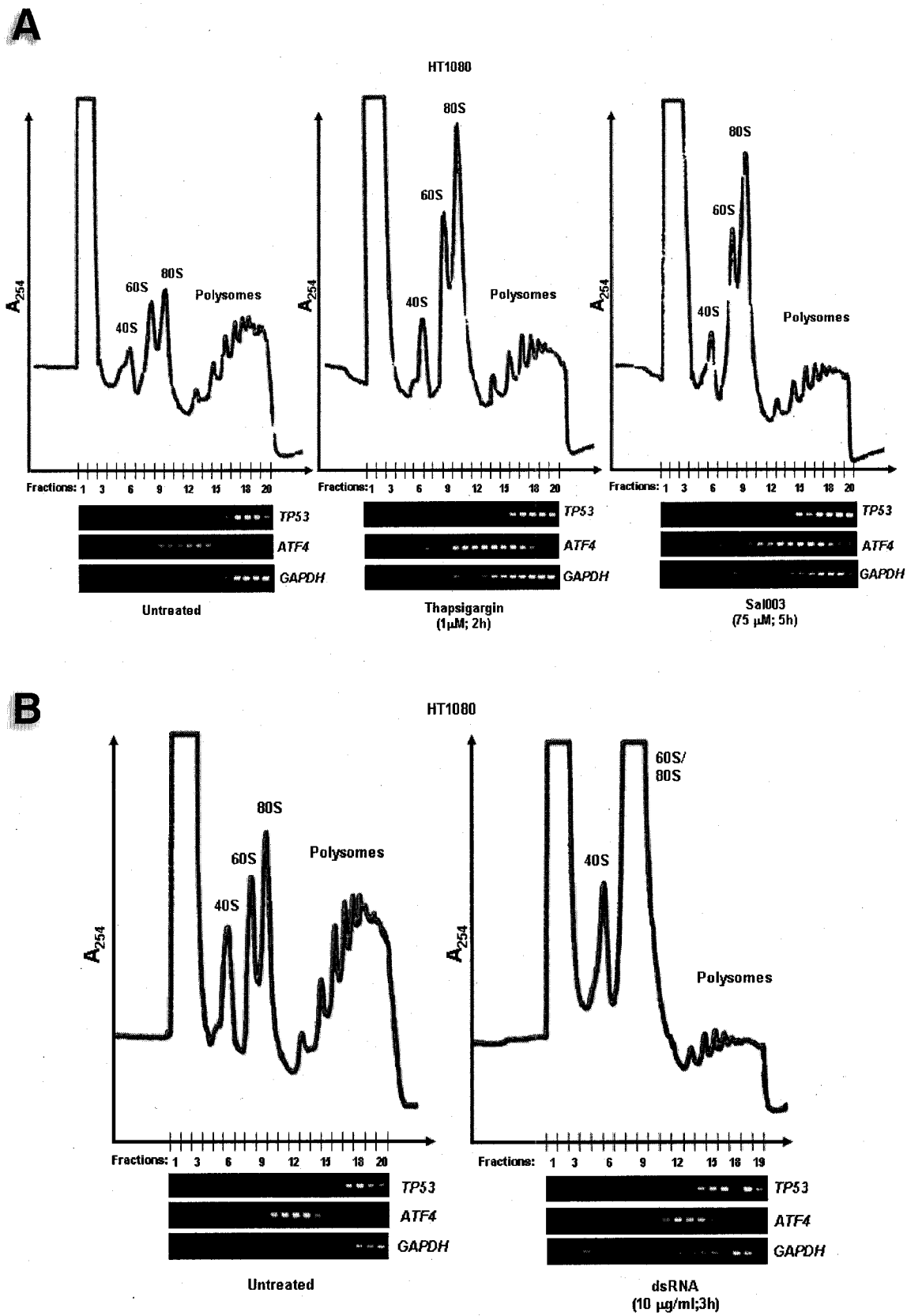
A
HT1080
A254
40S
60S
80S
Polysomes
Fractions: 1 3 6 9 12 15 18 20
TP53
ATF4
GAPDH
Untreated
Thapsigargin
(1μM; 2h)
Sal003
(75 μM; 5h)
B
HT1080
60S/
80S
Fractions: 1 3 6 9 12 15 18 19
Untreated
dsRNA
(10 μg/ml;3h)

Figure 44

3.2 eIF2α KINASE ACTIVITY IS SUFFICIENT TO DOWNREGULATE p53

3.2.1 An Inducible Form of eIF2α Kinase Downregulates p53

Although we determined that eIF2α phosphorylation and protein synthesis do not regulate p53 levels, we suspect that eIF2α kinase activity itself is required for this downregulation. However, many signaling pathways are activated in ER stressed or dsRNA treated cells, and it is therefore impossible to attribute the role of eIF2α kinase activity versus the activation of other pleiotropic pathways. To uncouple eIF2α kinase activity from stress, we took advantage of the fact that activation of eIF2α kinases is initiated by dimerization followed by *trans*-autophosphorylation. Normally this dimerization event is driven by the N-terminus regulatory domain of all eIF2α kinases. Therefore we needed a system that allows us to monitor eIF2α kinase activity without inducing other stress-inducing pathways.

In order to test the possibility and investigate specifically the role of eIF2α kinase activity in the regulation of p53, we employed a chimeric protein consisting of the bacterial Gyrase B protein (GyrB) fused to the kinase domain (KD) of human PKR (GyrB-PKR) (333). In the presence of the antibiotic coumermycin, the GyrB domains dimerize and induce the catalytic activity of the PKR kinase domain (Fig. 45A). Since the kinase domain of all eIF2α kinases is very similar in sequence and specificity (85), the GyrB-PKR system may faithfully represent not only PKR but all eIF2α kinases in terms of induction of their catalytic activity. We previously demonstrated that conditional

activation of GyrB-PKR in HT1080 cells in the presence of coumermycin leads to the induction of eIF2α phosphorylation and inhibition of global protein synthesis (177).

We used the HT1080/GyrB-PKR cells to look at the localization and expression of the endogenous wild type p53. The activation of wild type (WT) GyrB-PKR by coumermycin increased the cytoplasmic localization of p53 (Fig. 45B) as opposed to coumermycin-treated cells expressing the catalytically inactive GyrB-PKR K296H, in which localization of p53 remained nuclear (Fig. 45B). The nuclear localization of p53 was rescued by leptomycin B, an inhibitor of nuclear export, in coumermycin treated GyrB-PKR WT cells (data not shown) (291,314). Moreover, coumermycin treatment resulted in the downregulation of p53 protein levels and the induction of eIF2α phosphorylation in cells expressing GyrB-PKR WT but not in cells expressing the catalytically inactive GyrB-PKR K296H (Fig. 45C). We also noticed that the p53 protein levels in coumermycin-treated GyrB-PKR WT cells were recovered in the presence of MG132 (Fig. 46A) and partially decreased eIF2α phosphorylation levels (similar to Fig. 40B) through an as yet unidentified mechanism. Treatment with MG132 also prevented the cytoplasmic localization of p53 (Fig. 46B) despite the activation of GyrB-PKR.

Therefore inhibition of proteasome mediated degradation not only stabilizes p53 but it also retains it in the nucleus as previously observed (Fig. 41). These results indicate that GyrB-PKR WT induced p53 degradation by enhancing its nucleocytoplasmic shuttling.

Figure 45. A conditional form of eIF2α kinase downregulates p53.

(A) A chimeric kinase-inducible PKR fusion protein (GyrB-PKR) was generated by swapping the dsRNA-binding domain (dsRBD) of PKR with part of the gyrase B (GyrB) bacterial protein. In the presence of the antibiotic coumermycin, the GyrB domains dimerize, and induce the autophosphorylation and catalytic activity of the PKR kinase domain (KD).

(B) GyrB-PKR WT and K296H cells were treated with coumermycin (100 ng/ml) for 4h, and the localization of endogenous wild-type p53 was examined by immunofluorescence. Cell nuclei were visualized by DAPI staining. **(C)** GyrB-PKR WT and K296H cells were treated with coumermycin (100 ng/ml) for 4h. Protein extracts were subjected to immunoblot analysis with anti-p53 (DO-1), anti-phospho-Ser51-eIF2α, anti-eIF2α, and anti-actin antibodies.

A

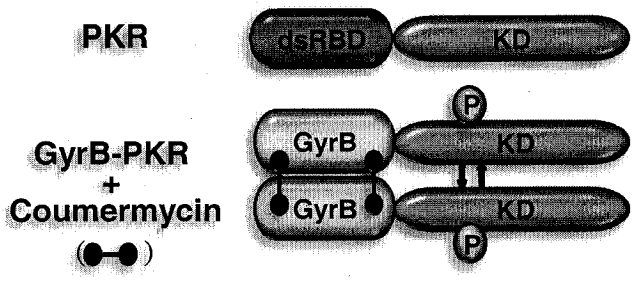

B

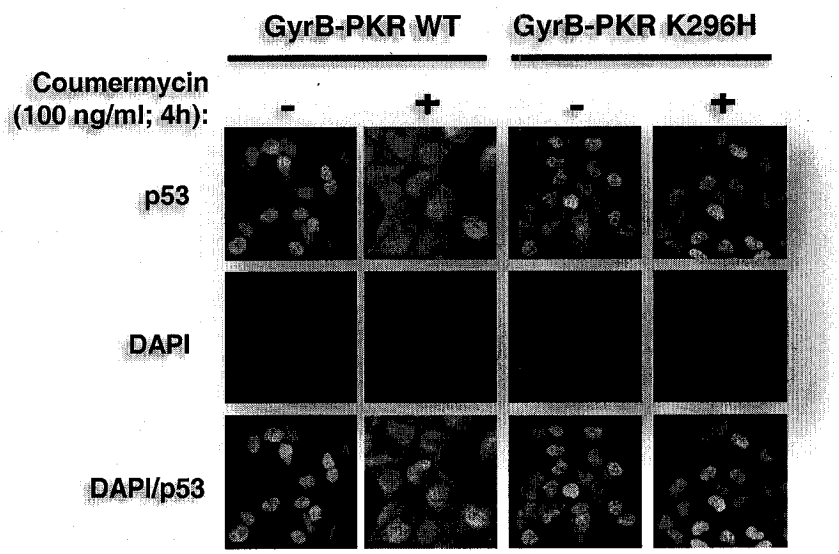

C

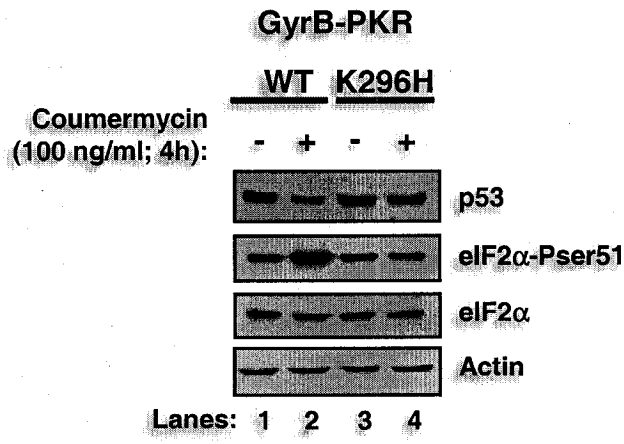

Figure 45

Figure 46. Disruption of the proteasome pathway rescues p53 from GyrB-PKR activation.

(A, B) GyrB-PKR WT cells were treated with coumermycin (100 ng/ml) for 4h and pre-treated with or without MG132 (10 μM), and protein extracts were subjected to immunoblot analysis **(A)** with anti-p53 (DO-1), anti-phospho-Ser51-eIF2α, and anti-eIF2α, antibodies. **(B)** The localization of endogenous wild-type p53 was examined by immunofluorescence. Cell nuclei were visualized by DAPI staining.

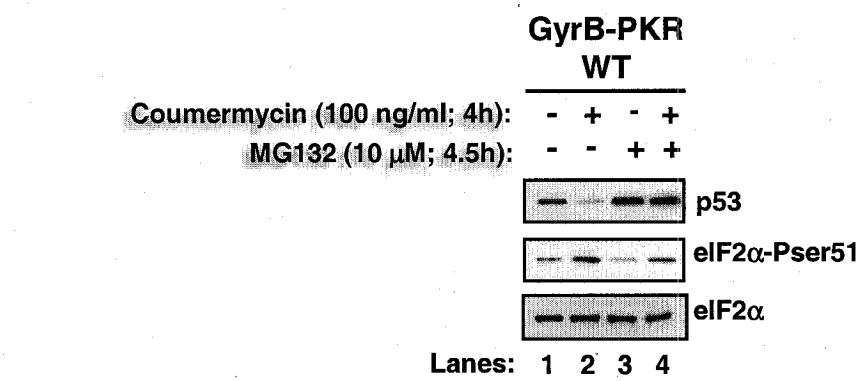
A
GyrB-PKR
WT
Coumermycin (100 ng/ml; 4h): - + - +
MG132 (10 μM; 4.5h): - - + +
p53
eIF2α-Pser51
eIF2α
Lanes: 1 2 3 4

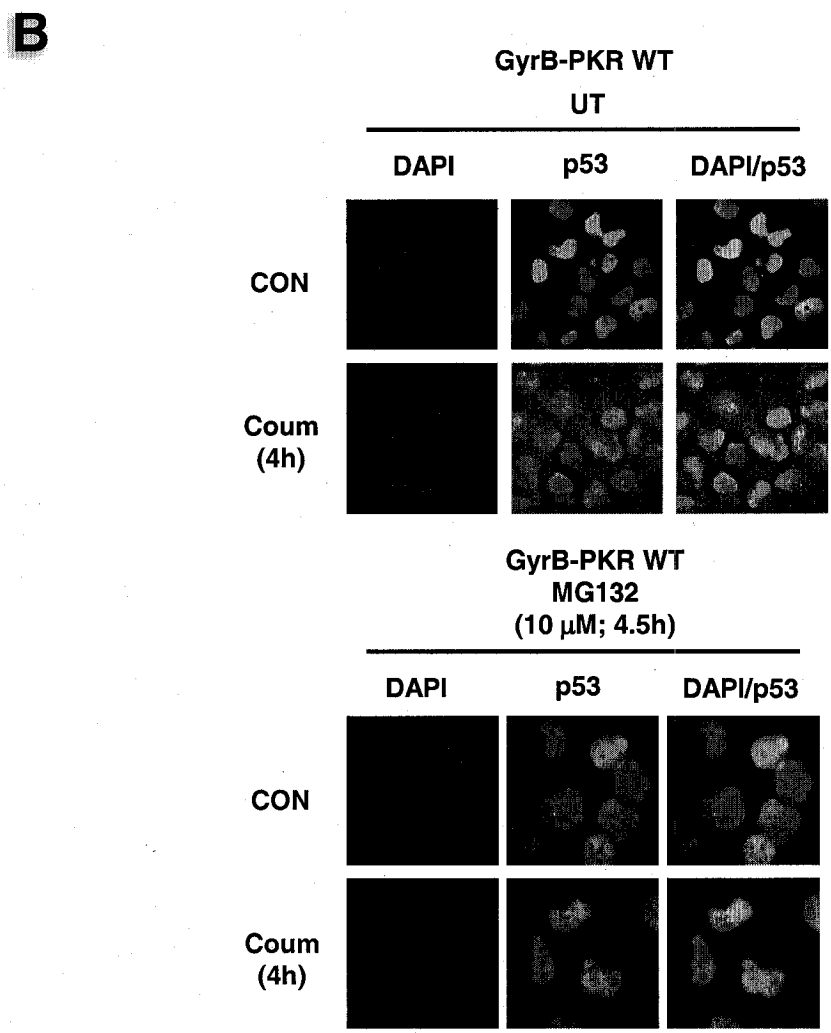
B
GyrB-PKR WT
UT
DAPI
p53
DAPI/p53
CON
Coum
(4h)
GyrB-PKR WT
MG132
(10 μM; 4.5h)
DAPI
p53
DAPI/p53
CON
Coum
(4h)

Figure 46

3.2.2 Activation of GyrB-PKR does not Alter *p53* mRNA Translation

We next investigated whether translation control affects *TP53* in the GyrB-PKR system by performing polysome profile analysis. Coumermycin treatment increased the levels of free 40S and 60S ribosomal subunits as well as inhibited translation initiation indicated by the large 80S peak (Fig. 47A, fractions 4-11). Translational inhibition correlated with a drastic disruption of the polysome fractions (Fig. 47A, fractions 12-20). However the disruption of the polysomes did not affect the polysomal distribution of *p53* mRNA in coumermycin treated GyrB-PKR cells (Fig. 47A, *TP53* panels). The *p53* mRNA was co-sedimented with the translated *ATF4* mRNA (Fig. 47A, *ATF4* panels) upon conditions that induce eIF2α phosphorylation. This suggests that *p53* and *ATF4* mRNA are both found in the polysomal pools where active translation occurs as previously observed (Fig. 44). The *GAPDH* mRNA clearly shows a shift towards the lower polysome pools and monosomes indicating a decrease in GAPDH translation (Fig 47A, *GAPDH* panels). These results imply that activation of eIF2α kinase activity does not affect *p53* mRNA translation and that the downregulation of p53 is translational independent.

In order to confirm that eIF2α did not play a role in p53 degradation, we knocked down eIF2α by siRNA in the GyrB-PKR cells. We reasoned that by knocking down eIF2α we should not be able to rescue p53 from degradation. Expression of eIF2α siRNA in GyrB-PKR WT cells led to >90% decrease of the endogenous eIF2α protein (Fig. 47B, third panel, lanes 3 and 4). When GyrB-PKR WT cells were subjected to coumermycin, p53 degradation occurred to the same extent in both cell types (Fig. 47B, first panel, lanes

2 and 4). This suggested that p53 downregulation occurs independently of eIF2α further supporting our previous findings (Fig. 42-43). These results provide evidence that eIF2α phosphorylation alone is not sufficient for the negative regulation of p53, further supporting the role that eIF2α kinases initiate a signaling pathway responsible for p53 degradation upon ER stress.

Figure 47. The downregulation of p53 by GyrB-PKR is not controlled by translation.

(A) GyrB-PKR WT cells were treated with coumermycin (100 ng/ml) for 4h. Cell lysates were separated on a sucrose gradient and subjected to polysome profile analysis followed by fractionation and RNA extraction as described in Materials and Methods. The positions of the polysomes and ribosomal subunits (40S, 60S, and 80S) are indicated above each corresponding peaks. Translation efficiency of *ATF4* mRNA, *TP53* mRNA, and *GAPDH* mRNA were determined by RT-PCR using specific primers and the RNA isolated from each polysome fractions.

(B) GyrB-PKR WT cells were transiently transfected with non-specific siRNA (GL-2) or eIF2α (eIF2αi) and then treated with coumermycin (100 ng/ml) for 4h. Cell extracts were subjected to immunoblot analysis with anti-p53, anti-phospho-Ser51-eIF2α, anti-eIF2α, and anti-actin antibodies.

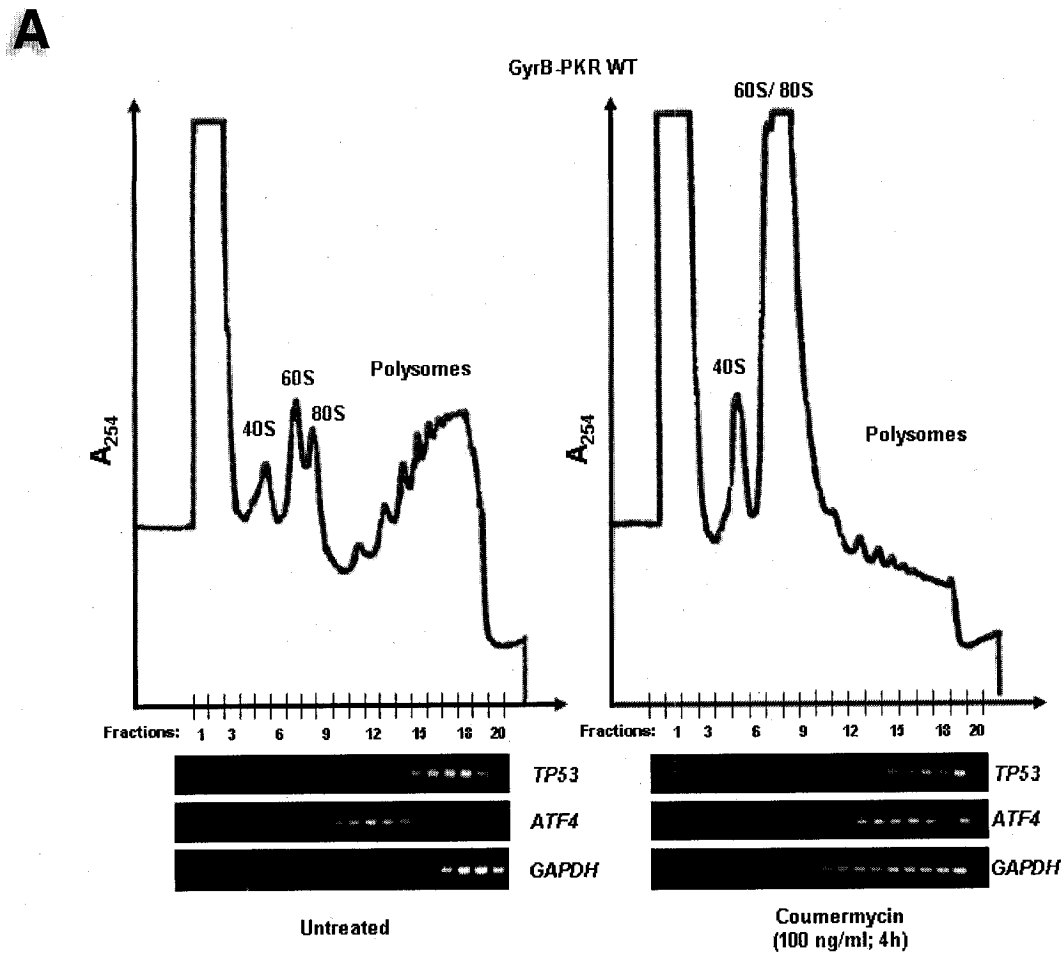
A
GyrB-PKR WT
60S/ 80S
40S
60S
80S
Polysomes
A254
Fractions: 1 3 6 9 12 15 18 20
TP53
ATF4
GAPDH
Untreated
Coumermycin
(100 ng/ml; 4h)

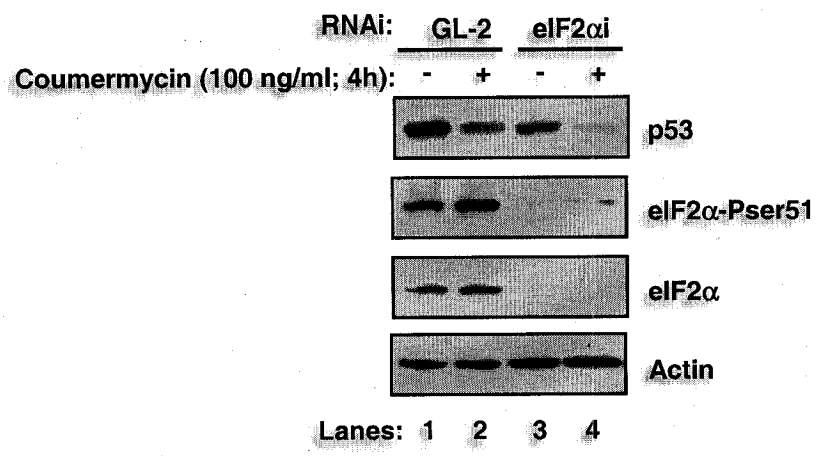
B
RNAi: GL-2 eIF2αi
Coumermycin (100 ng/ml; 4h): - + - +
p53
eIF2α-Pser51
eIF2α
Actin
Lanes: 1 2 3 4

Figure 47

3.3 eIF2α Kinases Induce p53 Degradation via GSK3β Activation

3.3.1 eIF2α Kinases Control GSK3β Localization and Activity

We previously showed that ER stress-inducing pharmacological compounds promote the nuclear translocation of GSK3β, which in turn induces the phosphorylation and nuclear export of p53 (263). It is well established that GSK3β is activated upon ER stress (263,305). However, upstream signaling events leading to GSK3β activation are still unknown. We therefore treated HT1080 cells with TG, Sal003 or transfected them with dsRNA and assessed the localization of GSK3β by immunofluorescence (Fig. 48A). Since dsRNA and ER stress induce eIF2α kinase activity as opposed to Sal003, they were the only two conditions that favored GSK3β nuclear localization. This supports our notion that eIF2α phosphorylation was not involved in this process since Sal003 did not alter GSK3β localization and remained perinuclear like in untreated cells (Fig. 48A). Similar results were obtained in A549 cells (data not shown).

We then measured GSK3 kinase activity in HT1080 cells by its capacity to phosphorylate the synthetic phospho-CREB substrate *in vitro*. GSK3 kinase activity increased after TG or dsRNA treatment in A549 (data not shown) and in HT1080 cells (Fig. 48B) but was unaffected in Sal003 treated cells. Moreover the increased nuclear localization of GSK3β (Fig. 48A) correlated with the increase of its kinase activity (Fig. 48B). Also the fact that localization and kinase activity of endogenous GSK3β was not affected by salubrinal treatment suggested that eIF2α phosphorylation alone is not responsible for GSK3 activation.

We next wanted to determine whether endogenous eIF2α kinases such as PERK and PKR are responsible for GSK3β activation. As PKR has been clearly implicated in virus infection (172) and PERK in the unfolded protein response in the ER (127), we used immortalized $PERK^{-/-}$ MEFs and the NIH3T3 PKR knockdown stable cell line (shPKR). These cells were respectively treated with TG or dsRNA, and the GSK3 activity was assessed as in Figure 48B. Thapsigargin treatment induced GSK3 activity in $PERK^{+/+}$ MEFs but not in $PERK^{-/-}$ MEFs (Fig. 49A) and dsRNA transfection increased GSK3 activity in control NIH 3T3 cells but not in shPKR cells (Fig. 49B). This induction of GSK3 kinase activity was abrogated in $PERK^{+/+}$ MEFS and control NIH 3T3 cells when 1-azakenpaullone (1-Aza) was used to inhibit GSK3 (Fig. 49). These results show that GSK3 activation is dependent on the activation of eIF2α kinases upon ER stress or dsRNA, and that GSK3β may be downstream to both PERK and PKR. These experiments advocate that eIF2α kinases downregulate p53 at least through a GSK3β dependent pathway.

Figure 48. PKR and PERK control GSK3β localization and activity in response to TG and dsRNA.

(A) HT1080 cells were treated with TG (1 μM), dsRNA (10 μg/ml) or Sal003 (75 μM) for 4 h and the localization of endogenous GSK3β was examined by immunofluorescence. Cell nuclei were visualized by DAPI staining. For quantitative analysis see Materials and methods.

(B) HT1080 cells were treated with TG (1 μM), dsRNA (10 μg/ml) or Sal003 (75 μM) for 4h and the activity of endogenous GSK3 was assessed by *in vitro* kinase assay as described in Materials and Methods.

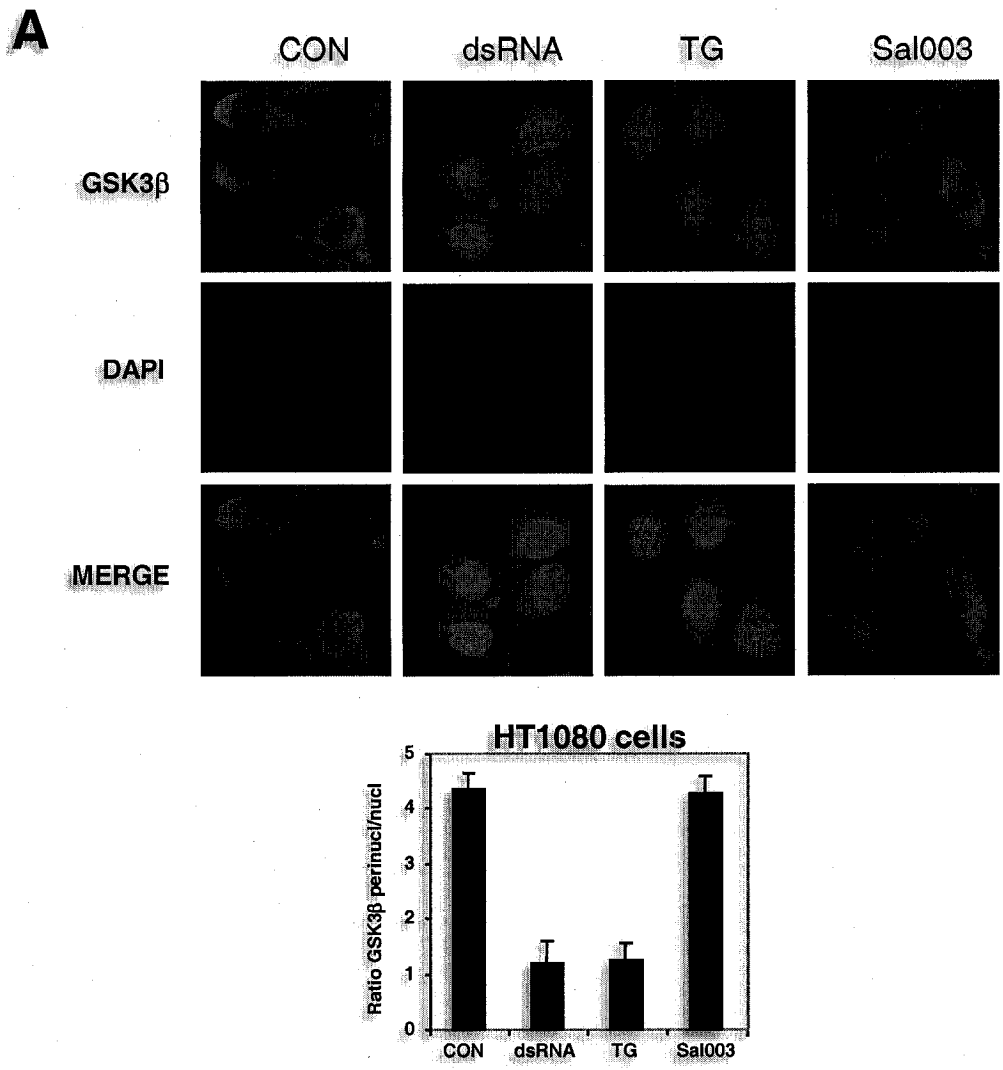
A
CON
dsRNA
TG
Sal003
GSK3β
DAPI
MERGE
HT1080 cells
Ratio GSK3β perinuc/nucl
0
1
2
3
4
5
CON
dsRNA
TG
Sal003
B
GSK3 activity (% of control)
0
50
100
150
200
CON
dsRNA
TG
Sal003

Figure 48

Figure 49. PERK and PKR control GSK3β activity in response to TG or dsRNA.

(A) $PERK^{+/+}$ and $PERK^{-/-}$ MEFs were treated with TG (1 μM), for 4h and the activity of endogenous GSK3 was assessed by *in vitro* kinase assay as described in Materials and Methods.

(B) NIH 3T3 stable cell lines expressing shRNA targeted against PKR (shPKR) cells were treated with dsRNA (10 μg/ml) for 4h and the activity of endogenous GSK3 was assessed by *in vitro* kinase assay as described in Materials and Methods. As a negative control of GSK3 activity, we used the GSK3β inhibitor 1-Aza-Kenpaullone (1 μM) in the kinase assays.

A

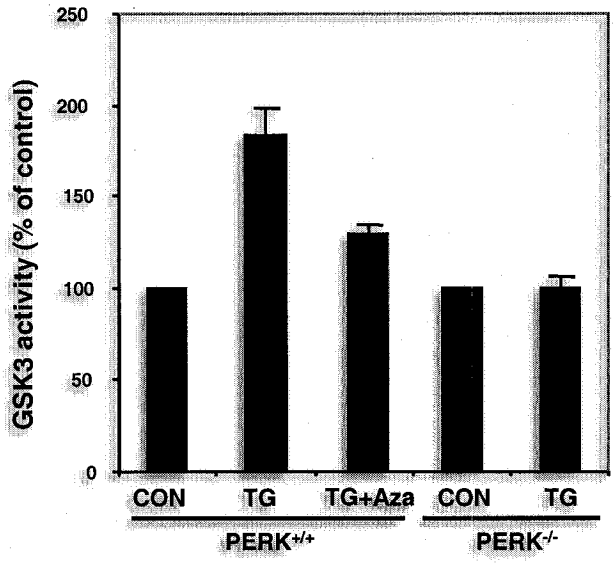
GSK3 activity (% of control)
250
200
150
100
50
0
CON
TG
TG+Aza
CON
TG
PERK+/+
PERK-/-

B

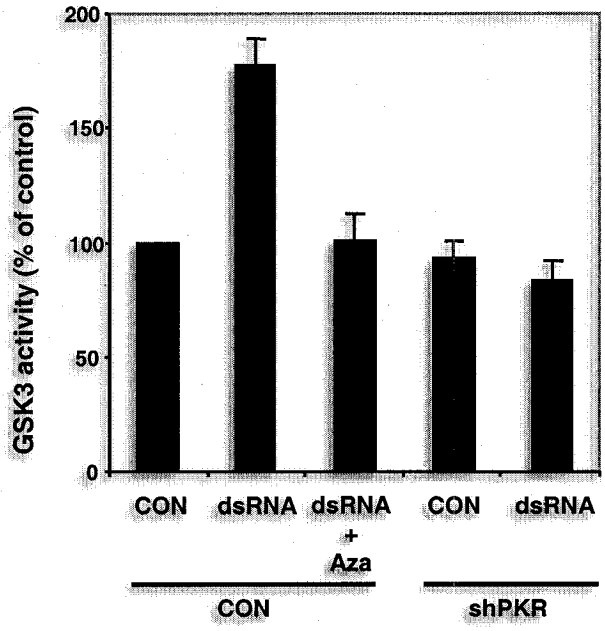
GSK3 activity (% of control)
200
150
100
50
0
CON
dsRNA
dsRNA + Aza
CON
dsRNA
CON
shPKR

Figure 49

3.3.2 GSK3β is Downstream of PERK and PKR upon ER Stress and dsRNA

From the previous observations, we reasoned that GSK3β is downstream to eIF2α kinases in response to ER stress and dsRNA. Therefore the absence of GSK3β would not affect eIF2α kinase activity and would thus recover p53 protein levels. We previously showed that loss of GSK3β prevented p53 degradation in response to ER stress (260). We used GSK3β$^{-/-}$ primary MEFs to determine the p53 protein levels in response to dsRNA (Fig. 50A). We observed 50-70% decrease in the p53 protein levels of dsRNA transfected GSK3β$^{+/+}$ primary MEFs (Fig. 50A, top panel). However, p53 protein levels were partially rescued (~50% recovery) in GSK3β$^{-/-}$ MEFs (Fig. 50A).

In order to exclude the possibility that eIF2α kinase activity was affected in GSK3β$^{-/-}$ MEFs, we tested whether these cells respond to ER stress or dsRNA to the same extent as their wild type counterparts. We determined that both cell types were able to induce eIF2α phosphorylation upon TG treatment (Fig. 50B) or dsRNA transfection (Fig. 50C). We concluded that absence of GSK3β did not prevent eIF2α kinase activity, and that GSK3β works downstream to PERK and PKR.

To confirm the downstream affect of GSK3β upon eIF2α kinase activation we used the GyrB-PKR cells. Treatment with 1-Aza rescued p53 from GyrB-PKR activation by coumermycin treatment (Fig. 51A, top panel, compare lane 4 with lane 3). The phosphorylation of eIF2α was not abolished by 1-Aza indicating that eIF2α kinase activity was not affected, and that the rescue of p53 was mainly due to the inhibition of GSK3β (Fig. 51A, fourth panel, lane 4). To validate this statement we investigated the

phosphorylation status of glycogen synthase, one of the well studied substrates of GSK3β (180). Coumermycin treatment induced glycogen synthase phosphorylation indicating that GSK3β activity was also stimulated by GyrB-PKR (Fig. 51A, second panel, lane 3). This was validated by performing GSK3 kinase assays similar to Fig. 48 and 49. GyrB-PKR WT activation induced GSK3 kinase activity but not in the kinase dead GyrB-PKR K296H cells (Fig. 51B). GSK3 activity was fully inhibited with the addition of 1-Aza (Fig. 51B), and the phosphorylation of glycogen synthase was abolished in combination with 1-Aza (Fig. 51A, second panel, lane 4).

Similarly, HT1080, U2OS, HCT116, and A549 cells treated with prolonged exposure (16h) to tunicamycin or thapsigargin induced glycogen synthase phosphorylation on Ser641/645, indicating that GSK3β activity was maintained throughout the ER stress response (Fig. 38A).

Overall, these data confirmed that GSK3β is downstream to eIF2α kinases and is required for the downregulation of p53 in response to ER stress or dsRNA. The partial rescue of p53 observed in GSK3β$^{-/-}$ MEFs suggests that perhaps eIF2α kinases induce other pathways that may be involved in the degradation of p53 or that GSK3α may compensate for the loss of GSK3β.

Figure 50. The downregulation of p53 by dsRNA and TG is mediated by GSK3β.

(A) Primary GSK3β$^{+/+}$ and GSK3β$^{-/-}$ MEFs were treated with dsRNA (10 μg/mL). Cell extracts were subjected to immunoblot analysis with anti-p53, anti-GSK3β, and anti-actin antibodies. The p53 levels were quantified and normalized to the actin levels and are presented as percentages underneath each lane.

(B, C) Primary GSK3β$^{+/+}$ and GSK3β$^{-/-}$ MEFs were treated with TG (**B**; 1 μM) or dsRNA (**C**; 10 μg/mL). Cell extracts were subjected to immunoblot analysis with anti-phospho-Ser51-eIF2α, and anti-eIF2α antibodies.

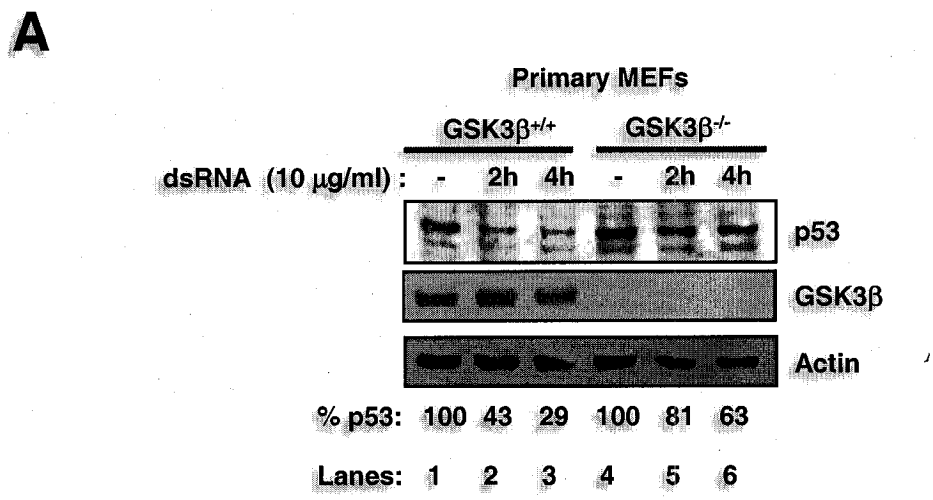
A
Primary MEFs
GSK3β+/+
GSK3β-/-
dsRNA (10 μg/ml) : - 2h 4h - 2h 4h
p53
GSK3β
Actin
% p53: 100 43 29 100 81 63
Lanes: 1 2 3 4 5 6

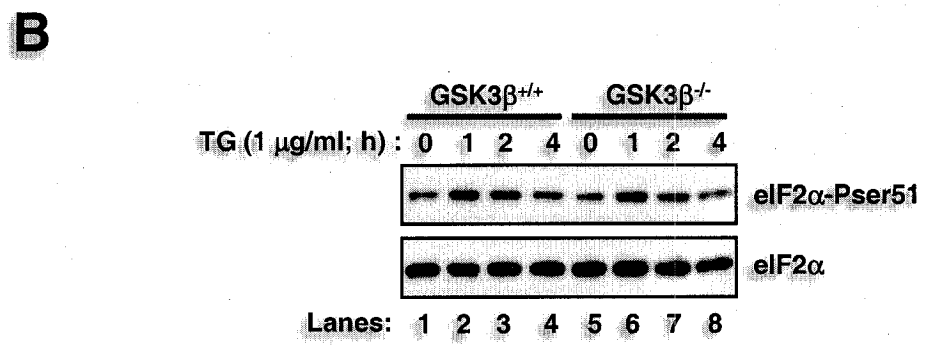
B
GSK3β+/+
GSK3β-/-
TG (1 μg/ml; h) : 0 1 2 4 0 1 2 4
eIF2α-Pser51
eIF2α
Lanes: 1 2 3 4 5 6 7 8

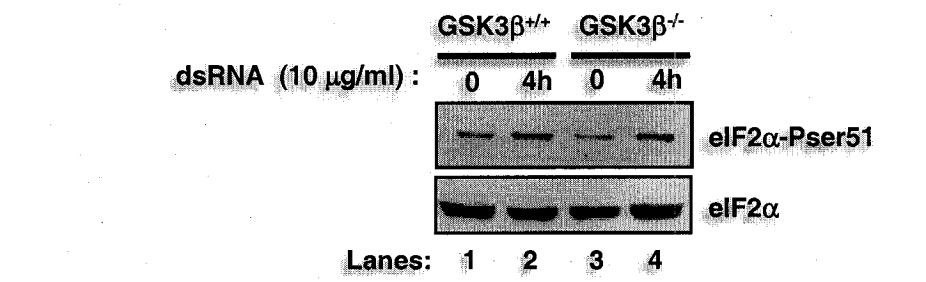
C
GSK3β+/+
GSK3β-/-
dsRNA (10 μg/ml) : 0 4h 0 4h
eIF2α-Pser51
eIF2α
Lanes: 1 2 3 4

Figure 50

Figure 51. Inhibition of GSK3β rescued p53 protein levels in GyrB-PKR cells.

(A) GyrB-PKR WT cells were treated with coumermycin (100 ng/ml) in the absence or presence of the GSK3β inhibitor 1-Aza-Kenpaullone (1 μM) for 4h. Protein extracts were subjected to immunoblot analysis with anti-p53 (DO-1), anti-phospho-Ser641/645-glycogen synthase, anti-glycogen synthase, anti-phospho-Ser51-eIF2α, anti-eIF2α, and anti-actin antibodies.

(B) GyrB-PKR WT and K296H cells were treated with coumermycin (100 ng/ml) for 4 h and the activity of endogenous GSK3 was assessed by *in vitro* kinase assay as described in Materials and Methods. As a negative control of GSK3 activity, we used the GSK3β inhibitor 1-Aza-Kenpaullone (1 μM) in the kinase assays.

A

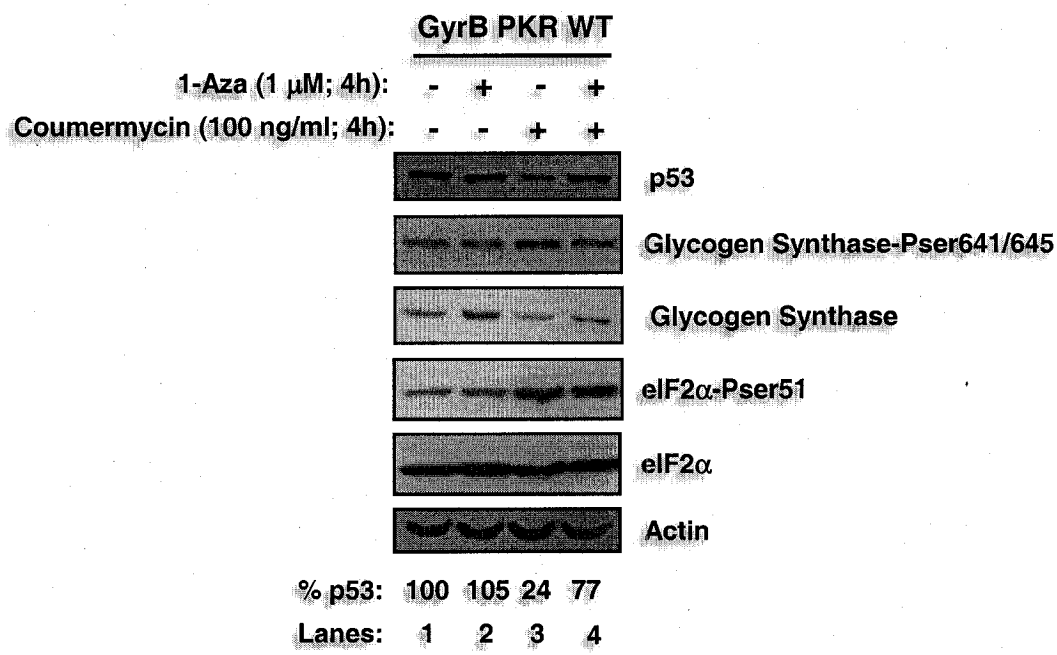
GyrB PKR WT
1-Aza (1 μM; 4h): - + - +
Coumermycin (100 ng/ml; 4h): - - + +
p53
Glycogen Synthase-Pser641/645
Glycogen Synthase
eIF2α-Pser51
eIF2α
Actin
% p53: 100 105 24 77
Lanes: 1 2 3 4

B

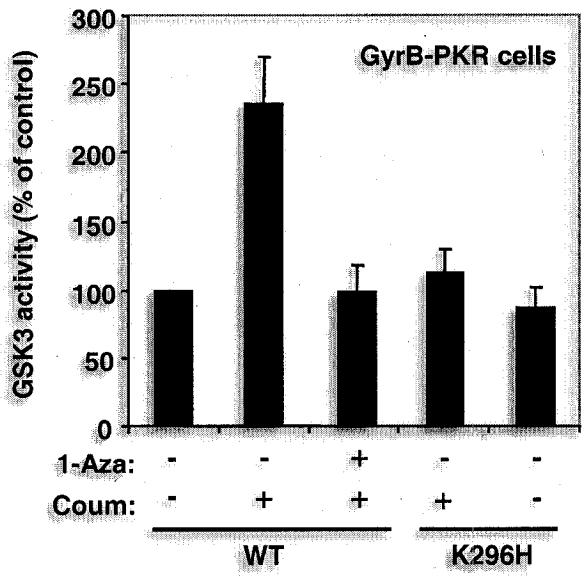
GyrB-PKR cells
GSK3 activity (% of control)
300
250
200
150
100
50
0
1-Aza: - - + - -
Coum: - + + + -
WT
K296H

Figure 51

CHAPTER IV – DISCUSSION

1. DISCREPANCIES BETWEEN PKR KNOCKOUT MICE

1.1 DISCREPANCIES IN PKR SIGNALING PATHWAYS

PKR was initially characterized as a protein kinase with an important role in the control of mRNA translation through its capacity to induce eIF2α phosphorylation (61,172). The transcriptional induction of the *pkr* gene by type I IFNs provided further evidence that PKR is a mediator of the antiviral and anti-proliferative effects of IFNs (311). The cloning of the human and mouse *PKR* cDNA (154,231,321,325) assisted in the identification of novel biological properties of the kinase in cultured cells. To date, numerous reports have assigned anti-proliferative and tumor suppressor functions *in vitro* to PKR and have implicated it in many signaling pathways that control gene expression at both translational and transcriptional levels (61,172). Since many of the important *in vitro* functions of PKR were not verified *in vivo*, attempts were made to generate $PKR^{-/-}$ mice.

The characterization of two different $PKR^{-/-}$ mice however did not yield the anticipated results. In addition, experiments with cells from the two $PKR^{-/-}$ mice have led to contradictory and confusing results concerning the PKR functions *in vivo*. Here, we demonstrate that neither of the two $PKR^{-/-}$ mice is completely devoid of PKR. The N-$PKR^{-/-}$ mouse (356) expresses a dsRNA-binding defective but catalytically active PKR protein, whereas the C-$PKR^{-/-}$ mouse (2) expresses an alternatively spliced form of the kinase with impaired catalytic properties but intact dsRNA-binding activity.

In regard to cell signaling, it was previously shown that N-$PKR^{-/-}$ MEFs display an impaired NF-κB activation in response to dsRNA and this defect was restored after

priming with IFNα/β or IFNγ possibly by the expression of a molecule that substitutes PKR function (356). Subsequent work with the N-PKR$^{-/-}$ MEFs concluded that PKR functions as an important signal transducer for the induction of IFN-stimulated genes through pathways that implicate interferon regulatory factor (IRF)-1 and NF-κB (190). Moreover, N-PKR$^{-/-}$ MEFs were found to be resistant to apoptotic death in response to dsRNA, TNFα or LPS providing further evidence for the role of PKR in stress-induced apoptosis (83). Work with the N-PKR$^{-/-}$ MEFs also established a requirement of the kinase for p38 MAPK activation (114) and for serine phosphorylation of Stat1α in response to IFNs (266). Recent studies have demonstrated that the defective NF-κB activation by dsRNA in the N-PKR$^{-/-}$ MEFs is due to the impaired IKK activation and phosphorylation of IκBα (56,364).

The above signaling defects of N-PKR$^{-/-}$ cells were not found in C-PKR$^{-/-}$ cells (2). Specifically, IFN signaling and transcriptional induction of IFN-inducible genes is normal in C-PKR$^{-/-}$ cells (2) indicating that the lack of the catalytic activity of PKR does not interfere with the Jak-Stat pathway. In accordance with this, we found that phosphorylation of Stat1 on serine 727 is not impaired in IFN-treated C-PKR$^{-/-}$ MEFs as opposed to N-PKR$^{-/-}$ MEFs (266). In regard to NF-κB activation, it has been documented that C-PKR$^{-/-}$ MEFs respond normally to dsRNA (157) or TNFα (2) suggesting that the catalytic activity of PKR is dispensable for NF-κB-mediated gene transcription. This is further supported by our data showing that induction of IκBα phosphorylation by dsRNA proceeds normally in C-PKR$^{-/-}$ MEFs compared to isogenic PKR$^{+/+}$ MEFs (Fig. 26A).

The above striking differences between both PKR$^{-/-}$ mice may be attributed to the expression of the PKR forms. It is possible that the N-terminal dsRNA-binding domain of PKR is essential for mediating some signaling properties of PKR, and therefore the lack of this domain in ES-mPKR may account for the signaling defects reported for N-PKR$^{-/-}$ MEFs. Specifically, PKR through its N-terminus domain may participate in cell signaling as a scaffold protein by mediating protein-protein interactions and/or subcellular localization and compartmentalization of the molecule. This would explain the lack of the signaling defects that were reported for N-PKR$^{-/-}$ cells in C-PKR$^{-/-}$ MEFs, since the latter cell type expresses SF-mPKR with an intact dsRNA-binding domain. This would also imply that PKR may have the capacity to modulate cell signaling independently of its enzymatic activity. Interestingly, a kinase-independent role of PKR has been reported for signaling pathways leading to the transcriptional activation of NF-κB and Stat1 (37,158,344).

1.2 Discrepancies in Virus Infection

Concerning viral infection, both PKR$^{-/-}$ mice exhibit a very modest susceptibility to viruses. Specifically, N-PKR$^{-/-}$ mice are susceptible to infection with EMCV (356), whereas C-PKR$^{-/-}$ mice are susceptible to VSV infection only after intranasal inoculation (11,313). Interestingly, a recent report demonstrates that the increased susceptibility of C-PKR$^{-/-}$ mice to VSV is dependent on the mouse strain, since animals with BALB/c genetic background are 5 orders of magnitude more sensitive to infection than those with 129SvEv background (93). Nevertheless, PKR$^{-/-}$ mice bred onto resistant 129SvEv background still exhibited a 10 fold increased sensitivity compared to the strain-matched

$PKR^{+/+}$ mice (93). These data raise the possibility that the signaling properties attributed to PKR may also be affected by mouse strain differences.

We also found that eIF2α phosphorylation in response to vesicular stomatitis virus infection is not impaired in C-$PKR^{-/-}$ MEFs compared to isogenic $PKR^{+/+}$ MEFs (Fig. 26B). This may indicate that the loss of the catalytic activity of PKR in C-$PKR^{-/-}$ cells could be compensated by another eIF2α kinase activated by virus infection. This is consistent with our previous observations that expression of the vaccinia virus K3L protein, which functions as a pseudo-substrate inhibitor of PKR (175), was still capable of enhancing translation from reporter gene constructs in transiently transfected C-$PKR^{-/-}$ MEFs (206). The newly identified eIF2α kinases PERK and GCN2 might be implicated in this process although it is not yet known how these enzymes are regulated in virus infected cells despite some recent studies suggesting their involvement in RNA viruses (28,165) and in herpes simplex virus 1 (HSV-1) infection (50).

In regard to an anti-viral role of PKR independently of eIF2α, the JNK and p38 MAPK pathways have been recently implicated in virus replication (56,156). Although, activation of p38 MAPK was partially impaired in N-$PKR^{-/-}$ MEFs (114), our experiments with C-$PKR^{-/-}$ MEFs showed normal patterns of activation of both JNK and p38 MAPK pathways in response to VSV or Sendai Virus (SeV) infection (data not shown).

The functional characterization of the ES-mPKR and SF1-mPKR proteins may provide some clues to molecular mechanisms of PKR activation. For example, current models for PKR activation propose that dsRNA binding to the dsRBMs leads to

structural rearrangement of PKR relieving an auto-inhibitory interaction between the dsRBD and the kinase domain (KD) (135,240,347). This facilitates the dimerization of the PKR kinase domain and its subsequent activation via a *trans*-inter-dimer autophosphorylation mechanism prior to substrate recognition (75,88). Based on this model, auto-inhibition of the KD by the dsRBD in ES-mPKR is not possible, since this protein lacks the dsRBM1 and half of the dsRBM2, and dimerization of the kinase domain itself could proceed independently of dsRNA-binding. Thus, the lack of an auto-inhibitory action may explain, at least in part, the constitutive activity of ES-mPKR *in vitro* and *in vivo*.

In regard to SF1-mPKR, its expression in certain mouse tissues might be indicative of a specific function of this protein (Fig. 25). Since induction of PKR activity proceeds through dsRNA-binding, dimerization and inter-phosphorylation, a predicted function of the SF1-mPKR protein is the inhibition of mPKR activity in a dominant negative fashion, as previously demonstrated for a similar catalytic inactive PKR form expressed in a mouse pre-B leukemia cell line (1). However, expression of SF1-mPKR in normal tissues is very little compared to the full-length PKR suggesting that a dominant negative effect of this protein could possibly be local and/or RNA specific. Alternatively, SF1-mPKR could function as an RNA-binding protein independently of PKR by modulating, for example, RNA editing (18), RNA trafficking (42), or RNA processing (179).

1.3 SUMMARY

In conclusion, our data clearly demonstrate that both $PKR^{-/-}$ animal models are incomplete knockouts, and this may account for the differential responses of the two $PKR^{-/-}$ cell types to various intracellular and extracellular signals. Considering the crucial biological functions that have been attributed to PKR in tissue culture systems *in vitro*, it is apparent that a complete disruption of the *pkr* gene may be necessary to verify the biological functions of the kinase *in vivo*.

2. ROLE OF PERK IN VSV INFECTION

2.1 CROSS-TALK BETWEEN PERK AND PKR

Our findings demonstrate an important role for PERK in VSV infection. We show that PERK-mediated eIF2α phosphorylation is induced in VSV infected cells, and this is accompanied by an inhibition of virus replication and apoptosis. However, it remains possible that additional control mechanisms are modulated by PERK in VSV infected cells. In fact, we demonstrate that activation of PKR is impaired in cells lacking PERK suggesting a functional cross-talk between the two kinases with PKR functioning downstream to PERK. Previous data showed that treatment of cells with thapsigargin and TNFα renders PKR active providing evidence for a role of the kinase in ER stress (262,309). More recent research indicated that ER stressed cells can induce the activation and nuclear translocation of PKR (248). Consistent with these findings, our data show the induction of PKR in ER stressed cells and the lack of its activation in $PERK^{-/-}$ cells (Fig. 35A).

At present, we do not know how PKR becomes activated by PERK. One possibility is that active PERK directly phosphorylates and activates PKR in the proximity of the ER. Alternatively, activation of PKR is mediated by another kinase that functions as an intermediate between the two eIF2α kinases (Fig. 52). Several studies have shown that the cellular inhibitor of PKR $p58^{IPK}$ (261), can also interact and inhibit PERK upon ER stress (334,353). This raises the possibility that the impaired PKR activation observed in ER stressed $PERK^{-/-}$ MEFs may be explained by the induction of unbound $p58^{IPK}$. The lack of PERK in these cells may release more $p58^{IPK}$ to the

cytoplasm where it can target and further inhibit PKR. However it is not yet known whether VSV infection regulates $p58^{IPK}$ expression.

Alternatively, PERK activation by VSV may be mediated by the viral proteins themselves. The VSV glycoprotein (G) oligomerizes in the ER prior to its transport to the cell surface (363). Misfolded and unassembled VSV-G is retained in the ER (77) where it interacts with the chaperone BiP, the inhibitor of PERK. Although VSV infection does not elicit the UPR (Fig. 37), it was recently shown that IRE1 can sense and bind directly to misfolded proteins, and induce its dimerization and activation (69). Since PERK has a homologous sensor domain to IRE1 (128), it is possible that PERK activation can be induced by direct binding of the VSV-G protein. Even though BiP is present in the ER lumen in millimolar concentrations, activation of PERK (by the release from BiP) would require large concentrations of unfolded proteins to compete with the free BiP pool in the ER. However, enveloped viruses induce the production of ER membranes so that the cell can cope with the load of viral membrane protein production (95,115). It is unclear if VSV behaves similarly, but we can speculate that this process may explain for the lack of UPR signaling during VSV infection despite PERK activation.

Nevertheless, VSV infection results in a powerful impairment of host gene expression due to the various combined actions of the virion components thus eliminating the majority of cellular ER-resident proteins. Combined with the limited load of viral ER-resident proteins early in the VSV replication life cycle, this ensures chaperone sufficiency and thereby does not produce ER stress or the UPR pathway (Fig. 37). As the VSV glycoprotein (G) is produced later in the life cycle, VSV-G may physically

associate with PERK to regulate viral protein accumulation in a PERK-dependent manner, thereby maintaining ER homeostasis.

As such, we conclude that VSV utilizes a novel pathway to activate PERK. Although this pathway is not currently known, we hypothesize that virus infection might induce protein-protein interactions and/or phosphorylation cascades leading to the activation of PERK in the ER.

2.2 Role of PERK in VSV-mediated Apoptosis

Regarding VSV-mediated apoptosis, our data implicate caspase-12 in this process (Fig. 32A). It was reported that upon ER stress, the cytosolic caspase-7 translocates to the ER surface, and associates with procaspase-12 thereby cleaving its prodomain to generate an active caspase-12 (Fig. 11) (267). Interestingly, VSV infection was shown to induce the activation of caspase-7 (143) and this may account, at least in part, for caspase-12 activation in infected cells.

Previous findings have shown that caspase-12 has been implicated in apoptosis induced by BVDV infection (165) indicating that this protease may play a role in virus-induced apoptosis in mouse cells. When $PERK^{+/+}$ and $PERK^{-/-}$ MEFs were treated with general caspase inhibitors prior to VSV infection, $PERK^{+/+}$ cells were rescued from VSV infection, as demonstrated by the absence of PARP cleavage (Fig. 32C). This suggested that caspases were involved in VSV-mediated apoptosis. However, $PERK^{-/-}$ MEFs were highly prone to PARP cleavage and VSV infection, despite caspase inhibition. This suggests that in the absence of PERK, the virus can utilize caspase-independent apoptotic pathways to induce PARP cleavage. This finding demonstrates that multiple caspase-

dependent and caspase-independent cell death pathways may be activated during VSV infection, and that PERK plays a role in modulating caspase function and activation. It is now understood that PARP is an important activator of caspase-independent cell death (149), and perhaps VSV can exploit some of these pathways to induce apoptosis. Undoubtedly, future experiments are needed to better characterize the fundamental pathways of VSV-induced apoptosis.

2.3 Summary

We have shown here that PERK appears to be a critical component of the innate immune response protecting the host against VSV infection. It does so, at least in part, through the activation of PKR. Thus, a cross-talk between PERK, PKR and possibly other eIF2α kinases is likely to exist and contribute to the antiviral mechanisms converging at the eIF2α phosphorylation level (Fig. 52). Although many viruses have evolved unique mechanisms to overcome PKR activation (171), it appears that some of these mechanisms also aim at inactivating PERK. For example, the HCV E2 protein (256) and the vaccinia virus K3L protein (306) are potent inhibitors of PERK as is the p58 PKR-inhibitor ($p58^{IPK}$) induced in cells infected with influenza virus (353). Thus, further investigation of the role of the eIF2α kinase family members in virus infection may yield important information about the translational mechanisms of virus replication, and lead to the discovery of unique pathways controlled by each of the eIF2α kinases with important implications against virus infection and associated disease.

Figure 52. Model depicting a cross-talk between PERK and PKR upon VSV infection.

VSV activates both PERK and PKR. Although PKR is thought to be activated by dsRNA produced during virus replication, the molecular mechanism(s) of PERK activation is not clear. Perhaps VSV infection induces protein-protein interactions or protein phosphorylation cascades resulting in PERK phosphorylation in the ER. PERK is upstream of PKR, and coordinated activation of both kinases is likely to be required for maximal eIF2α phosphorylation and full-scale shutdown of viral protein synthesis. PERK alone may not be sufficient to block virus replication unless PKR is present despite the sustained phosphorylation of eIF2α induced by PERK (thick arrow) in $PKR^{-/-}$ MEFs. This is also consistent with the impaired anti-viral response observed in $PKR^{-/-}$ MEFs after VSV infection.

PERK-PKR Cross-Talk in VSV Infection

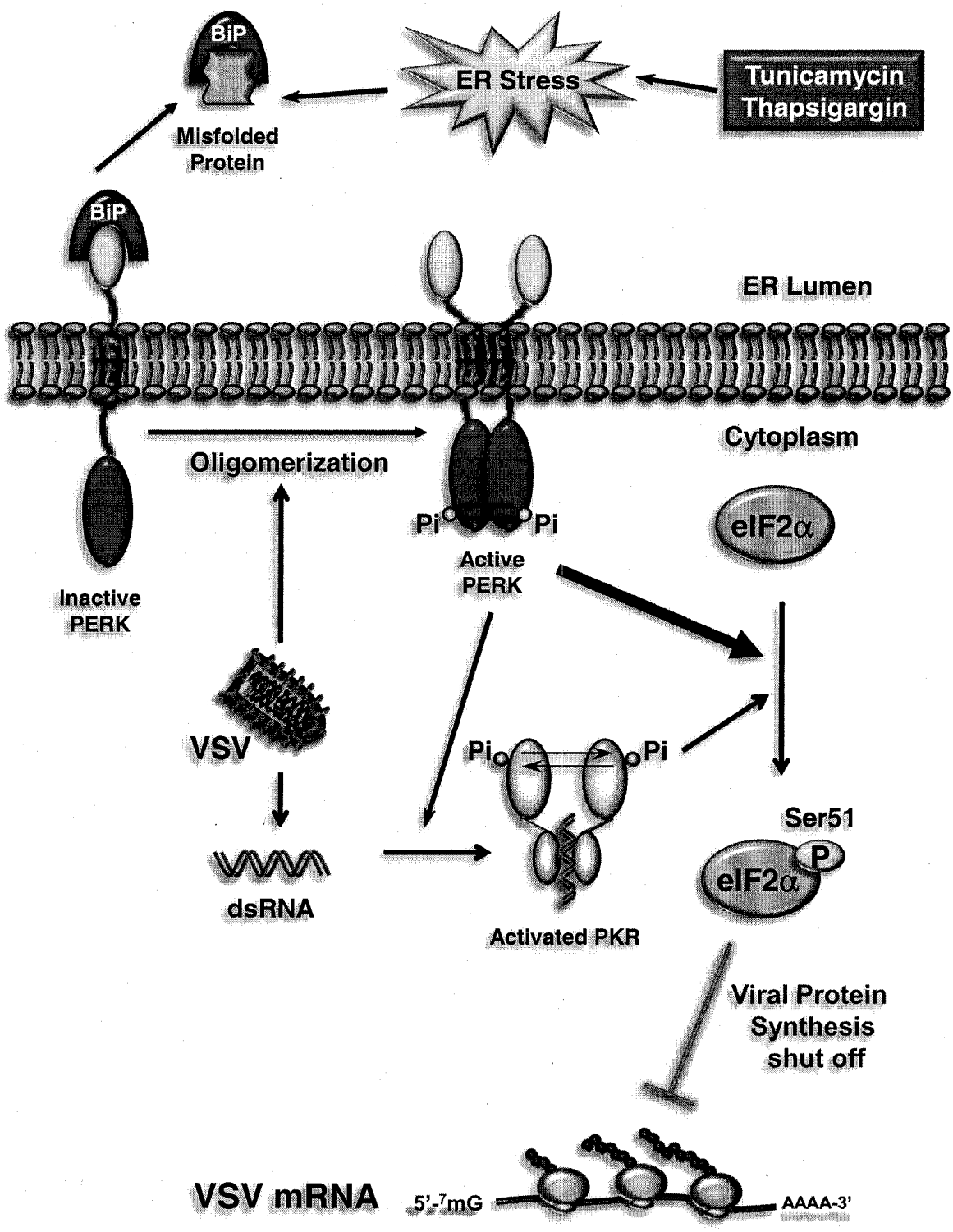

Figure 52

3. REGULATION OF P53 BY EIF2α KINASES

3.1 REGULATION OF GSK3β BY EIF2α KINASES

Herein, we report that activation of eIF2α kinases plays a critical role in down-regulating the p53 tumour suppressor protein, a key player in stress sensing and apoptotic signaling. We establish a novel functional cross-talk between the eIF2α kinases and p53. We demonstrated that eIF2α kinases participate in the nuclear export and proteasome-dependent degradation of p53 through a GSK3β-dependent but translational-independent pathway. A model illustrating our findings is shown in Figure 53. Thus, eIF2α kinase activation following ER stress or dsRNA regulates in parallel at least two distinct signaling pathways. The first is primarily dependent on eIF2α phosphorylation leading to a persistent inhibition of the global mRNA translation. The second is dependent on GSK3β activation resulting in the prolonged degradation of p53.

We identify GSK3β as a downstream effector of the eIF2α kinases which mediates p53 degradation (Fig. 49). GSK3β plays a role in a wide range of cellular processes and has been shown to phosphorylate many substrates including transcription and translation factors such as c-myc, eIF2Bε and p53 (64,89,263). Here, we show specifically that functional eIF2α kinases control GSK3β activity and its localization (Fig. 48A). This provides a new clue in our understanding of how thapsigargin (TG) induces GSK3β activity (305), and its nuclear localization (263) to mediate p53 nuclear export and degradation (260,263). One possibility is that GSK3β becomes activated by phosphorylation by kinase(s) that is (are) induced in response to PKR/PERK activation. Moreover, the eIF2α kinases may contribute to the control of factors that initiate GSK3β

activation and translocation. Here, we show that the eIF2α kinase/GSK3β pathway contributes to p53 degradation upon TG or dsRNA. Interestingly, it has been shown that DNA damage can induce the eIF2α kinase GCN2 (81) and that GSK3β activation and nuclear localization upon DNA damage resulted in p53 stabilization (340). However, it is still unclear whether eIF2α kinases control GSK3 activity and localization upon DNA damage. This apparent opposite regulation on p53 by GSK3β can be explained by the fact that different stimuli induce different p53 phosphorylation patterns and these patterns could determine the outcome of p53 stability and cellular response (281).

3.2 Downregulation of p53 Independent of Translation

Our data demonstrate that conditions activating eIF2α kinases induce p53 downregulation without involving the translational shut-off of *p53* mRNA despite the phosphorylation of eIF2α (Fig. 44 and 47).

Our results are partially in agreement with conclusions of findings reported by Marques *et al.* (226), who also showed the downregulation of p53 by dsRNA signaling and PKR activation. In this study, the authors concluded that the reduction in p53 protein expression is regulated at the translational level. However, they observed similarly to us that p53 protein levels can be recovered by proteasome inhibition with MG132 (Fig. 40B), supporting a role of the proteasome pathway for the decrease of p53 protein levels. In order to justify this apparent contradiction, we employed a method that directly measures translation: polysome profiling. We did not observe any changes in the sedimentation pattern of *p53* mRNA in contrast to *ATF4* mRNA (Fig. 44B) (125). Even if dsRNA induced a small shift of *p53* mRNA into lower polysomes, presumably due to the

disruption of high polysome fractions compared to TG treatment (Fig. 44A), the absence of *p53* mRNA in monosomes indicated that translation still proceeds. Moreover, the same conclusions were applied in our GyrB-PKR system, which mimics all eIF2α kinases in terms of induction of their catalytic activity (Fig. 47A). Furthermore, our data using Sal003 and the eIF2α knock-in cells excluded the role of eIF2α phosphorylation *per se* in p53 nuclear export and degradation (Fig. 42-43). Therefore, we conclude that the downregulation of p53 by dsRNA is independent of eIF2α and translation. This raises the question whether the downregulation of p53 by the eIF2α kinases is specific to p53. It will be therefore interesting to see if other proteins are regulated by a similar mechanism.

One possibility for *p53* mRNA to bypass eIF2α-dependent translation inhibition is characterization of Internal Ribosomal Entry Sites (IRES) that may mediate the translation of p53 as suggested recently (268,354). IRES-dependent translation upon eIF2α phosphorylation has been described for the *CAT-1* mRNA (351). Basically, the induction of *CAT-1* IRES activity requires both translation of a small upstream open reading frame (uORF) within the IRES and phosphorylation of eIF2α. Therefore, p53 may be regulated similarly upon conditions that induce eIF2α kinase activity.

3.3 eIF2α Kinases May Play a Role in the Regulation of the Proteasome Pathway

Our results suggest that eIF2α kinases may regulate specific proteins that are resistant to the translational effects of eIF2α phosphorylation by inducing their degradation via the proteasome pathway. The implication of ER stress in modulating the

ER-associated degradation (ERAD) pathway has been previously described (329). However, the role of eIF2α kinases and translational control in regulating the ERAD pathway or protein degradation is currently not known despite some studies that link translation to degradation (98,253). This implies that in some circumstances eIF2α kinases may regulate protein degradation rather than protein synthesis depending on the type of stress exerted on the cell. Therefore it is conceivable to speculate that the eIF2α kinases may contribute to the regulation of protein turnover through their capacity to phosphorylate or activate other unidentified substrates. To date only Nrf2 and p53 have been described as substrates to PERK and PKR, respectively (72,73).

3.4 Cytoprotective Effects of eIF2α Kinases

The eIF2α kinases contribute to stress adaptation and their activation is primarily cytoprotective. This notion is supported by the fact that eIF2α kinases facilitate NF-κB activation in response to diverse stimuli including amino acid starvation, UV irradiation, and ER stress (158,162,164). NF-κB is a key factor involved in many biological responses including inflammatory response and cell survival (168). However, when adaptation is not possible, stressed cells are eliminated by apoptosis through the activation of the JNK pathway and caspases-7, -12, and -3 (174,280). Inhibition of p53 activity by eIF2α kinases may represent an additional mechanism used by cells to adapt to various stress conditions that induce eIF2α kinase function. We previously showed that ER stress protects HCT116 cells from apoptosis in response to DNA damage and that ER stress impaired p53-dependent apoptosis (263). Recently published work by Li *et al.* report that ER stress-induced apoptosis resulted from p53-dependent activation of PUMA

and NOXA in MEFs (202). However, this conclusion is mainly based on immunoblot analysis performed with a p53 antibody (PAb240) that is known to recognize only the mutant form of p53 (109).

In contrast, our analysis in primary MEFs demonstrated that p53 was rapidly degraded upon TG treatment (Fig. 39A). Moreover, our data showed that PUMA protein levels were not induced after prolonged treatment of ER stress in HCT116, HT1080, U2OS and A549 cells (Fig. 38A). Similar results were found with NOXA except in U2OS cells, suggesting that various cancer cells may utilize multiple pathways to regulate NOXA independently of p53 following ER stress (Fig. 38A). Consistent with our observations, Armstrong *et al.* showed that the induction of NOXA-mediated apoptosis upon TG treatment was p53-independent (6). Our findings are also in opposition with those by Zhang *et al.*, who found that cytoprotective effects of ER stress resulted from the accumulation of p53 in HCT116 cells (365). By using the same conditions, our data clearly indicated that ER stress downregulates p53 protein levels in these cells (Fig. 38A). We have no explanation for these differences, however, our analysis using three additional cell lines was consistent with a recent report clearly showing that TG resulted in downregulation of p53 (6).

Moreover, our data showed an increase in phosphorylated glycogen synthase upon ER stress (Fig. 38A), a well known substrate correlating with GSK3β activation, and a role of GSK3β in p53 degradation as claimed in our previous conclusions (260,263). Consistent with our observations, Yamasaki *et al.* found that p53 was ubiquitinated and targeted for degradation in the cytoplasm by the ER-resident E3 ubiquitin ligase Synoviolin (352), whose expression is induced upon TG treatment (350). Taken together,

these data are consistent with the notion that p53 does not display any function or any transcriptional activity upon ER stress due to its degradation.

3.5 p53 and the Anti-viral Response

Our data suggest that dsRNA produced during virus replication may promote the downregulation of p53 protein levels in virus-infected cells. However, other studies have shown that the regulation of p53 during virus infection is dependent on the type of virus. For instance, VSV infection does not alter p53 protein levels whereas infection with encephalomyocarditis virus (ECMV), and human parainfluenza virus type 3 (HPIV3) downregulates p53 (226,320). Although these viruses have been shown to initiate an anti-viral response mediated via activation of PKR by dsRNA intermediates (11), the overall signaling pathways induced by these different viruses may determine the fate of p53 protein levels.

Also, IFNα/β treatment has been shown to induce p53 in order to contribute to the anti-viral response triggered by VSV infection (320). Studies have shown that two types of RNA helicases (RIG-I and MDA5) are essential for type I IFN production in response to distinct classes of RNA virus. RIG-I is required for the *in vivo* response to VSV, Newcastle disease virus (NDV), Sendai virus (SeV), and influenza virus (169,170). In contrast, MDA5 is the dominant receptor for poly(rI-rC), and is essential for the antiviral response to EMCV (113,170).

Therefore, the IFN response generated by various types of viruses may be utilized by the cell to limit virus replication either through induction of early apoptosis by stabilizing p53 or by turning off viral protein synthesis through eIF2α kinase activation.

Although dsRNA contributes to p53 destabilization, this effect may be counterbalanced by the changes in the nucleus in virus-infected cells activating a pathway similar to the DNA damage response, leading to p53 stabilization. For example, it is suggested that RNA viruses may interact with the nucleolus and perturb cellular functions (142). Perturbation of the nucleolus has been shown to stabilize p53 through oncogenic stress. The nucleolus-localized ARF protein has been shown to disrupt the Mdm2-p53 interaction, thus favoring the stabilization and accumulation of p53 (108). Since viral proteins are produced prior to genome replication (or dsRNA production), one can assume viral proteins that disrupt the nucleolus can potentially stabilize p53. In turn, this mechanism could counteract the degradation of p53 induced by dsRNA despite the activation of PKR.

Consequently, the nature of dsRNA recognition employed by the cell may explain the different ways in which differentially infected cells coordinate anti-viral immunity. Also, dsRNA signaling is one of the many pro-apoptotic pathways induced in virus-infected cells (279). Since, dsRNA is a by-product of virus replication, its ability to inhibit p53 raised some questions regarding the pro-apoptotic role of p53 in infected cells. The regulation of the anti-viral properties of p53 and the role of the eIF2α-dependent apoptotic pathway may contribute to current potential therapies such as the use of oncolytic viruses (20) aimed at destroying tumors carrying wild type p53.

3.6 Physiological Relevance to Cancer

It is well established that ER stress is linked to tumorigenesis (220). A recent report showed that ER stress induced cellular senescence in primary melanocytes without

the requirement of a functional p53 protein (82), supporting a direct role of ER stress in tumour suppression. However, several reports showed that PERK activation and eIF2α phosphorylation are induced under hypoxia (184,186), a physiological inducer of ER stress, and promotes tumor growth (31). Hypoxia is a condition that is common in solid tumors, making ER stress an important determinant of malignant progression. Although p53 induction under hypoxia is still controversial, some reports have provided evidence of the downregulation of p53 in conditions that were free from acidosis and maintained nutrient levels (254,288).

Taken together, our findings are consistent with a model where induction of PERK is associated with p53 degradation in hypoxic conditions. Given the role of p53 in tumor suppression, its downregulation and inactivation in conditions where eIF2α kinases are activated could provide growth advantages to cells and promote transformation. Therefore, we can speculate that activation of PERK in pathophysiological conditions may provide explanation for tumor resistance to radio/chemotherapies in cells harbouring wild type p53. In this regard, it is intriguing to address the degree to which PERK-mediated p53 inactivation contributes to cancer progression, in conjunction with other inactivating mechanisms (e.g. Mdm2 amplification, cytoplasmic sequestration, loss of ARF).

3.7 Summary

In conclusion, our data provide a molecular basis for the destabilization of p53 under conditions of eIF2α kinase activation. This allows the cell to adapt to disturbances in the normal function of the ER leading to p53 degradation, a necessary event to protect

cells against premature apoptosis. Further work is required to determine the intermediate signal(s) between eIF2α kinases and GSK3β. Such approach is crucial for the use of PERK and PKR as tools to discover therapeutic approaches for viral infection and cancer dysfunction.

Figure 53. Schematic model of eIF2α kinase mediated-p53 regulation in ER stressed cells.

When cells are exposed to ER stress, the eIF2α kinases activate different signaling pathways, one involved in translational control, another one controlling the activation of GSK3β leading to the induction of p53 phosphorylation on Ser315 and Ser376, as previously published. These phosphorylation events enhance the ubiquitination of p53 by Mdm2 and the cytoplasmic relocation of the tumour suppressor. As a result, p53 degradation occurs in the cytoplasm.

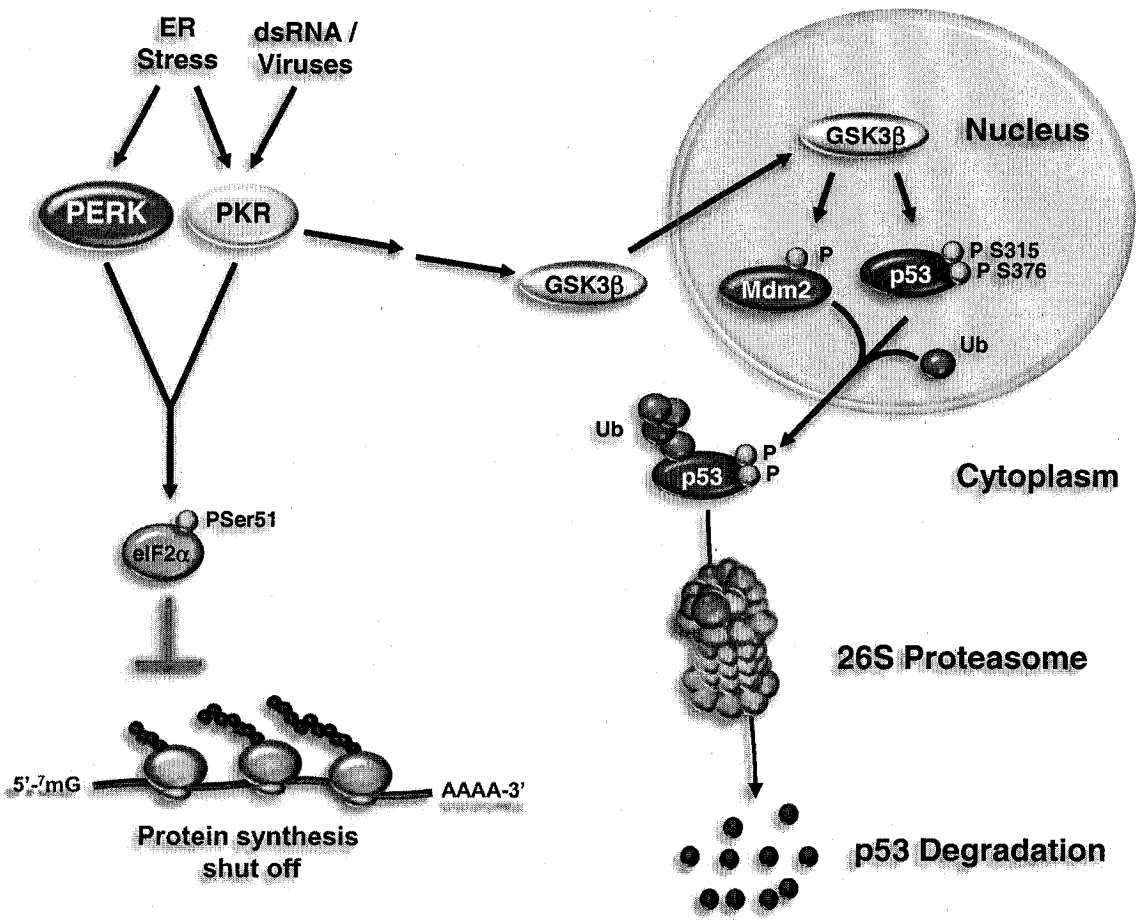
ER Stress
dsRNA / Viruses
PERK
PKR
GSK3β
Nucleus
GSK3β
P
Mdm2
p53
P S315
P S376
Ub
Ub
P
p53
P
Cytoplasm
PSer51
eIF2α
26S Proteasome
5'-7mG
AAAA-3'
Protein synthesis shut off
p53 Degradation

Figure 53

CHAPTER V – CONTRIBUTION TO THE ORIGINAL KNOWLEDGE

Research presented within this document has provided evidence that two distinct $PKR^{-/-}$ mice express truncated PKR proteins that may contribute to the controversial evidence observed regarding downstream signaling pathways mediated by dsRNA. Furthermore, we provide evidence of novel anti-viral and anti-apoptotic functions of PERK during VSV infection by regulating PKR activity. We also present new findings regarding the role of eIF2α kinases in promoting p53 downregulation independent of eIF2α-mediated translational inhibition. These studies are some of the first ones to demonstrate a role of eIF2α kinases in modulating p53 protein levels by promoting its nuclear export and degradation. Moreover, this document provides new insights into the molecular mechanisms regarding resistance to VSV infection, and the role of eIF2α kinases in the modulation of p53 upon conditions that induce ER stress. The candidate's major contributions are summarized as follows:

1. The candidate was the first to clone and characterize truncated proteins expressed in two distinct $PKR^{-/-}$ MEFs. These truncated proteins may contribute, at least in part, to the signaling differences observed between the two $PKR^{-/-}$ mice, and may explain the reason for the controversial evidence among them.

2. The candidate demonstrated for the first time, the activation of PERK in VSV infected MEFs. These experiments demonstrated that VSV induces PERK activation and subsequent eIF2α phosphorylation. These results provide further evidence that other eIF2α kinases are involved in mediating the

inhibition of viral protein synthesis, and explain the redundant eIF2α phosphorylation observed in VSV-infected PKR$^{-/-}$ MEFs.

3. Studies conducted by the candidate show, for the first time, that PERK may function upstream to PKR in VSV infection and upon ER stress. These data suggest that a cross-talk between two eIF2α kinases is required for resistance to VSV infection. This data may also explain the PKR activation observed during ER stress that remained elusive for almost one decade.

4. The candidate was first to describe the role of PERK in dsRNA-mediated activation of PKR. This may provide evidence that PERK may contribute to the interaction between PKR and dsRNA by mediating conformational changes prior to PKR activation.

5. Experiments performed by the candidate demonstrated that eIF2α kinases contribute to the downregulation of p53. This study provides further evidence to the transcriptional modulation functions mediated by eIF2α kinases. This suggests that eIF2α kinases play important roles in regulating transcription as well as translation.

6. The candidate provides evidence for the first time that the downregulation of p53 upon ER stress or dsRNA is not translational but rather degradation. This study suggests that translational control does not play a role in p53

downregulation suggesting that eIF2α kinases may play a role in the protein degradation machinery.

7. The candidate provides a novel finding that GSK3β activation is induced by eIF2α kinases. This suggests that the downregulation of p53 upon ER stress mediated by GSK3β is regulated by eIF2α kinase activity, and that eIF2α kinases may also play a role in glucose metabolism since GSK3β regulates glycogen synthesis.

CHAPTER VI – REFERENCES

References

1. **Abraham, N., M. L. Jaramillo, P. I. Duncan, N. Methot, P. L. Icely, D. F. Stojdl, G. N. Barber, and J. C. Bell**. 1998. The murine PKR tumor suppressor gene is rearranged in a lymphocytic leukemia. Exp. Cell Res. **244**:394-404.

2. **Abraham, N., D. F. Stojdl, P. I. Duncan, N. Methot, T. Ishii, M. Dube, B. C. Vanderhyden, H. L. Atkins, D. A. Gray, M. W. McBurney, A. E. Koromilas, E. G. Brown, N. Sonenberg, and J. C. Bell**. 1999. Characterization of transgenic mice with targeted disruption of the catalytic domain of the double-stranded RNA-dependent protein kinase, PKR. J. Biol. Chem. **274**:5953-5962.

3. **Adams, A., D. E. Gottschling, C. A. Kaiser, and T. Stearns**. 1997. Methods in Yeast Genetics. Cold Spring Harbor Laboratory Press, Plainview.

4. **Arava, Y.** 2003. Isolation of polysomal RNA for microarray analysis. Methods Mol. Biol. **224**:79-87.

5. **Aridor, M. and W. E. Balch**. 1999. Integration of endoplasmic reticulum signaling in health and disease. Nat. Med. **5**:745-751.

6. **Armstrong, J. L., G. J. Veal, C. P. Redfern, and P. E. Lovat**. 2007. Role of Noxa in p53-independent fenretinide-induced apoptosis of neuroectodermal tumours. Apoptosis.

7. **Baek, K. H.** 2003. Conjugation and deconjugation of ubiquitin regulating the destiny of proteins. Exp. Mol. Med. **35**:1-7.

8. **Baker, S. J., E. R. Fearon, J. M. Nigro, S. R. Hamilton, A. C. Preisinger, J. M. Jessup, P. vanTuinen, D. H. Ledbetter, D. F. Barker, Y. Nakamura, R. White, and B. Vogelstein**. 1989. Chromosome 17 deletions and p53 gene mutations in colorectal carcinomas. Science **244**:217-221.

9. **Baker, S. J., S. Markowitz, E. R. Fearon, J. K. Willson, and B. Vogelstein**. 1990. Suppression of human colorectal carcinoma cell growth by wild-type p53. Science **249**:912-915.

10. **Baker, S. J., A. C. Preisinger, J. M. Jessup, C. Paraskeva, S. Markowitz, J. K. Willson, S. Hamilton, and B. Vogelstein**. 1990. p53 gene mutations occur in combination with 17p allelic deletions as late events in colorectal tumorigenesis. Cancer Res. **50**:7717-7722.

11. **Balachandran, S., P. C. Roberts, L. E. Brown, H. Truong, A. K. Pattnaik, D. R. Archer, and G. N. Barber**. 2000. Essential role for the dsRNA-dependent protein kinase PKR in innate immunity to viral infection. Immunity. **13**:129-141.

12. **Ball, L. A. and G. W. Wertz**. 1981. VSV RNA synthesis: how can you be positive? Cell **26**:143-144.

13. **Ball, L. A. and C. N. White**. 1976. Order of transcription of genes of vesicular stomatitis virus. Proc. Natl. Acad. Sci. U. S. A **73**:442-446.

14. **Barber, G. N.** 2001. Host defense, viruses and apoptosis. Cell Death. Differ. **8**:113-126.

15. **Barber, G. N., S. Edelhoff, M. G. Katze, and C. M. Disteche**. 1993. Chromosomal assignment of the interferon-inducible double-stranded RNA-dependent protein kinase (PRKR) to human chromosome 2p21-p22 and mouse chromosome 17 E2. Genomics **16**:765-767.

16. **Barlev, N. A., L. Liu, N. H. Chehab, K. Mansfield, K. G. Harris, T. D. Halazonetis, and S. L. Berger**. 2001. Acetylation of p53 activates transcription through recruitment of coactivators/histone acetyltransferases. Mol. Cell **8**:1243-1254.

17. **Barr, J. N., S. P. Whelan, and G. W. Wertz**. 2002. Transcriptional control of the RNA-dependent RNA polymerase of vesicular stomatitis virus. Biochim. Biophys. Acta **1577**:337-353.

18. **Bass, B. L., K. Nishikura, W. Keller, P. H. Seeburg, R. B. Emeson, M. A. O'Connell, C. E. Samuel, and A. Herbert**. 1997. A standardized nomenclature for adenosine deaminases that act on RNA. RNA. **3**:947-949.

19. **Belkowski, L. S. and G. C. Sen**. 1987. Inhibition of vesicular stomatitis viral mRNA synthesis by interferons. J. Virol. **61**:653-660.

20. **Bell, J. C., K. A. Garson, B. D. Lichty, and D. F. Stojdl**. 2002. Oncolytic viruses: programmable tumour hunters. Curr. Gene Ther. **2**:243-254.

21. **Benchimol, S., P. Lamb, L. V. Crawford, D. Sheer, T. B. Shows, G. A. Bruns, and J. Peacock**. 1985. Transformation associated p53 protein is encoded by a gene on human chromosome 17. Somat. Cell Mol. Genet. **11**:505-510.

22. **Benchimol, S., D. Pim, and L. Crawford**. 1982. Radioimmunoassay of the cellular protein p53 in mouse and human cell lines. EMBO J. **1**:1055-1062.

23. **Bensaad, K., A. Tsuruta, M. A. Selak, M. N. Vidal, K. Nakano, R. Bartrons, E. Gottlieb, and K. H. Vousden**. 2006. TIGAR, a p53-inducible regulator of glycolysis and apoptosis. Cell **126**:107-120.

24. **Berger, M., N. Stahl, S. G. del, and Y. Haupt**. 2005. Mutations in proline 82 of p53 impair its activation by Pin1 and Chk2 in response to DNA damage. Mol. Cell Biol. **25**:5380-5388.

25. **Berger, M., S. R. Vogt, A. J. Levine, and Y. Haupt**. 2001. A role for the polyproline domain of p53 in its regulation by Mdm2. J. Biol. Chem. **276**:3785-3790.

26. **Berlanga, J. J., S. Herrero, and C. De Haro**. 1998. Characterization of the hemin-sensitive eukaryotic initiation factor 2alpha kinase from mouse nonerythroid cells. J Biol Chem. **273**:32340-32346.

27. **Berlanga, J. J., J. Santoyo, and H. C. de**. 1999. Characterization of a mammalian homolog of the GCN2 eukaryotic initiation factor 2alpha kinase. Eur. J. Biochem. **265**:754-762.

28. **Berlanga, J. J., I. Ventoso, H. P. Harding, J. Deng, D. Ron, N. Sonenberg, L. Carrasco, and H. C. de**. 2006. Antiviral effect of the mammalian translation initiation factor 2alpha kinase GCN2 against RNA viruses. EMBO J. **25**:1730-1740.

29. **Beroud, C. and T. Soussi**. 2003. The UMD-p53 database: new mutations and analysis tools. Hum. Mutat. **21**:176-181.

30. **Bertolotti, A., Y. Zhang, L. M. Hendershot, H. P. Harding, and D. Ron**. 2000. Dynamic interaction of BiP and ER stress transducers in the unfolded-protein response. Nat. Cell Biol. **2**:326-332.

31. **Bi, M., C. Naczki, M. Koritzinsky, D. Fels, J. Blais, N. Hu, H. Harding, I. Novoa, M. Varia, J. Raleigh, D. Scheuner, R. J. Kaufman, J. Bell, D. Ron, B. G. Wouters, and C. Koumenis**.

2005. ER stress-regulated translation increases tolerance to extreme hypoxia and promotes tumor growth. EMBO J. **24**:3470-3481.

32. **Bitko, V. and S. Barik**. 2001. An endoplasmic reticulum-specific stress-activated caspase (caspase-12) is implicated in the apoptosis of A549 epithelial cells by respiratory syncytial virus. J Cell Biochem. **80**:441-454.

33. **Blumberg, B. M., M. Leppert, and D. Kolakofsky**. 1981. Interaction of VSV leader RNA and nucleocapsid protein may control VSV genome replication. Cell **23**:837-845.

34. **Blumenthal, R., A. Bali-Puri, A. Walter, D. Covell, and O. Eidelman**. 1987. pH-dependent fusion of vesicular stomatitis virus with Vero cells. Measurement by dequenching of octadecyl rhodamine fluorescence. J. Biol. Chem. **262**:13614-13619.

35. **Bode, A. M. and Z. Dong**. 2004. Post-translational modification of p53 in tumorigenesis. Nat. Rev. Cancer **4**:793-805.

36. **Bond, G. L., W. Hu, and A. J. Levine**. 2005. MDM2 is a central node in the p53 pathway: 12 years and counting. Curr. Cancer Drug Targets. **5**:3-8.

37. **Bonnet, M. C., R. Weil, E. Dam, A. G. Hovanessian, and E. F. Meurs**. 2000. PKR stimulates NF-kappaB irrespective of its kinase function by interacting with the IkappaB kinase complex. Mol. Cell Biol. **20**:4532-4542.

38. **Both, G. W., S. A. Moyer, and A. K. Banerjee**. 1975. Translation and identification of the viral mRNA species isolated from subcellular fractions of vesicular stomatitis virus-infected cells. J. Virol. **15**:1012-1019.

39. **Boyce, M., K. F. Bryant, C. Jousse, K. Long, H. P. Harding, D. Scheuner, R. J. Kaufman, D. Ma, D. M. Coen, D. Ron, and J. Yuan**. 2005. A selective inhibitor of eIF2alpha dephosphorylation protects cells from ER stress. Science **307**:935-939.

40. **Boyd, S. D., K. Y. Tsai, and T. Jacks**. 2000. An intact HDM2 RING-finger domain is required for nuclear exclusion of p53. Nat. Cell Biol. **2**:563-568.

41. **Braithwaite, A. W., J. A. Royds, and P. Jackson**. 2005. The p53 story: layers of complexity. Carcinogenesis **26**:1161-1169.

42. **Bycroft, M., S. Grunert, A. G. Murzin, M. Proctor, and J. D. St**. 1995. NMR solution structure of a dsRNA binding domain from Drosophila staufen protein reveals homology to the N-terminal domain of ribosomal protein S5. EMBO J. **14**:3563-3571.

43. **Chan, H. M. and N. B. La Thangue**. 2001. p300/CBP proteins: HATs for transcriptional bridges and scaffolds. J. Cell Sci. **114**:2363-2373.

44. **Chefalo, P. J., J. Oh, M. Rafie-Kolpin, B. Kan, and J. J. Chen**. 1998. Heme-regulated eIF-2alpha kinase purifies as a hemoprotein. Eur. J Biochem. **258**:820-830.

45. **Chen, D., N. Kon, M. Li, W. Zhang, J. Qin, and W. Gu**. 2005. ARF-BP1/Mule is a critical mediator of the ARF tumor suppressor. Cell **121**:1071-1083.

46. **Chen, J. J.** 2000. Heme-regulated eIF2alpha kinase, p. 529-546. *In* N. Sonenberg, J. W. B. Hershey, and M. B. Mathews (ed.), Translational Control of Gene Expression. Cold Spring Harbor Laboratory Press, Cold Spring Harbor, New York.

47. **Chen, J. J., J. S. Crosby, and I. M. London**. 1994. Regulation of heme-regulated eIF-2 alpha kinase and its expression in erythroid cells. Biochimie **76**:761-769.

48. **Chen, J. J. and I. M. London**. 1995. Regulation of protein synthesis by heme-regulated eIF-2 alpha kinase. Trends Biochem. Sci. **20**:105-108.

49. **Chen, J. L., T. Das, and A. K. Banerjee**. 1997. Phosphorylated states of vesicular stomatitis virus P protein in vitro and in vivo. Virology **228**:200-212.

50. **Cheng, G., Z. Feng, and B. He**. 2005. Herpes simplex virus 1 infection activates the endoplasmic reticulum resident kinase PERK and mediates eIF-2alpha dephosphorylation by the gamma(1)34.5 protein. J. Virol. **79**:1379-1388.

51. **Chesler, D. A., J. L. Munoz-Jordan, N. Donelan, A. Garcia-Sastre, and C. S. Reiss**. 2003. PKR is not required for interferon-gamma inhibition of VSV replication in neurons. Viral Immunol. **16**:87-96.

52. **Chipuk, J. E., L. Bouchier-Hayes, T. Kuwana, D. D. Newmeyer, and D. R. Green**. 2005. PUMA couples the nuclear and cytoplasmic proapoptotic function of p53. Science **309**:1732-1735.

53. **Chipuk, J. E., T. Kuwana, L. Bouchier-Hayes, N. M. Droin, D. D. Newmeyer, M. Schuler, and D. R. Green**. 2004. Direct activation of Bax by p53 mediates mitochondrial membrane permeabilization and apoptosis. Science **303**:1010-1014.

54. **Chong, L. D. and J. K. Rose**. 1993. Membrane association of functional vesicular stomatitis virus matrix protein in vivo. J. Virol. **67**:407-414.

55. **Chowdary, D. R., J. J. Dermody, K. K. Jha, and H. L. Ozer**. 1994. Accumulation of p53 in a mutant cell line defective in the ubiquitin pathway. Mol. Cell Biol. **14**:1997-2003.

56. **Chu, W. M., D. Ostertag, Z. W. Li, L. Chang, Y. Chen, Y. Hu, B. Williams, J. Perrault, and M. Karin**. 1999. JNK2 and IKKbeta are required for activating the innate response to viral infection. Immunity. **11**:721-731.

57. **Chuikov, S., J. K. Kurash, J. R. Wilson, B. Xiao, N. Justin, G. S. Ivanov, K. McKinney, P. Tempst, C. Prives, S. J. Gamblin, N. A. Barlev, and D. Reinberg**. 2004. Regulation of p53 activity through lysine methylation. Nature **432**:353-360.

58. **Ciechanover, A., A. Orian, and A. L. Schwartz**. 2000. Ubiquitin-mediated proteolysis: biological regulation via destruction. Bioessays **22**:442-451.

59. **Clarke, P. A. and M. B. Mathews**. 1995. Interactions between the double-stranded RNA binding motif and RNA: definition of the binding site for the interferon-induced protein kinase DAI (PKR) on adenovirus VA RNA. RNA. **1**:7-20.

60. **Clemens, M. J.** 2001. Initiation factor eIF2 alpha phosphorylation in stress responses and apoptosis. Prog. Mol Subcell. Biol **27**:57-89.

61. **Clemens, M. J. and A. Elia**. 1997. The double-stranded RNA-dependent protein kinase PKR: structure and function. J. Interferon Cytokine Res. **17**:503-524.

62. **Clewley, J. P. and D. H. Bishop**. 1979. Assignment of the large oligonucleotides of vesicular stomatitis virus to the N, NS, M, G, and L genes and oligonucleotide gene ordering within the L gene. J. Virol. **30**:116-123.

63. **Clinton, G. M., B. W. Burge, and A. S. Huang**. 1978. Effects of phosphorylation and pH on the association of NS protein with vesicular stomatitis virus cores. J. Virol. **27**:340-346.

64. **Cohen, P. and S. Frame**. 2001. The renaissance of GSK3. Nat. Rev. Mol. Cell Biol. **2**:769-776.

65. **Coll, J. M.** 1995. The glycoprotein G of rhabdoviruses. Arch. Virol. **140**:827-851.

66. **Coll, J. M.** 1997. Synthetic peptides from the heptad repeats of the glycoproteins of rabies, vesicular stomatitis and fish rhabdoviruses bind phosphatidylserine. Arch. Virol. **142**:2089-2097.

67. **Connor, J. H. and D. S. Lyles**. 2002. Vesicular stomatitis virus infection alters the eIF4F translation initiation complex and causes dephosphorylation of the eIF4E binding protein 4E-BP1. J. Virol. **76**:10177-10187.

68. **Conti, C., P. Mastromarino, and N. Orsi**. 1991. Role of membrane phospholipids and glycolipids in cell-to-cell fusion by VSV. Comp Immunol. Microbiol. Infect. Dis. **14**:303-313.

69. **Credle, J. J., J. S. Finer-Moore, F. R. Papa, R. M. Stroud, and P. Walter**. 2005. On the mechanism of sensing unfolded protein in the endoplasmic reticulum. Proc. Natl. Acad. Sci. U. S. A **102**:18773-18784.

70. **Crighton, D., S. Wilkinson, J. O'Prey, N. Syed, P. Smith, P. R. Harrison, M. Gasco, O. Garrone, T. Crook, and K. M. Ryan**. 2006. DRAM, a p53-induced modulator of autophagy, is critical for apoptosis. Cell **126**:121-134.

71. **Cuddihy, A. R., S. Li, N. W. Tam, A. H. Wong, Y. Taya, N. Abraham, J. C. Bell, and A. E. Koromilas**. 1999. Double-stranded-RNA-activated protein kinase PKR enhances transcriptional activation by tumor suppressor p53. Mol. Cell Biol. **19**:2475-2484.

72. **Cuddihy, A. R., A. H. Wong, N. W. Tam, S. Li, and A. E. Koromilas**. 1999. The double-stranded RNA activated protein kinase PKR physically associates with the tumor suppressor p53 protein and phosphorylates human p53 on serine 392 in vitro. Oncogene **18**:2690-2702.

73. **Cullinan, S. B., D. Zhang, M. Hannink, E. Arvisais, R. J. Kaufman, and J. A. Diehl**. 2003. Nrf2 is a direct PERK substrate and effector of PERK-dependent cell survival. Mol. Cell Biol **23**:7198-7209.

74. **Damalas, A., A. Ben-Ze'ev, I. Simcha, M. Shtutman, J. F. Leal, J. Zhurinsky, B. Geiger, and M. Oren**. 1999. Excess beta-catenin promotes accumulation of transcriptionally active p53. EMBO J. **18**:3054-3063.

75. **Dar, A. C., T. E. Dever, and F. Sicheri**. 2005. Higher-order substrate recognition of eIF2alpha by the RNA-dependent protein kinase PKR. Cell **122**:887-900.

76. **Darnell, J. E., Jr.** 1997. STATs and gene regulation. Science **277**:1630-1635.

77. **de Silva, A. M., W. E. Balch, and A. Helenius**. 1990. Quality control in the endoplasmic reticulum: folding and misfolding of vesicular stomatitis virus G protein in cells and in vitro. J. Cell Biol. **111**:857-866.

78. **De, B. P. and A. K. Banerjee**. 1984. Specific interactions of vesicular stomatitis virus L and NS proteins with heterologous genome ribonucleoprotein template lead to mRNA synthesis in vitro. J. Virol. **51**:628-634.

79. **Deb, A., M. Zamanian-Daryoush, Z. Xu, S. Kadereit, and B. R. Williams**. 2001. Protein kinase PKR is required for platelet-derived growth factor signaling of c-fos gene expression via Erks and Stat3. EMBO J. **20**:2487-2496.

80. **DeLeo, A. B., G. Jay, E. Appella, G. C. DuBois, L. W. Law, and L. J. Old**. 1979. Detection of a transformation-related antigen in chemically induced sarcomas and other transformed cells of the mouse. Proc. Natl. Acad. Sci. U. S. A **76**:2420-2424.

81. **Deng, J., H. P. Harding, B. Raught, A. C. Gingras, J. J. Berlanga, D. Scheuner, R. J. Kaufman, D. Ron, and N. Sonenberg**. 2002. Activation of GCN2 in UV-irradiated cells inhibits translation. Curr. Biol. **12**:1279-1286.

82. **Denoyelle, C., G. bou-Rjaily, V. Bezrookove, M. Verhaegen, T. M. Johnson, D. R. Fullen, J. N. Pointer, S. B. Gruber, L. D. Su, M. A. Nikiforov, R. J. Kaufman, B. C. Bastian, and M. S. Soengas**. 2006. Anti-oncogenic role of the endoplasmic reticulum differentially activated by mutations in the MAPK pathway. Nat. Cell Biol. **8**:1053-1063.

83. **Der, S. D., Y. L. Yang, C. Weissmann, and B. R. Williams**. 1997. A double-stranded RNA-activated protein kinase-dependent pathway mediating stress-induced apoptosis. Proc. Natl. Acad. Sci. U. S. A **94**:3279-3283.

84. **Desforges, M., G. Despars, S. Berard, M. Gosselin, M. O. McKenzie, D. S. Lyles, P. J. Talbot, and L. Poliquin**. 2002. Matrix protein mutations contribute to inefficient induction of apoptosis leading to persistent infection of human neural cells by vesicular stomatitis virus. Virology **295**:63-73.

85. **Dever, T. E.** 2002. Gene-specific regulation by general translation factors. Cell **108**:545-556.

86. **Dever, T. E., J. J. Chen, G. N. Barber, A. M. Cigan, L. Feng, T. F. Donahue, I. M. London, M. G. Katze, and A. G. Hinnebusch**. 1993. Mammalian eukaryotic initiation factor 2 alpha kinases functionally substitute for GCN2 protein kinase in the GCN4 translational control mechanism of yeast. Proc. Natl. Acad. Sci. U. S. A **90**:4616-4620.

87. **Dever, T. E., L. Feng, R. C. Wek, A. M. Cigan, T. F. Donahue, and A. G. Hinnebusch**. 1992. Phosphorylation of initiation factor 2 alpha by protein kinase GCN2 mediates gene-specific translational control of GCN4 in yeast. Cell **68**:585-596.

88. **Dey, M., C. Cao, A. C. Dar, T. Tamura, K. Ozato, F. Sicheri, and T. E. Dever**. 2005. Mechanistic link between PKR dimerization, autophosphorylation, and eIF2alpha substrate recognition. Cell **122**:901-913.

89. **Doble, B. W. and J. R. Woodgett**. 2003. GSK-3: tricks of the trade for a multi-tasking kinase. J. Cell Sci. **116**:1175-1186.

90. **Donehower, L. A., M. Harvey, B. L. Slagle, M. J. McArthur, C. A. Montgomery, Jr., J. S. Butel, and A. Bradley**. 1992. Mice deficient for p53 are developmentally normal but susceptible to spontaneous tumours. Nature **356**:215-221.

91. **Donze, O., R. Jagus, A. E. Koromilas, J. W. Hershey, and N. Sonenberg**. 1995. Abrogation of translation initiation factor eIF-2 phosphorylation causes malignant transformation of NIH 3T3 cells. EMBO J **14**:3828-3834.

92. **Dornan, D., I. Wertz, H. Shimizu, D. Arnott, G. D. Frantz, P. Dowd, K. O'rourke, H. Koeppen, and V. M. Dixit**. 2004. The ubiquitin ligase COP1 is a critical negative regulator of p53. Nature **429**:86-92.

93. **Durbin, R. K., S. E. Mertz, A. E. Koromilas, and J. E. Durbin**. 2002. PKR protection against intranasal vesicular stomatitis virus infection is mouse strain dependent. Viral Immunol. **15**:41-51.

94. **Dutta, J., Y. Fan, N. Gupta, G. Fan, and C. Gelinas**. 2006. Current insights into the regulation of programmed cell death by NF-kappaB. Oncogene **25**:6800-6816.

95. **Egger, D., B. Wolk, R. Gosert, L. Bianchi, H. E. Blum, D. Moradpour, and K. Bienz**. 2002. Expression of hepatitis C virus proteins induces distinct membrane alterations including a candidate viral replication complex. J. Virol. **76**:5974-5984.

96. **El-Deiry, W. S., T. Tokino, V. E. Velculescu, D. B. Levy, R. Parsons, J. M. Trent, D. Lin, W. E. Mercer, K. W. Kinzler, and B. Vogelstein**. 1993. WAF1, a potential mediator of p53 tumor suppression. Cell **75**:817-825.

97. **Elbashir, S. M., J. Harborth, K. Weber, and T. Tuschl**. 2002. Analysis of gene function in somatic mammalian cells using small interfering RNAs. Methods **26**:199-213.

98. **Eley, H. L. and M. J. Tisdale**. 2007. Skeletal muscle atrophy: A link between depression of protein synthesis and increase in degradation. J. Biol. Chem.

99. **Esser, C., M. Scheffner, and J. Hohfeld**. 2005. The chaperone-associated ubiquitin ligase CHIP is able to target p53 for proteasomal degradation. J. Biol. Chem. **280**:27443-27448.

100. **Faria, P. A., P. Chakraborty, A. Levay, G. N. Barber, H. J. Ezelle, J. Enninga, C. Arana, D. J. van, and B. M. Fontoura**. 2005. VSV disrupts the Rae1/mrnp41 mRNA nuclear export pathway. Mol. Cell **17**:93-102.

101. **Feng, L., T. Lin, H. Uranishi, W. Gu, and Y. Xu**. 2005. Functional analysis of the roles of posttranslational modifications at the p53 C terminus in regulating p53 stability and activity. Mol. Cell Biol. **25**:5389-5395.

102. **Finlay, C. A., P. W. Hinds, and A. J. Levine**. 1989. The p53 proto-oncogene can act as a suppressor of transformation. Cell **57**:1083-1093.

103. **Fontoura, B. M., P. A. Faria, and D. R. Nussenzveig**. 2005. Viral interactions with the nuclear transport machinery: discovering and disrupting pathways. IUBMB. Life **57**:65-72.

104. **Forrester, K., S. Ambs, S. E. Lupold, R. B. Kapust, E. A. Spillare, W. C. Weinberg, E. Felley-Bosco, X. W. Wang, D. A. Geller, E. Tzeng, T. R. Billiar, and C. C. Harris**. 1996. Nitric oxide-induced p53 accumulation and regulation of inducible nitric oxide synthase expression by wild-type p53. Proc. Natl. Acad. Sci. U. S. A **93**:2442-2447.

105. **Fu, L. and S. Benchimol**. 1997. Participation of the human p53 3'UTR in translational repression and activation following gamma-irradiation. EMBO J. **16**:4117-4125.

106. **Fuerst, T. R., E. G. Niles, F. W. Studier, and B. Moss**. 1986. Eukaryotic transient-expression system based on recombinant vaccinia virus that synthesizes bacteriophage T7 RNA polymerase. Proc. Natl. Acad. Sci. U. S. A **83**:8122-8126.

107. **Furlong, E. E., T. Rein, and F. Martin**. 1996. YY1 and NF1 both activate the human p53 promoter by alternatively binding to a composite element, and YY1 and E1A cooperate to amplify p53 promoter activity. Mol. Cell Biol. **16**:5933-5945.

108. **Gallagher, S. J., R. F. Kefford, and H. Rizos**. 2006. The ARF tumour suppressor. Int. J. Biochem. Cell Biol. **38**:1637-1641.

109. **Gannon, J. V., R. Greaves, R. Iggo, and D. P. Lane**. 1990. Activating mutations in p53 produce a common conformational effect. A monoclonal antibody specific for the mutant form. EMBO J. **9**:1595-1602.

110. **Gebauer, F. and M. W. Hentze**. 2004. Molecular mechanisms of translational control. Nat. Rev. Mol. Cell Biol. **5**:827-835.

111. **Gil, J., J. Alcami, and M. Esteban**. 2000. Activation of NF-kappa B by the dsRNA-dependent protein kinase, PKR involves the I kappa B kinase complex. Oncogene **19**:1369-1378.

112. **Gil, J., J. Rullas, M. A. Garcia, J. Alcami, and M. Esteban**. 2001. The catalytic activity of dsRNA-dependent protein kinase, PKR, is required for NF-kappaB activation. Oncogene **20**:385-394.

113. **Gitlin, L., W. Barchet, S. Gilfillan, M. Cella, B. Beutler, R. A. Flavell, M. S. Diamond, and M. Colonna**. 2006. Essential role of mda-5 in type I IFN responses to polyriboinosinic:polyribocytidylic acid and encephalomyocarditis picornavirus. Proc. Natl. Acad. Sci. U. S. A **103**:8459-8464.

114. **Goh, K. C., M. J. deVeer, and B. R. Williams**. 2000. The protein kinase PKR is required for p38 MAPK activation and the innate immune response to bacterial endotoxin. EMBO J. **19**:4292-4297.

115. **Gosert, R., D. Egger, and K. Bienz**. 2000. A cytopathic and a cell culture adapted hepatitis A virus strain differ in cell killing but not in intracellular membrane rearrangements. Virology **266**:157-169.

116. **Gottifredi, V., S. Shieh, Y. Taya, and C. Prives**. 2001. p53 accumulates but is functionally impaired when DNA synthesis is blocked. Proc. Natl. Acad. Sci. U. S. A **98**:1036-1041.

117. **Graeber, T. G., J. F. Peterson, M. Tsai, K. Monica, A. J. Fornace, Jr., and A. J. Giaccia**. 1994. Hypoxia induces accumulation of p53 protein, but activation of a G1-phase checkpoint by low-oxygen conditions is independent of p53 status. Mol. Cell Biol. **14**:6264-6277.

118. **Grossman, S. R.** 2001. p300/CBP/p53 interaction and regulation of the p53 response. Eur. J. Biochem. **268**:2773-2778.

119. **Grossman, S. R., M. E. Deato, C. Brignone, H. M. Chan, A. L. Kung, H. Tagami, Y. Nakatani, and D. M. Livingston**. 2003. Polyubiquitination of p53 by a ubiquitin ligase activity of p300. Science **300**:342-344.

120. **Gu, W. and R. G. Roeder**. 1997. Activation of p53 sequence-specific DNA binding by acetylation of the p53 C-terminal domain. Cell **90**:595-606.

121. **Gu, W., X. L. Shi, and R. G. Roeder**. 1997. Synergistic activation of transcription by CBP and p53. Nature **387**:819-823.

122. **Guerra, S., L. A. Lopez-Fernandez, M. A. Garcia, A. Zaballos, and M. Esteban**. 2006. Human gene profiling in response to the active protein kinase, interferon-induced serine/threonine protein kinase (PKR), in infected cells. Involvement of the transcription factor ATF-3 IN PKR-induced apoptosis. J. Biol. Chem. **281**:18734-18745.

123. **Hainaut, P., T. Soussi, B. Shomer, M. Hollstein, M. Greenblatt, E. Hovig, C. C. Harris, and R. Montesano**. 1997. Database of p53 gene somatic mutations in human tumors and cell lines: updated compilation and future prospects. Nucleic Acids Res. **25**:151-157.

124. **Hammond, C. and A. Helenius**. 1994. Folding of VSV G protein: sequential interaction with BiP and calnexin. Science **266**:456-458.

125. **Harding, H. P., M. Calfon, F. Urano, I. Novoa, and D. Ron**. 2002. Transcriptional and translational control in the Mammalian unfolded protein response. Annu. Rev. Cell Dev. Biol. **18**:575-599.

126. **Harding, H. P., I. Novoa, Y. Zhang, H. Zeng, R. Wek, M. Schapira, and D. Ron**. 2000. Regulated translation initiation controls stress-induced gene expression in mammalian cells. Mol. Cell **6**:1099-1108.

127. **Harding, H. P., Y. Zhang, A. Bertolotti, H. Zeng, and D. Ron**. 2000. Perk is essential for translational regulation and cell survival during the unfolded protein response. Mol. Cell **5**:897-904.

128. **Harding, H. P., Y. Zhang, and D. Ron**. 1999. Protein translation and folding are coupled by an endoplasmic-reticulum-resident kinase. Nature **397**:271-274.

129. **Harding, H. P., Y. Zhang, H. Zeng, I. Novoa, P. D. Lu, M. Calfon, N. Sadri, C. Yun, B. Popko, R. Paules, D. F. Stojdl, J. C. Bell, T. Hettmann, J. M. Leiden, and D. Ron**. 2003. An integrated stress response regulates amino acid metabolism and resistance to oxidative stress. Mol. Cell **11**:619-633.

130. **Harms, K., S. Nozell, and X. Chen**. 2004. The common and distinct target genes of the p53 family transcription factors. Cell Mol. Life Sci. **61**:822-842.

131. **Harms, K. L. and X. Chen**. 2006. The functional domains in p53 family proteins exhibit both common and distinct properties. Cell Death. Differ. **13**:890-897.

132. **Harris, S. L. and A. J. Levine**. 2005. The p53 pathway: positive and negative feedback loops. Oncogene **24**:2899-2908.

133. **Haupt, Y., R. Maya, A. Kazaz, and M. Oren**. 1997. Mdm2 promotes the rapid degradation of p53. Nature **387**:296-299.

134. **Hayden, M. S., A. P. West, and S. Ghosh**. 2006. NF-kappaB and the immune response. Oncogene **25**:6758-6780.

135. **Herman, R. C.** 1987. Characterization of the internal initiation of translation on the vesicular stomatitis virus phosphoprotein mRNA. Biochemistry **26**:8346-8350.

136. **Hermeking, H. and D. Eick**. 1994. Mediation of c-Myc-induced apoptosis by p53. Science **265**:2091-2093.

137. **Hermeking, H., C. Lengauer, K. Polyak, T. C. He, L. Zhang, S. Thiagalingam, K. W. Kinzler, and B. Vogelstein**. 1997. 14-3-3 sigma is a p53-regulated inhibitor of G2/M progression. Mol. Cell **1**:3-11.

138. **Hernandez-Boussard, T., P. Rodriguez-Tome, R. Montesano, and P. Hainaut**. 1999. IARC p53 mutation database: a relational database to compile and analyze p53 mutations in human tumors and cell lines. International Agency for Research on Cancer. Hum. Mutat. **14**:1-8.

139. **Hinnebusch, A. G.** 1994. The eIF-2 alpha kinases: regulators of protein synthesis in starvation and stress. Semin. Cell Biol **5**:417-426.

140. **Hinnebusch, A. G.** 2000. Translational control of GCN4: Gene-specific regulation by phosphorylation of eIF2, p. 199-244. *In* N. Sonenberg, J. W. B. Hershey, and M. B. Mathews (ed.), Translational Control of Gene Expression. Cold Spring Harbor Laboratory Press, Cold Spring Harbor, New York.

141. **Hinzman, E. E., J. N. Barr, and G. W. Wertz**. 2002. Identification of an upstream sequence element required for vesicular stomatitis virus mRNA transcription. J. Virol. **76**:7632-7641.

142. **Hiscox, J. A.** 2007. RNA viruses: hijacking the dynamic nucleolus. Nat. Rev. Microbiol. **5**:119-127.

143. **Hobbs, J. A., R. H. Schloemer, G. Hommel-Berrey, and Z. Brahmi**. 2001. Caspase-3-like proteases are activated by infection but are not required for replication of vesicular stomatitis virus. Virus Res. **80**:53-65.

144. **Hoeflich, K. P., J. Luo, E. A. Rubie, M. S. Tsao, O. Jin, and J. R. Woodgett**. 2000. Requirement for glycogen synthase kinase-3beta in cell survival and NF-kappaB activation. Nature **406**:86-90.

145. **Hollstein, M., K. Rice, M. S. Greenblatt, T. Soussi, R. Fuchs, T. Sorlie, E. Hovig, B. Smith-Sorensen, R. Montesano, and C. C. Harris**. 1994. Database of p53 gene somatic mutations in human tumors and cell lines. Nucleic Acids Res. **22**:3551-3555.

146. **Hollstein, M., D. Sidransky, B. Vogelstein, and C. C. Harris**. 1991. p53 mutations in human cancers. Science **253**:49-53.

147. **Honda, R., H. Tanaka, and H. Yasuda**. 1997. Oncoprotein MDM2 is a ubiquitin ligase E3 for tumor suppressor p53. FEBS Lett. **420**:25-27.

148. **Honda, R. and H. Yasuda**. 2000. Activity of MDM2, a ubiquitin ligase, toward p53 or itself is dependent on the RING finger domain of the ligase. Oncogene **19**:1473-1476.

149. **Hong, S. J., T. M. Dawson, and V. L. Dawson**. 2004. Nuclear and mitochondrial conversations in cell death: PARP-1 and AIF signaling. Trends Pharmacol. Sci. **25**:259-264.

150. **Hu, M., L. Gu, M. Li, P. D. Jeffrey, W. Gu, and Y. Shi**. 2006. Structural basis of competitive recognition of p53 and MDM2 by HAUSP/USP7: implications for the regulation of the p53-MDM2 pathway. PLoS. Biol. **4**:e27.

151. **Iborra, F. J., D. A. Jackson, and P. R. Cook**. 2001. Coupled transcription and translation within nuclei of mammalian cells. Science **293**:1139-1142.

152. **Iborra, F. J., D. A. Jackson, and P. R. Cook**. 2004. Approaches for monitoring nuclear translation. Methods Mol. Biol. **257**:103-114.

153. **Iborra, F. J., D. A. Jackson, and P. R. Cook**. 2004. The case for nuclear translation. J. Cell Sci. **117**:5713-5720.

154. **Icely, P. L., P. Gros, J. J. Bergeron, A. Devault, D. E. Afar, and J. C. Bell**. 1991. TIK, a novel serine/threonine kinase, is recognized by antibodies directed against phosphotyrosine. J Biol Chem. **266**:16073-16077.

155. **Inoue, T., R. K. Geyer, Z. K. Yu, and C. G. Maki**. 2001. Downregulation of MDM2 stabilizes p53 by inhibiting p53 ubiquitination in response to specific alkylating agents. FEBS Lett. **490**:196-201.

156. **Iordanov, M. S., J. M. Paranjape, A. Zhou, J. Wong, B. R. Williams, E. F. Meurs, R. H. Silverman, and B. E. Magun**. 2000. Activation of p38 mitogen-activated protein kinase and c-Jun NH(2)-terminal kinase by double-stranded RNA and encephalomyocarditis virus: involvement of RNase L, protein kinase R, and alternative pathways. Mol. Cell Biol. **20**:617-627.

157. **Iordanov, M. S., J. Wong, J. C. Bell, and B. E. Magun**. 2001. Activation of NF-kappaB by double-stranded RNA (dsRNA) in the absence of protein kinase R and RNase L demonstrates the existence of two separate dsRNA-triggered antiviral programs. Mol. Cell Biol. **21**:61-72.

158. **Ishii, T., H. Kwon, J. Hiscott, G. Mosialos, and A. E. Koromilas**. 2001. Activation of the I kappa B alpha kinase (IKK) complex by double-stranded RNA-binding defective and catalytic inactive mutants of the interferon-inducible protein kinase PKR. Oncogene **20**:1900-1912.

159. **Jayakar, H. R., E. Jeetendra, and M. A. Whitt**. 2004. Rhabdovirus assembly and budding. Virus Res. **106**:117-132.

160. **Jeffrey, I. W., S. Kadereit, E. F. Meurs, T. Metzger, M. Bachmann, M. Schwemmle, A. G. Hovanessian, and M. J. Clemens**. 1995. Nuclear localization of the interferon-inducible protein kinase PKR in human cells and transfected mouse cells. Exp. Cell Res. **218**:17-27.

161. **Jenkins, J. R., K. Rudge, and G. A. Currie**. 1984. Cellular immortalization by a cDNA clone encoding the transformation-associated phosphoprotein p53. Nature **312**:651-654.

162. **Jiang, H. Y. and R. C. Wek**. 2005. GCN2 phosphorylation of eIF2alpha activates NF-kappaB in response to UV irradiation. Biochem. J. **385**:371-380.

163. **Jiang, H. Y. and R. C. Wek**. 2005. Phosphorylation of the alpha-subunit of the eukaryotic initiation factor-2 (eIF2alpha) reduces protein synthesis and enhances apoptosis in response to proteasome inhibition. J. Biol. Chem. **280**:14189-14202.

164. **Jiang, H. Y., S. A. Wek, B. C. McGrath, D. Scheuner, R. J. Kaufman, D. R. Cavener, and R. C. Wek**. 2003. Phosphorylation of the alpha subunit of eukaryotic initiation factor 2 is required for activation of NF-kappaB in response to diverse cellular stresses. Mol. Cell Biol. **23**:5651-5663.

165. **Jordan, R., L. Wang, T. M. Graczyk, T. M. Block, and P. R. Romano**. 2002. Replication of a cytopathic strain of bovine viral diarrhea virus activates PERK and induces endoplasmic reticulum stress-mediated apoptosis of MDBK cells. J. Virol. **76**:9588-9599.

166. **Jousse, C., S. Oyadomari, I. Novoa, P. Lu, Y. Zhang, H. P. Harding, and D. Ron**. 2003. Inhibition of a constitutive translation initiation factor 2alpha phosphatase, CReP, promotes survival of stressed cells. J. Cell Biol. **163**:767-775.

167. **Juan, L. J., W. J. Shia, M. H. Chen, W. M. Yang, E. Seto, Y. S. Lin, and C. W. Wu**. 2000. Histone deacetylases specifically down-regulate p53-dependent gene activation. J. Biol. Chem. **275**:20436-20443.

168. **Karin, M.** 1998. The NF-kappa B activation pathway: its regulation and role in inflammation and cell survival. Cancer J. Sci. Am. **4 Suppl 1**:S92-S99.

169. **Kato, H., S. Sato, M. Yoneyama, M. Yamamoto, S. Uematsu, K. Matsui, T. Tsujimura, K. Takeda, T. Fujita, O. Takeuchi, and S. Akira**. 2005. Cell type-specific involvement of RIG-I in antiviral response. Immunity. **23**:19-28.

170. **Kato, H., O. Takeuchi, S. Sato, M. Yoneyama, M. Yamamoto, K. Matsui, S. Uematsu, A. Jung, T. Kawai, K. J. Ishii, O. Yamaguchi, K. Otsu, T. Tsujimura, C. S. Koh, Reis E Sousa,**

Y. Matsuura, T. Fujita, and S. Akira. 2006. Differential roles of MDA5 and RIG-I helicases in the recognition of RNA viruses. Nature **441**:101-105.

171. **Katze, M. G., Y. He, and M. Gale, Jr.** 2002. Viruses and interferon: a fight for supremacy. Nat. Rev. Immunol. **2**:675-687.

172. **Kaufman, R. J.** 2000. The double-stranded RNA-activated protein kinase PKR, p. 503-527. *In* N. Sonenberg, J. W. B. Hershey, and M. B. Mathews (ed.), Translational Control of Gene Expression. Cold Spring Harbor Laboratory Press, Cold Spring Harbor, New York.

173. **Kaufman, R. J., M. V. Davies, V. K. Pathak, and J. W. Hershey**. 1989. The phosphorylation state of eucaryotic initiation factor 2 alters translational efficiency of specific mRNAs. Mol. Cell Biol. **9**:946-958.

174. **Kaufman, R. J., D. Scheuner, M. Schroder, X. Shen, K. Lee, C. Y. Liu, and S. M. Arnold**. 2002. The unfolded protein response in nutrient sensing and differentiation. Nat. Rev. Mol. Cell Biol. **3**:411-421.

175. **Kawagishi-Kobayashi, M., J. B. Silverman, T. L. Ung, and T. E. Dever**. 1997. Regulation of the protein kinase PKR by the vaccinia virus pseudosubstrate inhibitor K3L is dependent on residues conserved between the K3L protein and the PKR substrate eIF2alpha. Mol. Cell Biol. **17**:4146-4158.

176. **Kawauchi, J., C. Zhang, K. Nobori, Y. Hashimoto, M. T. Adachi, A. Noda, M. Sunamori, and S. Kitajima**. 2002. Transcriptional repressor activating transcription factor 3 protects human umbilical vein endothelial cells from tumor necrosis factor-alpha-induced apoptosis through down-regulation of p53 transcription. J. Biol. Chem. **277**:39025-39034.

177. **Kazemi, S., S. Papadopoulou, S. Li, Q. Su, S. Wang, A. Yoshimura, G. Matlashewski, T. E. Dever, and A. E. Koromilas**. 2004. Control of alpha subunit of eukaryotic translation initiation factor 2 (eIF2 alpha) phosphorylation by the human papillomavirus type 18 E6 oncoprotein: implications for eIF2 alpha-dependent gene expression and cell death. Mol. Cell Biol. **24**:3415-3429.

178. **Kebache, S., E. Cardin, D. T. Nguyen, E. Chevet, and L. Larose**. 2004. Nck-1 antagonizes the endoplasmic reticulum stress-induced inhibition of translation. J. Biol. Chem. **279**:9662-9671.

179. **Kharrat, A., M. J. Macias, T. J. Gibson, M. Nilges, and A. Pastore**. 1995. Structure of the dsRNA binding domain of E. coli RNase III. EMBO J. **14**:3572-3584.

180. **Kockeritz, L., B. Doble, S. Patel, and J. R. Woodgett**. 2006. Glycogen synthase kinase-3--an overview of an over-achieving protein kinase. Curr. Drug Targets. **7**:1377-1388.

181. **Kojima, E., A. Takeuchi, M. Haneda, A. Yagi, T. Hasegawa, K. Yamaki, K. Takeda, S. Akira, K. Shimokata, and K. Isobe**. 2003. The function of GADD34 is a recovery from a shutoff of protein synthesis induced by ER stress: elucidation by GADD34-deficient mice. FASEB J. **17**:1573-1575.

182. **Kondo, S., T. Murakami, K. Tatsumi, M. Ogata, S. Kanemoto, K. Otori, K. Iseki, A. Wanaka, and K. Imaizumi**. 2005. OASIS, a CREB/ATF-family member, modulates UPR signalling in astrocytes. Nat. Cell Biol. **7**:186-194.

183. **Kondo, S., A. Saito, S. I. Hino, T. Murakami, M. Ogata, S. Kanemoto, S. Nara, A. Yamashita, K. Yoshinaga, H. Hara, and K. Imaizumi**. 2006. BBF2H7, a novel transmembrane bZIP transcription factor, is a new type of ER stress transducer. Mol. Cell Biol.

184. **Koritzinsky, M., M. G. Magagnin, B. T. van den, R. Seigneuric, K. Savelkouls, J. Dostie, S. Pyronnet, R. J. Kaufman, S. A. Weppler, J. W. Voncken, P. Lambin, C. Koumenis, N. Sonenberg, and B. G. Wouters**. 2006. Gene expression during acute and prolonged hypoxia is regulated by distinct mechanisms of translational control. EMBO J. **25**:1114-1125.

185. **Koumenis, C., R. Alarcon, E. Hammond, P. Sutphin, W. Hoffman, M. Murphy, J. Derr, Y. Taya, S. W. Lowe, M. Kastan, and A. Giaccia**. 2001. Regulation of p53 by hypoxia: dissociation of transcriptional repression and apoptosis from p53-dependent transactivation. Mol. Cell Biol. **21**:1297-1310.

186. **Koumenis, C., C. Naczki, M. Koritzinsky, S. Rastani, A. Diehl, N. Sonenberg, A. Koromilas, and B. G. Wouters**. 2002. Regulation of protein synthesis by hypoxia via activation of the endoplasmic reticulum kinase PERK and phosphorylation of the translation initiation factor eIF2alpha. Mol. Cell Biol **22**:7405-7416.

187. **Kubbutat, M. H., R. L. Ludwig, A. J. Levine, and K. H. Vousden**. 1999. Analysis of the degradation function of Mdm2. Cell Growth Differ. **10**:87-92.

188. **Kuhen, K. L., X. Shen, E. R. Carlisle, A. L. Richardson, H. U. Weier, H. Tanaka, and C. E. Samuel**. 1996. Structural organization of the human gene (PKR) encoding an interferon-inducible RNA-dependent protein kinase (PKR) and differences from its mouse homolog. Genomics **36**:197-201.

189. **Kumar, A., J. Haque, J. Lacoste, J. Hiscott, and B. R. Williams**. 1994. Double-stranded RNA-dependent protein kinase activates transcription factor NF-kappa B by phosphorylating I kappa B. Proc. Natl. Acad. Sci. U. S. A **91**:6288-6292.

190. **Kumar, A., Y. L. Yang, V. Flati, S. Der, S. Kadereit, A. Deb, J. Haque, L. Reis, C. Weissmann, and B. R. Williams**. 1997. Deficient cytokine signaling in mouse embryo fibroblasts with a targeted deletion in the PKR gene: role of IRF-1 and NF-kappaB. EMBO Journal **16**:406-416.

191. **Kumar, K. U., S. P. Srivastava, and R. J. Kaufman**. 1999. Double-stranded RNA-activated protein kinase (PKR) is negatively regulated by 60S ribosomal subunit protein L18. Molecular & Cellular Biology **19**:1116-1125.

192. **Laine, A. and Z. Ronai**. 2006. Regulation of p53 localization and transcription by the HECT domain E3 ligase WWP1. Oncogene.

193. **Lane, D. P.** 1992. Cancer. p53, guardian of the genome. Nature **358**:15-16.

194. **Lane, D. P.** 1994. p53 and human cancers. Br. Med. Bull. **50**:582-599.

195. **Le Beau, M. M., C. A. Westbrook, M. O. Diaz, J. D. Rowley, and M. Oren**. 1985. Translocation of the p53 gene in t(15;17) in acute promyelocytic leukaemia. Nature **316**:826-828.

196. **Le, C. L., L. K. Linares, C. Paul, E. Julien, M. Lacroix, E. Hatchi, R. Triboulet, G. Bossis, A. Shmueli, M. S. Rodriguez, O. Coux, and C. Sardet**. 2006. E4F1 is an atypical ubiquitin ligase that modulates p53 effector functions independently of degradation. Cell **127**:775-788.

197. **Leaman, D. W., A. Salvekar, R. Patel, G. C. Sen, and G. R. Stark**. 1998. A mutant cell line defective in response to double-stranded RNA and in regulating basal expression of interferon-stimulated genes. Proc. Natl. Acad. Sci. U. S. A **95**:9442-9447.

198. **Lee, S. B., R. Bablanian, and M. Esteban**. 1996. Regulated expression of the interferon-induced protein kinase p68 (PKR) by vaccinia virus recombinants inhibits the replication of vesicular stomatitis virus but not that of poliovirus. J. Interferon Cytokine Res. **16**:1073-1078.

199. **Lee, S. B., Z. Melkova, W. Yan, B. R. Williams, A. G. Hovanessian, and M. Esteban**. 1993. The interferon-induced double-stranded RNA-activated human p68 protein kinase potently inhibits protein synthesis in cultured cells. Virology **192**:380-385.

200. **Leng, R. P., Y. Lin, W. Ma, H. Wu, B. Lemmers, S. Chung, J. M. Parant, G. Lozano, R. Hakem, and S. Benchimol**. 2003. Pirh2, a p53-induced ubiquitin-protein ligase, promotes p53 degradation. Cell **112**:779-791.

201. **Levine, A. J.** 1997. p53, the cellular gatekeeper for growth and division. Cell **88**:323-331.

202. **Li, J., B. Lee, and A. S. Lee**. 2006. Endoplasmic reticulum stress-induced apoptosis: multiple pathways and activation of p53-up-regulated modulator of apoptosis (PUMA) and NOXA by p53. J. Biol. Chem. **281**:7260-7270.

203. **Li, M., C. L. Brooks, N. Kon, and W. Gu**. 2004. A dynamic role of HAUSP in the p53-Mdm2 pathway. Mol. Cell **13**:879-886.

204. **Li, M., C. L. Brooks, F. Wu-Baer, D. Chen, R. Baer, and W. Gu**. 2003. Mono- versus polyubiquitination: differential control of p53 fate by Mdm2. Science **302**:1972-1975.

205. **Li, M., D. Chen, A. Shiloh, J. Luo, A. Y. Nikolaev, J. Qin, and W. Gu**. 2002. Deubiquitination of p53 by HAUSP is an important pathway for p53 stabilization. Nature **416**:648-653.

206. **Li, S. and A. E. Koromilas**. 2001. Dominant negative function by an alternatively spliced form of the interferon-inducible protein kinase PKR. J. Biol. Chem. **276**:13881-13890.

207. **Liang, S. H. and M. F. Clarke**. 2001. Regulation of p53 localization. Eur. J. Biochem. **268**:2779-2783.

208. **Lim, Y. P., T. T. Lim, Y. L. Chan, A. C. Song, B. H. Yeo, B. Vojtesek, D. Coomber, G. Rajagopal, and D. Lane**. 2006. The p53 knowledgebase: an integrated information resource for p53 research. Oncogene.

209. **Linke, S. P., K. C. Clarkin, L. A. Di, A. Tsou, and G. M. Wahl**. 1996. A reversible, p53-dependent G0/G1 cell cycle arrest induced by ribonucleotide depletion in the absence of detectable DNA damage. Genes Dev. **10**:934-947.

210. **Linzer, D. I. and A. J. Levine**. 1979. Characterization of a 54K dalton cellular SV40 tumor antigen present in SV40-transformed cells and uninfected embryonal carcinoma cells. Cell **17**:43-52.

211. **Linzer, D. I., W. Maltzman, and A. J. Levine**. 1979. The SV40 A gene product is required for the production of a 54,000 MW cellular tumor antigen. Virology **98**:308-318.

212. **Liu, G., T. Xia, and X. Chen**. 2003. The activation domains, the proline-rich domain, and the C-terminal basic domain in p53 are necessary for acetylation of histones on the proximal p21 promoter and interaction with p300/CREB-binding protein. J. Biol. Chem. **278**:17557-17565.

213. **Lozano, G. and A. J. Levine**. 1991. Tissue-specific expression of p53 in transgenic mice is regulated by intron sequences. Mol. Carcinog. **4**:3-9.

214. **Lu, L., A. P. Han, and J. J. Chen**. 2001. Translation initiation control by heme-regulated eukaryotic initiation factor 2alpha kinase in erythroid cells under cytoplasmic stresses. Mol Cell Biol **21**:7971-7980.

215. **Lu, P. D., H. P. Harding, and D. Ron**. 2004. Translation reinitiation at alternative open reading frames regulates gene expression in an integrated stress response. J. Cell Biol. **167**:27-33.

216. **Luo, J., M. Li, Y. Tang, M. Laszkowska, R. G. Roeder, and W. Gu**. 2004. Acetylation of p53 augments its site-specific DNA binding both in vitro and in vivo. Proc. Natl. Acad. Sci. U. S. A **101**:2259-2264.

217. **Luo, J., A. Y. Nikolaev, S. Imai, D. Chen, F. Su, A. Shiloh, L. Guarente, and W. Gu**. 2001. Negative control of p53 by Sir2alpha promotes cell survival under stress. Cell **107**:137-148.

218. **Luo, J., F. Su, D. Chen, A. Shiloh, and W. Gu**. 2000. Deacetylation of p53 modulates its effect on cell growth and apoptosis. Nature **408**:377-381.

219. **Ma, Y. and L. M. Hendershot**. 2003. Delineation of a negative feedback regulatory loop that controls protein translation during endoplasmic reticulum stress. J Biol Chem. **278**:34864-34873.

220. **Ma, Y. and L. M. Hendershot**. 2004. The role of the unfolded protein response in tumour development: friend or foe? Nat. Rev. Cancer **4**:966-977.

221. **Maki, C. G.** 1999. Oligomerization is required for p53 to be efficiently ubiquitinated by MDM2. J. Biol. Chem. **274**:16531-16535.

222. **Maki, C. G., J. M. Huibregtse, and P. M. Howley**. 1996. In vivo ubiquitination and proteasome-mediated degradation of p53. Cancer Res. **56**:2649-2654.

223. **Maltzman, W. and L. Czyzyk**. 1984. UV irradiation stimulates levels of p53 cellular tumor antigen in nontransformed mouse cells. Mol. Cell Biol. **4**:1689-1694.

224. **Mannen, K., M. Ohuchi, and K. Mifune**. 1982. pH-dependent hemolysis and cell fusion of rhabdoviruses. Microbiol. Immunol. **26**:1035-1043.

225. **Maran, A., R. K. Maitra, A. Kumar, B. Dong, W. Xiao, G. Li, B. R. Williams, P. F. Torrence, and R. H. Silverman**. 1994. Blockage of NF-kappa B signaling by selective ablation of an mRNA target by 2-5A antisense chimeras. Science **265**:789-792.

226. **Marques, J. T., D. Rebouillat, C. V. Ramana, J. Murakami, J. E. Hill, A. Gudkov, R. H. Silverman, G. R. Stark, and B. R. Williams**. 2005. Down-regulation of p53 by double-stranded RNA modulates the antiviral response. J. Virol. **79**:11105-11114.

227. **Matoba, S., J. G. Kang, W. D. Patino, A. Wragg, M. Boehm, O. Gavrilova, P. J. Hurley, F. Bunz, and P. M. Hwang**. 2006. p53 regulates mitochondrial respiration. Science **312**:1650-1653.

228. **Meraz, M. A., J. M. White, K. C. Sheehan, E. A. Bach, S. J. Rodig, A. S. Dighe, D. H. Kaplan, J. K. Riley, A. C. Greenlund, D. Campbell, K. Carver-Moore, R. N. DuBois, R. Clark, M. Aguet, and R. D. Schreiber**. 1996. Targeted disruption of the Stat1 gene in mice reveals unexpected physiologic specificity in the JAK-STAT signaling pathway. Cell **84**:431-442.

229. **Merrick, W. C. and J. W. Hershey**. 2000. The pathway and mechanism of eukaryotic protein synthesis, p. 31-70. *In* N. Sonenberg, J. W. B. Hershey, and M. B. Mathews (ed.), Translational Control of Gene Expression. Cold Spring Harbor Laboratory Press, Cold Spring Harbor, New York.

230. **Meurs, E., K. Chong, J. Galabru, N. S. Thomas, I. M. Kerr, B. R. Williams, and A. G. Hovanessian**. 1990. Molecular cloning and characterization of the human double-stranded RNA-activated protein kinase induced by interferon. Cell **62**:379-390.

231. **Meurs, E. F., Y. Watanabe, S. Kadereit, G. N. Barber, M. G. Katze, K. Chong, B. R. Williams, and A. G. Hovanessian**. 1992. Constitutive expression of human double-stranded RNA-activated p68 kinase in murine cells mediates phosphorylation of eukaryotic initiation factor 2 and partial resistance to encephalomyocarditis virus growth. J. Virol. **66**:5805-5814.

232. **Moll, U. M. and O. Petrenko**. 2003. The MDM2-p53 interaction. Mol. Cancer Res. **1**:1001-1008.

233. **Moll, U. M., S. Wolff, D. Speidel, and W. Deppert**. 2005. Transcription-independent pro-apoptotic functions of p53. Curr. Opin. Cell Biol. **17**:631-636.

234. **Morishima, N., K. Nakanishi, H. Takenouchi, T. Shibata, and Y. Yasuhiko**. 2002. An endoplasmic reticulum stress-specific caspase cascade in apoptosis. Cytochrome c-independent activation of caspase-9 by caspase-12. J. Biol. Chem. **277**:34287-34294.

235. **Mosner, J., T. Mummenbrauer, C. Bauer, G. Sczakiel, F. Grosse, and W. Deppert**. 1995. Negative feedback regulation of wild-type p53 biosynthesis. EMBO J. **14**:4442-4449.

236. **Moya, A., S. F. Elena, A. Bracho, R. Miralles, and E. Barrio**. 2000. The evolution of RNA viruses: A population genetics view. Proc. Natl. Acad. Sci. U. S. A **97**:6967-6973.

237. **Munger, K., M. Scheffner, J. M. Huibregtse, and P. M. Howley**. 1992. Interactions of HPV E6 and E7 oncoproteins with tumour suppressor gene products. Cancer Surv. **12**:197-217.

238. **Murphy, M., J. Ahn, K. K. Walker, W. H. Hoffman, R. M. Evans, A. J. Levine, and D. L. George**. 1999. Transcriptional repression by wild-type p53 utilizes histone deacetylases, mediated by interaction with mSin3a. Genes Dev. **13**:2490-2501.

239. **Nakagawa, T., H. Zhu, N. Morishima, E. Li, J. Xu, B. A. Yankner, and J. Yuan**. 2000. Caspase-12 mediates endoplasmic-reticulum-specific apoptosis and cytotoxicity by amyloid-beta. Nature **403**:98-103.

240. **Nanduri, S., F. Rahman, B. R. Williams, and J. Qin**. 2000. A dynamically tuned double-stranded RNA binding mechanism for the activation of antiviral kinase PKR. EMBO J. **19**:5567-5574.

241. **Nigro, J. M., S. J. Baker, A. C. Preisinger, J. M. Jessup, R. Hostetter, K. Cleary, S. H. Bigner, N. Davidson, S. Baylin, P. Devilee, and .** 1989. Mutations in the p53 gene occur in diverse human tumour types. Nature **342**:705-708.

242. **Nikolaev, A. Y., M. Li, N. Puskas, J. Qin, and W. Gu**. 2003. Parc: a cytoplasmic anchor for p53. Cell **112**:29-40.

243. **Norris, P. S. and M. Haas**. 1997. A fluorescent p53GFP fusion protein facilitates its detection in mammalian cells while retaining the properties of wild-type p53. Oncogene **15**:2241-2247.

244. **Novoa, I., H. Zeng, H. P. Harding, and D. Ron**. 2001. Feedback inhibition of the unfolded protein response by GADD34-mediated dephosphorylation of eIF2alpha. J. Cell Biol. **153**:1011-1022.

245. **Novoa, I., Y. Zhang, H. Zeng, R. Jungreis, H. P. Harding, and D. Ron**. 2003. Stress-induced gene expression requires programmed recovery from translational repression. EMBO J **22**:1180-1187.

246. **Offer, H., N. Erez, I. Zurer, X. Tang, M. Milyavsky, N. Goldfinger, and V. Rotter**. 2002. The onset of p53-dependent DNA repair or apoptosis is determined by the level of accumulated damaged DNA. Carcinogenesis **23**:1025-1032.

247. **Ohnishi, T., X. Wang, K. Ohnishi, H. Matsumoto, and A. Takahashi**. 1996. p53-dependent induction of WAF1 by heat treatment in human glioblastoma cells. J. Biol. Chem. **271**:14510-14513.

248. **Onuki, R., Y. Bando, E. Suyama, T. Katayama, H. Kawasaki, T. Baba, M. Tohyama, and K. Taira**. 2004. An RNA-dependent protein kinase is involved in tunicamycin-induced apoptosis and Alzheimer's disease. EMBO J. **23**:959-968.

249. **Oren, M., B. Bienz, D. Givol, G. Rechavi, and R. Zakut**. 1983. Analysis of recombinant DNA clones specific for the murine p53 cellular tumor antigen. EMBO J. **2**:1633-1639.

250. **Oren, M. and A. J. Levine**. 1983. Molecular cloning of a cDNA specific for the murine p53 cellular tumor antigen. Proc. Natl. Acad. Sci. U. S. A **80**:56-59.

251. **Oren, M., W. Maltzman, and A. J. Levine**. 1981. Post-translational regulation of the 54K cellular tumor antigen in normal and transformed cells. Mol. Cell Biol. **1**:101-110.

252. **Oyadomari, S., E. Araki, and M. Mori**. 2002. Endoplasmic reticulum stress-mediated apoptosis in pancreatic beta-cells. Apoptosis. **7**:335-345.

253. **Oyadomari, S., C. Yun, E. A. Fisher, N. Kreglinger, G. Kreibich, M. Oyadomari, H. P. Harding, A. G. Goodman, H. Harant, J. L. Garrison, J. Taunton, M. G. Katze, and D. Ron**. 2006. Cotranslocational degradation protects the stressed endoplasmic reticulum from protein overload. Cell **126**:727-739.

254. **Pan, Y., P. R. Oprysko, A. M. Asham, C. J. Koch, and M. C. Simon**. 2004. p53 cannot be induced by hypoxia alone but responds to the hypoxic microenvironment. Oncogene **23**:4975-4983.

255. **Parada, L. F., H. Land, R. A. Weinberg, D. Wolf, and V. Rotter**. 1984. Cooperation between gene encoding p53 tumour antigen and ras in cellular transformation. Nature **312**:649-651.

256. **Pavio, N., P. R. Romano, T. M. Graczyk, S. M. Feinstone, and D. R. Taylor**. 2003. Protein synthesis and endoplasmic reticulum stress can be modulated by the hepatitis C virus envelope protein E2 through the eukaryotic initiation factor 2alpha kinase PERK. J. Virol. **77**:3578-3585.

257. **Piu, F., A. Aronheim, S. Katz, and M. Karin**. 2001. AP-1 repressor protein JDP-2: inhibition of UV-mediated apoptosis through p53 down-regulation. Mol. Cell Biol. **21**:3012-3024.

258. **Piwnica-Worms, H. and J. D. Keene**. 1983. Sequential synthesis of small capped RNA transcripts in vitro by vesicular stomatitis virus. Virology **125**:206-218.

259. **Pluquet, O. and P. Hainaut**. 2001. Genotoxic and non-genotoxic pathways of p53 induction. Cancer Lett. **174**:1-15.

260. **Pluquet, O., L. K. Qu, D. Baltzis, and A. E. Koromilas**. 2005. Endoplasmic reticulum stress accelerates p53 degradation by the cooperative actions of Hdm2 and glycogen synthase kinase 3beta. Mol. Cell Biol. **25**:9392-9405.

261. **Polyak, S. J., N. Tang, M. Wambach, G. N. Barber, and M. G. Katze**. 1996. The P58 cellular inhibitor complexes with the interferon-induced, double-stranded RNA-dependent protein kinase, PKR, to regulate its autophosphorylation and activity. J. Biol. Chem. **271**:1702-1707.

262. **Prostko, C. R., J. N. Dholakia, M. A. Brostrom, and C. O. Brostrom**. 1995. Activation of the double-stranded RNA-regulated protein kinase by depletion of endoplasmic reticular calcium stores. J Biol Chem. **270**:6211-6215.

263. **Qu, L., S. Huang, D. Baltzis, A. M. Rivas-Estilla, O. Pluquet, M. Hatzoglou, C. Koumenis, Y. Taya, A. Yoshimura, and A. E. Koromilas**. 2004. Endoplasmic reticulum stress induces p53 cytoplasmic localization and prevents p53-dependent apoptosis by a pathway involving glycogen synthase kinase-3beta. Genes Dev.

264. **Rafie-Kolpin, M., P. J. Chefalo, Z. Hussain, J. Hahn, S. Uma, R. L. Matts, and J. J. Chen**. 2000. Two heme-binding domains of heme-regulated eukaryotic initiation factor-2alpha kinase. N terminus and kinase insertion. J Biol Chem. **275**:5171-5178.

265. **Rajendra, R., D. Malegaonkar, P. Pungaliya, H. Marshall, Z. Rasheed, J. Brownell, L. F. Liu, S. Lutzker, A. Saleem, and E. H. Rubin**. 2004. Topors functions as an E3 ubiquitin ligase with specific E2 enzymes and ubiquitinates p53. J. Biol. Chem. **279**:36440-36444.

266. **Ramana, C. V., N. Grammatikakis, M. Chernov, H. Nguyen, K. C. Goh, B. R. Williams, and G. R. Stark**. 2000. Regulation of c-myc expression by IFN-gamma through Stat1-dependent and -independent pathways. EMBO J. **19**:263-272.

267. **Rao, R. V., E. Hermel, S. Castro-Obregon, G. del Rio, L. M. Ellerby, H. M. Ellerby, and D. E. Bredesen**. 2001. Coupling endoplasmic reticulum stress to the cell death program. Mechanism of caspase activation. J. Biol. Chem. **276**:33869-33874.

268. **Ray, P. S., R. Grover, and S. Das**. 2006. Two internal ribosome entry sites mediate the translation of p53 isoforms. EMBO Rep. **7**:404-410.

269. **Roff, M., J. Thompson, M. S. Rodriguez, J. M. Jacque, F. Baleux, F. renzana-Seisdedos, and R. T. Hay**. 1996. Role of IkappaBalpha ubiquitination in signal-induced activation of NFkappaB in vivo. J. Biol. Chem. **271**:7844-7850.

270. **Rogel, A., M. Popliker, C. G. Webb, and M. Oren**. 1985. p53 cellular tumor antigen: analysis of mRNA levels in normal adult tissues, embryos, and tumors. Mol. Cell Biol. **5**:2851-2855.

271. **Romano, P. R., M. T. Garcia-Barrio, X. Zhang, Q. Wang, D. R. Taylor, F. Zhang, C. Herring, M. B. Mathews, J. Qin, and A. G. Hinnebusch**. 1998. Autophosphorylation in the activation loop is required for full kinase activity in vivo of human and yeast eukaryotic initiation factor 2alpha kinases PKR and GCN2. Mol. Cell Biol. **18**:2282-2297.

272. **Romano, P. R., S. R. Green, G. N. Barber, M. B. Mathews, and A. G. Hinnebusch**. 1995. Structural requirements for double-stranded RNA binding, dimerization, and activation of the human eIF-2 alpha kinase DAI in Saccharomyces cerevisiae. Mol. Cell Biol. **15**:365-378.

273. **Ron, D. and H. P. Harding**. 2000. PERK and translational control by stress in the endoplasmic reticulum, p. 547-560. *In* N. Sonenberg, J. W. B. Hershey, and M. B. Mathews (ed.), Translational

Control of Gene Expression. Cold Spring Harbor Laboratory Press, Cold Spring Harbor, New York.

274. **Rose, J. K.** 1977. Nucleotide sequences of ribosome recgonition sites in messenger RNAs of vesicular stomatitis virus. Proc. Natl. Acad. Sci. U. S. A **74**:3672-3676.

275. **Rose, J. K.** 1978. Complete sequences of the ribosome recognition sites in vesicular stomatitis virus mRNAs: recognition by the 40S and 80S complexes. Cell **14**:345-353.

276. **Rose, J. K. and D. Knipe**. 1975. Nucleotide sequence complexities, molecular weights, and poly(A) content of the vesicular stomatitis virus mRNA species. J. Virol. **15**:994-1003.

277. **Rose, J. K. and M. A. Whitt**. 2001. *Rhabdoviridae*: The Viruses and their Replication. Lippincott Williams and Wilkins, New York.

278. **Roth, W., P. Kermer, M. Krajewska, K. Welsh, S. Davis, S. Krajewski, and J. C. Reed**. 2003. Bifunctional apoptosis inhibitor (BAR) protects neurons from diverse cell death pathways. Cell Death. Differ. **10**:1178-1187.

279. **Roulston, A., R. C. Marcellus, and P. E. Branton**. 1999. Viruses and apoptosis. Annu. Rev. Microbiol. **53**:577-628.

280. **Rutkowski, D. T. and R. J. Kaufman**. 2004. A trip to the ER: coping with stress. Trends Cell Biol. **14**:20-28.

281. **Saito, S., H. Yamaguchi, Y. Higashimoto, C. Chao, Y. Xu, A. J. Fornace, Jr., E. Appella, and C. W. Anderson**. 2003. Phosphorylation site interdependence of human p53 post-translational modifications in response to stress. J. Biol. Chem. **278**:37536-37544.

282. **Sakaguchi, K., J. E. Herrera, S. Saito, T. Miki, M. Bustin, A. Vassilev, C. W. Anderson, and E. Appella**. 1998. DNA damage activates p53 through a phosphorylation-acetylation cascade. Genes Dev. **12**:2831-2841.

283. **Sambrook, J., E. F. Fritsch, and T. Maniatis**. 1989. Molecular Cloning: A Laboratory Manual. Cold Spring Harbor Laboratory Press, Plainview.

284. **Samuel, C. E., K. L. Kuhen, C. X. George, L. G. Ortega, R. Rende-Fournier, and H. Tanaka**. 1997. The PKR protein kinase--an interferon-inducible regulator of cell growth and differentiation. Int. J. Hematol. **65**:227-237.

285. **Sarnow, P., Y. S. Ho, J. Williams, and A. J. Levine**. 1982. Adenovirus E1b-58kd tumor antigen and SV40 large tumor antigen are physically associated with the same 54 kd cellular protein in transformed cells. Cell **28**:387-394.

286. **Scheuner, D., B. Song, E. McEwen, C. Liu, R. Laybutt, P. Gillespie, T. Saunders, S. Bonner-Weir, and R. J. Kaufman**. 2001. Translational control is required for the unfolded protein response and in vivo glucose homeostasis. Mol. Cell **7**:1165-1176.

287. **Schlegel, R., T. S. Tralka, M. C. Willingham, and I. Pastan**. 1983. Inhibition of VSV binding and infectivity by phosphatidylserine: is phosphatidylserine a VSV-binding site? Cell **32**:639-646.

288. **Schmaltz, C., P. H. Hardenbergh, A. Wells, and D. E. Fisher**. 1998. Regulation of proliferation-survival decisions during tumor cell hypoxia. Mol. Cell Biol. **18**:2845-2854.

289. **Schmidt, D. and S. Muller**. 2002. Members of the PIAS family act as SUMO ligases for c-Jun and p53 and repress p53 activity. Proc. Natl. Acad. Sci. U. S. A **99**:2872-2877.

290. **Schmidt, D. and S. Muller**. 2003. PIAS/SUMO: new partners in transcriptional regulation. Cell Mol. Life Sci. **60**:2561-2574.

291. **Schneiderhan, N., A. Budde, Y. Zhang, and B. Brune**. 2003. Nitric oxide induces phosphorylation of p53 and impairs nuclear export. Oncogene **22**:2857-2868.

292. **Schreiber, M., A. Kolbus, F. Piu, A. Szabowski, U. Mohle-Steinlein, J. Tian, M. Karin, P. Angel, and E. F. Wagner**. 1999. Control of cell cycle progression by c-Jun is p53 dependent. Genes Dev. **13**:607-619.

293. **Serrano, M., A. W. Lin, M. E. McCurrach, D. Beach, and S. W. Lowe**. 1997. Oncogenic ras provokes premature cell senescence associated with accumulation of p53 and p16INK4a. Cell **88**:593-602.

294. **Sharma, S., B. R. TenOever, N. Grandvaux, G. P. Zhou, R. Lin, and J. Hiscott**. 2003. Triggering the interferon antiviral response through an IKK-related pathway. Science **300**:1148-1151.

295. **Shaulian, E., M. Schreiber, F. Piu, M. Beeche, E. F. Wagner, and M. Karin**. 2000. The mammalian UV response: c-Jun induction is required for exit from p53-imposed growth arrest. Cell **103**:897-907.

296. **Shaulsky, G., N. Goldfinger, M. S. Tosky, A. J. Levine, and V. Rotter**. 1991. Nuclear localization is essential for the activity of p53 protein. Oncogene **6**:2055-2065.

297. **Shen, J., X. Chen, L. Hendershot, and R. Prywes**. 2002. ER stress regulation of ATF6 localization by dissociation of BiP/GRP78 binding and unmasking of Golgi localization signals. Dev. Cell **3**:99-111.

298. **Shi, Y., J. An, J. Liang, S. E. Hayes, G. E. Sandusky, L. E. Stramm, and N. N. Yang**. 1999. Characterization of a mutant pancreatic eIF-2alpha kinase, PEK, and co-localization with somatostatin in islet delta cells. J. Biol. Chem. **274**:5723-5730.

299. **Shi, Y., K. M. Vattem, R. Sood, J. An, J. Liang, L. Stramm, and R. C. Wek**. 1998. Identification and characterization of pancreatic eukaryotic initiation factor 2 alpha-subunit kinase, PEK, involved in translational control. Mol. Cell Biol. **18**:7499-7509.

300. **Shieh, S. Y., J. Ahn, K. Tamai, Y. Taya, and C. Prives**. 2000. The human homologs of checkpoint kinases Chk1 and Cds1 (Chk2) phosphorylate p53 at multiple DNA damage-inducible sites. Genes Dev. **14**:289-300.

301. **Shieh, S. Y., Y. Taya, and C. Prives**. 1999. DNA damage-inducible phosphorylation of p53 at N-terminal sites including a novel site, Ser20, requires tetramerization. EMBO J. **18**:1815-1823.

302. **Smith, G. E. and M. D. Summers**. 1980. The bidirectional transfer of DNA and RNA to nitrocellulose or diazobenzyloxymethyl-paper. Anal. Biochem. **109**:123-129.

303. **Smith, M. L., I. T. Chen, Q. Zhan, I. Bae, C. Y. Chen, T. M. Gilmer, M. B. Kastan, P. M. O'Connor, and A. J. Fornace, Jr.** 1994. Interaction of the p53-regulated protein Gadd45 with proliferating cell nuclear antigen. Science **266**:1376-1380.

304. **Smith, M. L. and Y. R. Seo**. 2002. p53 regulation of DNA excision repair pathways. Mutagenesis **17**:149-156.

305. **Song, L., P. De Sarno, and R. S. Jope**. 2002. Central role of glycogen synthase kinase-3beta in endoplasmic reticulum stress-induced caspase-3 activation. J. Biol. Chem. **277**:44701-44708.

306. **Sood, R., A. C. Porter, K. Ma, L. A. Quilliam, and R. C. Wek**. 2000. Pancreatic eukaryotic initiation factor-2alpha kinase (PEK) homologues in humans, Drosophila melanogaster and Caenorhabditis elegans that mediate translational control in response to endoplasmic reticulum stress. Biochem. J **346 Pt 2**:281-293.

307. **Soussi, T., F. C. Caron de, and P. May**. 1990. Structural aspects of the p53 protein in relation to gene evolution. Oncogene **5**:945-952.

308. **Squire, J., E. F. Meurs, K. L. Chong, N. A. McMillan, A. G. Hovanessian, and B. R. Williams**. 1993. Localization of the human interferon-induced, ds-RNA activated p68 kinase gene (PRKR) to chromosome 2p21-p22. Genomics **16**:768-770.

309. **Srivastava, S. P., K. U. Kumar, and R. J. Kaufman**. 1998. Phosphorylation of eukaryotic translation initiation factor 2 mediates apoptosis in response to activation of the double-stranded RNA-dependent protein kinase. J Biol Chem. **273**:2416-2423.

310. **St, C. S. and J. J. Manfredi**. 2006. The dual specificity phosphatase Cdc25C is a direct target for transcriptional repression by the tumor suppressor p53. Cell Cycle **5**:709-713.

311. **Stark, G. R., I. M. Kerr, B. R. Williams, R. H. Silverman, and R. D. Schreiber**. 1998. How cells respond to interferons. Annual Review of Biochemistry **67**:227-264.

312. **Stavridi, E. S., N. H. Chehab, A. Malikzay, and T. D. Halazonetis**. 2001. Substitutions that compromise the ionizing radiation-induced association of p53 with 14-3-3 proteins also compromise the ability of p53 to induce cell cycle arrest. Cancer Res. **61**:7030-7033.

313. **Stojdl, D. F., N. Abraham, S. Knowles, R. Marius, A. Brasey, B. D. Lichty, E. G. Brown, N. Sonenberg, and J. C. Bell**. 2000. The murine double-stranded RNA-dependent protein kinase PKR is required for resistance to vesicular stomatitis virus. J. Virol. **74**:9580-9585.

314. **Stommel, J. M., N. D. Marchenko, G. S. Jimenez, U. M. Moll, T. J. Hope, and G. M. Wahl**. 1999. A leucine-rich nuclear export signal in the p53 tetramerization domain: regulation of subcellular localization and p53 activity by NES masking. EMBO J. **18**:1660-1672.

315. **Stuart, E. T., R. Haffner, M. Oren, and P. Gruss**. 1995. Loss of p53 function through PAX-mediated transcriptional repression. EMBO J. **14**:5638-5645.

316. **Su, Q., S. Wang, D. Baltzis, L. K. Qu, A. H. Wong, and A. E. Koromilas**. 2006. Tyrosine phosphorylation acts as a molecular switch to full-scale activation of the eIF2alpha RNA-dependent protein kinase. Proc. Natl. Acad. Sci. U. S. A **103**:63-68.

317. **Sudhakar, A., A. Ramachandran, S. Ghosh, S. E. Hasnain, R. J. Kaufman, and K. V. Ramaiah**. 2000. Phosphorylation of serine 51 in initiation factor 2 alpha (eIF2 alpha) promotes complex formation between eIF2 alpha(P) and eIF2B and causes inhibition in the guanine nucleotide exchange activity of eIF2B. Biochemistry **39**:12929-12938.

318. **Sun, Y.** 2006. p53 and its downstream proteins as molecular targets of cancer. Mol. Carcinog. **45**:409-415.

319. **Takagi, M., M. J. Absalon, K. G. McLure, and M. B. Kastan**. 2005. Regulation of p53 translation and induction after DNA damage by ribosomal protein L26 and nucleolin. Cell **123**:49-63.

320. **Takaoka, A., S. Hayakawa, H. Yanai, D. Stoiber, H. Negishi, H. Kikuchi, S. Sasaki, K. Imai, T. Shibue, K. Honda, and T. Taniguchi**. 2003. Integration of interferon-alpha/beta signalling to p53 responses in tumour suppression and antiviral defence. Nature **424**:516-523.

321. **Tanaka, H. and C. E. Samuel**. 1994. Mechanism of interferon action: structure of the mouse PKR gene encoding the interferon-inducible RNA-dependent protein kinase. Proc. Natl. Acad. Sci. U. S. A **91**:7995-7999.

322. **Taylor, D. R., S. B. Lee, P. R. Romano, D. R. Marshak, A. G. Hinnebusch, M. Esteban, and M. B. Mathews**. 1996. Autophosphorylation sites participate in the activation of the double-stranded-RNA-activated protein kinase PKR. Mol. Cell Biol. **16**:6295-6302.

323. **Taylor, S. S., N. M. Haste, and G. Ghosh**. 2005. PKR and eIF2alpha: integration of kinase dimerization, activation, and substrate docking. Cell **122**:823-825.

324. **Terui, T., K. Murakami, R. Takimoto, M. Takahashi, K. Takada, T. Murakami, S. Minami, T. Matsunaga, T. Takayama, J. Kato, and Y. Niitsu**. 2003. Induction of PIG3 and NOXA through acetylation of p53 at 320 and 373 lysine residues as a mechanism for apoptotic cell death by histone deacetylase inhibitors. Cancer Res. **63**:8948-8954.

325. **Thomis, D. C., J. P. Doohan, and C. E. Samuel**. 1992. Mechanism of interferon action: cDNA structure, expression, and regulation of the interferon-induced, RNA-dependent P1/eIF-2 alpha protein kinase from human cells. Virology **188**:33-46.

326. **Thomis, D. C. and C. E. Samuel**. 1992. Mechanism of interferon action: autoregulation of RNA-dependent P1/eIF-2 alpha protein kinase (PKR) expression in transfected mammalian cells. Proc. Natl. Acad. Sci. U. S. A **89**:10837-10841.

327. **Thomis, D. C. and C. E. Samuel**. 1993. Mechanism of interferon action: evidence for intermolecular autophosphorylation and autoactivation of the interferon-induced, RNA-dependent protein kinase PKR. J. Virol. **67**:7695-7700.

328. **Tibbetts, R. S., K. M. Brumbaugh, J. M. Williams, J. N. Sarkaria, W. A. Cliby, S. Y. Shieh, Y. Taya, C. Prives, and R. T. Abraham**. 1999. A role for ATR in the DNA damage-induced phosphorylation of p53. Genes Dev. **13**:152-157.

329. **Tsai, B., Y. Ye, and T. A. Rapoport**. 2002. Retro-translocation of proteins from the endoplasmic reticulum into the cytosol. Nat. Rev. Mol. Cell Biol. **3**:246-255.

330. **Tuck, S. P. and L. Crawford**. 1989. Characterization of the human p53 gene promoter. Mol. Cell Biol. **9**:2163-2172.

331. **Tuck, S. P. and L. Crawford**. 1989. Overexpression of normal human p53 in established fibroblasts leads to their tumorigenic conversion. Oncogene Res. **4**:81-96.

332. **Turenne, G. A. and B. D. Price**. 2001. Glycogen synthase kinase3 beta phosphorylates serine 33 of p53 and activates p53's transcriptional activity. BMC. Cell Biol. **2**:12.

333. **Ung, T. L., C. Cao, J. Lu, K. Ozato, and T. E. Dever**. 2001. Heterologous dimerization domains functionally substitute for the double-stranded RNA binding domains of the kinase PKR. EMBO J. **20**:3728-3737.

334. **Van Huizen, R., J. L. Martindale, M. Gorospe, and N. J. Holbrook**. 2003. P58IPK, a novel endoplasmic reticulum stress-inducible protein and potential negative regulator of eIF2alpha signaling. J. Biol. Chem. **278**:15558-15564.

335. **van, H. R., J. L. Martindale, M. Gorospe, and N. J. Holbrook**. 2003. P58IPK, a novel endoplasmic reticulum stress-inducible protein and potential negative regulator of eIF2alpha signaling. J. Biol. Chem. **278**:15558-15564.

336. **VandePol, S. B., L. Lefrancois, and J. J. Holland**. 1986. Sequences of the major antibody binding epitopes of the Indiana serotype of vesicular stomatitis virus. Virology **148**:312-325.

337. **Vogelstein, B., D. Lane, and A. J. Levine**. 2000. Surfing the p53 network. Nature **408**:307-310.

338. **Wagner, R. R. and J. K. Rose**. 1996. Rhabdoviridae: The Viruses and Their Replication, p. 1121-1135. *In* B. N. Fields, D. M. Knipe, and P. M. Howley (ed.), Fields Virology, vol. 1. Lippincott-Raven Publishers, Philadelphia, PA.

339. **Wang, S., J. F. Raven, D. Baltzis, S. Kazemi, D. V. Brunet, M. Hatzoglou, M. L. Tremblay, and A. E. Koromilas**. 2006. The catalytic activity of the eukaryotic initiation factor-2alpha kinase PKR is required to negatively regulate Stat1 and Stat3 via activation of the T-cell protein-tyrosine phosphatase. J. Biol. Chem. **281**:9439-9449.

340. **Watcharasit, P., G. N. Bijur, J. W. Zmijewski, L. Song, A. Zmijewska, X. Chen, G. V. Johnson, and R. S. Jope**. 2002. Direct, activating interaction between glycogen synthase kinase-3beta and p53 after DNA damage. Proc. Natl. Acad. Sci. U. S. A **99**:7951-7955.

341. **Weger, S., E. Hammer, and R. Heilbronn**. 2005. Topors acts as a SUMO-1 E3 ligase for p53 in vitro and in vivo. FEBS Lett. **579**:5007-5012.

342. **Williams, B. R.** 1999. PKR; a sentinel kinase for cellular stress. Oncogene **18**:6112-6120.

343. **Willis, A. E.** 1999. Translational control of growth factor and proto-oncogene expression. Int. J. Biochem. Cell Biol. **31**:73-86.

344. **Wong, A. H., N. W. Tam, Y. L. Yang, A. R. Cuddihy, S. Li, S. Kirchhoff, H. Hauser, T. Decker, and A. E. Koromilas**. 1997. Physical association between STAT1 and the interferon-inducible protein kinase PKR and implications for interferon and double-stranded RNA signaling pathways. EMBO J. **16**:1291-1304.

345. **Woods, D. B. and K. H. Vousden**. 2001. Regulation of p53 function. Exp. Cell Res. **264**:56-66.

346. **Wu, S. and R. J. Kaufman**. 1996. Double-stranded (ds) RNA binding and not dimerization correlates with the activation of the dsRNA-dependent protein kinase (PKR). J. Biol. Chem. **271**:1756-1763.

347. **Wu, S. and R. J. Kaufman**. 1997. A model for the double-stranded RNA (dsRNA)-dependent dimerization and activation of the dsRNA-activated protein kinase PKR. J. Biol. Chem. **272**:1291-1296.

348. **Xirodimas, D. P., M. K. Saville, J. C. Bourdon, R. T. Hay, and D. P. Lane**. 2004. Mdm2-mediated NEDD8 conjugation of p53 inhibits its transcriptional activity. Cell **118**:83-97.

349. **Xu, Y.** 2003. Regulation of p53 responses by post-translational modifications. Cell Death. Differ. **10**:400-403.

350. **Yagishita, N., K. Ohneda, T. Amano, S. Yamasaki, A. Sugiura, K. Tsuchimochi, H. Shin, K. Kawahara, O. Ohneda, T. Ohta, S. Tanaka, M. Yamamoto, I. Maruyama, K. Nishioka, A. Fukamizu, and T. Nakajima**. 2005. Essential role of synoviolin in embryogenesis. J. Biol. Chem. **280**:7909-7916.

351. **Yaman, I., J. Fernandez, H. Liu, M. Caprara, A. A. Komar, A. E. Koromilas, L. Zhou, M. D. Snider, D. Scheuner, R. J. Kaufman, and M. Hatzoglou**. 2003. The zipper model of translational control: a small upstream ORF is the switch that controls structural remodeling of an mRNA leader. Cell **113**:519-531.

352. **Yamasaki, S., N. Yagishita, T. Sasaki, M. Nakazawa, Y. Kato, T. Yamadera, E. Bae, S. Toriyama, R. Ikeda, L. Zhang, K. Fujitani, E. Yoo, K. Tsuchimochi, T. Ohta, N. Araya, H. Fujita, S. Aratani, K. Eguchi, S. Komiya, I. Maruyama, N. Higashi, M. Sato, H. Senoo, T. Ochi, S. Yokoyama, T. Amano, J. Kim, S. Gay, K. Nishioka, A. Hukamizu, K. Tanaka, and T. Nakajima**. 2006. Cytoplasmic destruction of p53 by the endoplasmic reticulum-resident ubiquitin ligase 'Synoviolin'. EMBO J.

353. **Yan, W., C. L. Frank, M. J. Korth, B. L. Sopher, I. Novoa, D. Ron, and M. G. Katze**. 2002. Control of PERK eIF2alpha kinase activity by the endoplasmic reticulum stress-induced molecular chaperone P58IPK. Proc. Natl. Acad. Sci. U. S. A **99**:15920-15925.

354. **Yang, D. Q., M. J. Halaby, and Y. Zhang**. 2006. The identification of an internal ribosomal entry site in the 5'-untranslated region of p53 mRNA provides a novel mechanism for the regulation of its translation following DNA damage. Oncogene **25**:4613-4619.

355. **Yang, Y., C. C. Li, and A. M. Weissman**. 2004. Regulating the p53 system through ubiquitination. Oncogene **23**:2096-2106.

356. **Yang, Y. L., L. F. Reis, J. Pavlovic, A. Aguzzi, R. Schafer, A. Kumar, B. R. Williams, M. Aguet, and C. Weissmann**. 1995. Deficient signaling in mice devoid of double-stranded RNA-dependent protein kinase. EMBO J. **14**:6095-6106.

357. **Yao, Y. L. and W. M. Yang**. 2003. The metastasis-associated proteins 1 and 2 form distinct protein complexes with histone deacetylase activity. J. Biol. Chem. **278**:42560-42568.

358. **Yeung, M. C. and A. S. Lau**. 1998. Tumor suppressor p53 as a component of the tumor necrosis factor-induced, protein kinase PKR-mediated apoptotic pathway in human promonocytic U937 cells. J. Biol. Chem. **273**:25198-25202.

359. **Yoshida, H., K. Haze, H. Yanagi, T. Yura, and K. Mori**. 1998. Identification of the cis-acting endoplasmic reticulum stress response element responsible for transcriptional induction of mammalian glucose-regulated proteins. Involvement of basic leucine zipper transcription factors. J. Biol. Chem. **273**:33741-33749.

360. **Yoshida, H., T. Matsui, A. Yamamoto, T. Okada, and K. Mori**. 2001. XBP1 mRNA is induced by ATF6 and spliced by IRE1 in response to ER stress to produce a highly active transcription factor. Cell **107**:881-891.

361. **Yoshida, H., T. Okada, K. Haze, H. Yanagi, T. Yura, M. Negishi, and K. Mori**. 2000. ATF6 activated by proteolysis binds in the presence of NF-Y (CBF) directly to the cis-acting element responsible for the mammalian unfolded protein response. Mol. Cell Biol. **20**:6755-6767.

362. **Zacchi, P., M. Gostissa, T. Uchida, C. Salvagno, F. Avolio, S. Volinia, Z. Ronai, G. Blandino, C. Schneider, and G. Del Sal**. 2002. The prolyl isomerase Pin1 reveals a mechanism to control p53 functions after genotoxic insults. Nature **419**:853-857.

363. **Zagouras, P., A. Ruusala, and J. K. Rose**. 1991. Dissociation and reassociation of oligomeric viral glycoprotein subunits in the endoplasmic reticulum. J. Virol. **65**:1976-1984.

364. **Zamanian-Daryoush, M., T. H. Mogensen, J. A. DiDonato, and B. R. Williams**. 2000. NF-kappaB activation by double-stranded-RNA-activated protein kinase (PKR) is mediated through NF-kappaB-inducing kinase and IkappàB kinase. Molecular & Cellular Biology **20**:1278-1290.

365. **Zhang, F., R. B. Hamanka, E. Bobrovnikova-Marjon, J. Gordan, M. S. Dai, H. Lu, M. C. Simon, and J. A. Diehl**. 2006. Ribosomal stress couples the unfolded protein response to p53-dependent cell cycle arrest. J. Biol. Chem.

366. **Zhao, R., K. Gish, M. Murphy, Y. Yin, D. Notterman, W. H. Hoffman, E. Tom, D. H. Mack, and A. J. Levine**. 2000. Analysis of p53-regulated gene expression patterns using oligonucleotide arrays. Genes Dev. **14**:981-993.

367. **Zhu, S., P. R. Romano, and R. C. Wek**. 1997. Ribosome targeting of PKR is mediated by two double-stranded RNA-binding domains and facilitates in vivo phosphorylation of eukaryotic initiation factor-2. J. Biol. Chem. **272**:14434-14441.

368. **Zhu, S., A. Y. Sobolev, and R. C. Wek**. 1996. Histidyl-tRNA synthetase-related sequences in GCN2 protein kinase regulate in vitro phosphorylation of eIF-2. J Biol Chem. **271**:24989-24994.

369. **Zilfou, J. T., W. H. Hoffman, M. Sank, D. L. George, and M. Murphy**. 2001. The corepressor mSin3a interacts with the proline-rich domain of p53 and protects p53 from proteasome-mediated degradation. Mol. Cell Biol. **21**:3974-3985.

NUCLEAR SUBSTANCES AND RADIATION DEVICES LICENCE | PERMIS PORTANT SUR LES SUBSTANCES NUCLÉAIRES ET LES APPAREILS À RAYONNEMENT | Licence Number / Numéro de permis

I) TITULAIRE DE PERMIS

Conformément à l'article 24 (2) de la Loi sur la sûreté et la réglementation nucléaires, le présent permis est délivré à:

Hôpital Général Juif/
Jewish General Hospital
Sir Mortimer B. Davis
3755, chemin de la
Côte Ste-Catherine
Montréal (Québec)
H3T 1E2
Canada

Ci-après désigné sous le nom de «titulaire de permis»

II) PÉRIODE

Ce permis est valide du 1er août 2002 au 31 juillet 2007.

II) ACTIVITÉS AUTORISÉES

Le présent permis autorise le titulaire à avoir en sa possession, transférer, importer, exporter, utiliser et stocker les substances nucléaires et les équipements autorisés qui sont énumérés dans la section IV) du présent permis.

Le présent permis est délivré pour le type d'utilisation: études de laboratoire - 10 laboratoires ou plus où des radio-isotopes sont utilisés ou manutentionnés (836)

IV) SUBSTANCES NUCLÉAIRES ET ÉQUIPEMENT AUTORISÉ

ARTICLE	SUBSTANCE NUCLÉAIRE	SOURCE NON SCELLÉE QUANTITÉ MAXIMALE	ASSEMBLAGE DE LA SOURCE SCELLÉE QUANTITÉ MAXIMALE	ÉQUIPEMENT - FABRICANT ET MODÈLE
1	Carbone 14	400 MBq	s/o	s/o
2	Calcium 45	40 MBq	s/o	s/o
3	Cérium 141	100 MBq	s/o	s/o
4	Chrome 51	100 MBq	s/o	s/o
5	Fer 55	100 MBq	s/o	s/o
6	Fer 59	1 GBq	s/o	s/o
7	Hydrogène 3	2 GBq	s/o	s/o
8	Iode 125	1 GBq	s/o	s/o
9	Phosphore 32	5 GBq	s/o	s/o
10	Phosphore 33	100 MBq	s/o	s/o
11	Soufre 35	3 GBq	s/o	s/o
12	Scandium 46	100 MBq	s/o	s/o
13	Strontium 85	20 MBq	s/o	s/o
14	Césium 137	s/o	40 kBq	s/o
15	Césium 137	s/o	1480 kBq	Beckman LS (series)
16	Radium 226	s/o	370 kBq	PerkinElmer Wallac 1200 series LS Counters
17	Europium 152	s/o	740 kBq	PerkinElmer Wallac 1400 series LS Counters

La quantité totale d'une substance nucléaire non scellée possédée ne doit pas excéder la quantité maximale qui est indiquée pour une source non scellée correspondante. La quantité de substance nucléaire par source scellée ne doit pas excéder la quantité maximale indiquée par source scellée correspondante. Les sources scellées doivent être utilisées seulement dans l'équipement indiqué corrrespondant.

V) ENDROIT(S) OÙ LES ACTIVITÉS AUTORISÉES PEUVENT ÊTRE EXERCÉES

utilisées ou entreposées à (aux)

endroit(s) suivant(s):

Institut Lady Davis de Recherches Médicales
3755 chemin Côte Ste-Catherine
Montréal (Québec)

CONDITIONS

1. Interdiction visant l'utilisation chez les humains
Le permis n'autorise pas l'utilisation des substances nucléaires dans ou sur le corps d'une personne.
(2696-0)

2. Classification des zones, pièces et enceintes
Le titulaire de permis désigne chaque zone, pièce ou enceinte où on utilise plus d'une quantité d'exemption d'une substance nucléaire non scellée à un moment donné selon la classification suivante :

(a) de niveau élementaire si la quantité ne dépasse pas 5 LAI,
(b) de niveau intermédiaire si la quantité utilisée ne dépasse pas 50 LAI,
(c) de niveau supérieur si la quantité ne dépasse pas 500 LAI,
(d) de confinement si la quantité dépasse 500 LAI;
(e) à vocation spéciale, avec l'autorisation écrite de la Commission ou d'une personne autorisée par celle-ci.

À l'exception du niveau élementaire, le titulaire de permis n'utilise pas de substances nucléaires non scellées dans ces zones, pièces ou enceintes sans l'autorisation écrite de la Commission ou d'une personne autorisée par celle-ci.
(2108-1)

3. Liste des laboratoires
Le titulaire de permis tient à jour une liste de toutes les zones, salles et enceintes dans lesquelles plus d'une quantité d'exemption d'une substance nucléaire est utilisée ou stockée.
(2569-1)

4. Procédures de laboratoire
Le titulaire affiche en tout temps et bien en évidence dans les zones, les salles ou les enceintes où des substances nucléaires sont manipulées une affiche sur la radioprotection qui a été approuvée par la Commission ou une personne autorisée par la Commission et qui correspond à la classification de la zone, de la salle ou de l'enceinte.
(2570-1)

5. Surveillance thyroïdienne
La personne
a) qui utilise à un moment donné une quantité d'iode 125 ou d'iode 131 volatiles dépassant :
(i) 5 MBq dans une pièce ouverte,
(ii) 50 MBq dans une hotte,
(iii) 500 MBq dans une boîte à gants,
(iv) toute autre quantité dans une enceinte de confinement approuvée par écrit par la Commission ou une personne autorisée par celle-ci;
(b) qui est impliqué dans un déversement mettant en cause plus de 5 MBq d'iode 125 ou d'iode 131 volatiles;
(c) chez laquelle on détecte une contamination externe à l'iode 125 ou l'iode 131;
doit se prêter à un dépistage thyroïdien dans les cinq jours suivant l'exposition.
(2046-7)

6. Dépistage thyroïdien
Le dépistage de l'iode 125 et de l'iode 131 internes se fait :
(a) par mesure directe à l'aide d'un instrument capable de détecter 1 kBq d'iode 125 ou d'iode 131;
(b) par essai biologique approuvé par la Commission ou une personne autorisée par celle-ci.
(2600-1)

7. Essai biologique thyroïdien
Si la charge thyroïdienne dans une personne depasse 10 kBq d'iode 125 ou d'iode 131, le titulaire de permis doit présenter immédiatement un rapport préliminaire à la Commission ou à une personne autorisée par celle-ci. Dans un délai de 24 heures, la personne en question doit subir des essaies biologiques par une personne autorisée par la Commission à offrir un service de dosimétrie interne.
(2601-4)

8. Dosimétrie des extrémités
Le titulaire de permis veille à ce que toute personne qui manipule un contenant renfermant plus de 50 MBq de phosphore 32, de strontium 89, d'yttrium 90, de samarium 153 ou de rhénium 186 porte une bague dosimètre. Le dosimètre est fourni et lu par un service de dosimétrie autorisé par la Commission.
(2578-0)

9. Critères de contamination
En ce qui a trait aux substances nucléaires figurant au tableau «Classification des radionucléides» du guide sur les demandes de permis, le titulaire de permis veille à ce que :
(a) la contamination non fixée dans toutes les zones, pièces ou enceintes où on utilise ou stocke des substances nucléaires non scellées ne dépasse pas :
(i) 3 Bq/cm2 pour tous les radionucléides de catégorie A,
(ii) 30 Bq/cm2 pour tous les radionucléides de catégorie B,
(iii) 300 Bq/cm2 pour tous les radionucléides de catégorie C,
selon une moyenne établie pour une surface ne dépassant pas 100 cm2;
(b) la contamination non fixée pour toutes les autres zones ne dépasse pas :
(i) 0,3 Bq/cm2 pour tous les radionucléides de catégorie A,
(ii) 3 Bq/cm2 pour tous les radionucléides de catégorie B,
(iii) 30 Bq/cm2 pour tous les radionucléides de catégorie C,
selon une moyenne établie pour une surface ne dépassant pas 100 cm2.
(2642-2)

10. Déclassement
Avant le déclassement d'une zone, d'une pièce ou d'une enceinte où s'est déroulée l'activité autorisée, le titulaire de permis veille à ce que :
(a) la contamination non fixée pour les substances nucléaires figurant au tableau «Classification des radionucléides» du guide sur les demandes de permis ne dépasse pas :
(i) 0,3 Bq/cm2 pour tous les radionucléides de catégorie A,
(ii) 3 Bq/cm2 pour tous les radionucléides de catégorie B,
(iii) 30 Bq/cm2 pour tous les radionucléides de catégorie C,
selon une moyenne établie pour une surface ne dépassant pas 100 cm2;
(b) la mise en disponibilité de toute zone, pièce ou enceinte contenant une contamination fixée soit approuvée par la Commission ou une personne autorisée par celle-ci;
(c) toutes les substances nucléaires et tous les appareils à rayonnement ont été transférés conformément aux conditions du permis;
(d) tous les panneaux de mise en garde contre les rayonnements ont été retirés ou ont été rendus illisible.
(2571-2)

11. Stockage
Le titulaire :
a) veille à ce que seules les personnes autorisées par lui aient accès aux substances nucléaires radioactives ou aux appareils à rayonnement stockés;
b) veille à ce qu'à tout endroit occupé à l'extérieur de la zone, de la salle ou de l'enceinte de stockage le débit de dose provenant des substances ou appareils stockés ne dépasse pas 2,5 microSv/h;
c) a des mesures en place pour assurer que les limites de dose indiquées dans le Règlement sur la radioprotection ne sont pas dépassées en raison du stockage de ces substances ou appareils.
(2575-0)

12. Évacuation (laboratoires)
Lorsqu'il évacue des substances nucléaires non scellées dans une décharge municipale ou un réseau d'égouts, le titulaire de permis